

Sheffield Hallam University

The effect of piston design on hydrocarbon emissions in a spark ignited engine.

WILLCOCK, M.

Available from the Sheffield Hallam University Research Archive (SHURA) at:

<http://shura.shu.ac.uk/20539/>

A Sheffield Hallam University thesis

This thesis is protected by copyright which belongs to the author.

The content must not be changed in any way or sold commercially in any format or medium without the formal permission of the author.

When referring to this work, full bibliographic details including the author, title, awarding institution and date of the thesis must be given.

Please visit <http://shura.shu.ac.uk/20539/> and <http://shura.shu.ac.uk/information.html> for further details about copyright and re-use permissions.



287302

7/7/95 16:55
~~22/4/96~~ 18:30

Sheffield Hallam University
REFERENCE ONLY

ProQuest Number: 10701186

All rights reserved

INFORMATION TO ALL USERS

The quality of this reproduction is dependent upon the quality of the copy submitted.

In the unlikely event that the author did not send a complete manuscript and there are missing pages, these will be noted. Also, if material had to be removed, a note will indicate the deletion.



ProQuest 10701186

Published by ProQuest LLC (2017). Copyright of the Dissertation is held by the Author.

All rights reserved.

This work is protected against unauthorized copying under Title 17, United States Code
Microform Edition © ProQuest LLC.

ProQuest LLC.
789 East Eisenhower Parkway
P.O. Box 1346
Ann Arbor, MI 48106 – 1346

**THE EFFECT OF PISTON DESIGN ON HYDROCARBON EMISSIONS
IN A SPARK IGNITED ENGINE**

M. WILLCOCK

**A thesis submitted in partial fulfilment of the
requirements of
SHEFFIELD HALLAM UNIVERSITY
for the degree of Doctor of Philosophy**

December 1993

Collaborating Organisation: AE Piston Products Ltd

ABSTRACT

The Effect of Piston Design on Hydrocarbon Emissions in a Spark Ignited Engine

This thesis describes an investigation into the effect of piston design on hydrocarbon emissions from an spark ignited engine. The experimental investigation tested a series of three piston configurations against a standard design based on production dimensions. These tests examined the effect of top and 2nd land crevice volumes and absorption and desorption from lubricant on the cylinder liner as sources of hydrocarbon emissions. The operational conditions were steady state for all engine parameters. The work was performed on a modern four cylinder 16 valve engine with multi point fuel injection. Two fuels were used, a reference unleaded petrol and trimethyle pentane.

The results have shown that significant reductions in hydrocarbon emissions can be achieved by certain design changes. Reducing the top land height from 6mm to 2.8mm reduced emissions by up to 25% and creating a smoother surface on the cylinder liner wall reduced emissions by up to 28%. A method of assessing residual lubricant on the cylinder walls was developed from surface finish measurement and showed that the smoother surface finish would retain less oil and reduce the amount of fuel absorbed by the oil. The 2nd land volume was a secondary source having an effect at low speed low load conditions.

The hydrocarbon species were investigated with gas chromatography, the concentrations of these species were observed to change with each design, but not necessarily proportional to the total hydrocarbon emissions.

A model was developed to allow the prediction of changes to hydrocarbon emissions by altering various piston design parameters. In addition to modelling mixture flow into piston crevice volumes and absorption of fuel by lubricant on cylinder walls a basic combustion analysis allowed the prediction of combustion gas temperatures and the end point of combustion. In-cylinder oxidation could then be approximated. Results from this model gave good agreement with experimental results and was then used to assess the optimum piston design to reduce hydrocarbon emissions.

This research has demonstrated that component design and specification can be used to reduce hydrocarbon emissions from a spark ignited engine. The most significant parameters have been identified and methods of measurement developed. After considering current material and design constraints the dimensions for a low hydrocarbon emission piston was modelled and predicted 30% reduction in emissions.

CONTENTS

Section	Page No
List of Figures	i
List of Tables	viii
Notation	ix

CHAPTER 1. INTRODUCTION

1.1	Vehicle Emissions and legislation	1
1.2	Methods of Emission Control	2
1.3.	Objectives and Novel Aspects of this Research	5

CHAPTER 2. LITERATURE SURVEY

2.1	Early Research	8
2.2	Wall Quench and Crevice Volumes	9
2.3	Oil Effects	15
2.4.	Models for Combustion and Hydrocarbon Emissions	20
2.4.2.	Modelling of post flame oxidation	22
2.5.	Piston and Combustion Chamber Design	23
2.5.1	Piston Design	23

2.5.2.	Combustion Chamber Design	25
2.6	Cold starting of engines	27
2.7	Hydrocarbon Speciation and Fuels	
2.7.1	Hydrocarbon Species in Emissions	30
2.7.2.	Fuel Composition	31
2.7.3	Alternative fuels	33
2.8.	Conclusion	34

CHAPTER 3 EXPERIMENTAL

3.1	Test Rig Specification	37
3.1.1	The Engine	37
3.1.2.	Exhaust Gas Sampling	38
3.1.3.	Lubrication scheme	39
3.1.4.	Fuel scheme	40
3.1.5.	Pressure Transducers	40
3.1.6	Temperature Measurement	41
3.1.7.	Air Flow Measurement	41
3.2.	Exhaust Gas Analysis	41
3.2.1.	General Emissions	41
3.2.2	Gas Chromatograph Procedures	42
3.3	Operating and Test Procedures	
3.3.1	Test Procedures	45
3.3.2.	Engine Preparation	47
3.4.	Data Handling	48
3.4.1.	Engine and Emission Data	48
3.4.2.	Cylinder Pressure Data	49

CHAPTER 4. THEORETICAL

4.1	Introduction	55
4.1.2	Data Required for Calculations	55
4.2.	Piston Crevice Volume Effects	56
4.2.1.	Top Land Flow	57
4.2.2.	Flow into Ring Groove	58
4.2.3.	Flow into 2nd Land Crevice	59
4.2.4.	Test Calculations	60
4.2.4.1.	Flow Varying with Top Land Dimensions	61
4.2.4.2.	Flow Varying with 2nd Land Dimensions	62
4.3.	Absorption and Desorption of Fuel in Oil	
4.3.1.	Outline of Previously Developed Models	70
4.3.2.	Defining Values for $C_{\max} - C_{\min}$	73
4.3.3	Defining the Henry Constant	74
4.3.4	Test Runs of Computer Calculations	75
4.4.	Modelling of Oxidation of Crevice Mixture and desorbed fuel	81
4.4.1	Test Calculations	86
4.4.2.1	Mixture Ratio	86
4.4.2.2	Oxidation Varies with Piston Temperature	87
4.4.2.3	Changing Oxidation Rate	87
4.5.	Combustion Analysis	
4.5.1.	Heat Release Calculations from Pressure Data	91
4.5.2.	Combustion Gas Temperatures	94
4.5.3.	Checks on Heat Release	95
4.5.4.	Calculation Results	95
4.5.5.	Checks on Temperature.	96
4.5.6	Temperature Calculation Results	97

5. ENGINE TESTS	
5.1 Introduction	101
5.2. Repeatability Between Runs and Engine Builds	102
5.3. Standard Test	103
5.3.1. Standard Test Results	104
5.3.2. Gas Chromatography	105
5.4. Reducing top land crevice volume	116
5.4.2 Hydrocarbon Emissions	117
5.4.3. Gas Chromatography	118
5.5. Pressure Balanced 2nd Land Pistons	128
5.5.1. Hydrocarbon Emissions	129
5.5.2. Gas Chromatography	130
5.6. Cylinder Liner Surface finish Test	138
5.6.1 Defining Oil Layer Thickness	138
5.6.2. Hydrocarbon Emissions	141
5.6.3. Gas Chromatography	142
5.6.5. Surface Finish Performance	143
5.7. Predictive Calculation Results of Hydrocarbon Emissions	151
5.7.1. Changes to Crevice Volume for Piston Dimensions used in Experimental Tests	151
5.7.2. Cylinder Liner Surface Finish	153
5.8 Study of Some Factors effecting Hydrocarbon Emissions	153
5.9 Summary of Results	
5.9.1. Experimental Results	154
5.9.2. Gas Chromatography	154
5.9.3. Predictive Emissions	155

6. DISCUSSION

6.1	Introduction	162
6.2.1	Experimental Results from the Standard Test	162
6.2.2.	Pyrolysis and Oxidation of Emissions across Exhaust Manifold	162
6.2.3.	Effect of Single Component Fuel on Hydrocarbon Emissions	165
6.2.4.	The effect of different lubricant on Hydrocarbon emissions	166
6.3.	Comparison of Test Pistons against Standard	
6.3.1.	High Top Ring Piston Discussion	166
6.3.2	Enlarged 2nd Land Pistons Discussion	169
6.3.3.	Smooth Cylinder Liner Discussion	170
6.4.	Methods of Reducing Hydrocarbon Emissions	177
6.4.1.	Top Land Crevice Volume	177
6.4.2.	Cylinder Liner Surface Finish	178
6.5.	Optimum Piston and Liner Design	178

7 CONCLUSION

7.1.	Introduction	183
7.2.1	Experimental	183
7.2.2.	Gas Chromatography	184
7.3.	Modelling	184
7.4.	Piston Features for reducing Hydrocarbon Emissions	185

8. RECOMMENDATIONS FOR FUTURE WORK

- | | | |
|-----|---------------------------------------|-----|
| 8.1 | Pistons for Low Hydrocarbon Emissions | 187 |
| 8.2 | Extending the Predictive Model | 187 |

9. ACKNOWLEDGEMENTS 188

10. REFERENCES 189

APPENDICES

1. Engine Performance and Specific Emissions Calculations
2. Computer Program Listings and Input Data
3. Piston Dimensions for Engine Tests
4. Photographs of Engine and Instrumentation
5. Fuel and Oil Specification
6. Definitions of Surface Finish Parameters
7. Papers Published

List of Figures

	Page
1.1 Graph Showing Hydrocarbon Emissions against Air Fuel Ratio	7
3.1 Layout of engine and equipment	51
3.2 Inputs to Engine Control Unit	52
3.3 Sketch of Exhaust Port Sample Pipe	52
3.4 Emissions sampling circuit	53
3.5 Sealing cylinder head bolt	53
3.6 Engine lubrication circuit	54
3.7 Dual fuel circuit	54
4.1 Flow chart for complete model	63
4.2 Flow chart, crevice flow calculations	64
4.3 Pressure profile of piston crevice	65
4.4 Flow from top land, 2nd land and top ring groove	65
4.5 Top land mass flow, changes to top land volume	66
4.6 2nd Land pressure profile, changes to top land diameter	66
4.7 2nd Land mass flow, changes to top land diameter	67
4.8 Total crevice mass flow, changes in top land diameter	67

4.9	2nd Land pressure profile, changes to 2nd land volume	68
4.10	2nd Land mass flow, changes to 2nd land volume	68
4.11	Total crevice mass flow, changes to 2nd land volume	69
4.12	Values of $C_{\max} - C_{\min}$, with engine speed and piston position	77
4.13	Values of $C_{\max} - C_{\min}$, with piston position	77
4.14	Values of Henry Constant for trimethyle pentane, n-octane and m-xylene	78
4.15	Flow chart for calculation of absorption and desorption of fuel in lubricant	78
4.16	Fuel desorbed per degree crank angle	79
4.17	Cumulative mass of fuel desorbed	80
4.18	Flow chart of hydrocarbon oxidation	88
4.19	Effect of mixture ratio on the level of unburnt hydrocarbon	89
4.20	Effect of piston temperature on level of unburnt hydrocarbon	89
4.21	Effect of oxidation factor on level of unburnt hydrocarbon	90
4.22	Flow chart for combustion analysis	99
4.23	Calculated percentage fuel burnt and heat release per degree crank angle	100
4.24	Calculated combustion temperature per degree crank angle	100
5.1	Hydrocarbon emissions standard build, from exhaust	

port and Exhaust pipe.	109
5.2 Variation of hydrocarbon emissions from cylinder to cylinder and air fuel ratios	109
5.3 Nitric oxide emissions from standard build	110
5.4 Carbon Monoxide emissions from standard build	110
5.5 Flow of blow-by gases from standard build	111
5.6 Hydrocarbon emissions standard build, from Trimethyle Pentane Fuel	111
5.7 Hydrocarbon emissions from tests using another multigrade oil	112
5.8 Hydrocarbon emissions from tests using a synthetic lubricant	112
5.9 Gas Chromatograph plot of fuel vapour and emissions from Standard Build	113
5.10 Hydrocarbon species from standard build showing Percentage concentrations	114
5.11 Gas chromatograph Plot of emissions, fuel Trimethyle Pentane	115
5.12 Sketch of high top ring piston	120
5.13 Comparison of hydrocarbon emissions from exhaust pipe of high top ring pistons and standard build	121
5.14 Comparison of hydrocarbon emissions from exhaust port of high top ring pistons and standard build	121
5.15 Percentage change of hydrocarbon emissions from exhaust pipe of high top ring piston against standard build	122

5.16	Percentage change of hydrocarbon emissions from exhaust port of high top ring piston against standard build	122
5.17	Comparison of hydrocarbon emissions from exhaust pipe of high top ring pistons and standard build, Trimethyle Pentane Fuel	123
5.18	Comparison of blow-by flow from high top ring pistons and standard build	123
5.19	Gas chromatograph plot of emissions from high top ring pistons	124
5.20	The 13 selected species from high top ring pistons	125
5.21	Change in alkanes from high top ring pistons against standard build	125
5.22	Change in alkenes from high top ring pistons against standard build	126
5.23	Change in aromatics from high top ring pistons against standard build	126
5.24	Drawing of the enlarged 2nd land piston	132
5.25	Comparison of hydrocarbon emissions from exhaust pipe of enlarged 2nd land pistons and standard build	133
5.26	Comparison of hydrocarbon emissions from exhaust port of enlarged 2nd land pistons and standard build	133
5.27	Comparison of hydrocarbon emissions enlarged 2nd land pistons, Trimethyle Pentane Fuel	134
5.28	Comparison of blow-by flow from enlarged 2nd land pistons and standard build	134

5.29 Gas Chromatograph plot of emissions from enlarged 2nd land pistons	135
5.30 The 13 selected species from enlarged 2nd land pistons	136
5.31 Change in alkanes from enlarged 2nd land pistons against standard build	136
5.32 Change in alkenes from enlarged 2nd land pistons against standard build	137
5.33 Change in aromatics from enlarged 2nd land pistons against standard build	137
5.34 Surface finish traces from standard liners and smooth liners	144
5.35 Bearing area curve showing shaded area of oil	145
5.36 Comparison of hydrocarbon emissions from exhaust pipe of smooth liner and standard build	146
5.37 Comparison of hydrocarbon emissions from exhaust port of smooth liner and standard build	146
5.38 Comparison of hydrocarbon emissions from smooth liner and standard build Trimethyle Pentane Fuel	147
5.39 Comparison of blow-by flow from smooth liner and standard build	147
5.40 Gas chromatograph plot of emissions from smooth liner	148
5.41 The 13 selected species from smooth liner	149

5.42 Change in alkanes from smooth liner against standard build	149
5.43 Change in alkenes from smooth liner against standard build	150
5.44 Change in aromatics from smooth liner against standard build	150
5.45 Predicted crevice flow for piston dimensions used in tests, high top ring pistons and enlarged 2nd land pistons	156
5.46 Effect of top ring height on desorption of fuel	156
5.47 Normalised hydrocarbon emissions from high top ring pistons measured and predicted	157
5.48 Normalised hydrocarbon emissions from enlarged 2nd land pistons measured and predicted values	157
5.49 Predicted 2nd land crevice flow for enlarged 2nd land piston	158
5.50 Predicted total crevice flow for smooth liner piston	158
5.51 Normalised hydrocarbon emissions from smooth liner measured and predicted	159
5.52 Percent changes to hydrocarbon emissions for design variations	159
5.53 Measured normalised hydrocarbon emissions from engine variations	160
5.54 Total Alkanes, Alkenes and Aromatics compared against standard build	160

5.55 Predicted normalised hydrocarbon emissions from each engine variation	161
6.1 Percentage change in hydrocarbon emissions across exhaust manifold	174
6.2 Percentage change in species across exhaust manifold	174
6.3 Percentage change in hydrocarbon emissions from smooth liner tests	175
6.4 Gas chromatograph plot from oil vapour	176
6.5 Sketch of Optimum Piston	180
6.6 Optimum piston design, 2nd land flow	181
6.7 Optimum piston design, top land flow	181
6.8 Optimum piston design, total crevice flow	182
6.9 Comparison of normalised emissions between optimum pistons and standard	182

List of Tables

	Page
3.1 Gas Chromatograph method	43
3.2 Engine test points	44
3.3 Schematic of tests performed	46
3.4 Engine running-in schedule	50
4.1 Assumed inputs for calculations	55
4.2 Inputs for modelling absorption/desorption	76
4.3 Ignition and combustion completion timing	96
4.4 Combustion chamber temperatures at inlet and outlet	98
5.1 Test Programme	101
5.2 Comparison of sfc and efficiency for all builds	103
5.3 Standard piston dimensions	103
5.4 Identified hydrocarbon species	107
5.5 High top ring piston dimensions	117
5.6 Enlarged 2nd land piston dimensions	129
5.7 Cylinder liner surface finish parameters	141
5.8 Smooth liner piston dimensions	141
5.9 Piston dimensions for high top ring and enlarged 2nd land Pistons	151
6.1 Gas Chromatograph data, unburnt fuel and products Trimethyle Pentane fuel	164
6.2 Exhaust gas temperatures at exhaust pipe and ports	165
6.3 Optimum piston dimensions	179

NOTATION

A = Area	m^2
Cd = Coefficient of Discharge	
C _p = Specific Heat at constant pressure,	kJ/kgK
C _v = Specific Heat at constant volume,	kJ/kgK
C* = mass fraction fuel in oil	
C* _{eq} = mass fraction of fuel in oil at equilibrium.	
D = Piston Diameter	m
d = Cylinder Diameter	m
F _{O2} = exhaust oxygen percent	
H _c = Henry Constant	
h = channel width	m
k = area ratio ring gap/crevice area	
m = Mass	kg
m _c = mass of mixture in crevice	kg
M _r = Mol weight of mixture	
N = engine speed	rpm
P = Cylinder Pressure	N/m^2
P _i = inlet pressure	N/m^2
P _o = Atmospheric pressure	N/m^2
Q = Heat Release	kJ/kg
Q _f = Calorific Value of fuel	kJ/kg
R _o = Universal gas constant	kJ/kgK
Re = Renolds number	
T _p = Piston temperature	K
U = Internal energy	kJ
V _c = crevice volume	m^3
W = channel length, ring width	m

X = Mixing Ratio

x = Mol Fraction

y/s = Piston displacement from TDC

θ = Crank Angle, degrees

ρ_o = oil density kg/m³

μ_{gas} = Dynamic Viscosity kg/ms

SUBSCRIPTS

u = pressure upstream

d = down stream

f = fuel

c = Crevice mixture

ABBREVIATION

AFR = air fuel ratio

ATC = After Top Dead Centre

bmep = Brake Mean Effective Pressure

sfc = specific fuel consumption

1. INTRODUCTION

1.1 Vehicle Emissions and legislation

The scale of car ownership in many countries has increased dramatically in the past three decades and the demand for personal private transport continues to increase. It has been observed that no developed country has yet reached saturation for the number of cars for the population Cragg (1). Saturation is predicted when 90% of the population eligible to drive has a vehicle. This is assumed to be 650 cars per thousand (cpt) people for the overall population. In Britain the cpt is currently approximately 330, the forecasts are that the cpt will increase to between 529 and 608 by the year 2025.

This increase has coincided with a heightened awareness of the environment by the general population, and has created pressure to improve air quality, but not to restrict car usage and availability. National governments and international organisations whilst appreciating these demands also have to concede to the demands of the car industry which is of major importance to world and national economies. Legislation has been introduced to compel manufacturers to reduce vehicle emissions, but not to restrict the growth in vehicle numbers. The continuing increase in vehicle numbers will create greater pressure to reduce emissions even further.

The legislation varies across the developed world. The state of California, USA has usually set the trends for the

whole of the USA and has a strong influence on European legislation. The limits set there are very tight and call for the gradual introduction of ultra low and zero emissions vehicles by the year 2000. With reference to hydrocarbon emissions the current requirements for California are for HC + NOx of 0.4 g/km. In Europe the current limits for HC + NOx is 0.97 g/km. But further legislation under the European Consolidated Directive 11 (ECD 11) will bring this down to 0.45 g/km in 1996. Proposals for ECD 111 are for 0.2 g/km in 1999.

1.2 Methods of Emission Control

The main toxic emissions from spark ignition engines are carbon monoxide, hydrocarbons and nitric oxides. Also, because of the greenhouse effect the monitoring of carbon dioxide could be introduced. With improvements to the control of air/fuel mixture control and ignition control the emissions from vehicle have been reduced, but not sufficiently with the increasing number of vehicles, further methods of reduction were required.

The current method of control to meet European standards is the after treatment of emissions by a three way catalytic converter. This has caused considerable controversy, because of the need to operate the engine at a stoichometric air fuel ratio of 14.7:1. This reduces the engine efficiency and increases fuel consumption and production of CO₂. A further disadvantage to this method is catalyst performance during a cold engine start. The catalyst takes several minutes to reach operating

temperature during which time the engine emits high levels of pollutants.

An alternative to this method is lean burn combustion and the use of an oxidation catalyst. The engine design enables it to operate at air fuel ratios between 18:1 and 22:1. Comparison against stoichiometric combustion, before catalyst after treatment, lean burn gives lower carbon monoxide and nitric oxide emissions and a slight increase in hydrocarbon emissions, which can be oxidised by the catalyst. The high air fuel ratios also improve fuel consumption and reduce carbon dioxide emissions. At air fuel ratios of 22:1 engine misfires start to occur and hydrocarbon emissions increase, this puts the limit on lean air fuel ratios.

Both these methods of control reduce levels of emissions, but do not eradicate them. The severe legislation being introduced require all aspects of engine design and control to be focused on reducing emissions. It would be preferable to reduce the levels of pollutants at source, because catalyst units are expensive and the cost has to be passed to the consumer, though it seems unlikely that the required levels will be met without some exhaust after treatment.

The origin of hydrocarbon emissions within the engine have been researched extensively and the major sources have been identified, these are;

Crevice volumes; the fuel mixture is trapped in crevices where the flame cannot penetrate.

Absorption; the fuel is absorbed into the lubricant on

the cylinder walls this is desorbed after combustion.

Bulk quench; incomplete combustion of mixture in the chamber and occurs under poor combustion conditions.

Surface quench; as the flame approaches the cooler combustion chamber walls the flame is extinguished.

The hydrocarbon emissions varying with air fuel ratio are shown in Figure 1.1. It can be seen that at air fuel ratios at and weaker than stoichiometric the emissions are at their lowest and least sensitive. In a correctly adjusted engine emissions from poor combustion will be very small at these conditions. The emissions at this point are mainly due to crevice volumes and absorption of fuel into the cylinder lubricant.

The hydrocarbons as pollutants are a wide mixture of compounds, usually referred to as species, some of these are toxic for example benzene is a known carcinogen with no safe limit of exposure. Additionally with the aid of sunlight these hydrocarbons combine with the nitric oxide emissions to form smog. The smog forming potential of each species is dependent upon its reactivity, in the USA this is now leading to legislation to set limits on alkenes (hydrocarbon compounds with a double carbon-carbon bond making it more reactive) in fuel and vehicle emissions. The extra processing of fuel to reduce alkenes increases the energy consumed during refining, with higher costs and producing more CO₂.

1.3. Objectives

The objective of this research was to investigate the impact of design and specification of the piston and cylinder liner on hydrocarbon emissions and to demonstrate how this can reduce engine out hydrocarbon emissions. This research was not directed at combustion within the cylinder but with related phenomena of how fuel evades combustion at the periphery of the combustion chamber, ie crevice volumes and fuel absorption into lubricant.

This research had have two main activities, experimental engine tests and a mathematical model.

The experimental work involved testing a series of piston designs for there impact on hydrocarbon emissions. These designs were developed from studies of previous research which identified possible sources of hydrocarbon emissions. The pistons tested would alter one feature at a time, so that only one source of emissions is affected. To perform these experiments a complex test rig was designed and built. This allow the accurate measurement of engine operating conditions, performance and emissions. This included the measurement of combustion pressure in the cylinder per degree crank angle this provided a basis for the modelling. Because of the interest in hydrocarbon species in vehicle emissions a gas chromatograph was used to analyze the species and how their relative concentration is affected by the piston design.

The objective of the modelling was to simulate the effect of piston design changes on hydrocarbon emissions. The model included mass flow of hydrocarbon emissions from each source and oxidation during expansion and exhaust, too achieve this a combustion model to predict the end point of combustion and

gas temperatures is included. This model can then be verified by the experimental work.

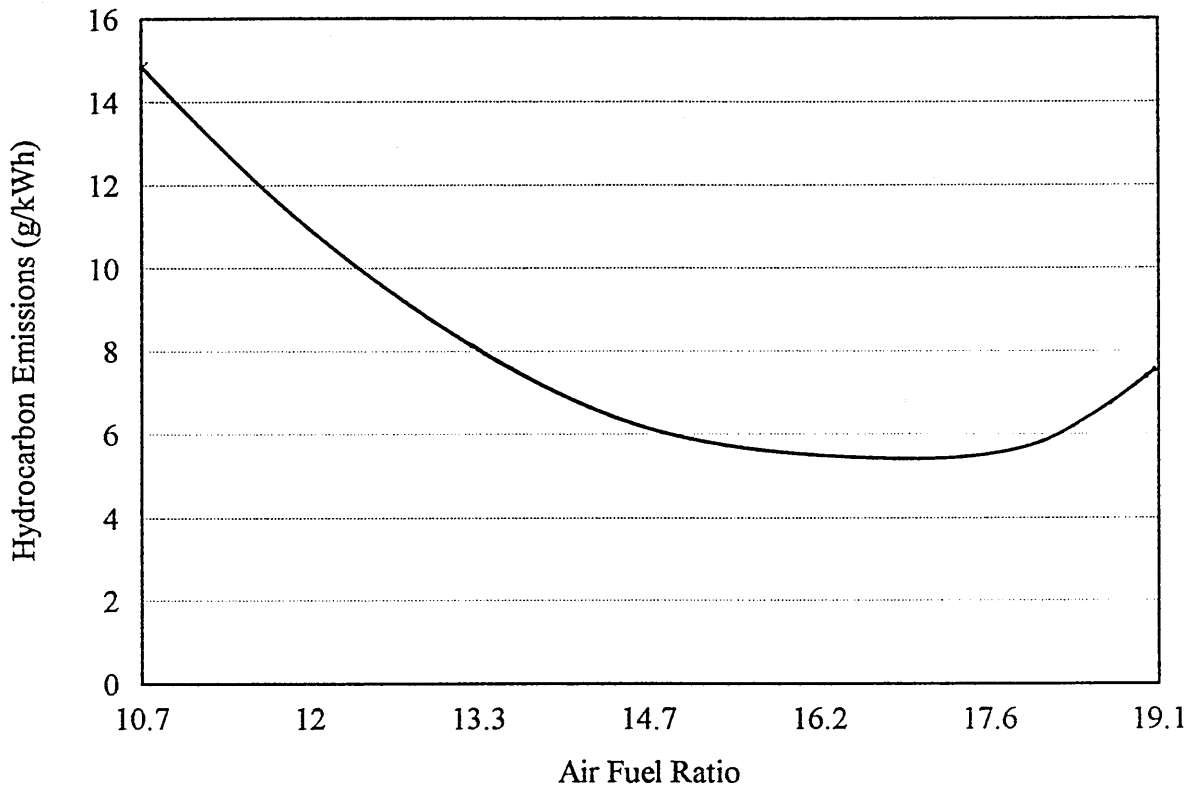


Figure 1.1 Hydrocarbon emissions varying with air fuel ratio

2. LITERATURE SURVEY

2.1 Early Research

The investigation of hydrocarbon emissions from internal combustion engines fall into two broad categories;

1, sources of emissions and possible methods of reduction.

2, Theoretical model to predict emissions from various sources.

The problems caused by vehicle emissions were first recognised in the 1950's, and researches began to investigate the sources of these emissions within the engine. One of the major causes of emissions was thought to be wall quench, as the flame approached the cooled walls of the combustion chamber it was extinguished leaving some unburned fuel. Daniel (2) investigated this using high speed photography. A quench layer was observed with a thickness of between 0.012" and 0.02", it was concluded that a large part of the hydrocarbons emitted would be from this source. In further work Daniel and Wentworth (3) took samples from inside the cylinder of a single cylinder test engine for the analysis of hydrocarbons during combustion, expansion and exhaust. When samples were taken close to the wall of the cylinder the hydrocarbon concentrations increased. In further tests the hydrocarbons in the exhaust pipe were sampled it was

observed that with leaner ratios, ie $>16.9:1$ some reaction took place after the gases left the cylinder. It was also noted that some reactions took place during the expansion and exhaust strokes.

2.2 Wall Quench and Crevice Volumes

In a study of the mass flow rate of hydrocarbon in the exhaust Tabaszynski et al (4) used a fast sampling valve mounted in the exhaust manifold of a single cylinder engine. Two peaks in emissions were observed these occurred at the start and end of exhaust stroke. The source of these peaks were from entrainment of cylinder head quench layer and from the vortex motion caused by the piston scraping the boundary layer on the cylinder wall which contains unburnt fuel from the piston crevices. The relative contributions to the total emissions were approximately equal, but this can vary with cylinder geometry.

Wentworth (5) and (6) continued in this field and observed that the 'crevice effect' may be a special case of quench in particular the piston-ring-cylinder crevices. In a series of tests Wentworth investigated the effect on emissions of ring gap size and position and number of piston rings. He observed that blow-by gases comprised of 85% carburetted mixture. From his results he conjectured that this gas is forced down this route by cylinder pressure and is unburned due to wall quench, some of this gas does make its way back into the

cylinder during exhaust. He concluded that 'the reduction of crevices is an obvious direct approach to reducing hydrocarbon emissions.' Wentworth goes on to develop a test piston and ring which effectively reduce blow-by and emissions, from these results he conjectures that approximately 50% of hydrocarbon emissions originate from the crevices.

Some attempts were made to model the wall quench affect. Wiess and Keck (7) had some success but concluded that emissions from quench layers were are not a significant contribution to exhaust emissions. Turning to crevice effects and oxidation times in the combustion chamber and developed the following model.

$$t_r = \frac{1}{[HC]} \cdot \frac{d[HC]}{dt} = A(P_{O_2}/P_0)^b \cdot e^{-E/RT} \dots [1]$$

Where t_r = oxidation time

P_{O_2} = partial pressure oxygen

A, b, E = Constants

This model indicated that unburnt fuel entering the chamber during expansion is oxidised, but during blow down the temperature in the cylinder drops bellow 1000 K and so the reaction time increases and oxidisation is greatly reduced. Unburnt mixture from crevices arrive after the temperature has dropped and will pass into the exhaust. Some discrepancy with experimental results are observed and are explained as mixture from crevices entering the chamber before the end of the expansion stroke which the model does not cover.

Lorusso et al (8) also investigated quench layers,

taking samples from close to the wall of the cylinder. It was observed that oxidation products were found almost immediately after flame arrival and were dispersed quickly, 'suggesting that the material in the quench layer is rapidly and extensively oxidised.' Calculations showed that the quench layer would only yield approximately 9% of total exhaust emissions.

The post quench oxidation of the wall quench layer was also observed by Heywood and Keck (9). Noting that levels of hydrocarbon due to wall quench were only 2% of those predicted, he stated that 'This implies virtually complete post-quench oxidation of the quench layer'. Further tests showed that crevice volumes were the dominant source of HC emissions, and that up to 10% of the charge can be contained in the crevice regions.

Haskell and Legate (10) investigated the effect of the piston top land crevice on HC emissions. It was proposed that an increase in the top land clearance would result in an increase in hydrocarbon emissions. Experiment showed this increase to be linear until a certain clearance was reached, then there was a dramatic drop in emissions. Haskell postulated that at this clearance the flame could propagate into this volume. However after a period of time deposits accumulated reducing this volume and the emissions then increased. A brief investigation was made into the temperature effects on top land clearance. It was found to reduce as temperature increased due to the different coefficients of expansion of the steel liner and the aluminium piston.

It was suggested that this was the effect which lead to reduced emissions when engine speed and load were increased.

The flow from the piston-cylinder crevices was observed by Namazian and Heywood (11) and (12) using schlieren photographic techniques. From these photographs flow was observed from spark plug and piston-cylinder crevices. There were two types of flow observed from the piston-cylinder crevice; at 30 to 50 degrees after top centre (ATC) flow was observed this flow was from the piston top land it was also noted that gases still flowed into regions behind and between the rings and that this occurs until the pressures have equalised. As the exhaust stroke starts and the cylinder pressure drops this flow reverses. A jet like flow was observed. A reasonably successful model of this flow was developed. The power and efficiency are significantly affected by these crevice effects with losses ranging between 2% and 7%.

These earlier works clearly established the crevice volumes in the combustion chamber as a source of unburnt fuel which would form part of the total exhaust hydrocarbon emissions. Other researches now strove to define these crevice volumes and develop predictive models of emissions from this source.

After the analysis of samples taken from within the cylinder, Panesar et al (13) devised a non-dimensional parameter for the crevice effect.

$$\frac{V_{ct}}{V_{st}} = \frac{\text{Total Crevice Volume}}{\text{Total Swept Volume}} = \frac{(V + AD + LD + ED)n}{D/4.S.n} \quad . . [2]$$

Where; V = Spark plug crevices including threads, AD = Cross section on a radial basis, ie gaskets & valves, LD = Ring pack and piston top lands and ED = Ring pack assumption

From this an expression for the flow rate of exhaust emissions was developed.

An important aspect of the crevice effect is the flow into and out of these crevices at different times in the combustion cycle. Although an investigation into oil consumption Miyachika(14) investigated the effect of blow-by flow through the second land and reverse flow carrying oil back into the chamber after the combustion stroke. A model was developed to predict inter-ring pressures and the flows which resulted. It was demonstrated that the second land pressure was an important factor in this flow. Ring gaps were used to control this pressure and thus the reverse flow. Namazian and Heywood (12) has shown that this flow is important in the return of unburned mixture back into the cylinder after combustion. Developing this model Kue et al (15) combined this with an additional model for predicting piston ring friction. The value of blow-by was used as a check against data from engine tests. The model was ran for several variables, cylinder wall temperature, top and 2nd ring end gap area and crevice volume behind the top ring. It was observed that the most sensitive variable was the wall temperature. Comparison with the test data showed that it predicted the correct trends but usually underestimated the actual levels. Several factors might account for this, the main one being

predicting the wall temperature.

In a follow up paper Reitz and Kue (16) combined this model with a multi-dimensional engine-flow and combustion model to investigate the effect of crevice flow upon combustion and top land crevice dimensions. The model indicated that crevice flow had very little influence on combustion. When considering the hydrocarbon emissions it was shown that predicted trends with speed and load were consistent with measurements. These calculations indicated that crevice out flow before 70 ATDC is oxidised by the high cylinder temperatures.

The top land had a strong influence upon the 2nd land crevice flow. The crevice width, clearance between piston and cylinder was observed to control the flow reducing the gap reduced the flow. The model was found to be insensitive to Top land height. This was not compared against engine tests with these top land alterations.

A hypothetical crevice volume was used by Hymas et al (17) to investigate storage and release mechanisms in the combustion chamber. Using propane as fuel, samples were taken from the cylinder and exhaust port. Gas chromatography identified that more than 80% by mass of in-cylinder hydrocarbons are fuel. Tests at varying speeds indicated that the storage parameter increased with speed.

$$\text{Storage parameter } S = \frac{A}{A^*}$$

Where; A = Parameter proportional to volume stored

A* = Reference value of A

In-cylinder hydrocarbons were seen to increase as the exhaust emissions decreased with increase in speed. The increase in the storage parameter was seen as a change in emphasis of the storage mechanism. The increase in in-cylinder hydrocarbons suggested that crevice volumes rather than the absorption of fuel as a source of hydrocarbon emissions. However, it must be noted that propane as a fuel is far less absorbent in oil than a normal unleaded fuel with approximately 45% of highly absorbent aromatics.

2.3 Oil Effects

Another source of exhaust hydrocarbons is the absorption of fuel in the lubrication oil layer during compression and combustion followed by its desorption during expansion and exhaust.

These oil effects have been investigated by several researches. Kaiser (18) carried out a series of experiments in a combustion chamber. A metal plate was smeared with oil and placed in the chamber. By applying different amounts of oil the effect of the layer thickness could be investigated. Unfortunately the time scale was too long to be directly applied to IC engines. In later research by Kaiser (19) an engine was used and oil was injected onto the top of the piston. It was observed that 50% of the increase in emissions were unburned fuel, Kaiser concluded that steady state oil layers in engines can play an important role in HC emissions.

Experimental work on the absorption effect has

focused on the effect of different types and viscosities of oil, a range of fuels have also been tried. Adamczyk et al (20) and (21) tried various oils with a mixture of methanol and ethane as fuel in a closed combustion chamber. The oils were in two groups, polar and non polar. It was found that unburnt fuel was the principal effluent after combustion and that fuel oil combinations of unmatched polarity produced significantly lower emissions. It was observed that the Henry constant and molecular weight of oils affected the emissions and that values of Henry constant multiplied by molecular weight gave an indication of the absorption of fuel into the oil.

Further investigation was undertaken by Ishizawa and Takagi (22) who ran a series of experiments with pistons in a lubricant free state. Their observations showed a significant difference the non lubricated piston generally emitted 1000 ppm less hydrocarbon emissions than lubricated pistons. It was concluded that this is due to fuel being absorbed into the lubricating oil. Some tests were carried out with different oil layer thickness although the thickness of the layer was only a qualitative comparison HC emissions were observed to decrease as the oil layer decreased. It was observed that blow-by decreased with the presence of oil due to the improved seal caused by the presence of oil, though emissions were not dependent on this.

With the development of a fast sampling valve mounted in the combustion chamber Yates (23) was able to analyse emissions during the combustion and expansion of the cycle. Reporting on the results Yates (24) discussed the high

levels of fuel (iso-octane) which were measured later in the expansion stroke. The valve was mounted in the cylinder liner above the area swept by the top ring. It was postulated that because this area was well oiled that the high level of fuel was being emitted from this oil and diffusing outward. Measurements further away from the wall showed lower levels at the same crank angle.

An investigation by Schramm and Sorenson (25) observed the effect of different oil viscosities on HC emissions. It was found that different oils did vary the emissions this was due to the difference in the fuels solubility into different oils this is defined by Henry's law.

Henry constant was approximated by the following equation.

$$H' = \frac{(R \times T)}{V_r \times M_i} \dots \dots \dots [3]$$

Where R is the gas constant, T temperature, V_r the specific retention volume and M_i the molar weight of the lubricant.

There have been several attempts to model this effect and these models are based on two controlling equations. These are:

The diffusion equation; conservation of gaseous fuel species.

$$\frac{dZ}{dt} - D_i \cdot \frac{d^2Z}{dx^2} = 0 \dots \dots \dots [4]$$

Where Z is mass fraction of fuel absorbed into oil layer. D_i is the diffusion coefficient, t and x are time and spatial coordinates.

Henry's law; the absorption of fuel vapour by the oil film,

$$x = 1/K \cdot P \quad [5]$$

Where x is the mole fraction in solution of species P is the partial pressure solute, K is Henry's constant

The model developed by Carrier et al (26) was based the model on the diffusion of fuel into and out of an oil layer of thickness x . It was observed that there was a strong link between the desorption of fuel and engine speed. This was thought to be more dependent on the oil temperature and thickness than directly to speed. The later model by Dent and Lakshminarayanan (27) was a comprehensive model bringing in crevice effects and post flame oxidation into the model to predict total hydrocarbon emissions. The basis of this model is the convective mass flux, which is dependent on both the diffusion and Henry's law. For the region i this was defined as;

$$dm/dt = \{ m''A_i + \rho \cdot Z \} m \, dA/dt \quad . . . [6]$$

Where dm/dt is the rate of change of fuel content of i , m'' is the convective mass flux, A is the surface area of i , ρ and Z are the density and thickness of oil layer, m is the mass fraction of fuel in oil in i , dA/dt is the rate of change of area i .

It was concluded that the trends shown by the model generally agreed with experiments made over a wide range

of engine operating conditions. The emissions were observed to decrease with an increase in speed, this was due the reduced cycle time to allow absorption and desorption to occur, increase in oil temperature also increases the Henry number thus reducing the fuel vapour absorbed, the temperature also increases with load. Another factor which affects the absorption of fuel is the oil layer thickness. Observations showed that the oil thicknesses should be kept to a minimum compatible with adequate lubrication.

The absorption /desorption effect has also been modelled by Korematsu (28). This includes many variables such as engine speed, load, AFR and oil layer thickness. The basis for this model was the diffusion equation.

This was developed to give an expression relating the mass of fuel emitted per unit of piston movement. Some results are shown from this model. This is then extended by inclusion into a synthetic model which also calculates cylinder pressure, inter ring gas pressure, oil layer thickness and fuel diffusion into oil. Further work was undertaken by Korematsu and Takahashi (29) to confirm this model. This was achieved with by experiment with the addition of oil onto the piston crown and comparing this with the results from an extended model to include this extra oil. The predictions were a satisfactory match with experiment and it was concluded that by these indirect means that this model was valid.

In an experimental investigation Gatellier et al (30) selected fuels and lubricants with combinations of high and low solubility. Two fuels and lubricants were chosen

for a series of tests which showed that hydrocarbon emissions were significantly affected by the solubility of the fuel-oil couple, lower solubility gives lower emissions. Using commercial gasoline with the two lubricants also showed some influence on hydrocarbon emissions. A further study with a single cylinder engine adapted for running with no lubricant was undertaken. The same link was shown with the selected fuels and lubricants when these were added after testing with no lubricant. Commercial gasoline showed a much smaller interaction with the lubricants. It was suggested that only 10% of hydrocarbon emissions could be accredited to absorption-desorption. However, this work was carried out at a fixed speed of 2000 rpm, previous investigations have shown a strong link to engine speed, absorption occurring at higher levels with lower speeds.

2.4 Modelling of Emissions

The modelling of combustion processes has been of interest for a long time and large amount of literature has been published on the subject. The following covers some of this literature as it relates to hydrocarbon emissions.

2.4.1 Models for Combustion and Hydrocarbon Emissions

One of the early developments in this field was made by Rassweiler and Withrow (31) using high speed photography of combustion and cylinder pressure measurement. The photographs enabled an empirical method of defining the

polytropic index (n) to be developed. From this the mass fraction burned could be approximated. This was compared with pressure data and pressure rise due to combustion.

The use of engine pressure data to model combustion has continued, Stone and Green-Armytage (32) compared an improved version of the Rassweiler model to a more complex two zone model. The simple model had only a single value for the polytropic index. The basis of the two zone model, unburnt and burnt gas zones, was the calculation of internal energy from pressure against volume data for each zone. The results of this comparison indicated only minor differences when predicting the times for 10, 50 and 90% mass fraction burnt. This difference was averaged at 2.18%. The similarity was probably due to the almost constant temperature of the burnt gas over the combustion process and so effects of heat transfer and dissociation are uniform over a major part of combustion. The more complex model could however yield more information on the combustion process.

A general model for combustion and hydrocarbon emissions was constructed by Lavoie and Blumberg (33). The combustion was modelled for elements within the chamber. Each element of charge has two regions, an adiabatic core and thermal boundary layer. The basis of the model is the 1st law of thermodynamics, and expressions are derived for internal energy, heat loss and work done. This fundamental model for combustion has formed the base for most of the subsequent models developed by other researches. However the predictions for hydrocarbon emissions are inaccurate because when published (1980) the sources of emissions were

seen as wall quench and crevice volumes.

A more recent model by Schramm and Sorenson (34) included crevice effects and absorption/desorption. The model predicted general trends for most engine variables. The decrease in hydrocarbon emissions with load were predicted. This was explained by the increase in oil temperature which reduces the absorption of fuel into oil, and an increase in post flame oxidation. However the crevice effect was simplified to account for just one major crevice this being the volume behind the top piston ring.

2.4.2. Modelling of post flame oxidation

The oxidation of hydrocarbons in the cylinder and exhaust ports of an engine has a large impact upon the tail pipe emission. It is thought that 50% of hydrocarbons which escape combustion are oxidised in the cylinder and exhaust ports. The study and modelling of the oxidation processes contributes to the understanding of the fate of unburnt fuel. A considerable amount of modelling has been done on this aspect of emissions research. Bascunana et al (35) used an exhaust gas reactor to study oxidation rates in the exhaust for CO and HC's. A more detailed model for oxidation in the exhaust port was developed by Caton and Heywood (36). The main observation from this was that oxidation was strongly dependent upon the bulk gas temperature and residence time in the exhaust port. The oxygen content has a lesser effect. The fraction reacted can vary between 9% and 38% depending upon speed and load.

conditions of the engine. The fraction oxidised increased with increasing speed and decreasing load. Using the fast sampling valve designed by Yates (22) the species during the combustion gases passage through the engine were investigated by Bennet et al (37). A large drop in total hydrocarbon emissions were observed between the cylinder and the exhaust port which was greater than the drop predicted by Caton and Heywood (36). The fuel species was observed to drop between the cylinder and exhaust port while the products of pyrolyses show a distinct rise.

2.5. Piston and Combustion Chamber Design

In a general discussion considering the improvements to engine efficiency which could be achieved by design solutions, Crouch et al (38) covered a large selection of possibilities. Many of these were improvements to the inlet and induction systems, variable valve timing or variable inlet geometry. Cold start improvements were also covered these suggestions concentrated on improving the coolant circuit and methods for reducing volume of oil involved in cold starting. Investigating the reduction of reciprocating and rotating mass by reducing mass of pistons and gudgeon pin indicated that a 4% reduction of friction mean effective pressure (fmep) could be achieved. This would improve fuel consumption by 2.5%.

2.5.1 Piston Design

Many aspects of piston design will affect hydrocarbon

emissions Kamp and Essig (39) investigated these, this investigation was for diesel engines and much of the discussion covered bowl design in the piston crown. There are two common points of interest, oil consumption and pressure balancing inter ring volumes. The impact of piston design on combustion in spark ignition engines was investigated by Gupta and Jiang (40). The use of bowls in the piston to promote squish from the sides of the piston, and thus increase the turbulence levels in the chamber. This did impact on the combustion and formation of pollutants, but no clear trend was commented upon or could be defined from the results presented. However, the objective of the paper was to report on a numerical analysis method.

The major friction loss in an engine is that caused by the piston-ring-cylinder interface and ring friction accounts for 75% of this. To reduce this Furuhamma et al (41) developed a two ring piston. This had other advantages of reduced piston mass and reduced piston height. This would be expected to improve power output and reduce fuel consumption. The problems associated with this were increased blow-by and oil consumption, these were discussed in a further publication Furuhamma et al (42). With the two ring piston it was observed that the temperature profile of the pistons were altered. The piston rings are the main route for heat flow from the piston, removing a piston ring increased the piston temperature. Modelling indicated that the temperature above the compression ring was decreased by moving the ring upwards, no comment on the possible effects on

emissions were made. Frank and Heywood (43) investigated the temperature effects on emissions in a stratified charge engine. This is a considerably different problem to normal homogeneous charge engines. However, the results of dropping the temperature had little significance to the overall hydrocarbon emissions. Slight increases in emissions were observed, but the control of piston temperature was achieved by the coolant temperature, this would affect the whole engine. The absorption of fuel in oil as discussed in section 2.3 is dependent on oil temperature on the cylinder walls which would also be affected by coolant temperature, this may account for the slight increase observed at lower temperatures.

2.5.2. Combustion Chamber Design

Another source of hydrocarbon emissions is from poor combustion. Efforts have been made to improve combustion by developing the combustion chamber design. One aspect of this is the use high air / fuel ratios, referred to as lean burn because more air is supplied than is necessary for stoichiometric combustion. Douaud et al (44) investigated the part load combustion with various shaped combustion chambers. They found that chamber geometry, heat state of spark plug, ignition energy, local physico-chemical and aerodynamic conditions can affect the start of ignition. It was observed that increase in burn velocity could indirectly improve combustion.

In an investigation into the development of lean

burn engines Benjamin et al (45) also tried a selection of combustion chamber designs. These were cylinder head designs with different valve configurations, the piston was flat topped.

Using a criteria of HC + NOx against specific fuel consumption, an open 4 valve design was chosen for further development because of better breathing and reduced pumping losses. A test engine was built and its performance mapped. It was concluded that this design could be further developed to give improved fuel economy and power while meeting emission control directives.

Benjamin et al (46) continued this development and were successful in running the engine at AFR's of 22:1. They investigated the in-cylinder flow of the engine and found the following characteristics.

- 1, Barrel swirl occurs during induction about a centre line perpendicular to the cylinder axis.

- 2, During compression barrel swirl vortex is enhanced due to conservation of momentum.

- 3, Towards TDC the vortex is distorted and therefore breaks down.

This leads to good mixing during induction and compression, and a stable condition for combustion. It was felt that further research in this area could significantly improve combustion characteristics. Similar work by de Boer (47) confirmed these conclusions. The development of lean burn engines has continued Fraidle (48) discussed three features of 4 valve lean burn engines which could be used to reduce emissions

and boost fuel economy. These were:-

- 1 Torque characteristics which show little variation across a wide range of engine speeds.
- 2 Emissions from engine are generally lower.
- 3 Good fuel economy .

Some possible methods of improvement were suggested these included, variable valve timing, variable intake systems and port throttling. This would give improved specific fuel consumption and allow higher rates of exhaust gas recirculation leading to lower emissions. The problems associated with lean mixture combustion are caused by the slower burning rates and are, increases in cyclic variability, partial burning and misfires. Hu et al (49) investigated methods for improving lean combustion by further enhancement of turbulence before combustion. Experiments were undertaken altering the inlet ports to affect the induced tumbling vortex. Increasing the vortex strength did improve lean combustion giving lower variability and improving the engines performance, hydrocarbon emissions increases slightly. This was thought to be due to early flame quenching causing incomplete combustion.

2.6 Cold starting of engines

An important area of emissions research is during the first few minutes of operation from a cold start. In this time fuel consumption and unburned hydrocarbon emissions are high also catalysts are not effective at temperatures

below 250 deg C. In measurements of thermal transients during a cold start Stone et al (50) observed that the wall temperature of the combustion chamber rises rapidly and approaches its equilibrium temperature.

Also cylinder pressure measurement indicated that imep was not affected by the cold combustion chamber. From this it was concluded that poor combustion during warm-up is not the source of high emissions or fuel consumption. However, the bmep increased with time showing that the fmep decreased as the engine warmed up. It was concluded that high engine fuel consumption is due to friction in the cold engine and poor mixture preparation. Similar findings were made by Andrews et al (51) and (52) and Sorrel and Stone (53).

The effect of cold starting on component temperature was investigated by Kaplan and Heywood (54). Modelling involved heat transfer from combustion and friction to calculate component temperatures. The hydrocarbon emissions from crevices were then calculated by taking in consideration the changes in crevice volume. The model gave expected results for temperatures and showed that the main route for heat transfer from the piston was through the piston rings. Also that the oil temperature lagged behind other component temperatures, because it gained heat only from secondary sources. Crevice volume calculations showed a strong link with temperature and the clearance against time differed depending upon the speed and load of the engine. The decrease in volume was quicker for higher speeds and loads. This was shown to have a substantial effect on hydrocarbon emissions. This model was not

compared against actual engine tests. However, a later investigation by the United Kingdom Engine Emissions Consortium (UKEEC) (55) used several test engines. Operating conditions were tightly controlled in a series of tests in which several causes of hydrocarbon emissions were investigated and their impact upon cold start emissions observed. A sealed crevice piston was developed for these tests. After 100 seconds from a cold start the emissions were reduced by 30%. This indicated that during cold starts the crevice volume is a significant source of hydrocarbon emissions. Another source of emissions was shown to be mixture preparation. Although other phenomena were investigated these were the most significant during cold start conditions.

The use of a hypothetical crevice volume developed by Hymas et al (17), was used to model the storage mechanism during a cold start by Brown and Woods (56). Samples were taken from the cylinder and exhaust port. Using propane as fuel and gas chromatography it was observed that from in-cylinder samples 95% was unburned fuel. It was also noted that no substantial oxidation occurred in the cylinder during first 15 seconds of engine operation. After 2 minutes of operation the storage mechanism resembled those of a fully warmed up engine. It was suggested that both fuel and products undergo the same processes of storage and release.

2.7. Hydrocarbon Speciation and Fuels

2.7.1 Hydrocarbon Species in Emissions

The emissions discussed previously have been hydrocarbons in general. However, the emissions contain a large number of different hydrocarbon species, some of which are more harmful than others. In a study of emissions from vehicles on the road by Bailey (57), some of the species identified were, ethylene, i-pentane, toluene, benzene, methane and acetylene. Gas chromatography has often been used as a research tool to identify the particular species emitted and also to observe whether emissions are unburnt fuel or combustion products. This has been used extensively, Daniel (58) was one of the first researchers to report on these investigations. Since this early work gas chromatography equipment has developed considerably.

Investigating fuel effects Dempster and Shore (59) used unleaded petrol and Trimethyl pentane to which varying amounts of toluene and benzene was added. Using modern equipment, which allows detailed resolution of hydrocarbons from C1 to C4 and analysis up to C8, 22 compounds were identified. The combustion products were the major fraction of hydrocarbon emissions although unburnt fuel was present. With the trimethyl pentane the emissions produced a large array of compounds, though fewer than with petrol as fuel. Variations were also shown with engine operating conditions.

2.7.2. Fuel Composition

There are three main types of hydrocarbon species found in fuel and emissions, these are;

- 1 Parafins (Alkanes) Single bonds between carbons.
- 2 Olefins (Alkenes) Some double bonds between carbons
- 3 Aromatics Based on a C6 benzene ring with alternate double bonds.

Oxygenates such as Aldehydes are also present. Increasingly the composition of the fuel is being studied for its impact on emissions, this has been encouraged by the advancement of catalyst technology and the need for continued reduction of vehicle emissions. The work covered in this section will give only a brief view of alternative fuels and their effect on emissions, because it is a major area of research on its own more suitable to chemical engineers. In a wide ranging report Koehl et al (60) reviewed several research projects covering a wide area of emissions research, of importance in this review was the investigation of NOx and HC emissions varying with fuel composition and the increasing importance of the aromatic content of fuel and emissions. The basic findings on these subjects are:

- 1, The effects of fuel composition on the mass of HC,CO and NOx are inconclusive because several parameters would vary simultaneously. For example variations in emissions with aromatic content may be attributed to the changes in distillation characteristics of the whole fuel.

- 2, The olefin (alkenes) fraction of exhaust emissions

are directly proportional to the sum of olefins and paraffins (alkanes) in the fuel. The C₂, C₃ and C₄ olefins are combustion products.

3, Aromatic emissions are proportional to aromatics in fuel, though benzene and toluene increase as a result of pyrolysis of heavier aromatics.

The aromatics were observed to vary with engine variables, Ninomiya and Biggers (61). The equivalence ratio has a considerable effect upon benzene and toluene both decreasing as this increases. Benzene in the exhaust also increases with increased toluene in the fuel. It was found that the levels of these aromatics in the exhaust is directly proportional to the total aromatics in the fuel.

Single component fuels from each of the three groups were used in investigation by Shore et al (62). The fuels used were 2,2,4, trimethyl pentane, 2,4,4-trimethyl pent-1-ene and toluene. General observations were that toluene gave higher levels of unburnt fuel and total emission than the other fuels, but gave the lowest post catalyst emissions. The composition of emissions from 2,2,4, trimethyl pentane and 2,4,4-trimethyl pent-1-ene were similar and consisted of mainly alkenes plus methane. However, the interaction between different fuel components in normal fuel may be different to using a single component fuel. The influence of fuel quality and composition was discussed by Booth et al (63) it was observed that the magnitude of fuel effects on emissions is much smaller than the changes achieved by changes in engine and catalyst technology. It was also pointed out that because of increased refinery processing required for

modified fuels the overall energy cost and production of CO₂ is much greater.

2.7.3. Alternative fuels

The use of methanol was reviewed by Kowalewicz (64). This fuel has many benefits over gasoline, it produces less soot, can be burnt at much leaner mixture levels which improves efficiency and reduces carbon monoxide hydrocarbon and nitric oxide emissions. However, it still requires energy to produce methanol, but this is less than that required for gasoline. Also if produced from biomass it does not contribute to the greenhouse effect.

The use of compressed natural gas as an engine fuel is being investigated for its impact on emissions and engine efficiency. In a wide ranging investigation Wallace et al (65) assessed the performance and durability of a natural gas fuelled van. The total hydrocarbons were significantly reduced due to improved fuel preparation and elimination of fuel enrichment during cold starts. The engine performance and emissions of a modern 4 valve engine were investigated by Jaaskelainen and Wallace (66) Significant reductions in the emissions were observed from natural gas. The absorption of fuel into oil layers on the cylinder wall are a major source of hydrocarbon emissions, one of the many factors which control this is the solubility of one hydrocarbon species into another. Natural gas has a low solubility in oil, poor vaporisation of petrol also leads to it being absorbed into the oil layer. This change in the fuel being absorbed accounts for the majority of the

reduced emissions.

2.8. Conclusion

Although it is difficult to compare levels of emissions from different papers with the many types of test engines and conditions used. It can generally be observed that significant reductions have been achieved, Booth et al (63) observed that in a six year period from 1983 emissions from vehicles were reduced by 50 to 60 %. The continuing rise in the number of vehicles counteracts this success.

From this survey it can be observed that there are three main sources of hydrocarbon emissions these being:

- 1 Fuel mixture being compressed into crevices, such as clearance volume between piston and cylinder, where it escapes combustion and then flows back into combustion chamber and to exhaust.

- 2 The fuel is absorbed in the lubricating oil layer on the cylinder wall during combustion, as cylinder pressure drops it is then desorbed so escaping combustion.

- 3 Bulk quench caused by poor combustion or mixture preparation especially at part load.

A lesser effect is the quenching of the flame as it approaches the combustion chamber walls, this is mostly oxidised later in the cycle.

It has also been observed that operating conditions of the engine affect hydrocarbon emissions. The emissions are reduced by increasing speed and/or load being most notable. Other variables which affect emissions are, ignition timing, air fuel ratio and operating temperatures. An

important source of hydrocarbon emissions is during cold starting where poor mixture preparation and high friction torque combine to produce poor engine operation.

Gas chromatography is contributing to this research by improving the understanding of combustion, post combustion oxidation processes and the affect of different fuels on emissions.

There are various means of reducing hydrocarbon emissions such as reducing crevice volumes controlling oil layers on the cylinder wall. Improving combustion characteristics will also reduce emissions, the lean burn technology being a viable method of achieving this. Some reduction in emissions can be achieved by the use of alternative fuels but the possible reductions are less than can be achieved by improvements to engines and catalysts. These fuels also have a greater energy demand for refining and processing.

With the previous research several models for predicting Hydrocarbon emissions have been developed, but the processes are usually dealt with in isolation especially the crevice effect and the absorption effect. The piston and liner has an affect on both these phenomena. These models tend not to deal with component specification especially for modelling the absorption effect. Several areas which require further investigation can be outlined.

1 The piston crevices are a source of hydrocarbon emissions. But this crevice region is formed from separate volumes, to reduce emissions further the most critical dimensions should be identified and controlled to minimise

flow back into the combustion chamber. These dimensions include the total top and second land volume and the ratio between the top land height and clearance.

2 The two main sources of hydrocarbon emissions linked to piston design are crevice volumes and absorbed fuel in oil layers. It has not been determined how much these contribute to total emissions and which is the dominant source.

3 What impact can the continued development of component specification have in achieving significant reductions in hydrocarbon emissions. Does the component specification effect the hydrocarbon speciation process.

3 EXPERIMENTAL

3.1 Test Rig Specification

The engine to be used in experimental work was mounted in a sound proof cell newly constructed for this type of research. The test engine and instrumentation was mounted to the designs and specifications described below Figure 3.1 shows the general layout of the engine and equipment.

3.1.1 The Engine

The test engine was a 1.4 litre 16 valve overhead cam Rover engine. The original throttle body injection manifold was adapted to a multipoint injection system. This engine is well suited to research because of its modular construction which eases dismantling and rebuilding and the installation of instrumentation and other alterations required for research. An important feature is that it had wet cylinder liners. This reduces the problems of liner distortion during bolting down of the cylinder head. It also allows the installation of new cylinder liners for each change of piston design. This helps ensure consistent starting conditions for each change of piston design and the possibility of changing the cylinder liner specifications.

The engine was coupled to a Schenk eddy current dynamometer, operated with a constant speed setting which allowed torque to be controlled by the throttle setting.

The engine was controlled by an engine control unit, ECU. This monitored engine speed, throttle position, manifold depression and coolant and inlet air temperatures. From this information the ECU controlled the fuel injector duration and ignition timing to settings from the engine control programme, a schematic diagram of these inputs is given in Figure 3.2. Modifications to the programme and wiring system enabled external control of air fuel ratio and ignition timing. Adjustments were made by connecting potentiometers to the inputs for the coolant and air temperature sensors. Air fuel ratio was controlled by air temperature sensor and coolant temperature controlled the ignition timing.

3.1.2. Exhaust Gas Sampling

Stainless steel pipes were fitted to the exhaust manifold to take samples from the exhaust port of each cylinder. To ensure that a representative sample was obtained for each cylinder the sample was taken from the centre of the port and facing into the flow. The sample pipe ended level with the joint between manifold and cylinder head this ensured that sample was taken from the same distance from exhaust valves of approximately 120mm, this is shown in Figure 3.3. A sampling point was placed in the main exhaust pipe also from centre of pipe facing into the flow. Thermocouples were mounted at each sample point to record exhaust gas temperature. The sample pipes were brought together and passed through a heated line to the analysers. This prevented the loss of sample by its being

dissolved into condensate which would form in a cool sample line. A series of valves at each end of this line enabled the choice of sample and analyser to be made, Figure 3.4. The sample circuit was purged regularly with compressed air. Exhaust gas samples were sent to the following instruments;

Multi-gas Analyser for CO₂, CO, O₂, NO_x and HC (NDIR).

Gas Chromatography to analyse HC species.

3.1.3. Lubrication scheme

In a series of tests it was planned to lubricate the cylinder head with a different lubricant than the base of the engine. A method of separating the cylinder head lubrication from that of the crank shaft and pistons was designed and implemented. The engine has an aluminium engine block. To reduce weight long high tensile bolts pass through the cylinder head, engine block and bearing rail to take the tensile load. Clearance around these bolts provide passage for crank case gases, blow-by, into the cylinder head and returning oil into the sump. Small inserts were machined and fitted to the cylinder head and block where the bolts passed through. This allowed sufficient clearance for the bolts alone. A seal was achieved with "O" rings, Figure 3.5. The lubricant could be fed from an external pump unit or via external piping from engine lubrication pump. Figure 3.6. The lubricant used throughout the engine is a CEC reference oil (RL-139/4) unless otherwise stated, the specification is given in Appendix 5

The alterations to the lubrication scheme required the external routing of crank case gases, blow-by. A circuit was designed to enable measurement of this gas flow or route it back into the engine inlet. The gas flow was measured by rotameters. To even out the flow a small surge tank was installed in the pipe line, together with a trap to catch oil and moisture.

3.1.4. Fuel scheme

Fuel flow was measured by timing the flow of a known volume. Fuel temperature was checked to allow for variations in fuel density with temperature.

In any combustion process the fuel is important. Throughout this research programme two fuels were used. The main fuel was a reference fuel, unleaded petrol (CEC RF-08-A-85). A second fuel was used this was 2.2.4. trimethyl pentane, often referred to as iso-octane which is a C_8H_{18} hydrocarbon. Specifications for both fuels are given in Appendix 5. The fuels were stored under low pressure nitrogen to prevent evaporation.

It was possible to change over from petrol to this fuel and back again whilst the engine was running. A system was designed to enable fuels to be switched. This included separate tanks and pumps and a valve system to prevent contamination of one fuel by the other, Figure 3.7, shows the circuit diagram.

3.1.5. Pressure Transducers

Piezoelectric pressure transducers were mounted

into the cylinder head for measuring combustion chamber pressures. They were flush mounted to reduce the creation of extra crevices. The mounting scheme was supplied by Rover Group.

3.1.6 Temperature Measurement

Temperature measurement were taken at all exhaust gas sampling points, cooling water on entering and leaving the engine, intake air at the laminar flow meter and in the manifold, and sump oil. The thermocouples were K type, and the data was plotted by chart recorders. These temperatures provided an accurate check on the operation of the engine, for correct setting of timing and other parameters and fault diagnosis.

3.1.7. Air Flow Measurement

Air flow into the engine was measured a by laminar flow meter. A plenum was used to damp out any dynamic fluctuations and the system was calibrated against a standard B.S. flow meter.

3.2. Exhaust Gas Analysis

3.2.1. General Emissions

Exhaust emissions were measured using a Richard Oliver Multigas Analyser. This measured the levels of the major pollutants by several methods:-

A non dispersive infra-red system analysed carbon dioxide, carbon monoxide and total hydrocarbon (propane). Each gas had a dedicated analyser. Nitric Oxides measured by a chemiluminescent analyser

This equipment was calibrated with two gas mixtures;

1 Tri-blend, CO₂ 16%, CO 8%, and propane 1600 ppm, nitrogen balance.

2 NO₂ 4000 ppm, nitrogen balance.

This system had a programmed calibration procedure. In addition further checks were also made. Sampling from the engine whilst it was not in operation gave a check on any retained sample from previous tests. This test was carried out daily before starting the engine, and usually gave readings of approximately 5 ppm. Calibration gas was also fed to the sample line at the engine and readings checked to ensure that the sample was not lost or contaminated.

3.2.2 Gas Chromatograph Procedures

A description of the gas chromatograph and its operating methods are set out below.

The sample was carried to the gas chromatograph through a heated sample line without being diluted or filtered. A Perkin Elmer 8600 GC was used with a wall coated open tubular column, the stationary phase being, CP-Sil-5 CB, column length 50m and inside diameter 0.32 mm. This equipment gave good resolution of a wide range of hydrocarbons from C1 to C9. The method used is described in Table 3.1.

Table 3.1. Gas Chromatograph Method

Temperature Programme

	Temperature 1 = 30 (deg C)
	Iso time = 2 minutes
	Ramp 1 = 4 (deg C/minute)
	Temperature 2 = 200 (deg C)

Injector Temperature	100 (deg C)
Detector Temperature	250 (deg C)
Carrier Gas	Helium
Flow Rate	1 (ml/minute)
Injector	Automatic heated gas sampling valve with 0.1 ml sample loop
Detection	Flame Ionisation Detector

The compounds separated with the method above from a sample of exhaust emissions required identification, three different methods were used;

1 Calibration gases, Mixtures of lighter hydrocarbon compounds of known concentration were readily available. These could be analysed by a separate run of the gas chromatograph or mixed with the emission sample. The retention times of the sample were then compared with the calibration mix. The drawing up of a retention index enabled prediction of unidentified compounds.

The retention times of n-alkanes, ie straight chain molecules, are proportional to the number of carbon atoms. For the index n-alkanes are given values in multiples of a hundred dependent on the carbon number. These values are plotted against the retention time. From this graph the retention index number for other compounds can be found. The compound can be identified from published tables of retention indices, Matukuma (67). The identity of these compounds were then confirmed by calibration with a sample

of the particular compound.

2 Gas chromatography with mass spectrometry. This produced a table of possible compounds for each peak by matching their characteristic emission spectra with that obtained from the sample. Each possible compound was listed with the percentage accuracy of its fit with the actual sample. There was usually an approximate 90% probability of the sample being the compound selected.

Also by comparison with other research on similar engines, Wallace and May (67) have also undertaken the identification of hydrocarbon species from the Rover K16 engine.

The various methods for identifying the hydrocarbon species are not totally reliable, because other similar compounds could have the same retention time. A peak could be another compound or a mixture of similar compounds. This uncertainty increases with increasing retention time. For lighter hydrocarbons with few isomer variations the identification is reliable. The higher the number of carbon atoms in a compound there is a larger number of isomeric variations and other compounds of a similar size. Having performed the identification from three methods the probability that the peaks are correctly identified is approximately 90%.

The flame ionisation detector connected to the gas chromatograph gives an output proportional to the carbon atoms present. The actual amount of a particular compound, was found by dividing the carbon atoms detected by the number of carbon atoms in that compound. The constant of

proportionality could be found from the calibration gases. The data processing of the GC also calculated the relative quantity of each compound as a percentage of the total area of the GC plot.

3.3 Operating and Test Procedures

3.3.1 Test Procedures

As part of the preparation for engine testing, the procedures had to be planned to ensure the required data was recorded and consistent conditions obtained for each test. The test points at which the engine would be set for steady state tests were first identified. System checks and lists of required readings could then be planned. A computer spread sheet was design for entering readings. This set out the order for taking results, would form a test routine and also ensure that all readings were recorded.

Table 3.2 Test Points

Test ID	Speed(RPM)	Torque(Nm)	bmep(bar)
A	1500	11.1	1.0
B	1500	29.1	2.62
C	2000	22.2	2.0
D	2500	61.1	5.5
E	3500	Wide Open Throttle	

The tests were to be run at steady state, the engine set at five speed and load settings. This allowed a sufficient range of speeds and loads to cover the engine's capabilities, Table 3.2. These test points were chosen from those used by manufacturers for research, to allow some

comparison with other research.

The ignition timing was optimised for each test point by observing peak cylinder pressure and torque. Although the ignition advance varied peak pressure occurred between 13° and 15° ATDC. Advancing ignition any further created detonation in the engine. Retarding ignition caused a drop in peak pressure and torque. The setting of the potentiometer was recorded and it was observed that this was repeatable between tests. The air fuel ratio was set at 15:1 using the Multigas analyzer. This was slightly lean of the stoichiometric value of 14.2:1 for the reference petrol, this gave an equivalence ratio of 0.95. A graph of hydrocarbon emissions against air/ fuel ratio, Figure 1.1, shows that the level of emissions are least sensitive slightly lean of stoichiometric. Careful adjustment was required to obtain correct torque and air fuel ratio settings. Inlet manifold depression, exhaust gas pressure were checked with manometers to ensure consistent conditions. Before taking readings the engine operating conditions were allowed to stabilise.

Exhaust samples were taken from the exhaust pipe below the manifold, and from the exhaust port of each cylinder simultaneously. Separate samples were also taken at the exhaust port of each cylinder. These samples are referred to as ALL, ALL4 and 1,2,3,4, respectively. The schematic for testing at each test point is set out in Table 3.3.

Table 3.3. Test Schematic

Sample Point	Fuel	
	Petrol	Trimethyl pentane
Exhaust pipe (ALL)	THC, GC,	THC, GC,
Cyl 1	THC, GC,	THC, GC.
Cyl 2	THC	THC
Cyl 3	THC	THC
Cyl 4	THC	THC
All 4	THC, GC	THC

THC = Total hydrocarbons
GC = Gas chromatograph

3.3.2. Engine Preparation

Careful preparation was required to ensure repeatable engine operation from each test. At the completion of a test, after dismantling the engine was cleaned carefully to remove deposits from combustion chamber. All valves were lightly reground to ensure they sealed correctly.

Before the commencement of the steady state tests after rebuilding the engine a running-in period was given. This ensured that piston rings and liner had worn to a stable surface finish. This period was carefully controlled with a planned schedule of operating speeds and loads, Table 3.4. This allowed for emissions testing to monitor emissions of the engines early life.

The health and safety aspects of these experiments were also considered. During the first series of tests

levels of noise and poisonous emissions were monitored in the laboratory. Safe operating procedures were adopted in consultation with the university safety officer.

3.4. Data Handling

3.4.1. Engine and Emission Data

Data from these experiments were entered onto two computer spread sheets, enabling all the calculations to be performed automatically.

1 Engine data; engine performance information, brake mean effective pressure (bmep), brake power corrected for ambient conditions, specific fuel consumption (sfc), air and fuel flow rates, physical air fuel ratio and volumetric and thermal efficiency.

2 Emission data, with the transfer of specific fuel consumption to this file specific emissions of carbon monoxide, nitric oxide and hydrocarbon were calculated in units of g/kWh.

Further spread sheets were used for analysis to produce statistical information. From this data from eight steady state tests could be given as an average, the variance of this data was taken as plus and minus one standard deviation about the average. The graphs of this data are in this format.

Details of the calculations can be found in Appendix 1.

3.4.2. Cylinder Pressure Data

The pressure transducer in the cylinder head was linked to an AVL 646 high speed data acquisition system, triggered by a shaft encoder fitted to the crankshaft, enabling combustion pressure to be defined with respect to crank angle. The software allowed the average of several cycles to be calculated and stored on computer disc for later analysis.

Table 3.4 Running-in Schedule

Torque (Nm)	Speed (rpm)	Duration
DAY 1		
Warm up 15	1500	10 minutes
31	1875	30
Emission test		100
31	2800	30
31	3750	30
62	4475	30
Emission test		
Engine off		
DAY 2		
Warm up 15	1500	10
93	4375	30
WOT	2500	30
WOT	3750	30
Emission test		
Engine off		
DAY 3		
Warm up 15	1500	10
62	5000	30
93	6250	30
WOT	4675	30
Emission test		
Engine off		
DAY 4		
Warm up 15	1500	10
WOT	5625	30
WOT	6250	30
Emission test		100
Engine off		

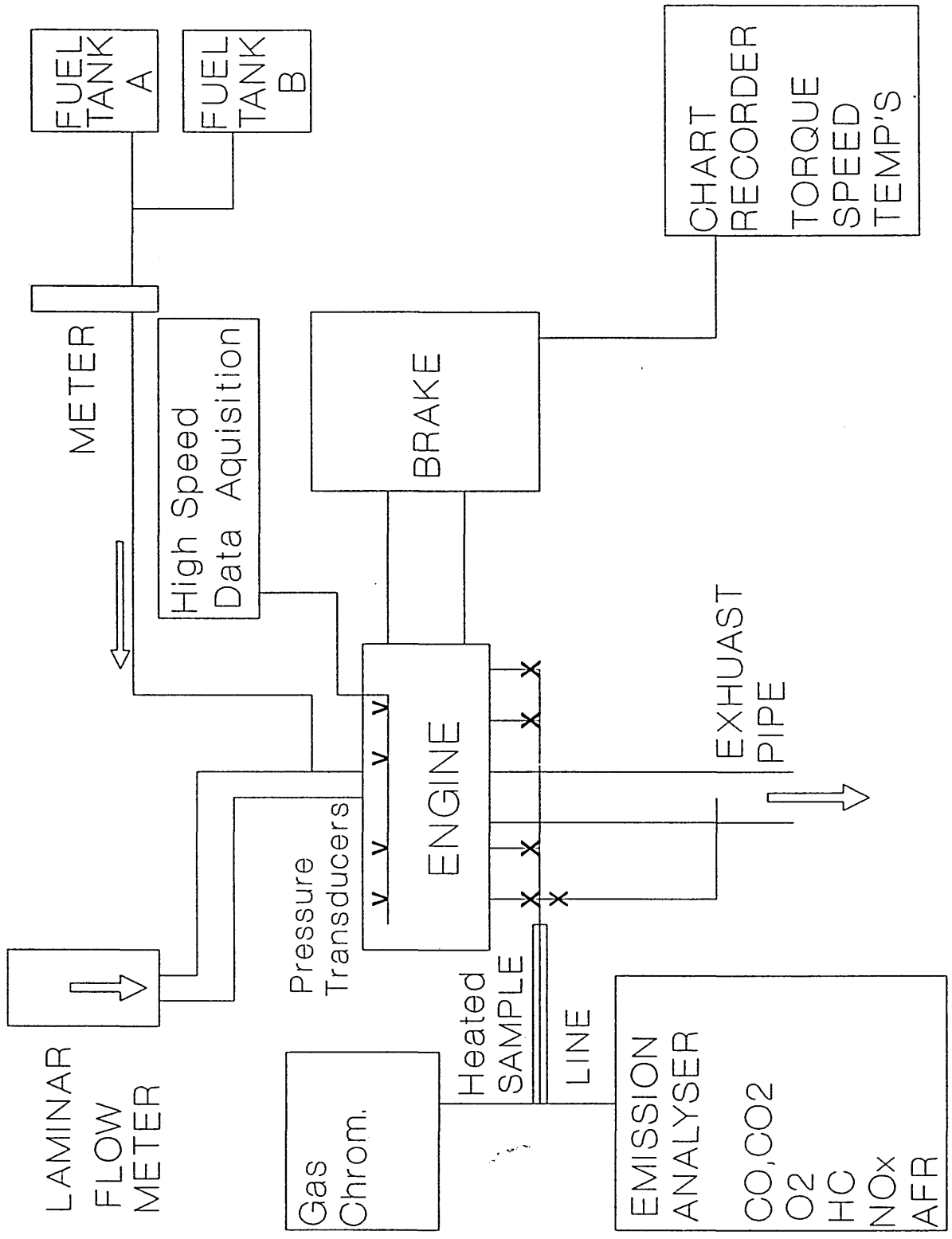


Figure 3.1 Schematic Layout of Engine Test Equipment

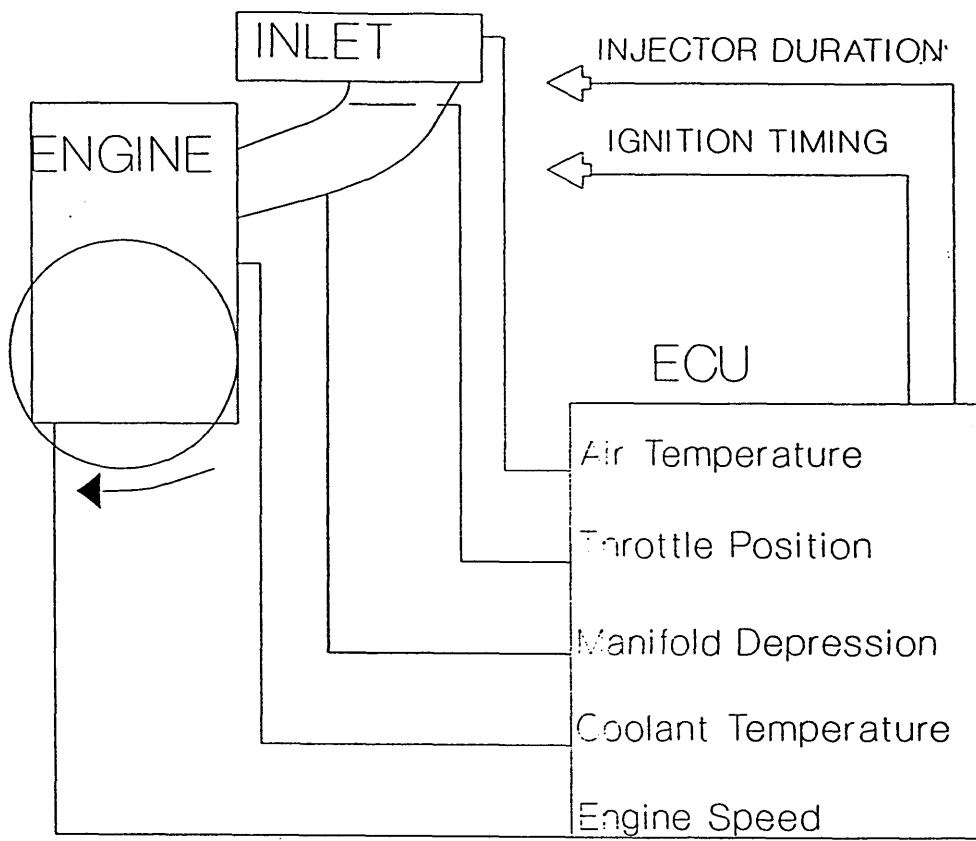


Figure 3.2 Inputs for engine control unit

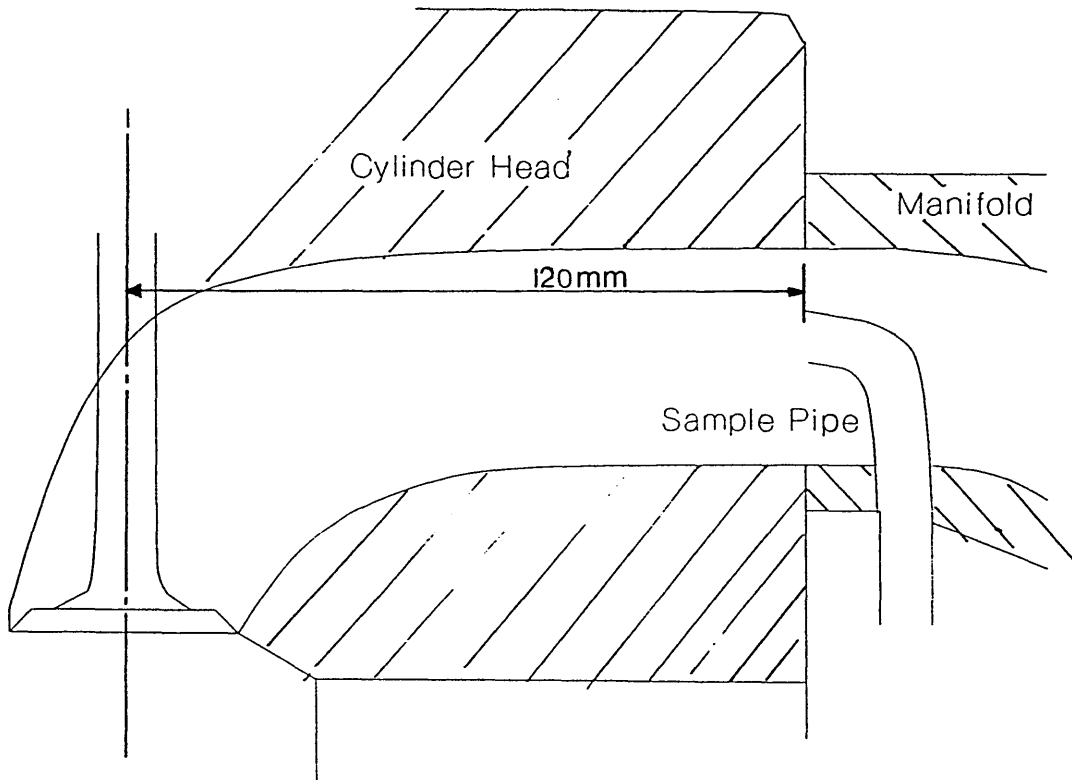


Figure 3.3 Sketch of exhaust port showing position of sampling valve

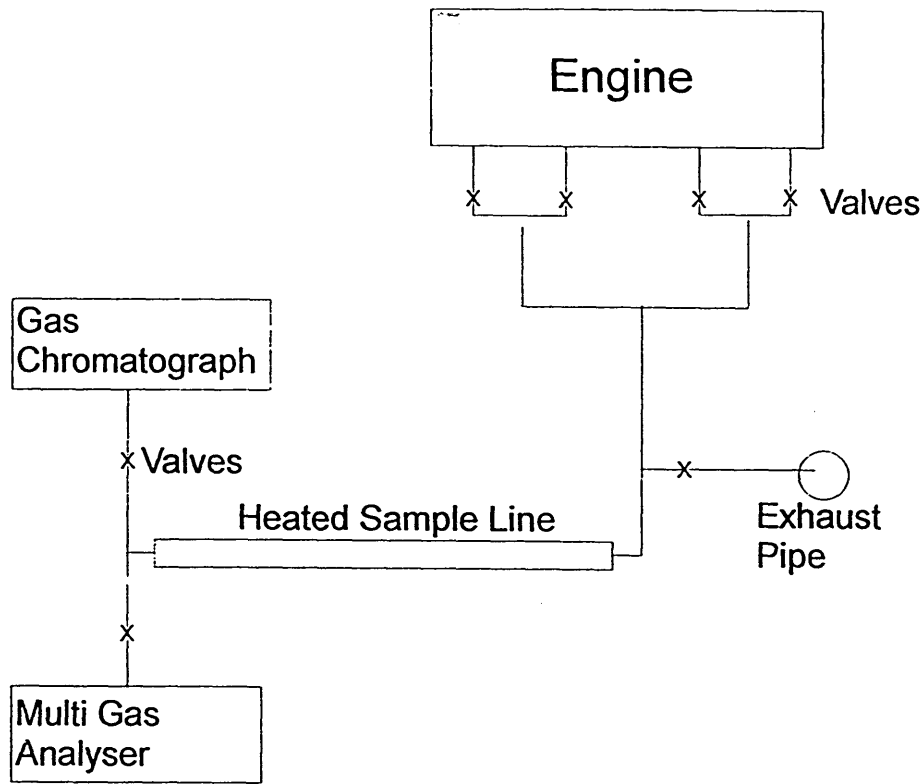


Figure 3.4 Exhaust emissions sampling circuit

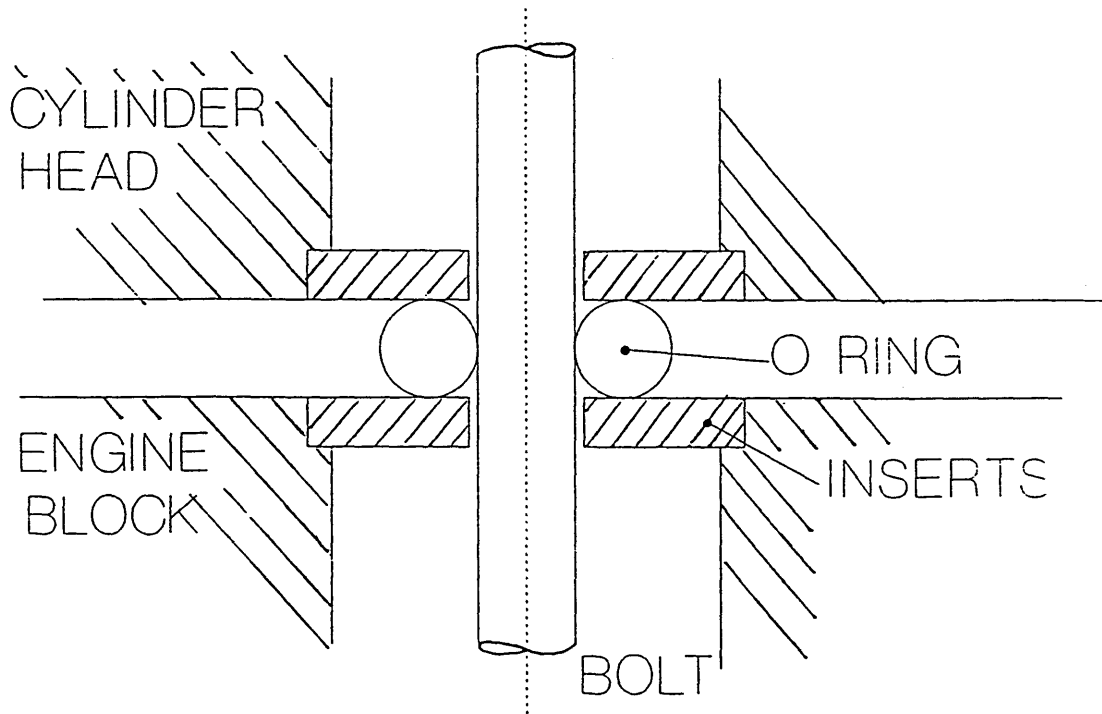


Figure 3.5 Scheme from Sealing Cylinder Head Bolts

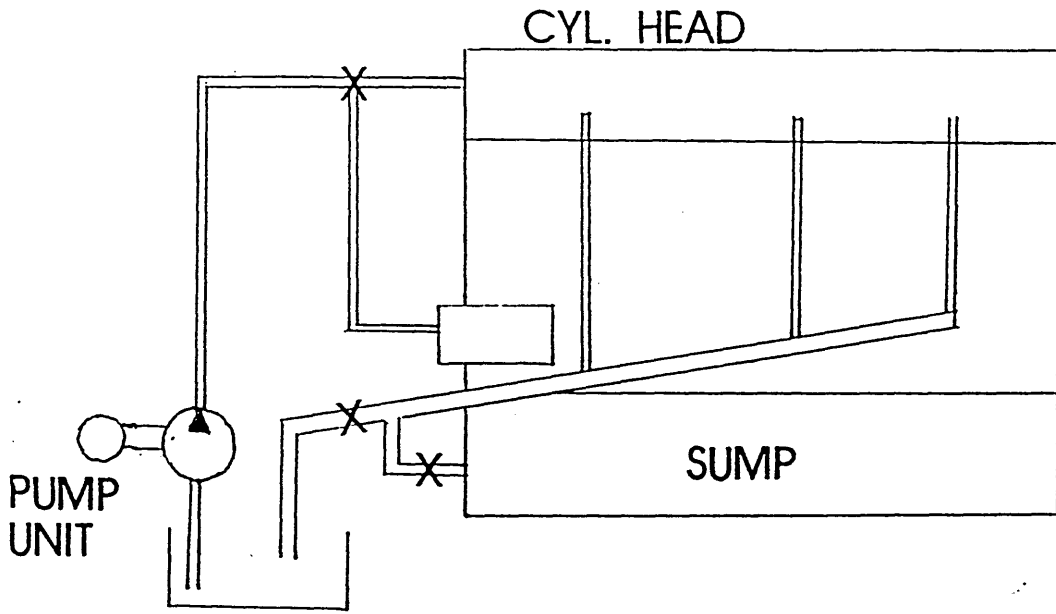


Figure 3.6 External Lubrication Circuit for Cylinder Head

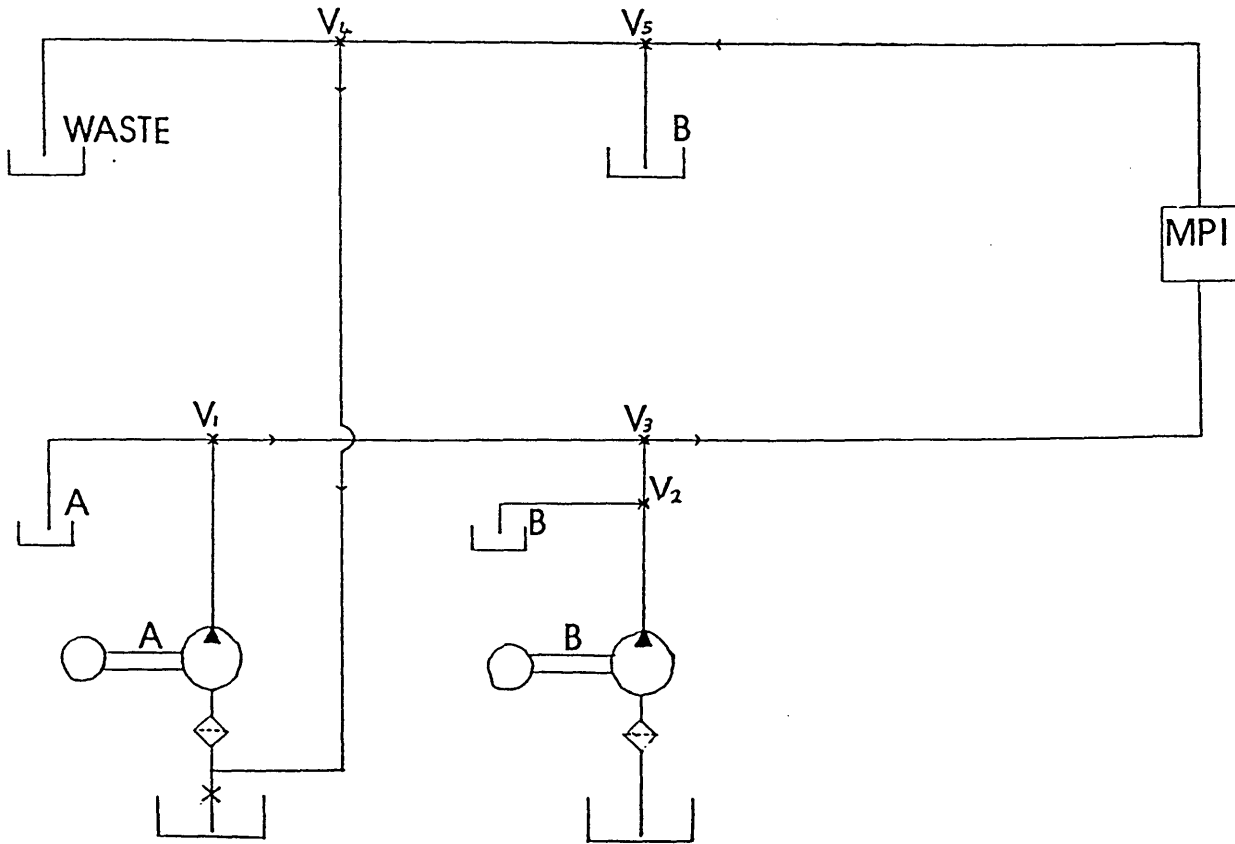


Figure 3.7 Dual Fuel Circuit

4. THEORETICAL

4.1. Introduction

To develop the theoretical basis for the model to predict changes in hydrocarbon emissions from piston design, only those formation mechanisms related to piston features are considered. The origins under consideration are, crevice flow from piston lands and ring grooves and absorption and desorption of fuel from cylinder liner wall. A basic analysis of combustion and oxidation processes must also be included as these have an impact on the sources being considered. The flow chart for the whole set of calculations is given in Figure 4.1.

Table 4.1 Source of assigned values

Term	Obtained from
Piston Dimensions	Measured before tests (cold)
Liner Dimensions	" " " "
Ambient air Condition (pressure, humidity and temperature)	Obtained from tests
Air at inlet port (manifold depression and temperature)	" " "
Engine speed/load	" " "
Cylinder pressure	" " "
Piston and liner temperature	Assumed from literature

4.1.2 Data Required for Calculations

For these calculations there are many terms which must be assigned values. There were three methods of achieving this. Measurement of components before testing, measurement

during engine tests and approximations from published literature. These are set out in Table 4.1

4.2. Piston Crevice Volume Effects

The piston-cylinder crevice volumes have been shown to be a major source of hydrocarbon emissions by several researches. Some of these researches have produced models to predict emissions, with varying degrees of complexity, these are discussed in the literature survey. The basis of this study is the top land volume, which can be seen as two inter-linked volumes, top land and the volume behind the top piston ring. Flow into and out of the 2nd land through the ring gap is included. The computer programme for these calculations uses pressure data per degree crank angle. Figure 4.2 is the flow chart for crevice flow calculations, a listing of the computer programme is given in Appendix 2.

Assumptions

All piston and cylinder dimensions are based on cold components.

The piston is always positioned centrally in the liner
All gases entering piston crevices are unburnt mixture
Fuel/air mixture is homogeneous and behaves similar to a perfect gas.

The flow of gas is isothermal

The gas temperature is equal to piston temperature and is constant during steady state operation.

Piston rings remain on base of ring groove

Blow-by is ignored.

4.2.1. Top Land Flow

The calculation of flow into and out of the top land crevice volume is based on the gas laws, mixture flows into this region as it is compressed by increasing pressure.

$$\text{From } PV_C = \frac{m_C R_o T_p}{M_r}$$

$$m_C = \frac{PV_C M_r}{R_o T_p}$$

Where P = Cylinder pressure N/m^2
 V_C = crevice volume m^3
 m_C = mass of mixture in crevice kg
 M_r = Mol weight of mixture
 R_o = Universal gas constant kJ/kg K
 T_p = Piston temperature K

In differential form

$$\frac{dm_C}{d\theta} = \frac{V_C M_r}{R_o T_p} \frac{dP}{d\theta}$$

$$dm_C = \int_{P_2}^{P_1} \frac{V_C M_r}{R_o T_p} dP$$

$$dm_C = \frac{V_C M_r}{R_o T_p} (P_1 - P_2) \dots \dots \dots [1]$$

Equation 1 is the change in mass per degree crank angle for a mass flow rate;

$$m = \frac{V_c M_r \cdot N \cdot 6}{R_o T_p} (P_1 - P_2) \quad (\text{kg}) \quad \dots \dots \dots [2]$$

+ive flow out of crevice volume
-ive flow into crevice volume

4.2.2. Flow into Ring Groove

From Kue et al (15) the flow into this region is treated as an isothermal compressible flow through a narrow channel.

$$\left(\frac{m}{A}\right)^2 = \frac{P_u - P_d}{RT \left[\frac{4fW}{D} + 2 \ln \left(\frac{P_u}{P_d} \right) \right]} \quad \dots \dots \dots [3]$$

For laminar flow $f = 24/Re$ and $Re = \frac{m \cdot D}{A \mu_{gas}}$

Generally $2 \ln(P_u/P_d) \ll 4W/D$

So Eq [3] reduces to;

$$\left(\frac{m}{A}\right) = \frac{h^2}{24W\mu_{gas}RT_p} (P_u - P_d) \quad \dots \dots \dots [4]$$

where h = channel width m

W = channel length, ring width m

P_u and P_d = pressure upstream and down stream N/m^2

D = hydraulic diameter = $2h$

$$\mu_{gas} = 3.3 \times 10^{-7} \times T^{0.7} \quad \text{Ns/m}^2$$

4.2.3. Flow into 2nd Land Crevice

The flow into 2nd land is based on incompressible flow through an orifice. From Bernoulli's equation and Continuity of mass;

Bernoulli eq'n.

$$\frac{(P_2 - P_1)}{\rho} + \frac{(C_2^2 - C_1^2)}{2} + g(Z_2 - Z_1) = -w_s - w_f \quad [a]$$

Note No w_s and no significant change in height $Z_2 = Z_1$

Neglect friction, assume no change in ρ

Continuity eq'n

$$\rho_2 C_2 A_2 = \rho_1 C_1 A_1 \quad [b]$$

$$\frac{P_2}{\rho} + \frac{C_2^2}{2} = \frac{P_1}{\rho} + \frac{C_1^2}{2}$$

$$C_1 = C_2 \frac{A_2}{A_1}$$

$$\text{Let } \frac{A_2}{A_1} = k$$

Thus

$$\frac{C_2^2}{2} (1 - k^2) = \frac{P_1 - P_2}{\rho}$$

$$C_2 = \left[\frac{2(P_1 - P_2)}{\rho(1 - k^2)} \right]^{\frac{1}{2}}$$

$$\text{but } V = CA$$

$$V = A_2 \left[\frac{2(P_1 - P_2)}{\rho(1 - k^2)} \right]^{\frac{1}{2}}$$

$$\text{also } m = \rho CA$$

$$m = A_2 \left[\frac{2(P_1 - P_2)}{\rho(1 - k^2)} \right]^{\frac{1}{2}}$$

Including a coefficient of discharge gives

$$m = C_d \cdot A \left[\frac{2(P_1 - P_2)}{(1 - k^2)} \right]^{\frac{1}{2}} \quad [5]$$

Where C = velocity m/s
V = volume flow m³/s
A = area of ring gap m²
P₁ = pressure at ring gap N/m²
m = mass flow rate kg/s
k = area ratio ring gap/crevice area
C_d = coefficient of discharge = 0.86

The pressure in the 2nd land is then calculated;
from gas laws

$$P_2 = \frac{m_2 R_0 T_p}{M_r V_2} \quad [6]$$

4.2.4. Test Calculations

A series of computer runs of the above calculations were made to demonstrate the effect of various piston dimensions on crevice flow, results from calculations using actual piston dimensions are discussed in section 5.2.

The pressure profiles for the three regions are shown in Figure 4.3, the ring groove pressure closely follows the cylinder pressure peaking at the same magnitude but with a lag of 2° crank angle. The lag is constant through the cycle. The 2nd land pressure peaks considerably later in the cycle at approximately 50° ATC, but with a much lower magnitude. An overlap of 2nd land pressure occurs until the

pressures stabilise. The flows caused by these pressures are shown in Figure 4.4 the main crevice flow is from the top land and peaks at approximately 25° ATC. Flow from the ring groove peaks at a similar time and is approximately a fifth of the top land flow.

A further series of computer runs were performed with varying piston dimensions. The main variables are; piston top land diameter, top land height and extra 2nd land volume.

4.2.4.1 Top Land Dimensions

Reducing the top land volume has a significant effect on the top land flow, and changing either the piston ring height or piston diameter had a similar effect on the flow, Figure 4.5 shows the total flow into the crevice volumes the flow being proportional to the top land volume.

The changes to the top land diameter has an affect on the flow into the 2nd land, because of the effect on the top ring gap area. This was shown with calculations changing the ratio between top land height and diameter keeping a constant volume. Figure 4.6 shows the pressure profiles for the 2nd land, demonstrating the lower pressure due to increasing piston diameter. The impact this has on flow can be seen in Figure 4.7 where flow into and out of 2nd land is reduced with increasing diameter. The timing of the flow back into the top land is also altered occurring approximately 10° later. The impact on total crevice flow is shown in Figure 4.8, where the small changes to back flow from 2nd land crevice occurs at approximately 50° ATC.

4.2.4.2. 2nd Land Crevice Volume

The changes to 2nd land volume have no effect on the top land volume, but has a significant effect on 2nd land pressure and flow. Increasing volume reduces the pressure Figure 4.9 and changes the flow profile, Figure 4.10. The flow into the region is not affected, but the lower pressure with increased volume reduces the return flow. The changes to second land flow has little effect on the total flow, Figure 4.11.

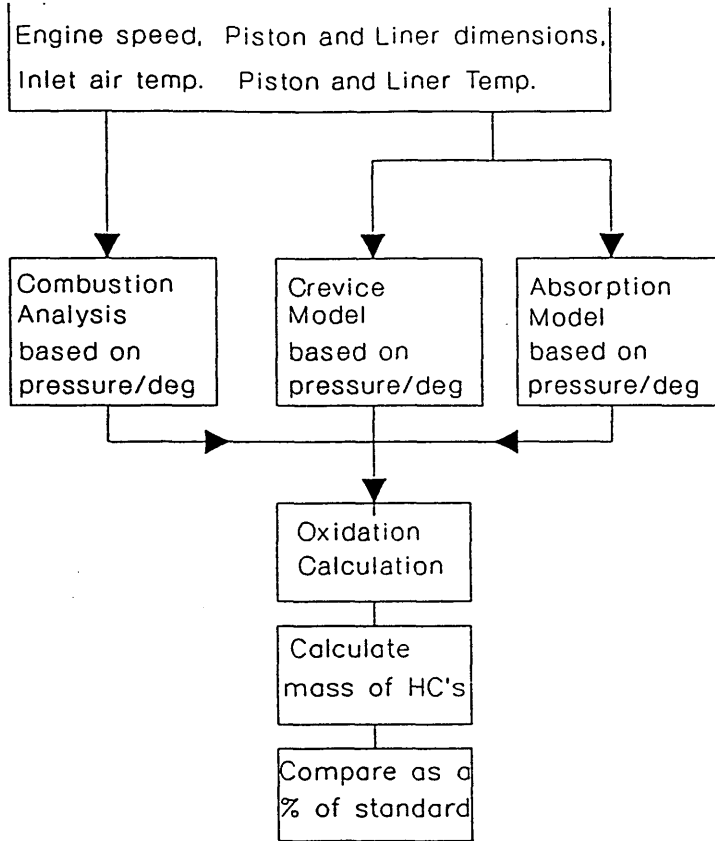


Figure 4.1.a. Flow chart for prediction of hydrocarbon emissions

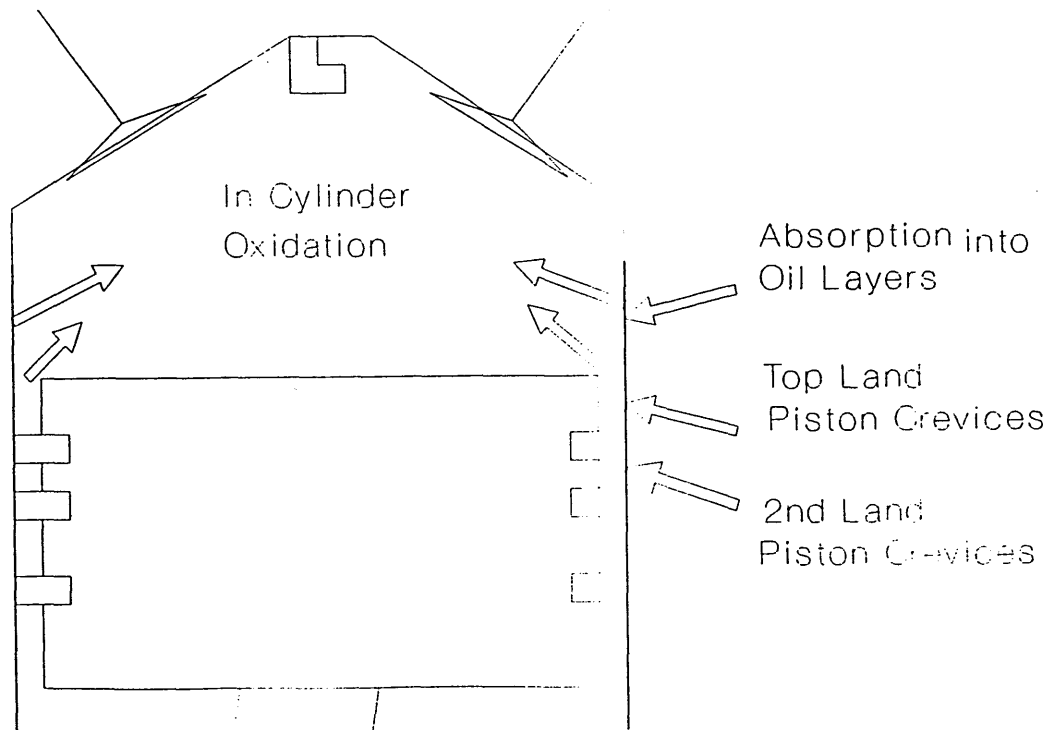


Figure 4.1.b. Sources of hydrocarbon emissions included in model

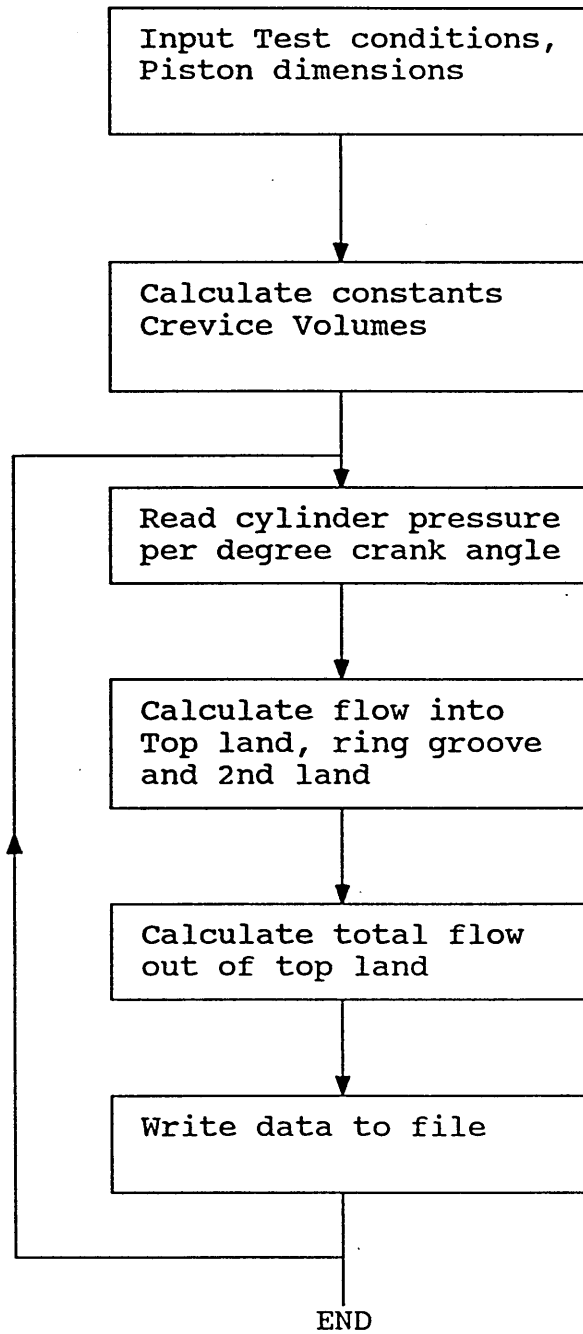
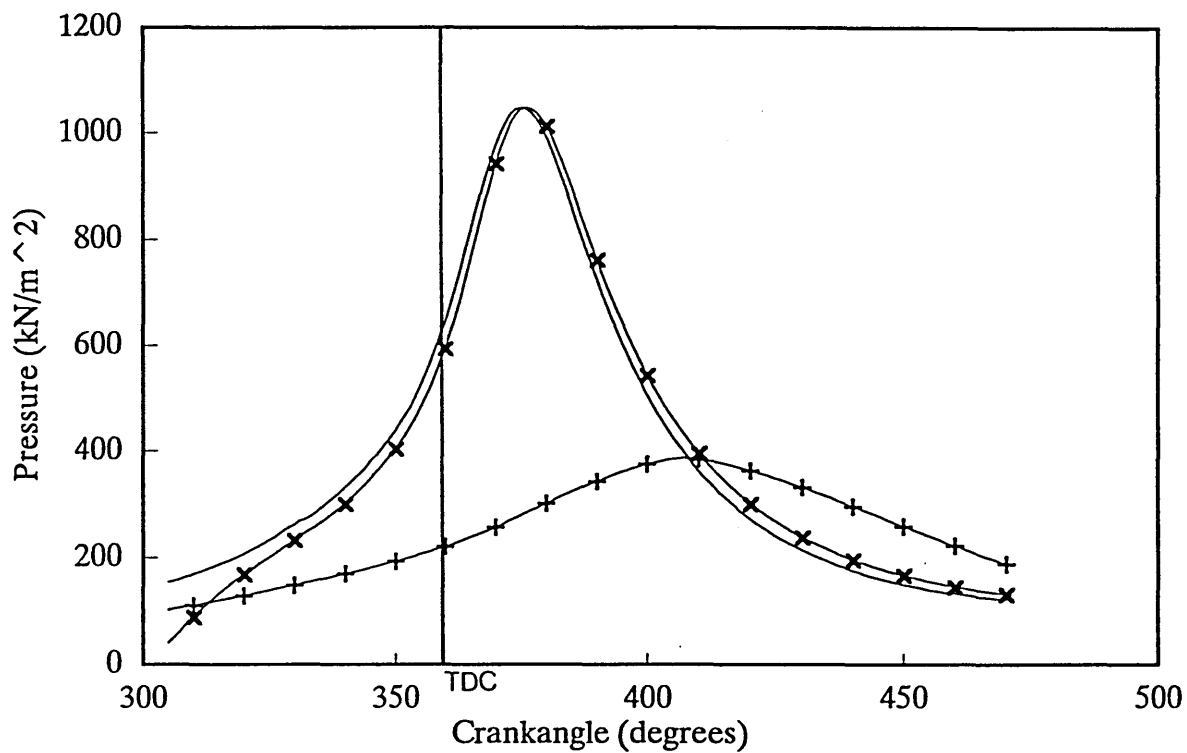
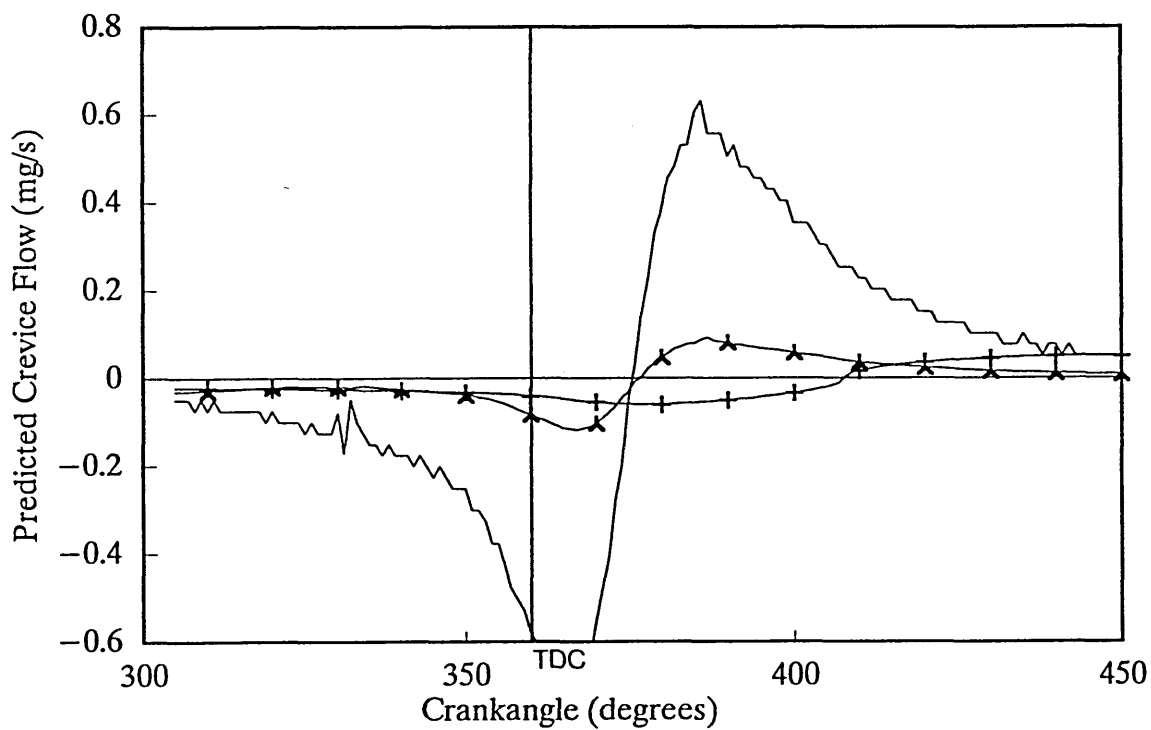


Figure 4.2 Flow Chart for Crevice Model



— Cylinder Pressure x Ring Groove Pressure + 2nd Land Pressure
 Figure 4.3 Actual Cylinder pressure and predicted ring groove and 2nd land pressure profile, Standard Piston, 1500 rpm 1 bar bmep



— Top Land + 2nd Land ^ Top ring groove
 Figure 4.4 Predicted flow profiles from piston crevice regions
 Standard Piston, 1500 rpm 1 bar bmep

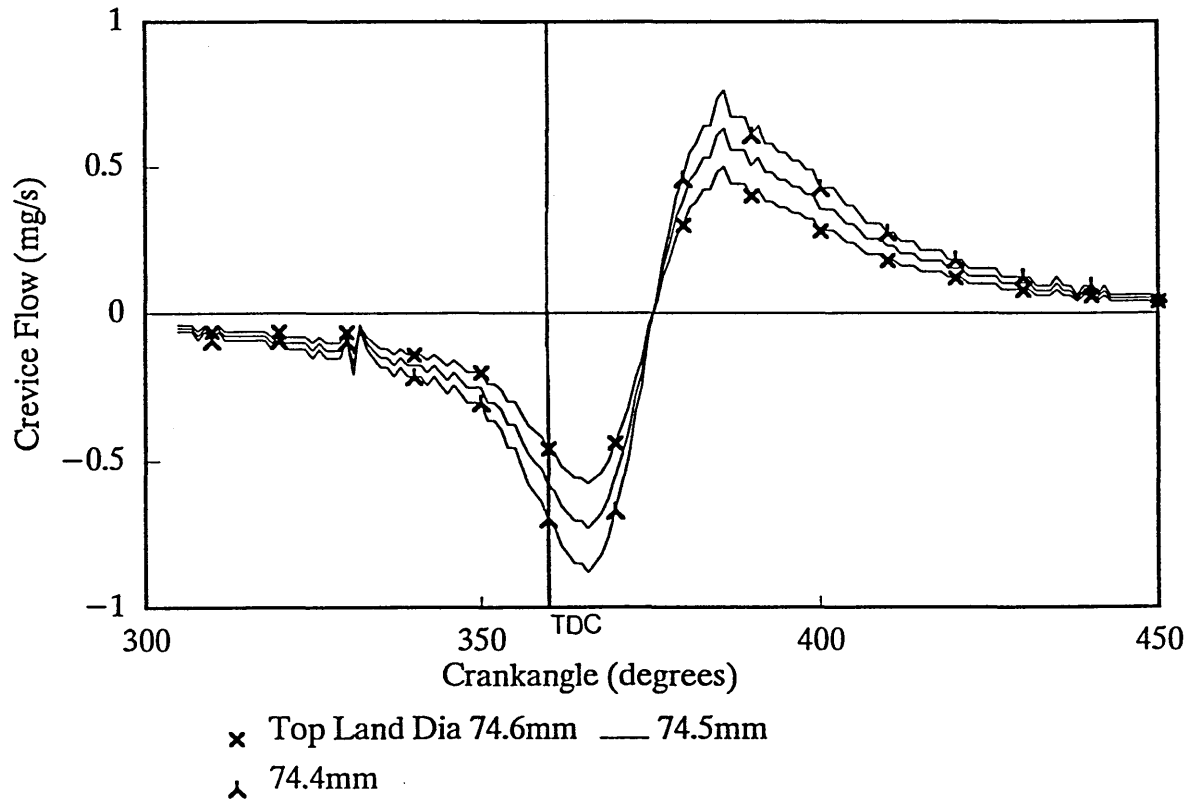


Figure 4.5 Predicted flow into top land varying with top land diameter
 Constant top land height, 1500 rpm 1 bar bmep

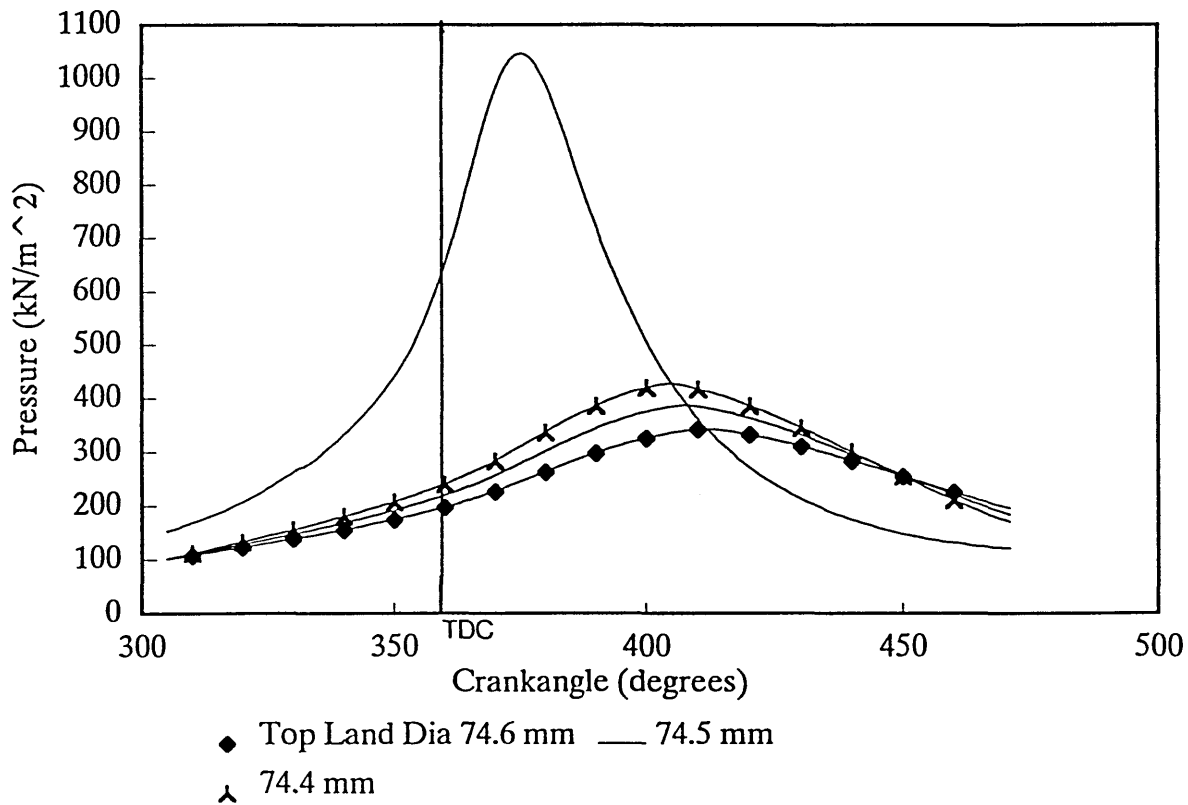
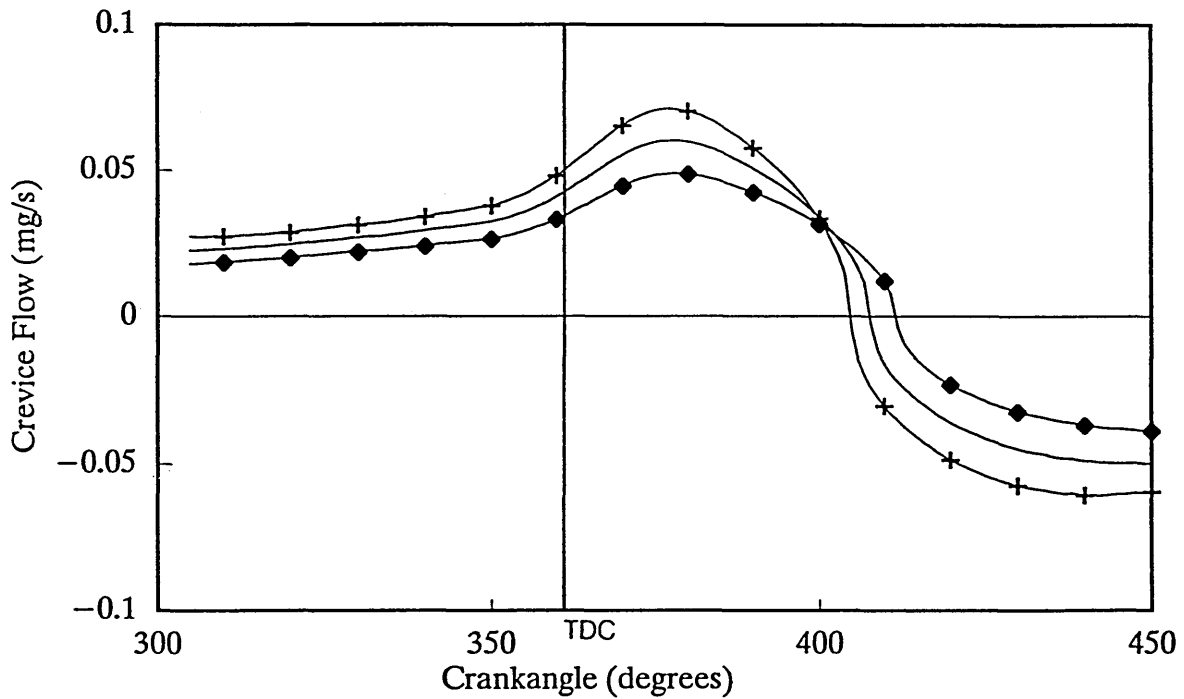
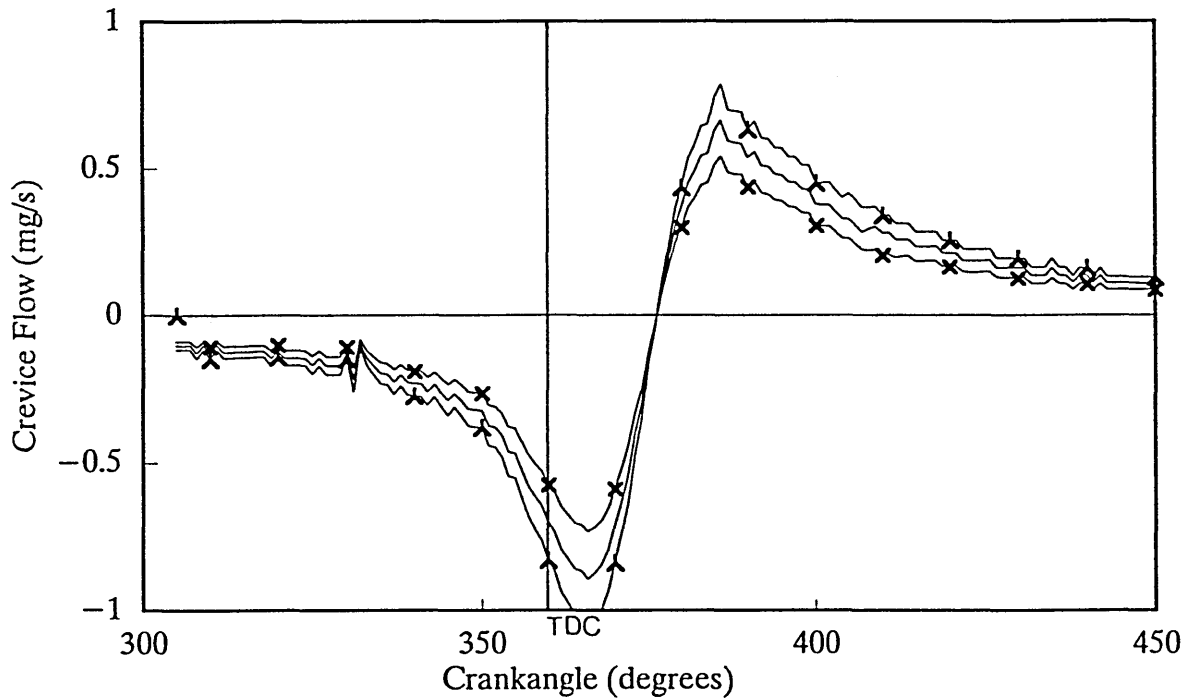


Figure 4.6 Change in 2nd land pressure with piston top land diameter
 1500 rpm 1 bar bmep



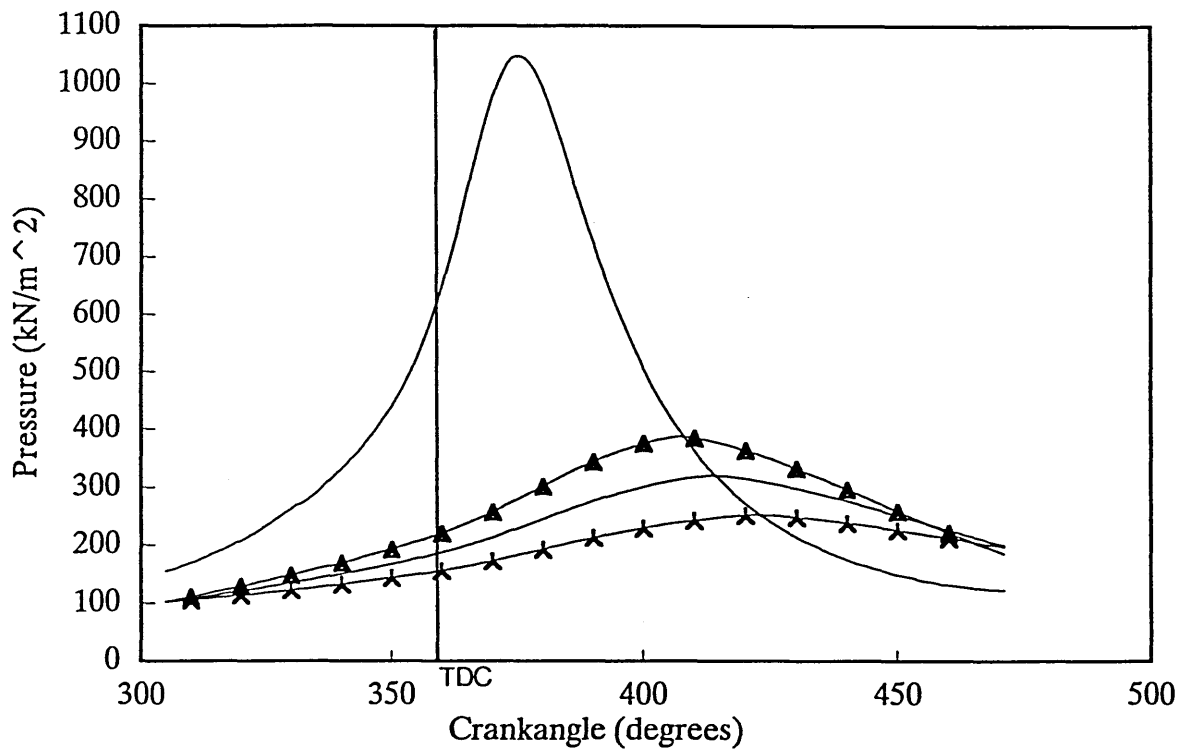
◆ Top Land Dia 74.6mm — 74.5mm
 + 74.4mm

Figure 4.7 Flow into 2nd land varying with top land diameter
 Constant top land height, 1500 rpm 1 bar bmep



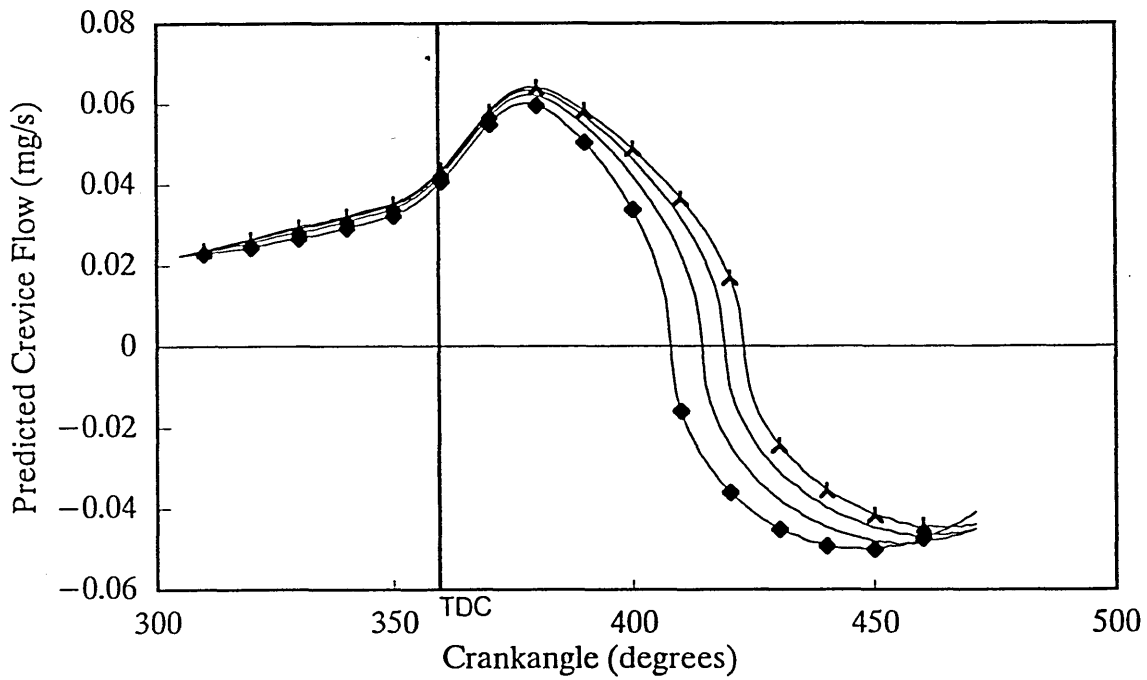
× Top Land Dia 74.6mm — 74.5mm
 ▲ 74.4mm

Figure 4.8 Predicted total flow with changes in top land diameter
 1500 rpm 1 bar bmep



▲ Extra Volume.0 — Extra Vol. 0.1 ✕ Extra vol. 0.3

Figure 4.9 Change in predicted 2nd land pressure with 2nd land volume
1500 rpm 1 bar bmep



◆ Extra Vol 0 cm³ — Vol 0.1cm³
 - - - Vol 0.2cm³ ✕ Extra Vol 0.3cm³

Figure 4.10 Predicted change in 2nd land flow with increase in 2nd land volume
1500 rpm 1 bar bmep

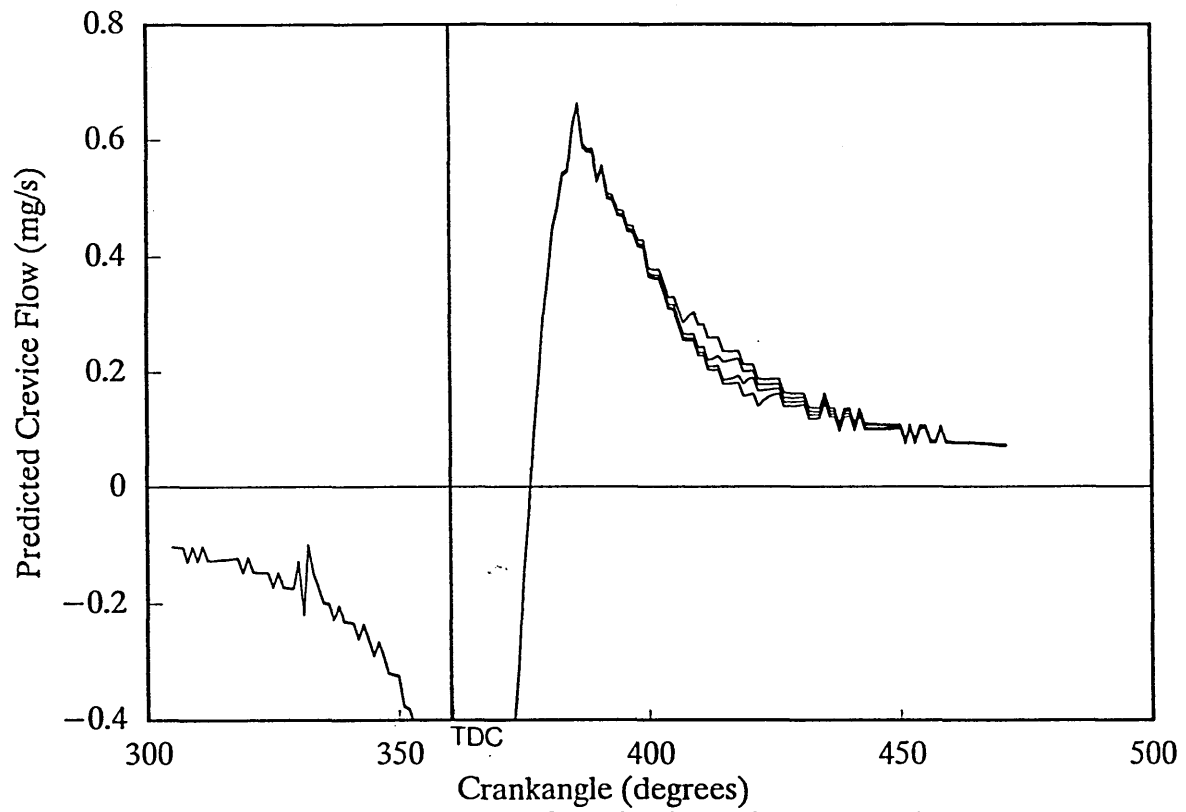


Figure 4.11 Predicted total flow out of crevice flow with increase in 2nd land volume
1500 rpm 1 bar bmep

4.3. Absorption and Desorption of Fuel in Oil

4.3.1 Previously Developed Models

The absorption of fuel by the lubricating oil on the cylinder wall during the compression and combustion strokes and the desorption of this fuel during expansion and exhaust has been recognised as a major source of hydrocarbon emissions, see literature survey part 2.3.

There are many variables to consider; lubricating oil characteristics including viscosity, type of fuel, and engine operating conditions are an example. The use of reference lubricating oil and fuel and testing at five fixed operating conditions (see experimental development) holds these variables constant. This enabled a particular variable of interest to be investigated. The oil layer thickness has been shown to have a significant effect on this source of emissions. It is also something which can be controlled by component design and specification, which brings it into the scope of this investigation. The purpose of modelling absorption/desorption is to investigate the impact of changes to the oil layer thickness on hydrocarbon emissions for comparison with the experimental work undertaken in this research.

Several researchers have modelled the absorption /desorption effect, the following will build upon some of these models. Three models were considered:-

The cylinder wall is split into 4 regions with varying amounts of contact with unburned mixture. The following is the general formula for all regions;

$$\frac{dm_i}{dt} = m'' \cdot A_i + \rho \cdot Z \sum_{j=1,4} m_{fi} \cdot \frac{dA_{ij}}{dt} \quad \dots \dots [1]$$

Where dm_i = rate of change of fuel content of region i

and Z = density and thickness of oil layer

m_{fi} = mass fraction of fuel in oil in region i

dA/dt = rate of change in area of region i

m'' = convective mass flux across gas phase boundary layer.

$$m'' = \frac{g^*G \cdot g^*F [m_{fG} - m_{fF} \cdot N_{hc}]}{(N_{hc} \cdot g^*G + g^*F)}$$

m_{fi} = mass of fuel in oil in region i

N_{hc} = Henry number

$g^*G = h/C_p$ and $g^*F = \rho \cdot D/x$

D = Diffusion coefficient

2 Schramm and Sorenson (33)

The basis of this model was to determine the mass concentration of fuel in the oil and its distance from the cylinder wall. This was based on the diffusion equation.

$$\frac{dc}{dt} - D \frac{d^2c}{dx^2} = 0 \quad \dots \dots [2]$$

Where c = the mass concentration of fuel in oil

D = the diffusion coefficient

Boundary Conditions.

$$dC/dx (0,t) = 0$$

$$C (1,0) = F(t)$$

$$C (x,0) = 0$$

3 Korematsu (28)

$$dm_f = (C_{\max} - C_{\min}) \cdot \pi \cdot D_c \cdot x \cdot \rho \cdot C^*_{eq} \cdot dy \quad [3]$$

Where dm_f gives the mass of fuel emitted for increment of oil layer dy .

$$\text{From Henry Law's, } C^*_{eq} = (M_f/M_o) \cdot (P/H) \cdot Y_f \quad . . . [3a]$$

C^*_{eq} = mass fraction of fuel in oil at equilibrium.

C^* = mass fraction fuel in oil

$c = C^*/C^*_{eq}$ (non dimensional)

$C_{\max} - C_{\min}$ = fuel emitted from oil in a cycle

D_c = Cylinder diameter (m)

x = Oil layer thickness (m)

ρ = oil density (kg/m³)

The model chosen here was that developed by Korematsu, because this gave the mass of fuel emitted in increments down the cylinder bore, with a direct relation to the oil layer thickness.

4.3.2. Defining Values for $C_{\max} - C_{\min}$

The term $C_{\max} - C_{\min}$ is dependent on engine speed, position of piston throughout the cycle and oil layer thickness. These values are based on the following.

The term C^* is the mass of fuel in the oil layer and is defined by the conservation of fuel species.

$$\frac{dC^*}{dt} = D \cdot \frac{d^2 C^*}{dx^2}$$

D is the diffusion coefficient

This is normalised to $C_m = \frac{C^*}{C_{eq}^*}$

The mean value of C_m is given by C . The maximum and minimum values of C in the cycle are C_{\max} and C_{\min} respectively. The values of C are displayed graphically by Korematsu (28). From these graphs the values of C_{\max} and C_{\min} can be approximated and gives the following function for variations in speed and piston position;

$$(C_{\max} - C_{\min}) = (N \cdot M_1 + k) + M_2 \cdot y/s \quad [4]$$

Where N = engine speed (rpm)

$$M_1 = -1.972E-4$$

$$k = 1.1304$$

$$M_2 = -0.44$$

y/s = Piston displacement from TDC/Length of stroke

Values for $C_{\max} - C_{\min}$ are given in text of Korematsu

(29) these are compared against the predicted values from equation [4] in Figures 4.12 and 4.13.

4.3.3 Defining the Henry Constant

An important aspect of this modelling is to define the solubility of fuel in oil. To define this Henry's Law is assumed to be applicable for the absorption of a vapour by the oil film. The partial pressure of fuel vapour at the interface is related to the mole fraction of the fuel dissolved into the oil film.

$$H_c = \frac{P_f}{n_f} \quad [5]$$

Where H_c = the Henry Constant (N/m²)

P_f = the partial pressure of fuel vapour (N/m²)

n_f = Mol fraction of fuel dissolved on oil film.

Defining the Henry Constant for modelling purposes with multigrade oils and gasoline is very difficult, because both solvent and diluent are complex mixtures of many hydrocarbon compounds. Previous researches have simplified this by assuming the lubricating oil behaves as squalane C₃₀H₆₂. The absorption of the many individual fuel component can then be investigated. Chappelow and Prausnitz (69) defined the Henry constant for methane, ethane, propane and n-butane. These definitions were used by Dent and Lakshminarayanan (27) to extrapolate for n-octane. This gave the following relationship:-

$$\text{Log (Hc)} = -1.921 + 0.013.(T - 300) \dots [6]$$

A completely different approach was used by Schramm and Sorenson (25). A gas-liquid chromatography method was developed using the particular lubricating oil as the stationary phase. By this method several lubricating oils were assessed using trimethyle pentane and m-xylene as fuels. It was observed that the lubricants gave similar results for each fuel, Figure 4.14 shows the Henry Constants derived by these two research teams.

For approximating the Henry Constant in the model the relationship [6] will be adopted. It can be seen in Figure 4.14 that values for n-octane from equation 6 are lower than for trimethyle pentane and similar to m-Xylene (an aromatic C₈ compound), from Schramm and Sorenson (25). This equation will probably give reasonable values for the Henry Constant for the reference fuel which contains a high concentration of aromatic compounds.

4.3.4 Test Runs of Computer Calculations

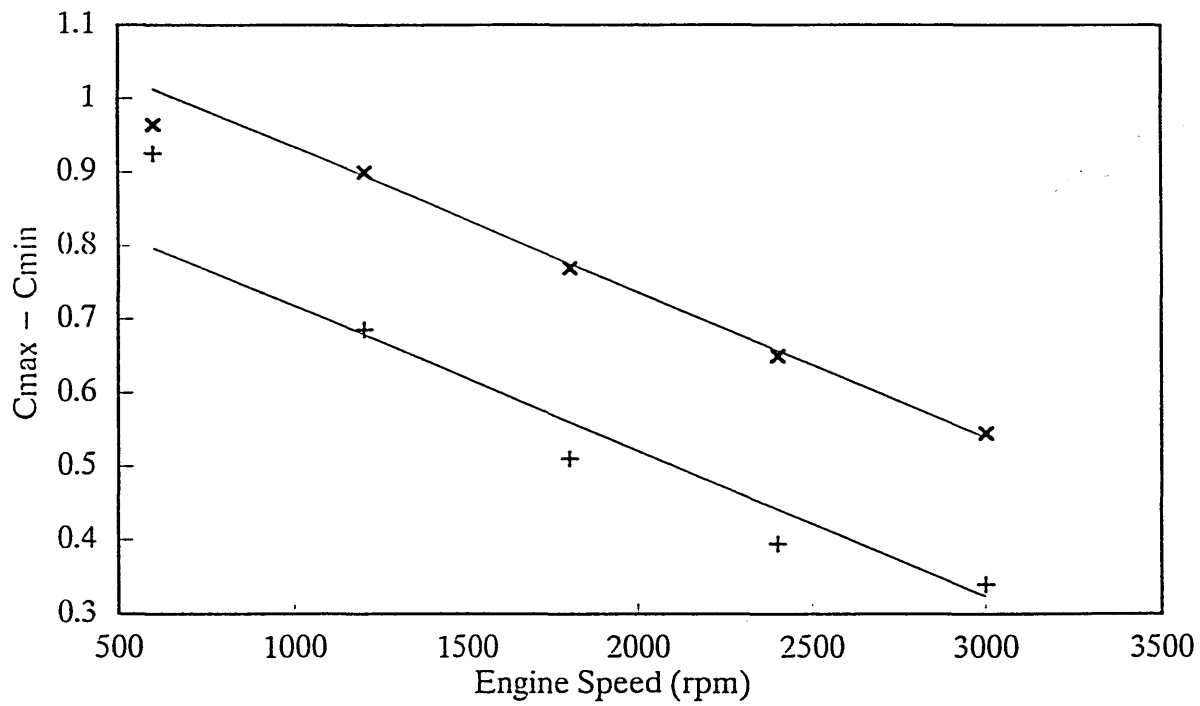
To demonstrate that the model was correctly predicting known trends for varying engine conditions a series of test calculations were made. A listing of this programme is given in Appendix 2. Table 4.2. gives the input conditions used in these calculations. The test calculations used cylinder pressure data obtained at 1500 rpm 1 bar bmep. Figure 4.15 is a flow chart for the programme.

The mass of fuel released per degree is shown in Figure 4.16. The desorption peaks at 25° ATC during the rapid decrease in pressure. Also the large reduction in desorbed fuel due to cylinder liner temperature is very apparent. The link with temperature can also be seen in Figure 4.17, which shows the total fuel desorbed in a cycle. The reduction in desorption caused by increase in speed is small. However, in a real engine an increase in speed would also increase the temperature.

Table 4.2. Input Conditions for Absorption/Desorption

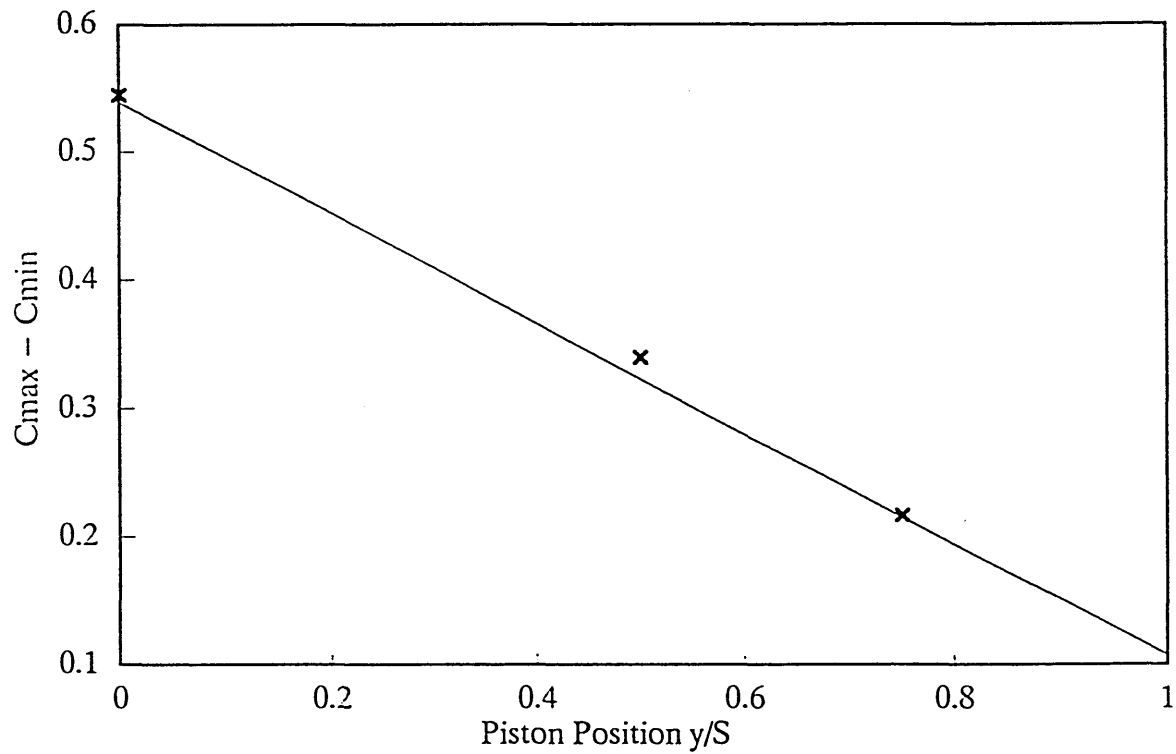
	Liner Temperatures °C				
Oil Layer	120	135	140	145	160
0.244 μ m			B		
0.233 μ m	A,B,C	A,B,C,	A,B,C,	A,B,C	A,B,C
0.222 μ m	A,B,C	A,B,C	A,B,C	A,B,C	A,B,C
0.215 μ m	A,B,C	A,B,C	A,B,C	A,B,C	A,B,C

For engine speeds A = 1000 rpm, B = 1500 rpm, C = 2000rpm



— $y/S = 0$, Predicted — $y/S = 0.5$, Predicted
 × $y/S = 0$, Korematsu + $y/S = 0.5$, Korematsu

Figure 4.12 Values of $C_{max} - C_{min}$ for increasing engine speed at TDC $y/S = 0$ and 90 ATDC $y/S = 0.5$



— Predicted Values × Values from Korematsu

Figure 4.13 Values of $C_{max} - C_{min}$ for different piston positions at TDC $y/S = 0$

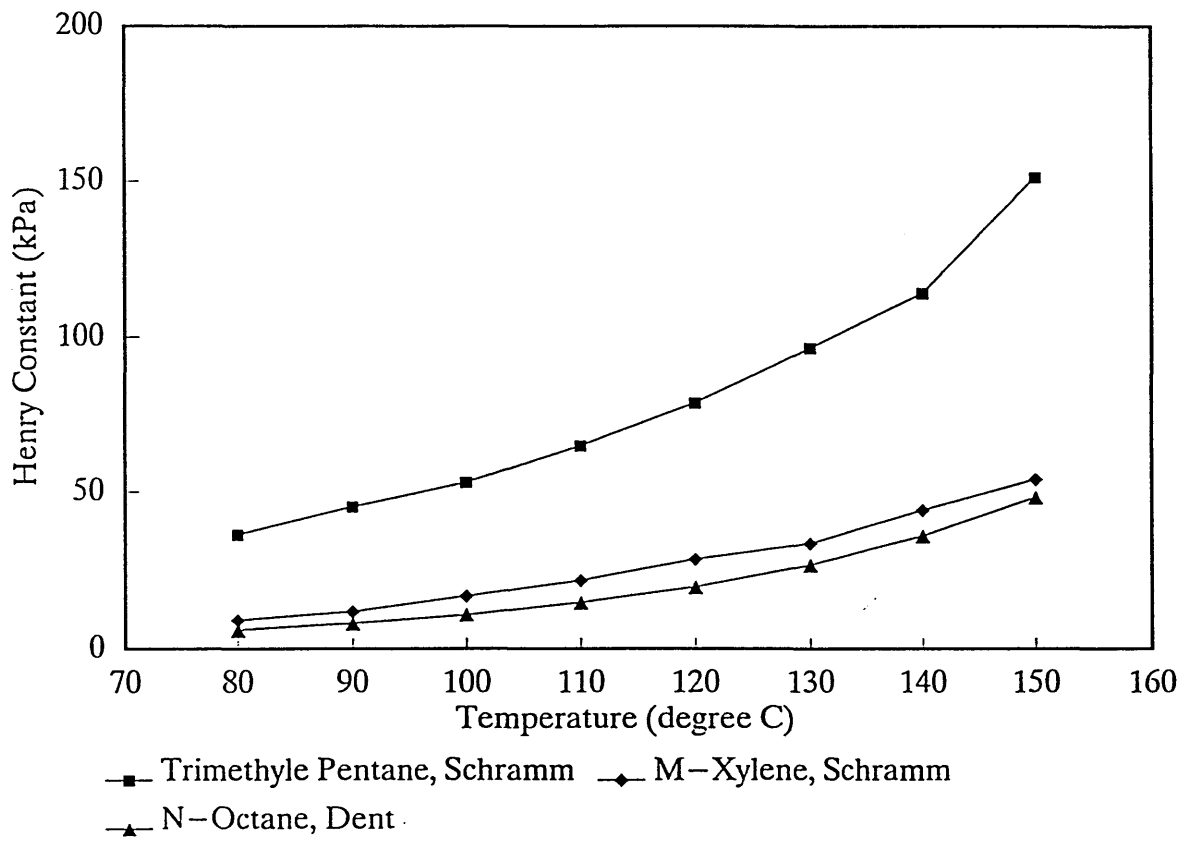


Figure 4.14 Henry Constant as predicted for different C8 hydrocarbons

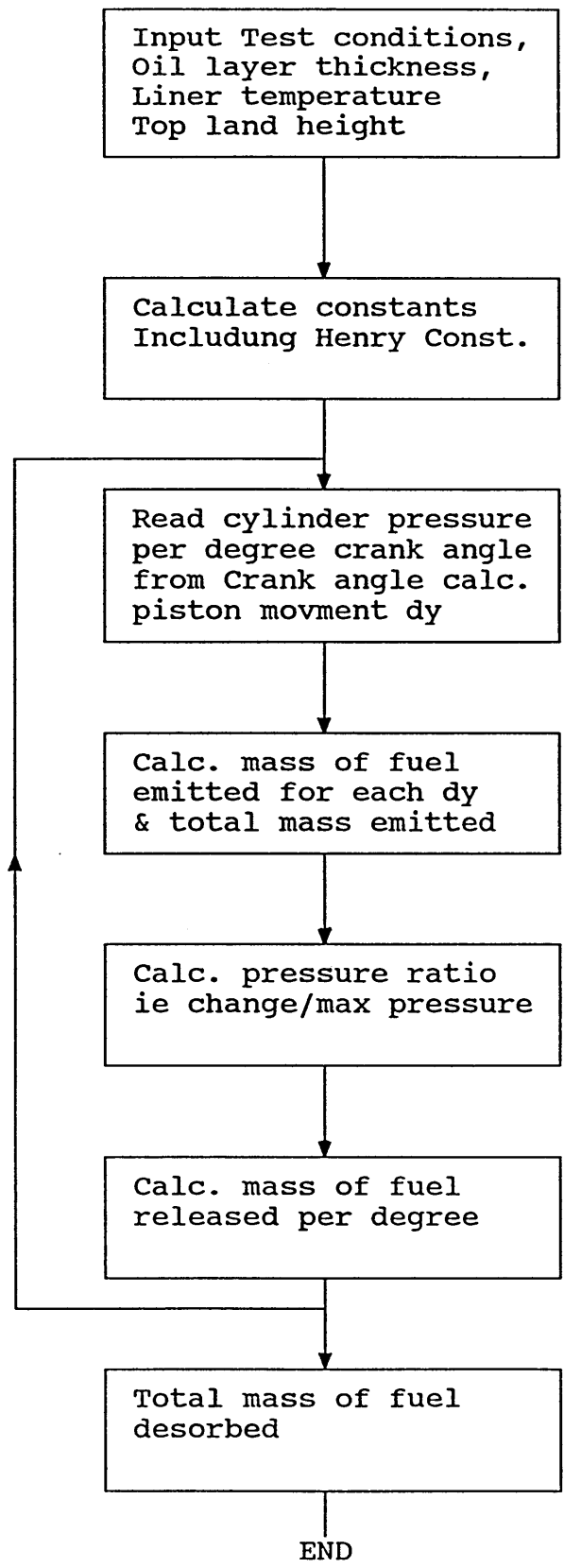


Figure 4.15 Flow Chart for Absorption/Desorption Model

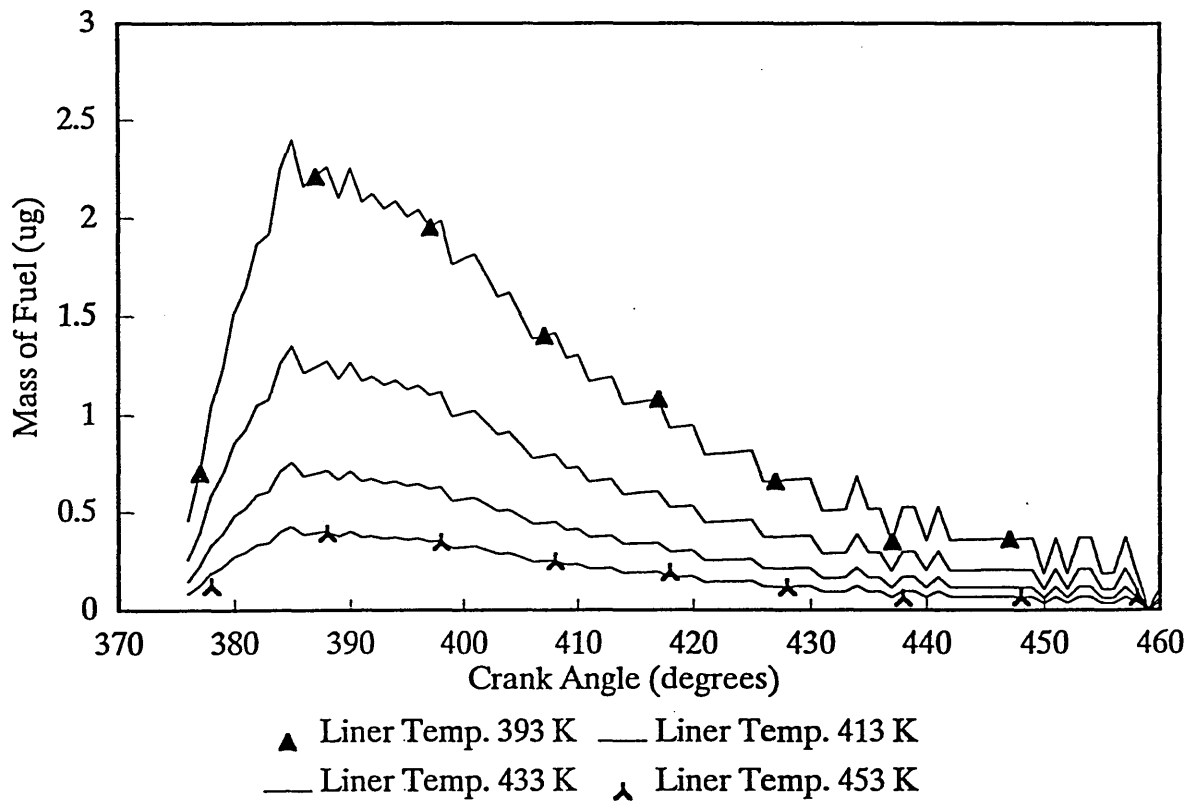


Figure 4.16 Fuel desorbed from lubricant per degree crank angle
 Variation in cylinder liner temperature, Standard Piston, 1500 rpm 1 bar bmep

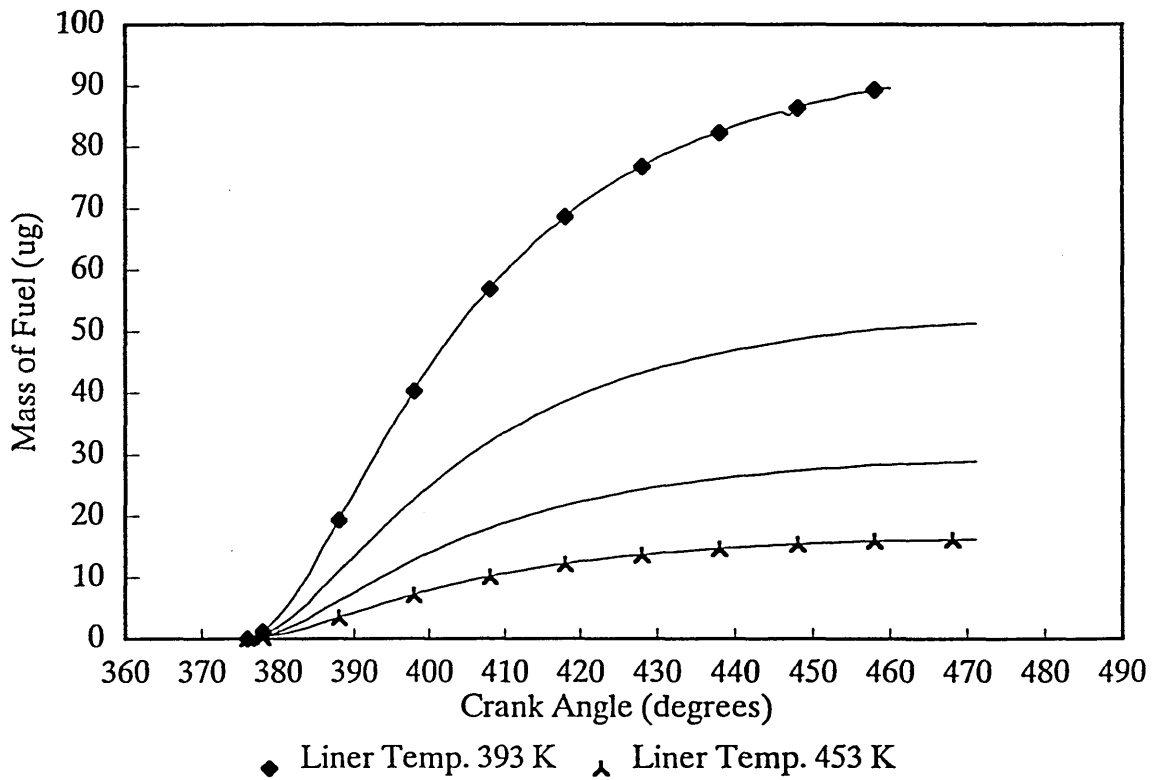


Figure 4.17 Predicted cumulative fuel desorbed from lubricant,
 Variations in liner temperature, Standard Piston, 1500 rpm 1 bar bmep

4.4. Modelling of Oxidation of Crevice Mixture and Desorbed Fuel as it returns to the Combustion Chamber

The level of oxidation undergone by the returning fuel has a large influence on the total engine out hydrocarbon emissions. The crevice mixture as it returns to the chamber occurs at low velocities and in the form of a wiped layer as the piston descends. During the exhaust stroke a vortex forms as the pistons scrapes this mixture off cylinder walls Namazian and Heywood (12). Some mixing between crevice and bulk cylinder gases occurs due to the vortex. This mixing results in an increase in temperature of the crevice gases resulting in some oxidation occurring. Oxidation is temperature critical, and the temperature is controlled by the amount of mixing which occurs. Defining the amount of mixing due to the vortex would require more information and a more complex model than is justified in the current research. To simplify this a ratio of mixing will be used.

1. No mixing

Crevice gases remain close to the cylinder wall and during the exhaust stroke the vortex does not allow any mixing with cylinder gases. Thus the temperature remains close to the piston temperature and molecular fractions of HC's remain as for original mixture.

2. Complete Mixing

Crevice gases mix completely with cylinder gases as

the vortex progresses ahead of the piston. Because of relative masses the gas temperature remains the same as cylinder gases. Mass fractions are across the total mass of the cylinder.

3. Partial Mixing

The crevice gases remain close to the cylinder wall, but some interaction with cylinder gases occurs due to turbulence and diffusion in the vortex. For this case assume that C_p and density are the same for crevice and cylinder gases; then from basic heat exchange

$$Q = m_c C_p T_c = m_g C_p T_g$$

$$m_c T_c = m_g T_g$$

Thus Crevice gas temp $T = \frac{X T_c + T_g}{(X + 1)}$ [1]

Where X is the ratio of gas mix

$$X = m_c / m_g$$

The flow characteristics as calculated from models indicate that partial mixing is the most likely option.

There have been many studies of the calculations for the oxidation rate, for example Weiss and Keck (7). However, the evaluation of some of the constants were not accurate. This gave variations between experimental data and calculated results which were high. However, a much simpler concept was discussed, that of a sudden freezing temperature. At this temperature all oxidation would halt

due to the much longer time constant for oxidation reactions. The function for the sudden freezing temperature from Wiess and Keck (7) was given as;

$$T_{sf} = \frac{1320}{(1 + 0.02 \cdot \ln(F_{O_2} \cdot 100 \cdot P_i / P_o))} \quad [2]$$

Where F_{O_2} = exhaust oxygen percent

P_i = inlet pressure (N/m²)

P_o = Atmospheric pressure. (N/m²)

It was also concluded that mixing of crevice mixture was rapid, but not instantaneous.

The concept of the model used in this investigation will be to evaluate the Mol fraction of crevice mixture and desorbed fuel mixing with burnt gases in the cylinder. Then, using simple heat transfer between the mixing gases to approximate its temperature. This can be compared with the sudden freezing temperature to evaluate how much oxidation occurs. Above this temperature complete oxidation will occur, but below it oxidation continues at a reduced rate. This will be defined as a percentage of the initial Mol fraction.

Assumptions

Cylinder gases are all burnt gas

At 15:1 AFR, O₂ Concentration 1.4 % and Mol weight = 59.57

For unburnt mixture 1 Mol fuel requires 56.38 Mol air,

ie crevice Mol weight = 57.38

Mol fractions of fuel and air with a mixture ratio of X.

Refer to Appendix 1 for calculations of mol weights

For Crevice Mixture

$$\text{Mol Fraction } x_i = \frac{n_i}{n} = \frac{\text{Number of Mols of Component}}{\text{Number of Mols of Mixture}}$$

$$\text{Mol fraction HC } x_{\text{HC}} = \frac{1}{57.38 + X \cdot 59.57} \quad [3a]$$

For Desorbed Fuel

$$\text{Mol fraction HC } x_{\text{HCa}} = \frac{1}{1 + 0.8 \cdot X \cdot 59.57} \quad [3b]$$

$$\text{Mol fraction O}_2 \text{ } x_{\text{O}_2} = \frac{11.81}{57.38 + X \cdot 59.57} \quad [3c]$$

This sets the Mol fraction at the start, however, on a release per crank angle basis the temperature varies and the residual HC's from previous crank angles have also to be considered. For the oxidation per crank angle the mass flow out of the crevices per degree will be added to the previous mass out flow and the amount of oxidation recalculated as one. This will require the mass fraction to be calculated at each step for the new mixture of crevice and cylinder gases. Also to be included is the mass of fuel desorbed from oil layers.

$$x_{i2\text{Hct}} = \frac{m_c \cdot x_{i1} + \frac{m_c \cdot x_{i2\text{HCr}}}{m_c + X} + dm \cdot x_{\text{HCa}}}{(m_c + X \cdot m_c + dm)} \quad [4]$$

Where m_c = mass flow from crevice

dm = fuel desorbed from oil layers, both per degree
crank angle.

x_{i2Hct} = Total mol fraction of HC's at 2

x_{i2HCr} = Residual mol fraction of HC's at 2

For the mass fraction of O_2

$$x_{i2t0} = x_{i2Hct} \cdot 11.81$$

So for the Mol fraction at a crank angle the temperature of this mixture is calculated and then a change in Mol fraction is assumed. This is subtracted from the initial Mol fraction to give the residual Mol fraction.

$$x_{i2HCr} = x_{i2Hct} - dx_i$$

If the temperature is greater than the sudden freeze temperature, then dx_i is equal to x_{i2Hct} . For lower temperatures a lower level of oxidation occurs.

The residual fraction at exhaust valve opening will be taken as the final value. The actual mass of unburned fuel can then be calculated.

$$n_i = \frac{m}{M} \quad \text{and} \quad x_i = \frac{n_i}{n} \quad n = \frac{m_c + m_b}{M}$$

Thus $n_i = x_{iHCex} \cdot n$

$$n_i = x_{iHCex} \cdot \frac{(m_c + m_b)}{M_{ex}}$$

$$m_{HC} = M_{HC} \cdot n_i$$

$$m_{HC} = M_{HC} \cdot x_{iHCex} \cdot \frac{m_c (X + 1)}{X \cdot M_{ex}} \quad . . . [5]$$

4.4.1 Test Calculations

A series of calculations were performed to assess the sensitivity of the model to the assumed variables. The data for these calculations were based on pressure data taken at 1500 rpm 1 bar bmep and 2500rpm 5.5 bar bmep. The flow chart for the computer programme is given in Figure 4.18 and a listing is given in appendix 2. The variables covered are mixture ratio and piston temperature, variations in piston and liner details are covered in discussions of crevice and absorption calculations.

4.4.2.1. Mixture Ratio

The mixture ratio of the crevice mixture and desorbed fuel into the combustion chamber gases is used to approximate the temperature of these mixing gases, Equation [1], and the Mol. fraction of hydrocarbons in this mixture. The level of unburnt hydrocarbons are shown in Figure 4.19 for mixture ratios from 0.2 to 0.9. This shows a considerable reduction in hydrocarbons as the mixture level approaches one. The largest decrease occurs between 0.2 and 0.5. For further calculations a mixture ratio of 0.6 was chosen as this level is less sensitive than lower levels but does not give complete mixing.

4.4.2.2. Piston Temperature

The temperature of the crevice gases are usually assumed to be the piston temperature. Measurement of piston temperatures and calculated temperatures, Furuhamo et al (41) and (42), indicate that the temperature varies between 520° K and 570° K. This varies with speed and load, Figure 4.20 indicates that piston temperature has slightly more effect at higher speeds and loads.

4.4.2.3. Oxidation Rate

Once the temperature of the mixture of crevice, desorbed fuel and combustion gases drops below the sudden freezing temperature the oxidation rate reduces but does not stop. For these calculations the change in the mass fraction dx_i is scaled by a factor of less than one. Figure 4.21 shows the effect this has on oxidation. For further calculations an oxidation factor of 0.5 will be used.

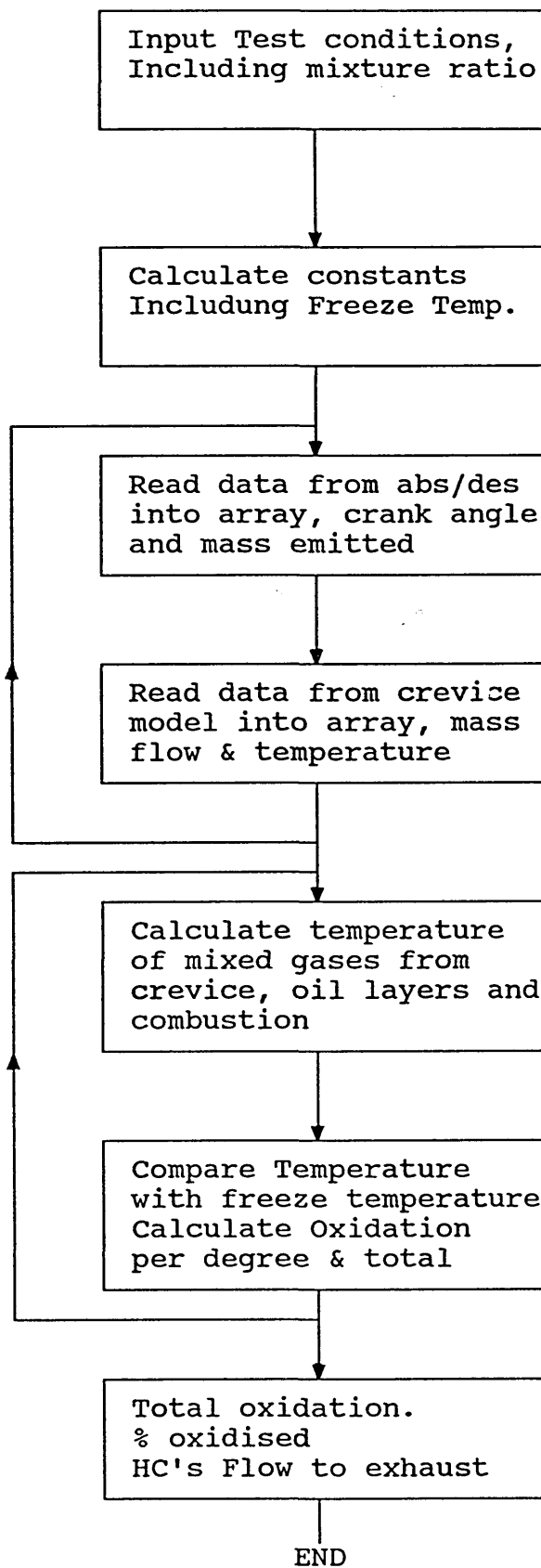


Figure 4.18 Flow Chart for Oxidation Model

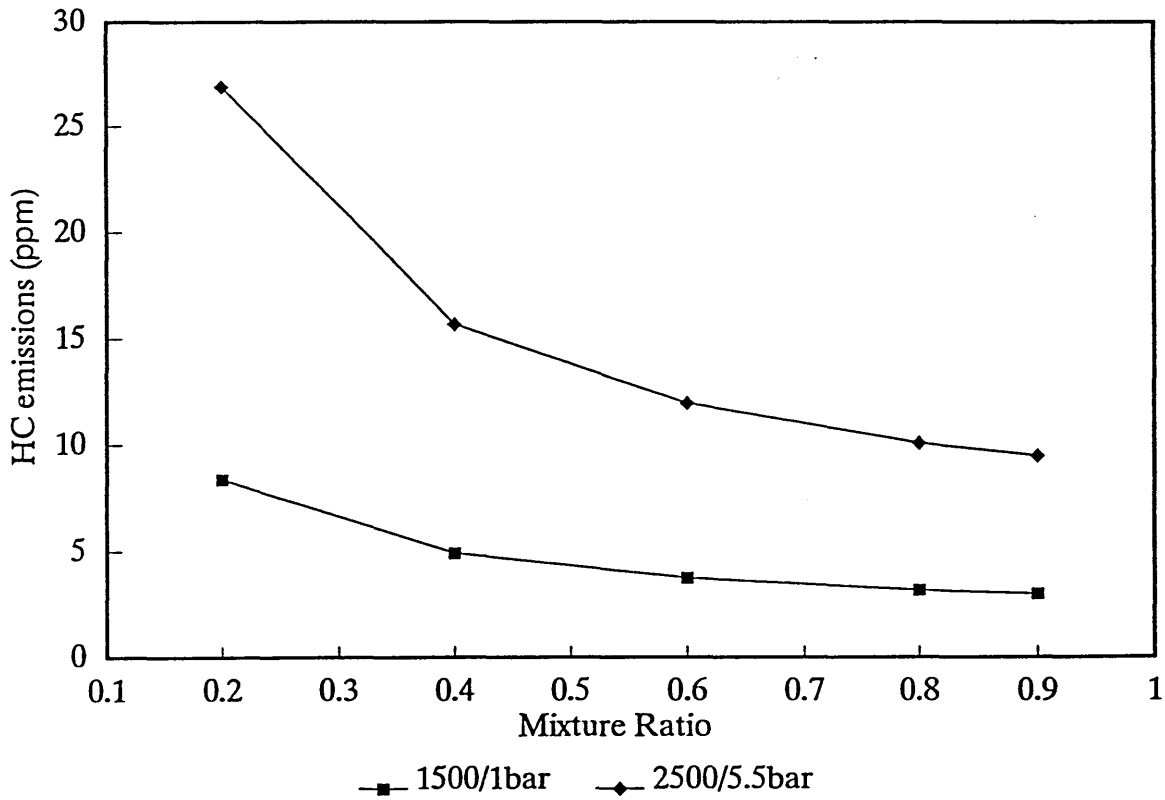


Figure 4.19 Total predicted HC emissions with different mixing ratios into combustion chamber gases, Standard Piston, 15:1 AFR

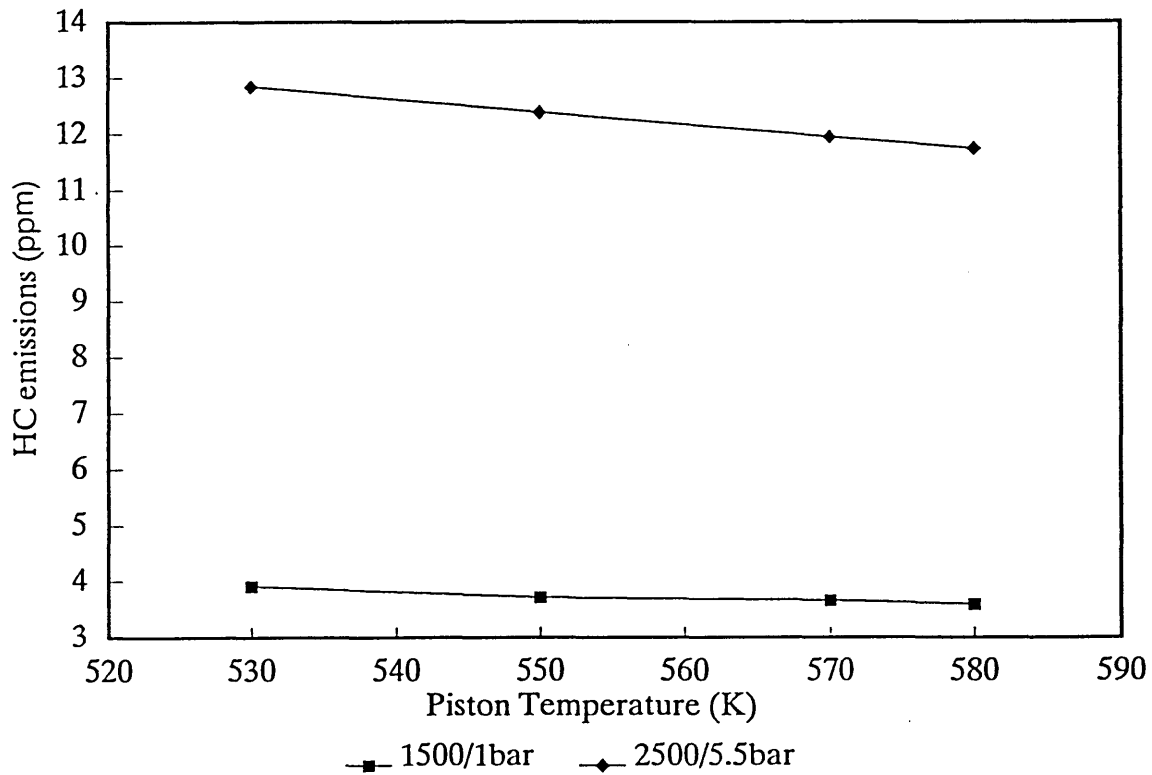


Figure 4.20 Total predicted HC emissions with increasing piston temperature Standard Piston, 15:1 AFR

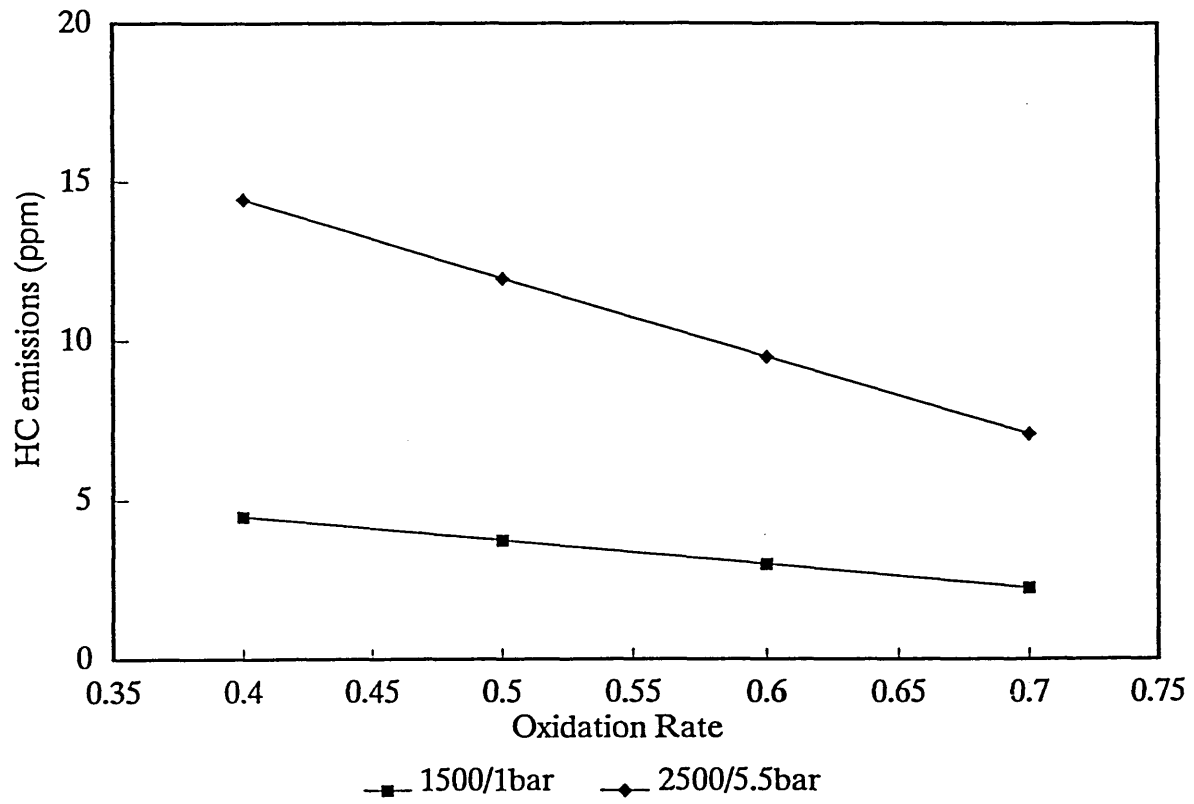


Figure 4.21 Total predicted HC emissions with different oxidation rates
Standard Piston, 15:1 AFR

4.5. Combustion Analysis

4.5.1. Heat Release Calculations from Pressure Data

Although the modelling being undertaken for this research is aimed at calculating the effects of crevice volumes and absorption of fuel into oil layers, an analysis of combustion heat release is required to derive cylinder temperatures and mass fraction burnt through the cycle. This will provide data for the calculation of oxidation rates of hydrocarbon emissions from the above sources before they leave the combustion chamber.

The details of the fuel, combustion equations, definitions of air fuel ratios and Mol weights reactants are given in Appendix 1.

There are many combustion models of varying complexity described in the literature. These are discussed in detail by Heywood (70). However Stone and Green-Armytage (32) in comparing a basic model with more complex ones observed only minor differences in the predicted times for 10, 50 and 90% mass fraction burnt. Since the aim of this modelling is an approximation of the completion of burning and combustion temperatures a simple model will be used. The basis of this model is the 1st law of thermodynamics. A flow chart is given in Figure 4.22.

Assumptions

No heat transfer to cylinder walls, cylinder head or piston.

Air/Fuel mixture behaves as a perfect gas.

$$dQ = dU + dW \quad [1]$$

For a small change in volume per degree crank angle assuming a perfect gas.

$$dU = m.C_v.dT \quad \text{and} \quad dW = PdV$$

Hence

$$dQ = m.C_v.dT + P.dV \quad [2]$$

Also $PV = mRT$

In differential form

$$V.dP + P.dV = m.R.dT + m.T.dR + R.T.dm$$

R and m are constant

$$V.dP + P.dV = m.R.dT \quad [3]$$

Substituting [3] into [2] gives

$$dQ = \frac{C_v}{R} . (V.dP + P.dV) + P.dV \quad [4]$$

But

$$C_p - C_v = R \quad \text{and} \quad \frac{C_p}{C_v} = \gamma$$

Thus

$$dQ = \frac{C_v}{C_p - C_v} . (V.dP + P.dV) + P.dV$$

$$dQ = \frac{C_v . (V.dP + P.dV) + P.dV . (C_p - C_v)}{C_p - C_v}$$

$$dQ = \frac{C_v . V . dP + C_p . P . dV}{C_p - C_v}$$

Thus

$$dQ = \frac{V \cdot dP + \gamma P \cdot dV}{\gamma - 1} \dots \dots \dots [5]$$

The rate of change of heat flow with crank angle

$$\frac{dQ}{d\theta} = \frac{V \cdot \frac{dP}{d\theta} + \gamma P \cdot \frac{dV}{d\theta}}{\gamma - 1}$$

Also $Q = m_f \cdot Q_f$

$$\frac{dQ}{d\theta} = Q_f \cdot \frac{dm_f}{d\theta}$$

Q_f = Calorific value of fuel

m_f = mass of fuel burnt

Therefore

$$dm_f = \frac{dQ}{Q_f}$$

Where dm_f is the fuel burnt in creating an incremental heat flow dQ

Thus the total mass of fuel burnt

$$m_{ft} = \int_{\theta_1}^{\theta_2} \frac{dQ}{Q_f}$$

Where θ_1 = Angle at establishment of flame kernel

θ_2 = End of Burning

For any crank angle θ_i the amount of fuel burned for a change of crank angle from θ_1 to θ_i is;

$$m_{fi} = \int_{\theta_1}^{\theta_i} \frac{dQ}{Q_f}$$

As a percentage,

$$m_i \% = \frac{\sum_{\theta_1}^{\theta_2} dQ}{\sum_{\theta_1}^{\theta_2} d\theta} \times 100 \quad \dots \dots \dots [6]$$

Where θ_1 = Crank angle after which no negative heat release occurs.

θ_2 = Crank angle when total heat release is a maximum

4.5.2. Combustion Gas Temperatures

For the calculation of gas temperatures based on the pressure data obtained from tests.

Assume the gas follows the polytropic non flow process

$$pv^n = \text{constant}$$

since $Pv = mRT$, it follows that

$$\frac{T_1}{T_2} = \left(\frac{P_1}{P_2} \right)^{n-1/n}$$

In differential form

$$\frac{T_1}{(T_1 + dT)} = \left[\frac{P}{(P_1 + dP)} \right]^{(n-1)/n}$$

Thus the change in temperature, dT , is given by

$$dT = \left[\left(\frac{P_1 + dP}{P_1} \right)^{(n-1)/n} - 1 \right] \cdot T_1 \quad \dots \dots \dots [7]$$

Value of n is determined from

$$P_1 v_1^n = P_2 v_2^n$$

Thus
$$n = \frac{\text{Log}(P_1/P_2)}{\text{Log}(v_2/v_1)} \dots \dots \dots [8]$$

4.5.3. Checks on Heat Release

Heat release

$$dQ = Q_f \cdot dm_f$$

For total heat release over the cycle

$$Q_{\text{tot}} = Q_f \cdot \text{mass of fuel inducted}$$

$$m_m = \frac{P_i \cdot V_i}{R \cdot T_i}$$

i denotes the conditions at inlet valve closure

m_m is the mass of inducted mixture.

Since
$$m_m = m_{\text{air}} + m_{\text{fuel}}$$

For an AFR of 15:1,
$$m_m = 15 \cdot m_{\text{fuel}} + m_{\text{fuel}} = 16m_{\text{fuel}}$$

Thus
$$Q_{\text{tot}} = \frac{Q_f \cdot m_m}{16}$$

4.5.4. Calculation Results

A computer programme was written to perform these calculations and a listing of this is given in Appendix 2. The heat release calculations compare well with results from previous researches for the burn duration. It was observed that the burn duration was similar at each test point, beginning at the spark the initial rise in heat

release occurred at approximately 12° BTDC and rapid burning between TDC and 20° ATDC. Figure 4.23 shows the percent burnt and heat release per degree. This is similar to the data presented by Stone and Green-Armytage (32).

The Main objective of these calculations was to define the end point of combustion for the purpose of calculating oxidation of unburnt hydrocarbons from crevices and oil layers. This end point has been assumed to be the crank angle when 100% burnt is reached. The ignition timing and combustion end points are given in Table 4.3

Table 4.3 Ignition and Combustion Completion Timing.

Test Point	Ignition °BTDC	Combustion End °ATDC
1500/1 bar	28°	25°
1500/2.62	23°	25°
2000/2bar1	20°	30
2500/5.5	20°	28°
3500/WOT	15°	28°

4.5.5. Checks on Temperature

There are no temperature measurements from the combustion chamber, but temperatures at the inlet and exhaust ports are measured. The predictions of induced mixture temperature can be compared with measured inlet temperatures.

The exhaust gas predictions are more difficult to

compare because of the heat transfer occurring in the exhaust port. Allowing for this, a difference of between 50 to 100 K from predictions to actual measured values will be likely.

4.5.6 Temperature Calculation Results

These calculations yielded a temperature profile throughout the cycle, giving a peak in the temperature shortly after peak pressure. Figure 4.24 displays the temperatures calculated at 1500 rpm 1 bar bmep. The measured temperatures are given in Table 4.4. The temperature at inlet was measured in the manifold and is the average over the cycle. The in-cylinder calculation is taken as the average over inlet valve opening period. The calculations gave close agreement. Exhaust gas temperatures were measured at the exhaust port approximately 100mm down stream of the valve and is the average over the cycle. The calculated in-cylinder exhaust gas are the average of valve open duration. The calculated temperatures were lower than those measured at the ports, but are usually within the 100°C range, allowance was made for this in the oxidation calculations for which these temperature calculations were performed.

Table 4.4 Combustion Chamber Temperatures

Test Point	Temperature °C	
	Measured at inlet port	Measured at exhaust port
1500/1bar	58.7	510
1500/2.62	56	554
2000/2bar	54.7	597
2500/5.5	47.5	698
3500/WOT	46.4	745

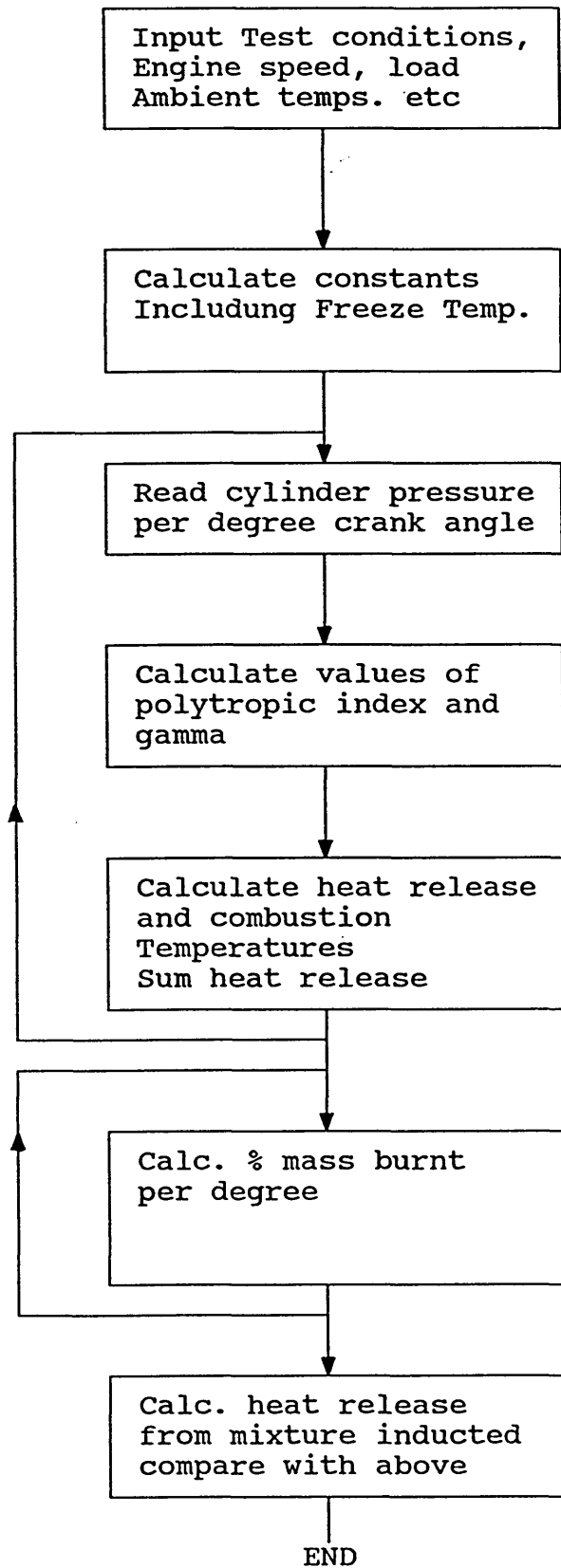


Figure 4.22 Flow Chart for Combustion Analysis

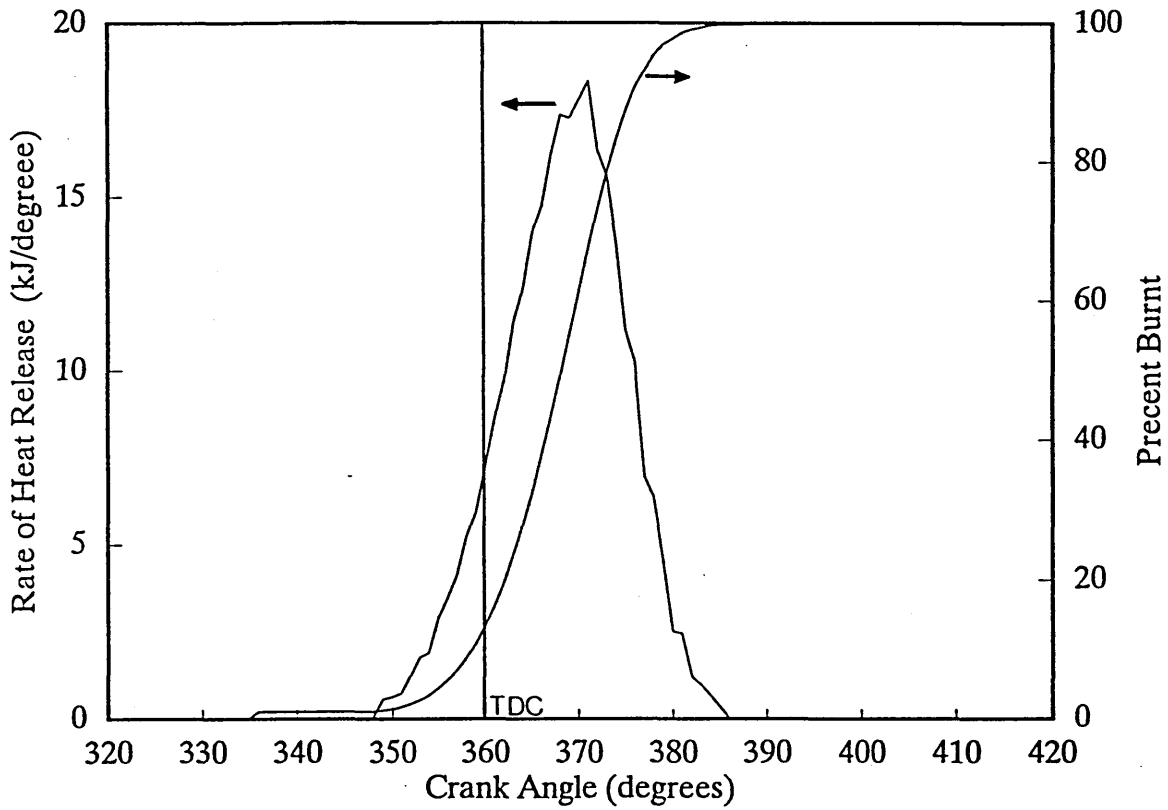


Figure 4.23 Heat release and percentage burnt from combustion model calculations pressure data at 1500 rpm 1 bar bmep, 15:1 AFR, 28 deg timing

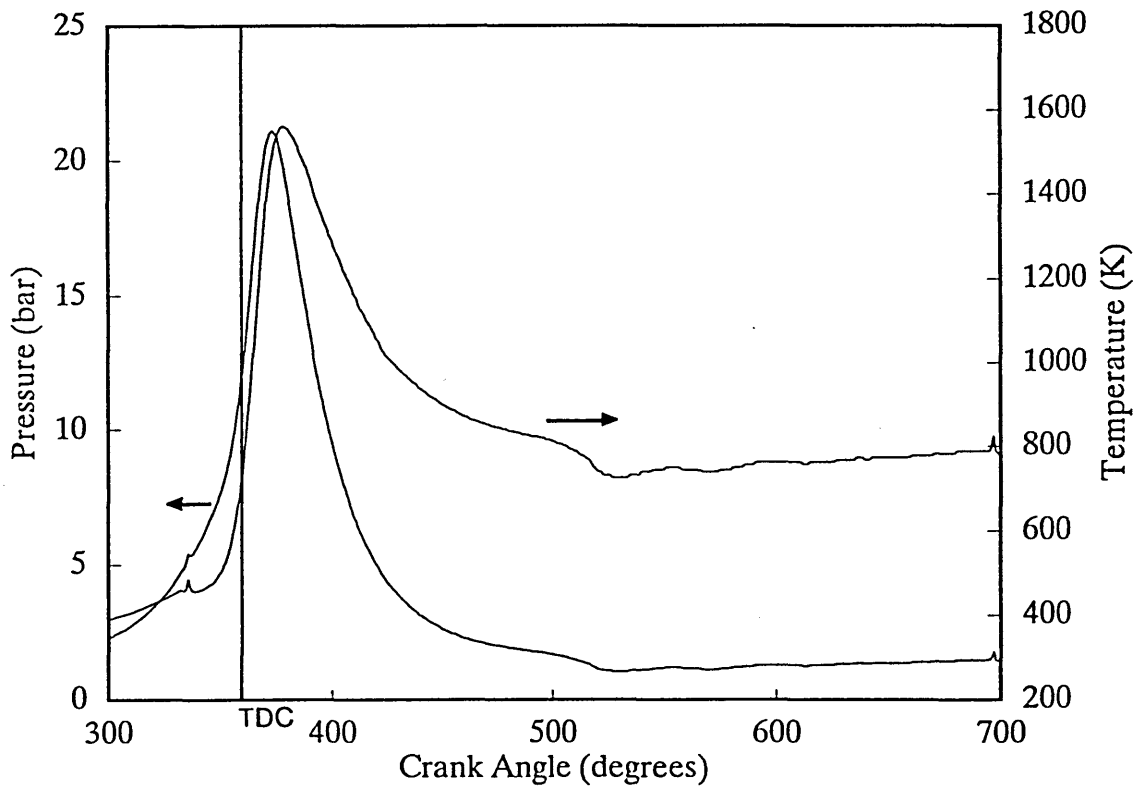


Figure 4.24 Cylinder Pressure and Predicted Temperature from combustion model from pressure data taken at 1500 rpm 1 bar bmep, 15:1 AFR, 28 deg Timing

5. ENGINE TESTS

5.1 Introduction

During the course of this research a series of five engine tests were performed, each with a different piston-liner configuration. The test programme is set out in Table 5.1. As preparation for each of these tests the pistons and liners were accurately measured in the metrology laboratory. This included roundness and surface finish measurements. The surface finish was also measured after the test run. These measurements were used to calculate the crevice volumes and oil layer thickness. Piston and liner dimensions used in these tests are given in Appendix 3.

Table 5.1 Test Programme

Date	Test	Engine Format
June 91	Commissioning	As Production
Jan. 92	Standard	Base line for later tests
June 92	High Top Ring	High top ring pistons, Cylinder liners as Standard
Oct. 92	Smooth Liner	Pistons as Standard Smooth cylinder liners
March 93	Enlarged 2nd Pistons	Vee groove in piston 2nd land, Cyl. liners Standard

The first of these tests was a commissioning test for the equipment and was fitted with normal production pistons and liners. There were three objectives for this test.

- 1, To learn how to operate and obtain accurate results from equipment and instrumentation.

- 2, Ensure equipment and instrumentation were correctly installed and operating to specification.
- 3, Develop and improve test procedures

Result for this test are not reported, because they are not comparable with later tests due to installation of additional instrumentation to the engine.

5.2. Repeatability Between Tests and Engine Builds

To enable reliable hydrocarbon emission comparisons between engine builds repeatability of engine operating conditions must be demonstrated. Experience gained in the first test indicated that engine speed could be set to ± 10 rpm from the dynamometer at a constant speed setting. The torque was dependent on the throttle adjustment and could be set to ± 0.3 Nm of the desired torque. Table 5.2 shows that this produced consistent power output for each test. Therefore any change in the engine's performance would be observed in an observable trend in specific fuel consumption, thermal and volumetric efficiencies. These were found to compare very closely with the standard build, Table 5.2 compares the average data for each build at 2000rpm 2bar bmep. These are average readings subject to a similar variability. Coolant and oil temperatures were monitored, emissions were sampled only when these had stabilised at temperatures identified during the standard test.

Table 5.2 Comparison of Performance with Standard build

	Variation from Standard at 2000 rpm 2bar bmep		
	High Top Ring	Smooth liner	Enlarged 2nd Land
Power kW	-0.4 %	-0.2 %	-1.3 %
bsfc g/kWh	-3.4 %	-1.3 %	+2.3 %
Thermal Efficiency	0.0 %	0.0 %	-5.0 %
Volumetric Efficiency	-0.0 %	+3.4 %	+3.4 %
NOx g/kWh	-12.2 %	-13.4 %	+14.4 %

5.3. Standard Test

After the initial test, the modifications discussed in Chapter 3 were undertaken and the next test was prepared. The objective of this test was to define a standard for comparison with future piston designs. The set of pistons and liners for this test were machined to closer tolerances than production pistons to reduce crevices to a minimum, Table 5.3 gives the average piston and liner dimensions and the crevice volumes arising from them, actual dimensions are listed in Appendix 3.

Table 5.3 Standard Piston and Liner Dimensions

	Diameter	Height	Crevice Volume mm ³	
			Top Land	Ring Groove Volume
Top Land	74.55mm	6 mm	296.35	359.9
2nd Land	74.441mm	3.85mm	241.83	422.9

To ensure an accurate standard set of emission and operational data a large number of runs were made with this set of pistons. Each day's test data was critically assessed before testing commenced the following day any variation in operating conditions which would affect the emissions were identified, the run was repeated if necessary.

5.3.1. Standard Test Results

Emissions data from each test point was recorded. Accumulated data for each test point was brought together and the average and standard deviation were calculated. Average hydrocarbon emissions at each test point taken at the exhaust port and pipe are plotted in Figure 5.1. The error bars show the standard deviation. It can be seen that for most test points the standard deviation is quite small, between 2.8% and 5.5% of the average. This graph shows the high level of oxidation which occurs in the exhaust manifold. Variations between each cylinder were observed, Figure 5.2, shows this and the air fuel ratio at 2000 rpm 2 bar bmep. Variations in the air fuel ratio are due to the inlet manifold and injector timing not giving consistent mixture preparation for each cylinder. Nitric oxide and carbon monoxide emissions are plotted in Figures 5.3 and 5.4 and follow trends predicted by literature. Although hydrocarbon emissions are of primary interest these others were also monitored to ensure consistency of test data.

The flow of crankcase gases (blow-by), Figure 5.5. was measured, this can affect hydrocarbon emissions and is

an indication that piston rings are sealing effectively. In addition to the tests on the reference unleaded petrol tests were also performed with trimethyle pentane as fuel. The hydrocarbon emissions from these tests are plotted in Figure 5.6. Although the level of emissions are larger than for petrol they both follow a similar trend with substantially lower emissions at 3500 rpm wide open throttle.

Two further tests were carried out using two different engine lubricants to compare hydrocarbon emissions, a multi grade from a different source and a fully synthetic lubricant. The hydrocarbon emissions were little changed from either oil, Figures 5.7 and 5.8. Gas chromatography also gave similar results.

5.3.2. Gas Chromatography

The results were obtained using the methods specified in chapter 3.2.2. The objectives for using gas chromatography were to identify changes in the balance of species from the different piston/liner configurations. This would complement the total emission data and supply further information by identifying whether the hydrocarbon emissions were unburnt fuel or products of pyrolysis. Previous research has identified up to sixty species in exhaust emissions. For a comparison of piston designs only the largest and most significant species were chosen. These were a selection of the three main types of hydrocarbon compound found in emissions, Alkanes, Alkenes and Aromatics. Each group contains fuel components and pyrolysis products. Thirteen species were chosen, because

these were the largest and most consistent peaks which were detected in the standard test. These usually accounted for approximately 75% of the total gas chromatograph trace, and are listed in Table 5.4.

Alkanes have only single bonds between carbon atoms and the general formula for these compounds is C_nH_{2n+2} , where n is the number of carbon atoms. They are often referred to as saturated hydrocarbons because they are the least reactive of these groups and do not react readily with certain reagents.

Alkenes are similar to the alkanes except that they have one double carbon-carbon bond, the general formula is C_nH_{2n} . They are referred to as unsaturated, because the double bond makes them more reactive.

Aromatics are cyclic unsaturated compounds with several double carbon-carbon bonds. The base for these is usually the benzene ring containing 6 carbon atoms forming a hexagon with alternate double bonds. Additional methyl groups (CH_3) can be attached to this ring to form toluene (1 methyl group) and the xylenes (2 methyl groups). The general formula is C_nH_{2n-6} .

It can be observed from Figure 5.9, GC plots from reference unleaded gasoline and emissions, that there was a significant reduction in the number of peaks detected in the emissions than from fuel. Also, unburned fuel species do not survive the combustion process in equal proportions, and some C1 to C3 hydrocarbons are not present in gasoline but are products of incomplete combustion. Many components of fuel are not detected in the emissions. Dempster and

Shore (59), identified that a greater part of the hydrocarbon emissions would be combustion products. The percentage concentration of these species are plotted in Figure 5.10 and shows the predominance of product species over fuel species.

Table 5.4 Selected Hydrocarbon Species

peak No	Group and Name	Formula
ALKANES		C_nH_{2n+2}
1	Methane	CH_4
3	Ethane	C_2H_6
6	Butane	C_4H_{10}
9	2,2,4, Trimethyle pentane	C_8H_{18}
10	2,4, Dimethyle hexane	C_8H_{18}
ALKENES		C_nH_{2n}
2	Ethene (ethylene)	C_2H_4
4	Propene (propylene)	C_3H_6
5	Isobutene	C_4H_8
7	pent-1-ene	C_5H_{10}
AROMATICS		C_nH_{2n-6}
8	Benzene	C_6H_6
11	Toluene	C_7H_8
12	P-Xylene	C_8H_{10}
13	O-Xylene	C_8H_{10}

The use of trimethyle pentane as fuel indicates the level of pyrolysis which can occur, because it is a single component fuel other hydrocarbons detected in the emissions must originate from this compound there being no other source for the concentrations measured. Figure 5.11 shows a gas chromatograph plot of an emissions sample taken at 2000 rpm 2 bar bmep. From the data generated with gas chromatography trimethyle pentane comprised 48% of the hydrocarbons detected by the gas chromatograph. Other

species detected were pent-1-ene 22.6 %, propene 10.6 % and ethene 8.5 %. These species are products of pyrolysis formed from trimethyle pentane, similar results were observed by Dempster and Shore (59).

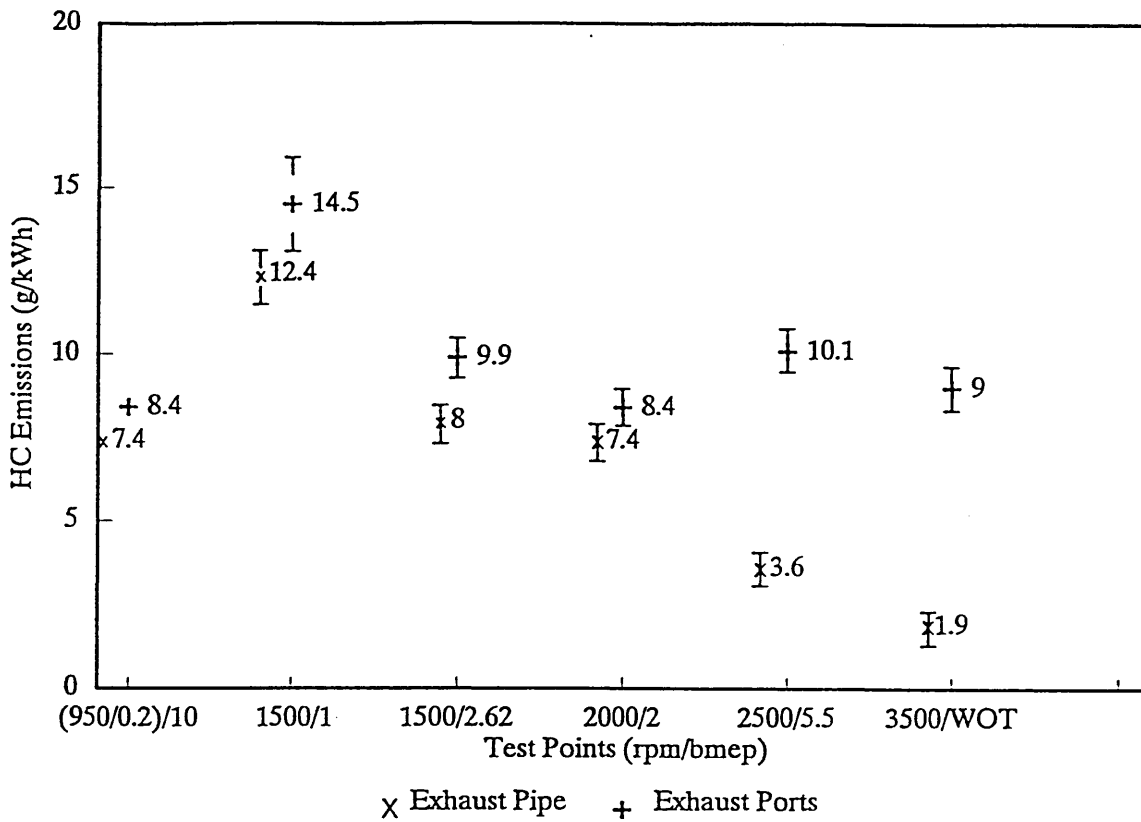


Figure 5.1 Hydrocarbon Emissions from standard build, a comparison between samples taken at the exhaust ports and pipe.

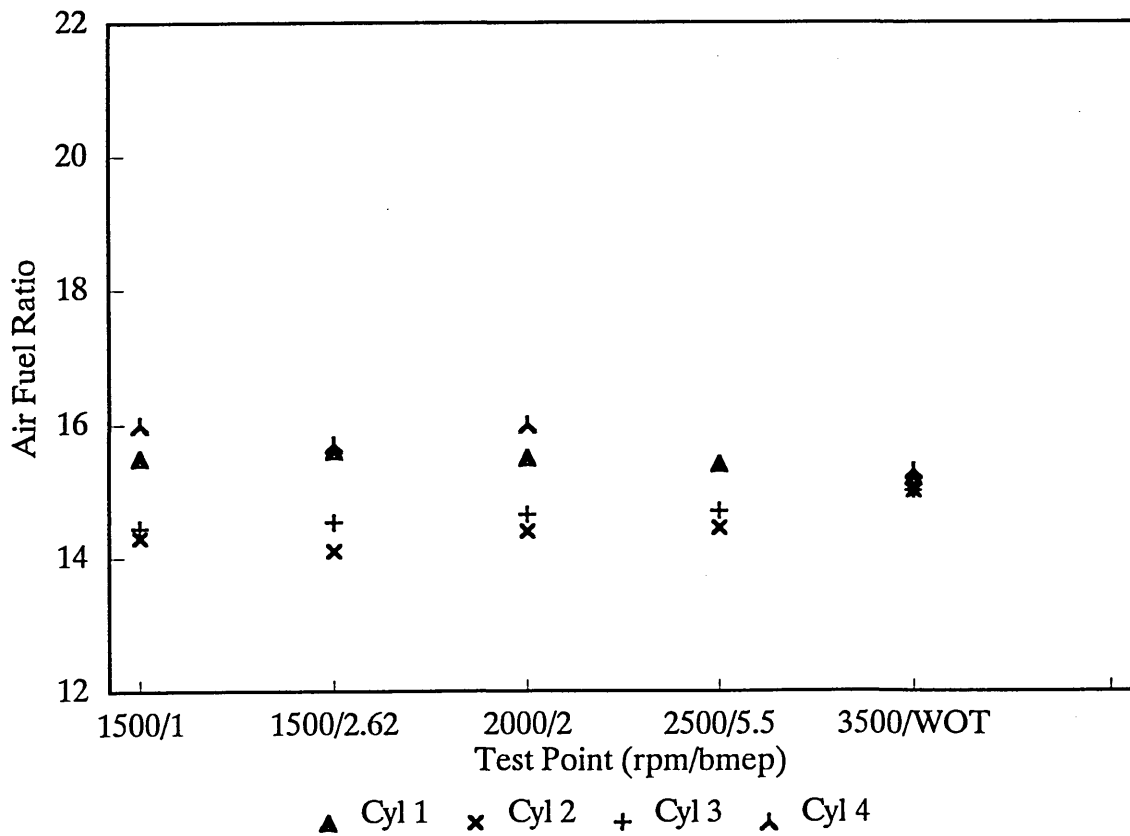


Figure 5.2 Variation in air fuel ratio between cylinders

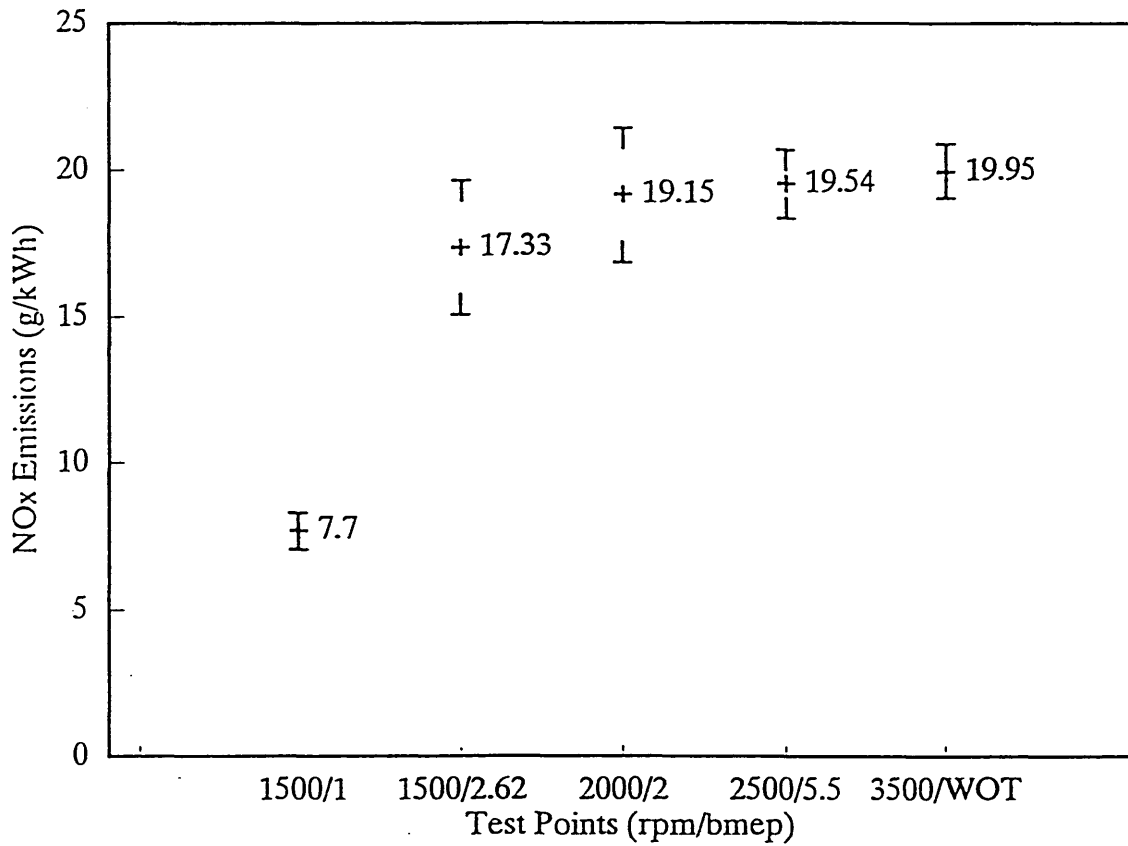


Figure 5.3 Nitric oxide emissions from standard pistons

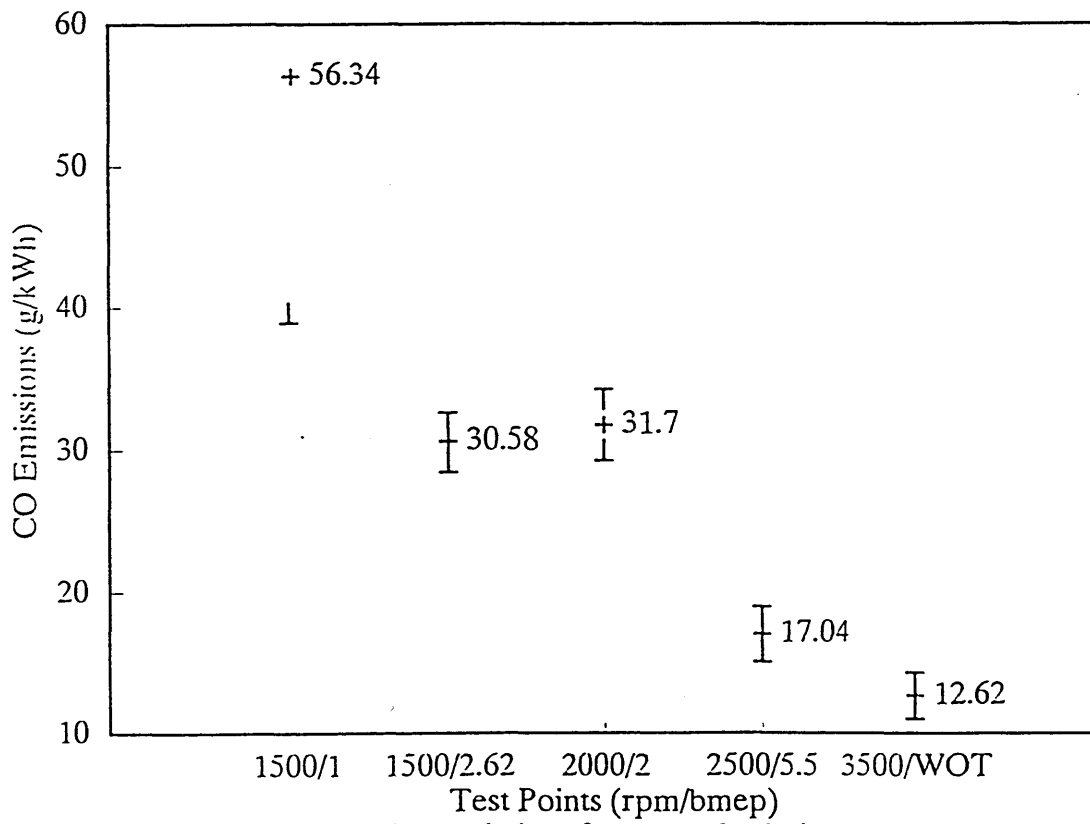


Figure 5.4 Carbon monoxide emissions from standard pistons

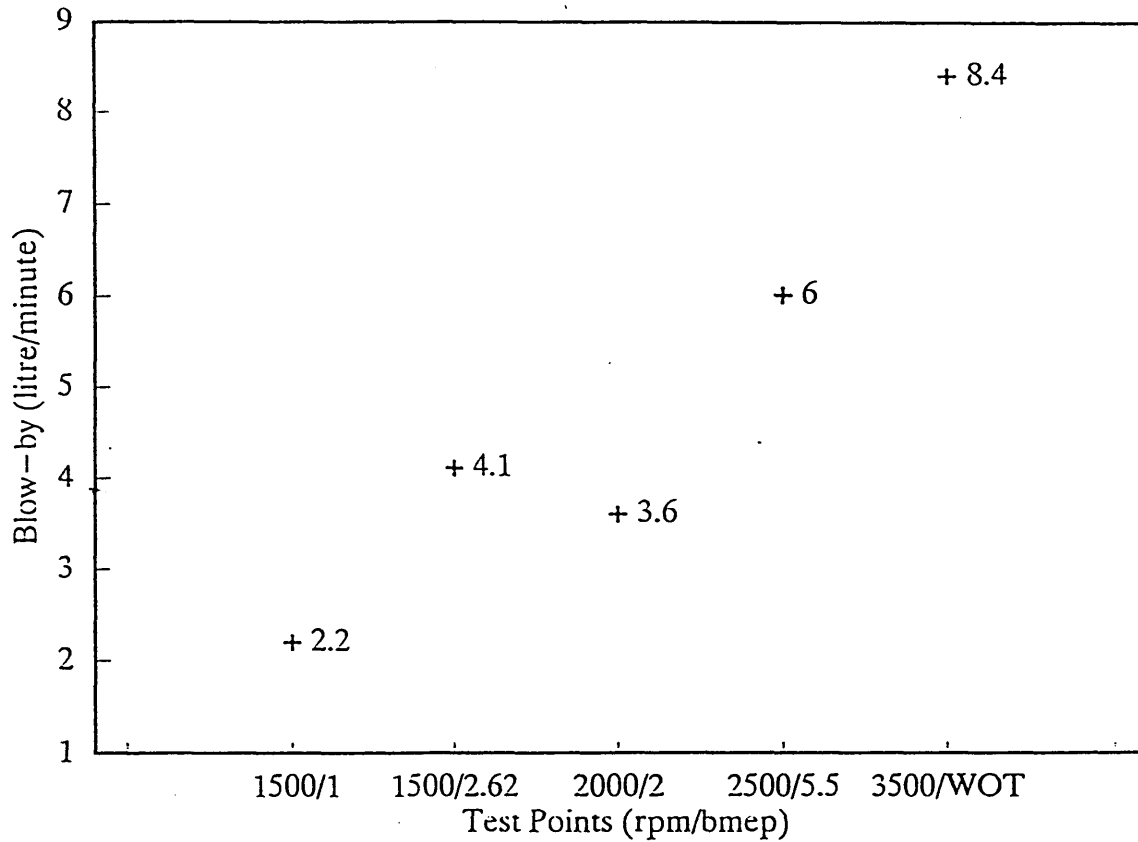


Figure 5.5 Blow-by from standard pistons

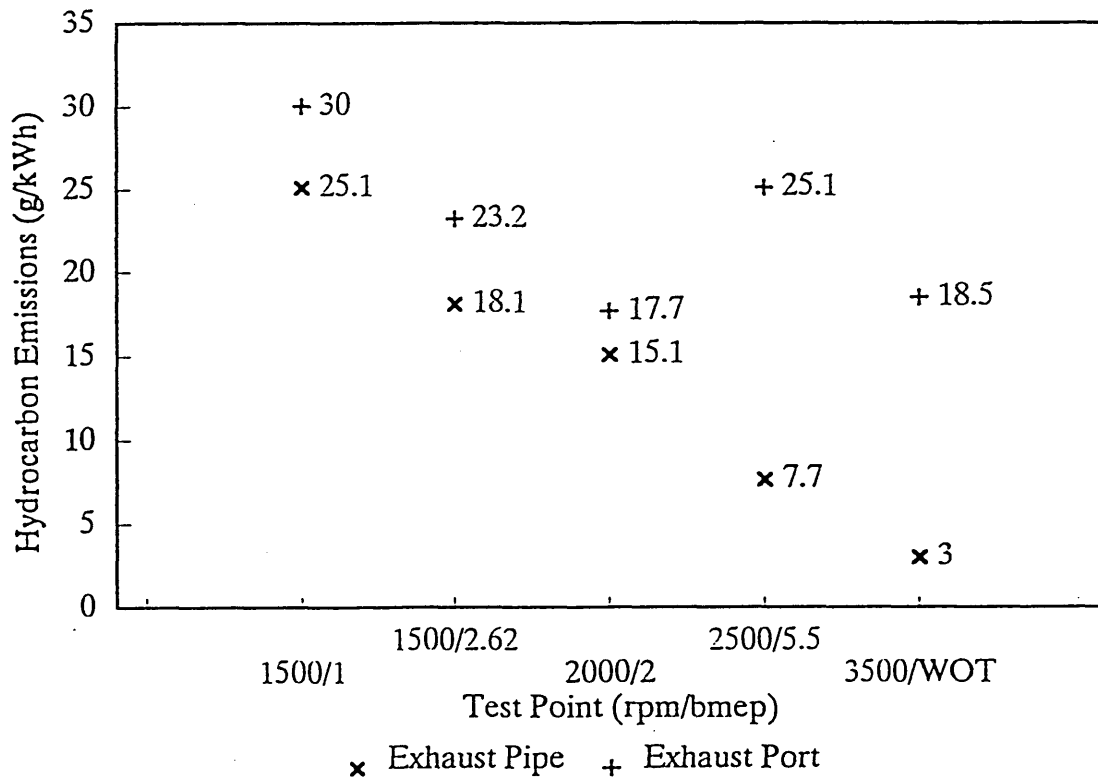


Figure 5.6 Hydrocarbon Emissions from standard build from port and pipe. Trimethyle pentane as fuel

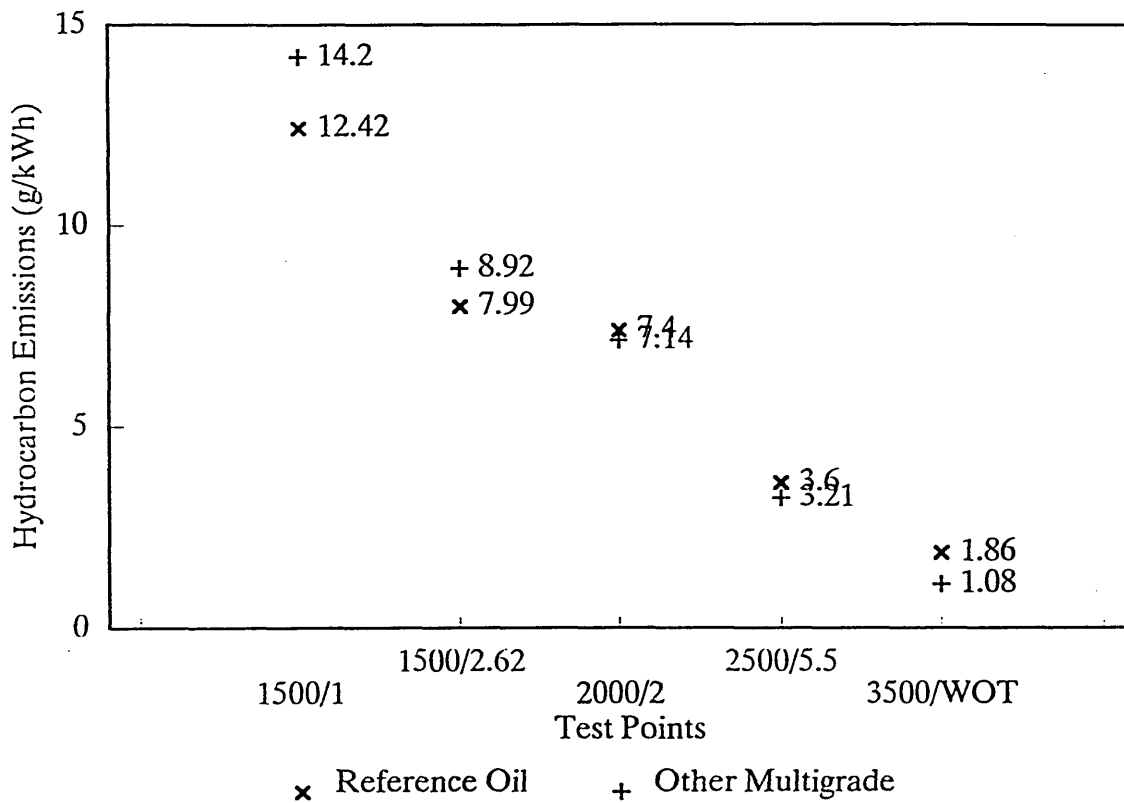


Figure 5.7 Comparison of hydrocarbon emissions from reference oil and a different multigrade oil

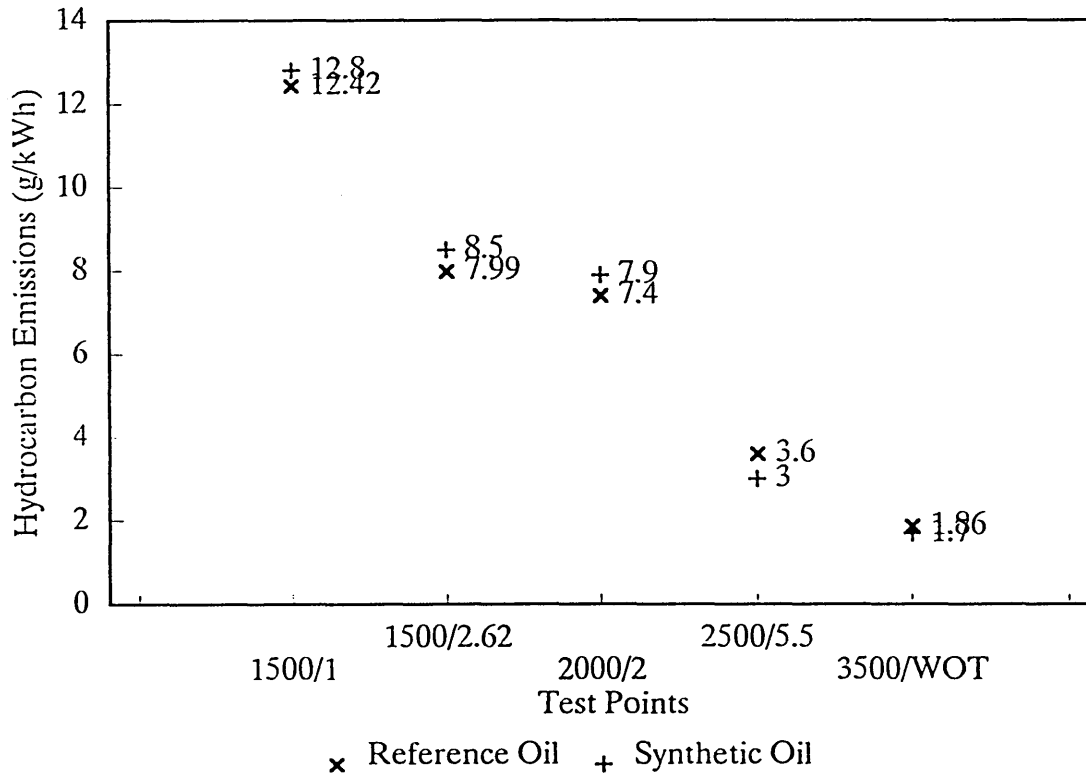


Figure 5.8 Comparison of hydrocarbon emissions from reference oil and synthetic oil

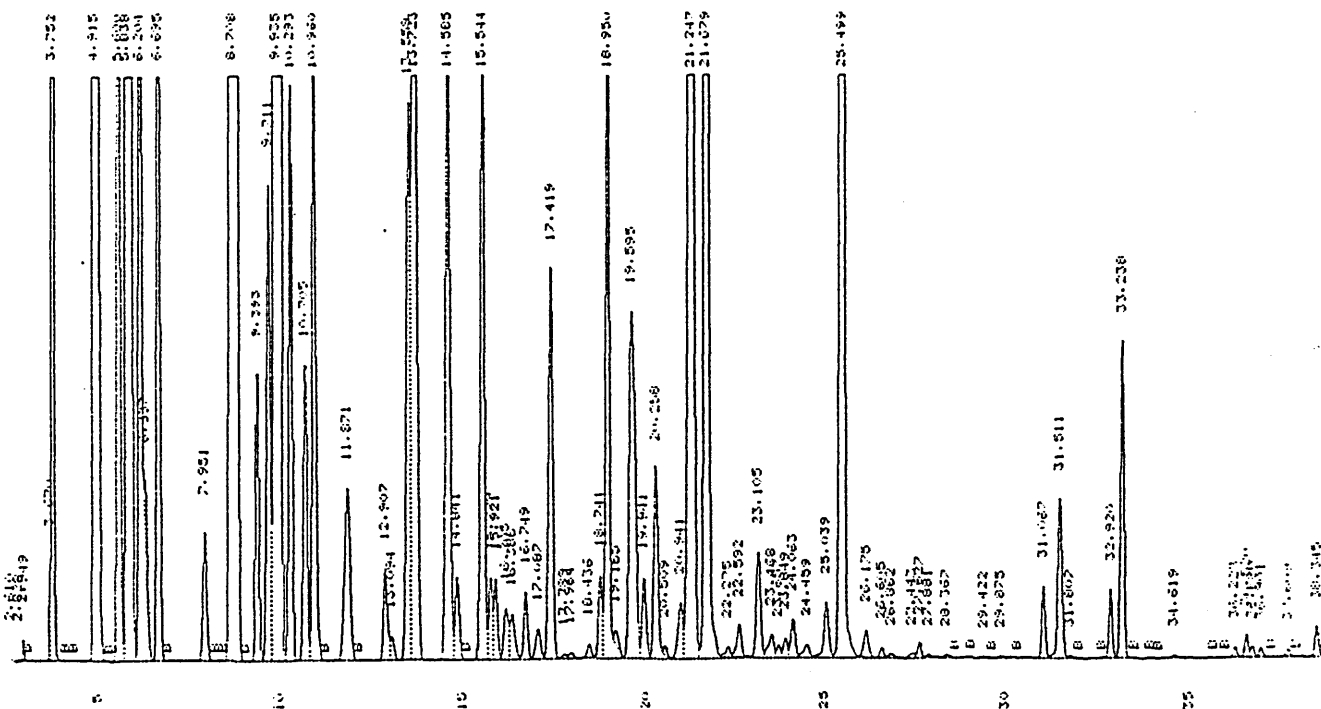


Figure 5.9 a Gas chromatography plot of reference fuel

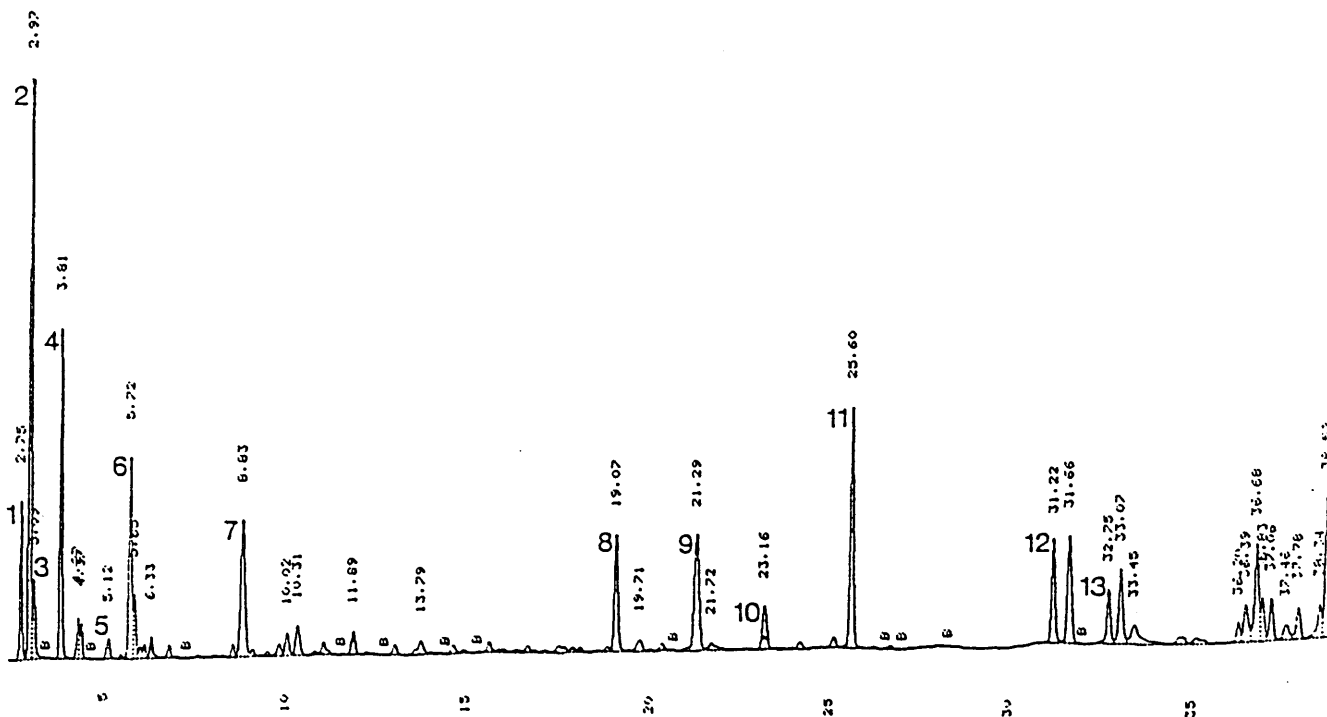


Figure 5.9 b GC plot of emissions at 2500 rpm 5.5 bar bmep using standard pistons

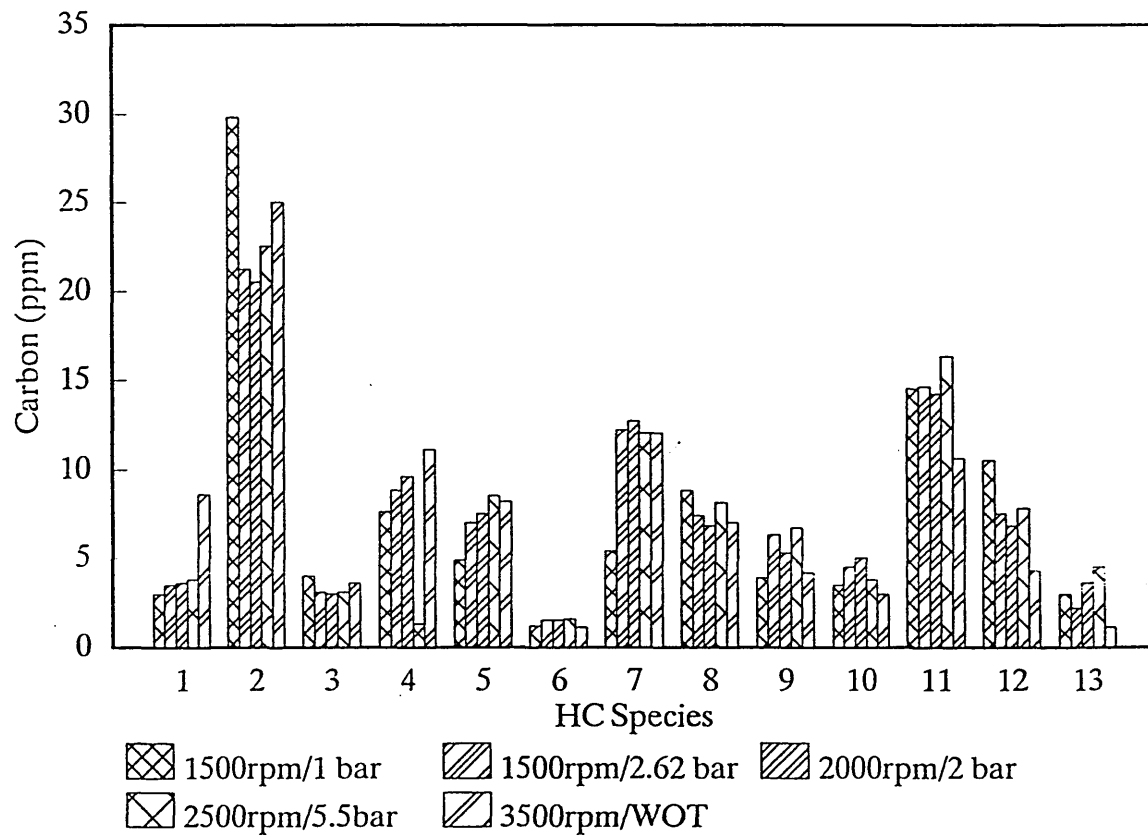


Figure 5.10 Percentage concentrations of 13 hydrocarbon Species from Standard Build

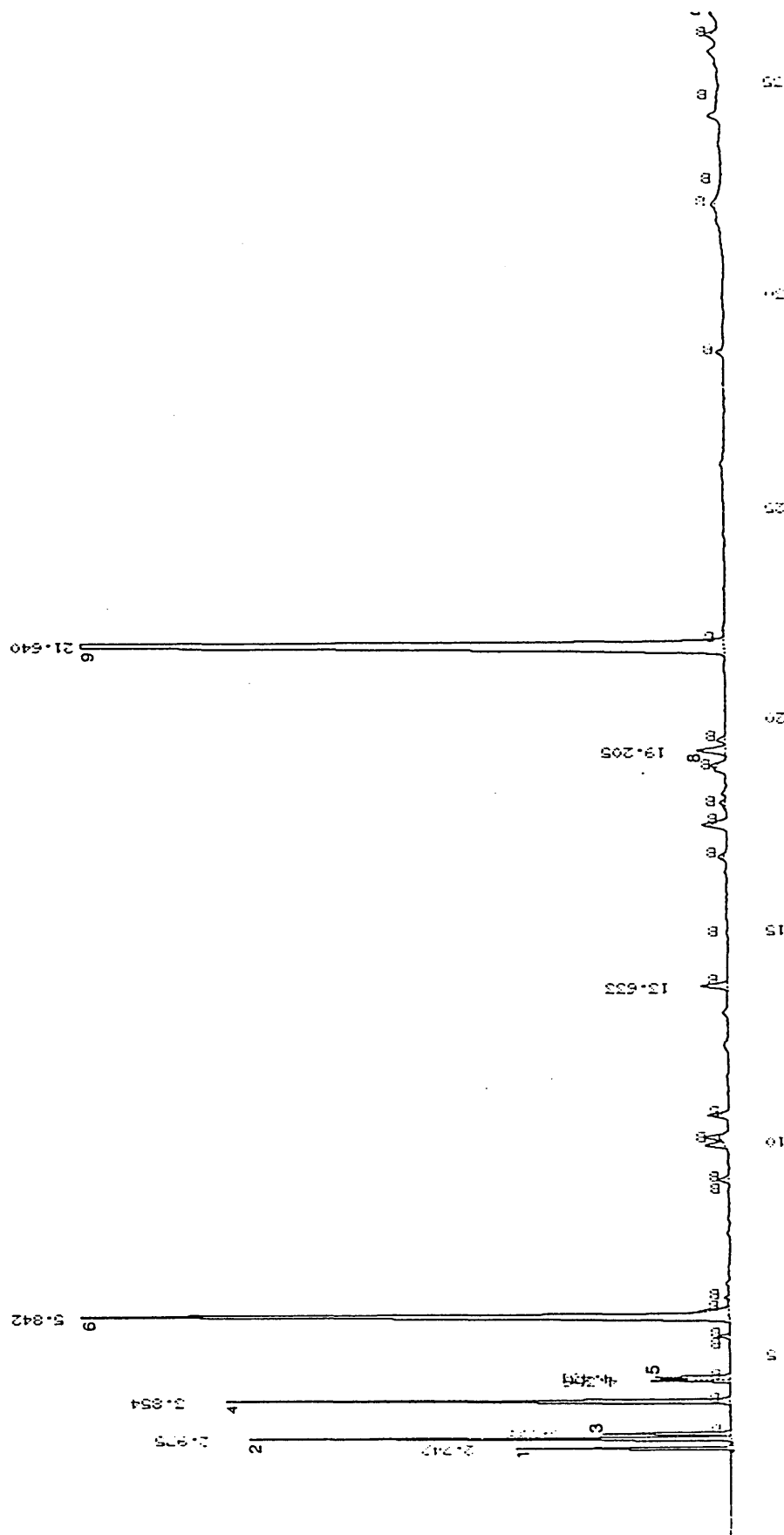


Figure 5.11 Gas chromatograph plot Using Trimethyl Pentane as fuel, sample taken at 2000 rpm 2 bar bmep

5.4. Reducing Top Land Crevice Volume

The effect that the top land has on hydrocarbon emissions is well reported. Namazian and Heywood [12] showed that the reduction in emissions was directly proportional to the top land crevice volume. In a series of tests, Wentworth [5] used a piston and ring configuration to completely seal off the piston crevice volume, achieving significant reductions in emissions. However, it was the objective of this research to produce practical designs suitable for use in modern automotive engines.

A set of pistons were manufactured with the smallest top land which could be run without failure in this engine for the type of testing performed. The top land height was 2.8 mm, compared with the standard of 6mm. The 2nd piston ring was also moved up the piston. This had the effect of reducing the top land volume, but kept the 2nd land volume similar to the standard pistons. A sketch of this piston is given in Figure 5.12. The 2nd land volume is also a source of hydrocarbon emissions, and it was the intention to change only one source at a time. This has given the pistons a very large 3rd land volume, but this is not thought to affect the emissions as mixture entering this region flows into the crankcase as blow-by. Detailed measurement of pistons and liners indicated that the top land crevice volume was reduced by 35%. If the volume behind top ring groove is included as part of the top land crevice region the reduction in volume was only 16.9%.

The average crevice volumes for these pistons are listed in Table 5.5, Actual piston dimensions are given in Appendix 3. The cylinder liner was as standard test.

Table 5.5 High Top Ring Piston and Liner Dimensions

	Dia	Height	Crevice Vol mm ³	% change relative to Standard	
				top land	including ring groove
Top Land	74.38mm	2.8 mm	192.197	-35	-16.9
2nd Land	74.45mm	3.85mm	200.93	+16	+6.2

5.4.2 Hydrocarbon Emissions

Hydrocarbon emissions were successfully and repeatably obtained for a series of 5 runs. Significant reductions in hydrocarbon emissions were observed at most test points. Figure 5.13 compares these emissions at the exhaust pipe with those from standard pistons. Exhaust port emissions are shown in Figure 5.14. From these graphs it can be seen that the greatest reductions occur at the higher speeds and loads. The standard deviation bands are similar at each test point, but there are only two test points where these error bands do not overlap. The reductions achieved are shown as a percentage of the standard in Figures 5.15 and 5.16. At higher speeds, reductions were over 25%. Similar reduction in hydrocarbon emissions were observed with trimethyle pentane as fuel, Figure 5.17. Blow-by

measurement, Figure 5.18, does not follow a consistent trend for all test points.

5.4.3. Gas Chromatography

The gas chromatography results indicated that the reduction in emissions were not uniform for all hydrocarbon species. Figure 5.19 is a plot taken at 2000 rpm 2 bar bmep. For comparison between standard and high top ring pistons the ppm value for a particular species from the standard build is subtracted from the value for the high top ring piston. Figure 5.20 compares the species at each test point. Positive bars show an increase from the standard.

For further comparison the details of the speciation require closer inspection. The three main groups of compounds will be treated separately, these are; Alkanes, Alkenes and Aromatics.

The differences in Alkanes are plotted in Figure 5.21. All have been reduced in concentration, the reduction being greater for the fuel species, 2,2,4 trimethyl pentane and 2,4, dimethyl hexane. At some test points 2,2,4, trimethyl pentane is not detected and apart from the anomaly at 1500 rpm 1 bar bmep, 2,4, dimethyl hexane is reduced to very small amounts. The amount by which 2,4, dimethyl hexane is reduced decreases as the speed and load increase. This trend can be observed in Figure 5.21. Methane and ethane are reduced by a lesser amount.

The Alkenes, Figure 5.22, have also been reduced,

particularly Pent-1-ene and ethene.

The aromatics indicate an increasing trend with higher loads although at low load there is a decrease in emissions. At higher loads there is a significant increase in the xylenes. Both benzene and toluene produce a lesser proportion of emissions than for standard pistons, Figure 5.23

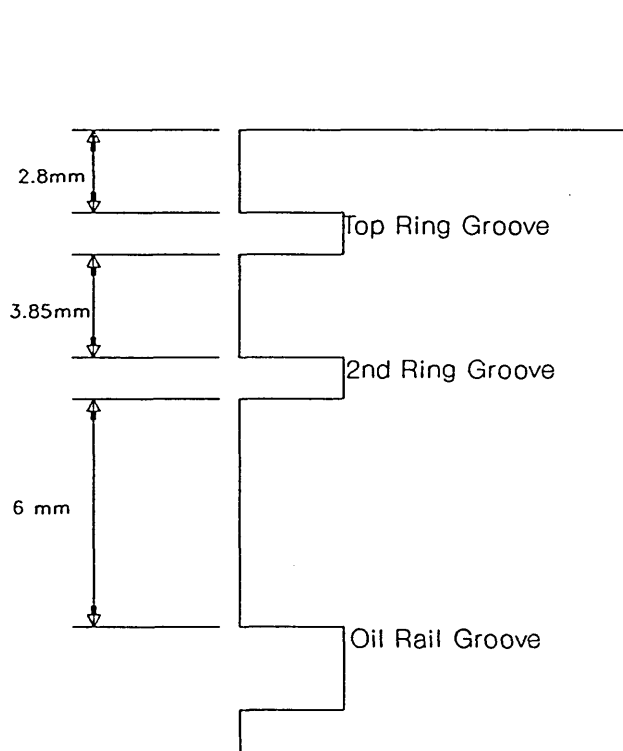


Figure 5.12 High Top Ring Piston

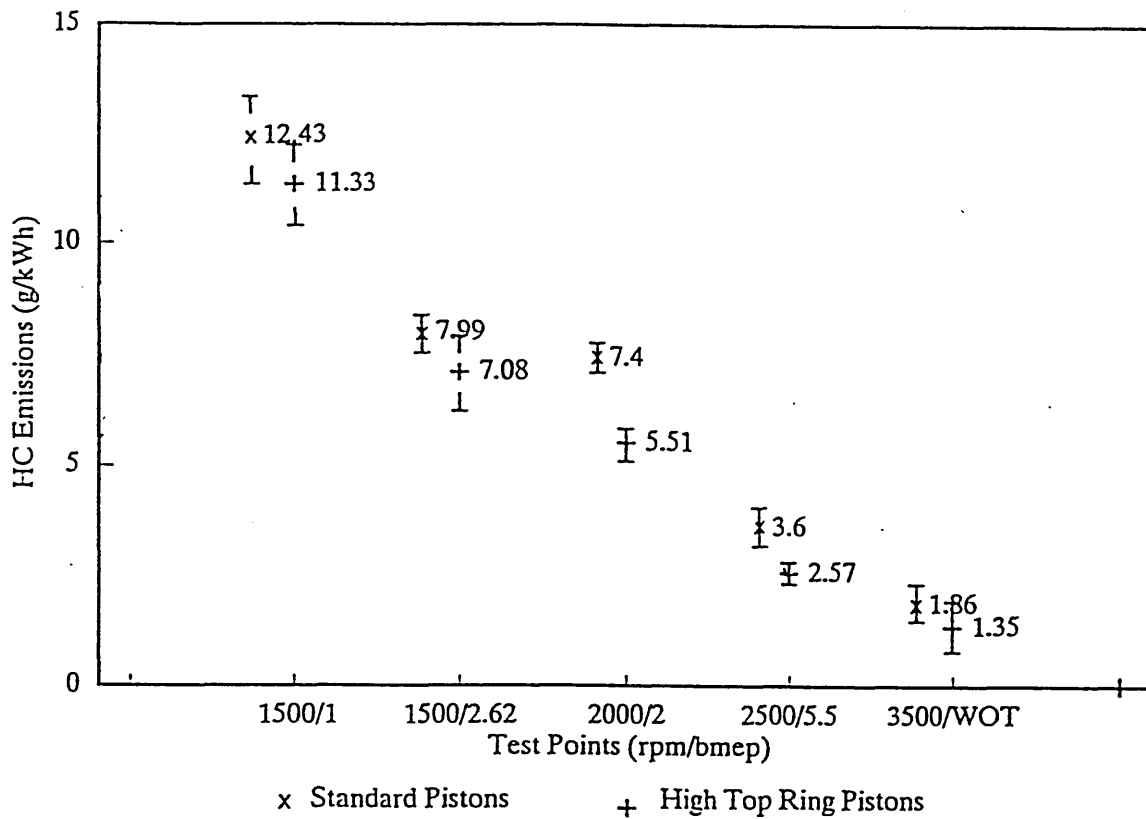


Figure 5.13 Comparison of Hydrocarbon Emissions from standard and High Top Ring Pistons, at Exhaust Pipe

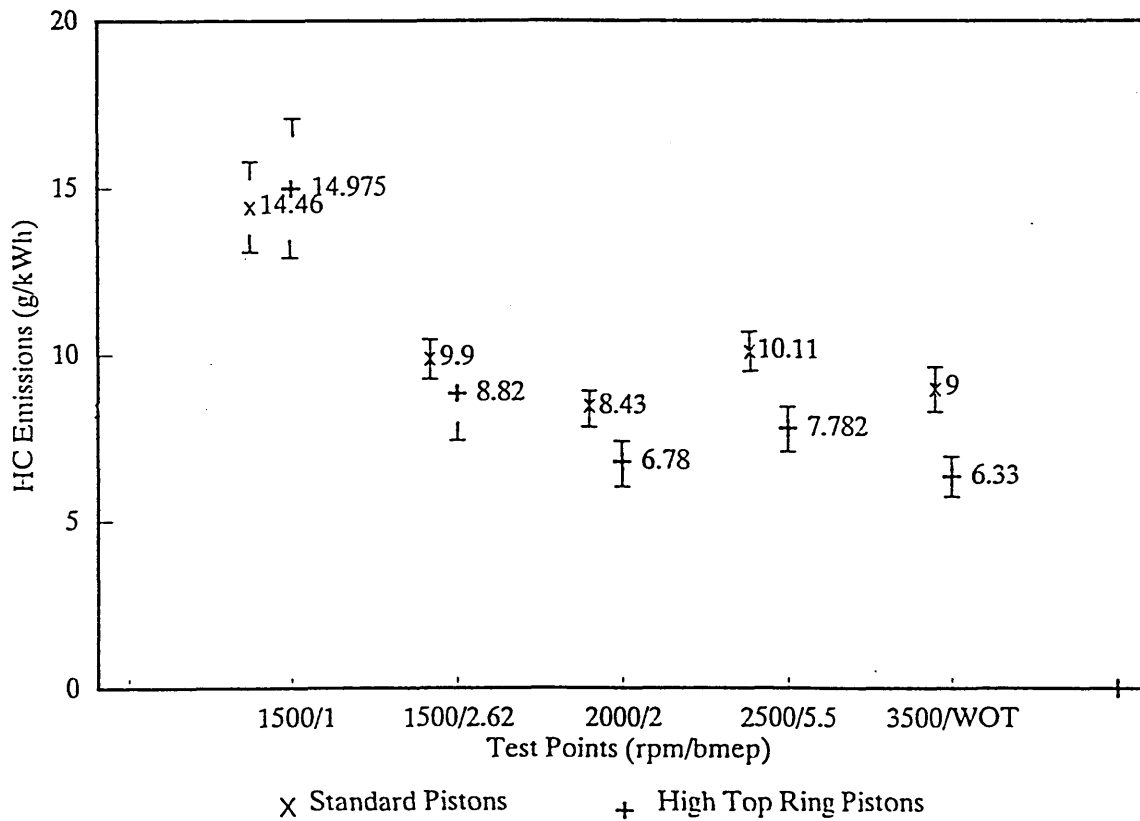


Figure 5.14 Comparison of Hydrocarbon emissions between standard pistons and high top ring pistons, samples taken at the exhaust ports.

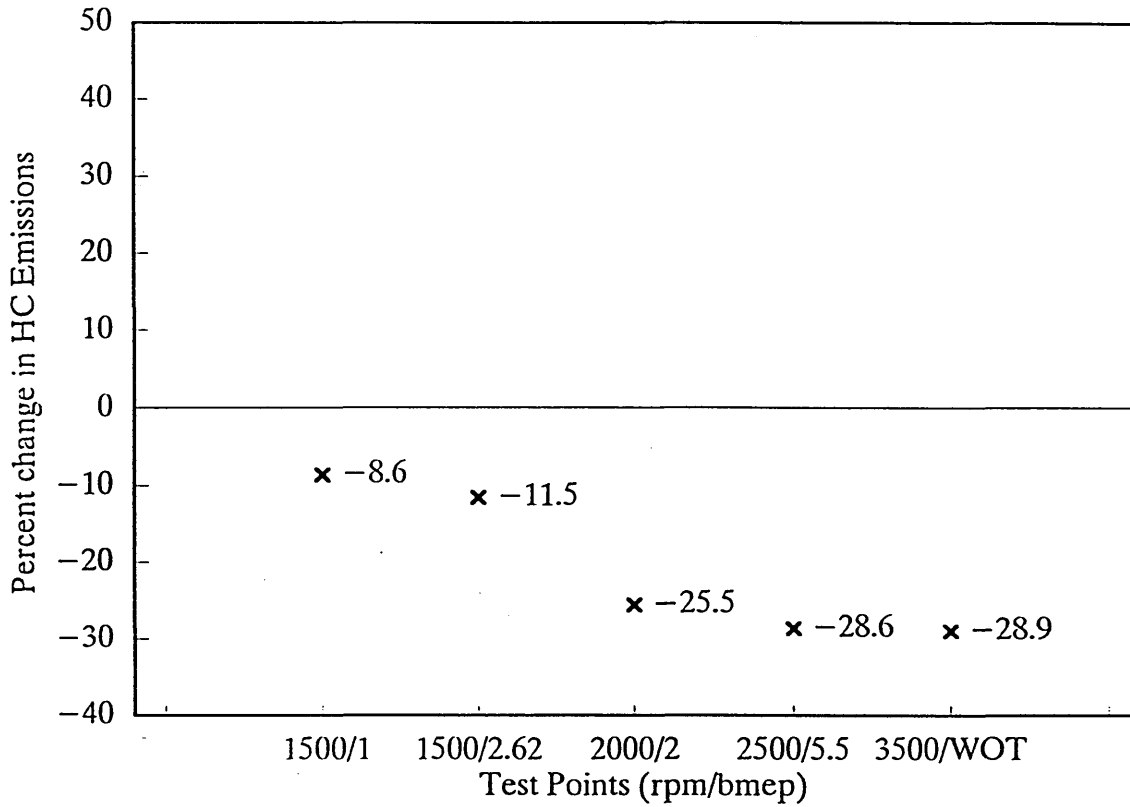


Figure 5.15 Percentage change in hydrocarbon emissions for crevice volume changes High top ring piston at exhaust pipe.

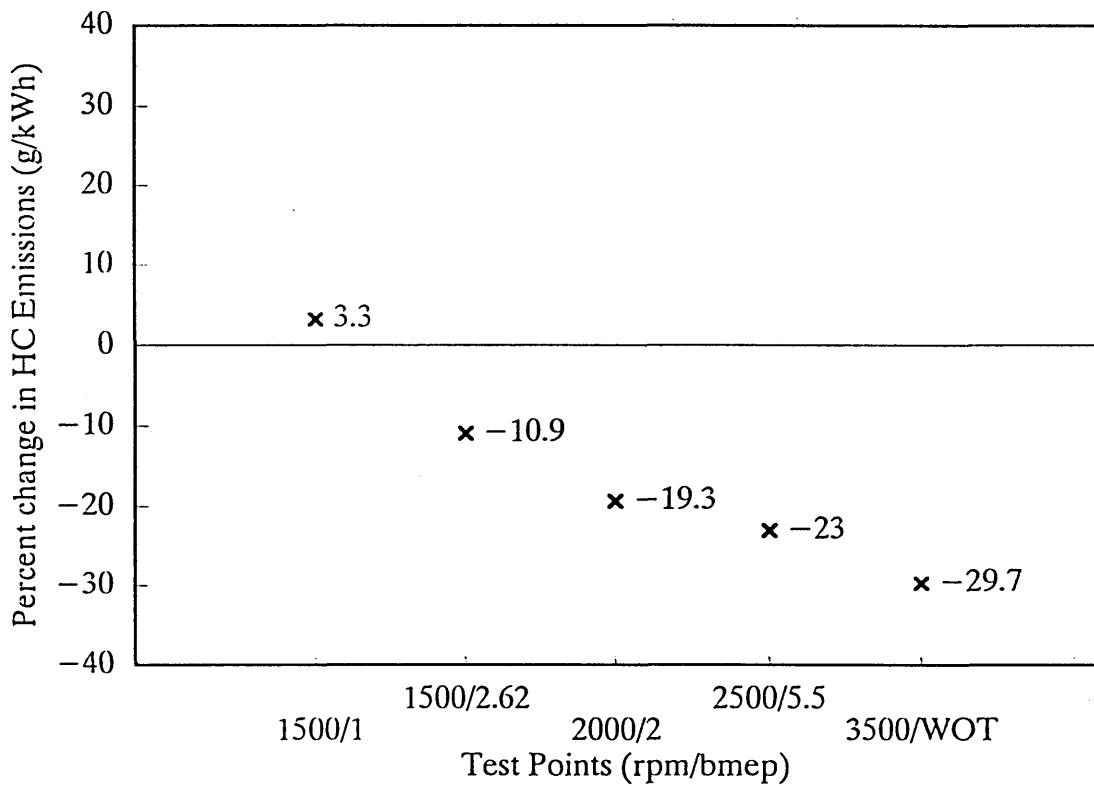


Figure 5.16 Percentage change in hydrocarbon emissions for changes in crevice volume High top ring pistons at exhaust ports.

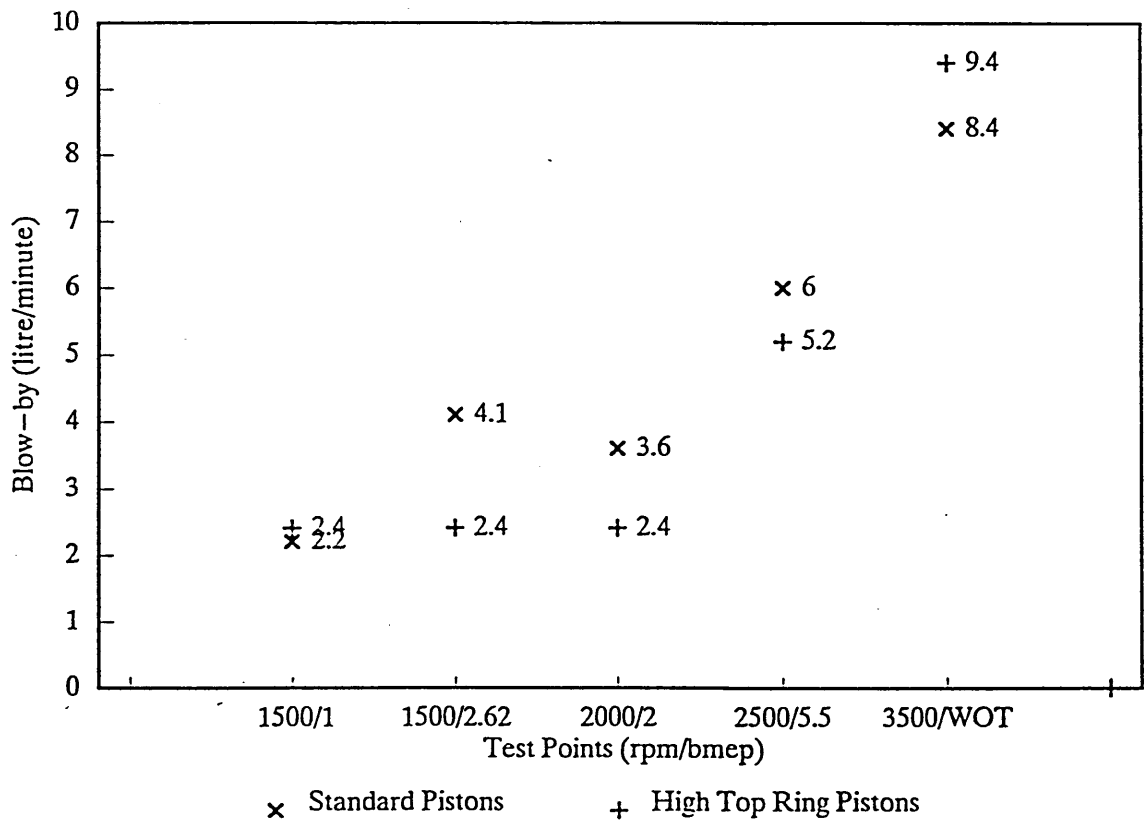


Figure 5.18 Comparison of Blow-by between Standard and High Top Ring Pistons

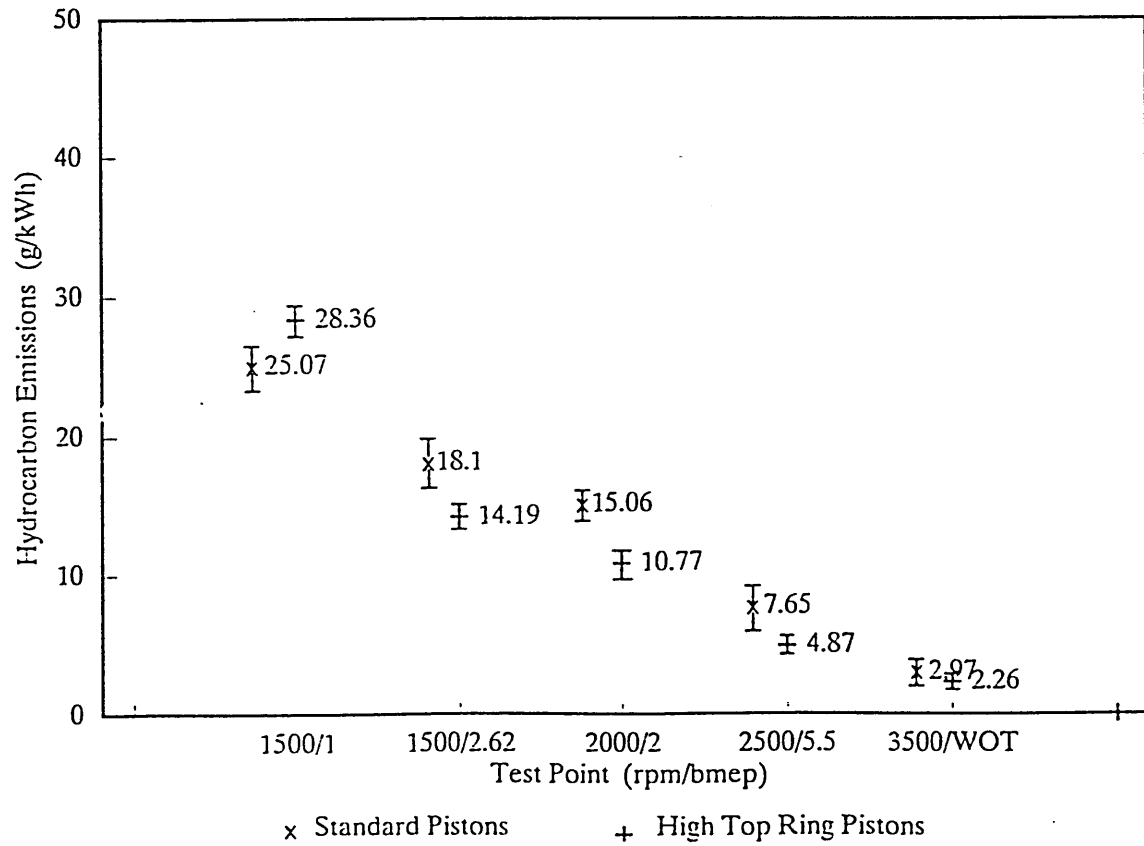


Figure 5.17 Comparison of Hydrocarbon Emissions from standard and High Top Ring Pistons, Trimethyle Pentane Fu

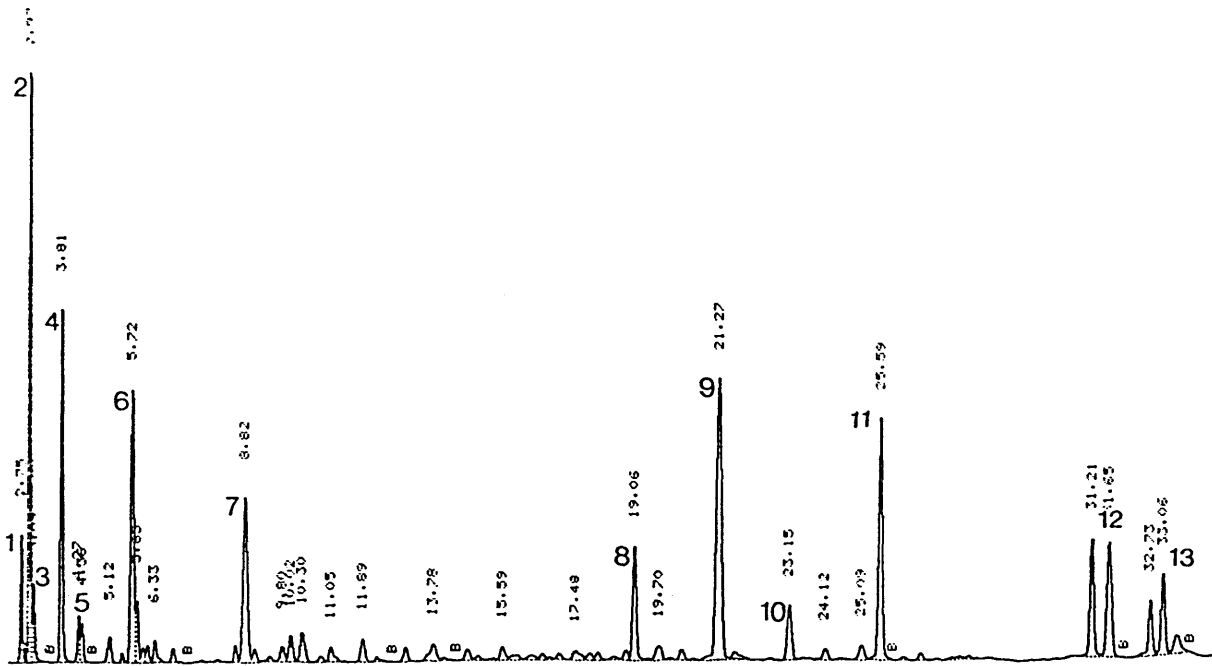


Figure 5.19.a. Gas chromatograph plot from standard pistons, sample taken at 2000 rpm 2 bar bmep

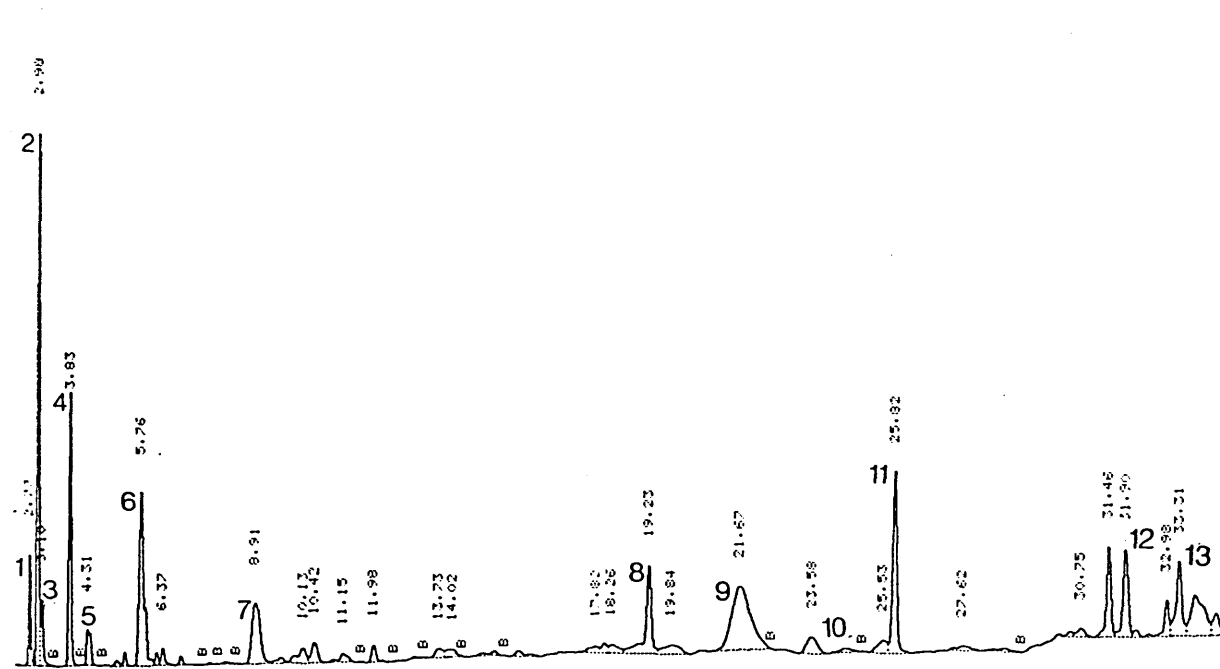


Figure 5.19.b. Gas chromatograph plot from high top land pistons, sample taken at 2000 rpm 2 bar bmep

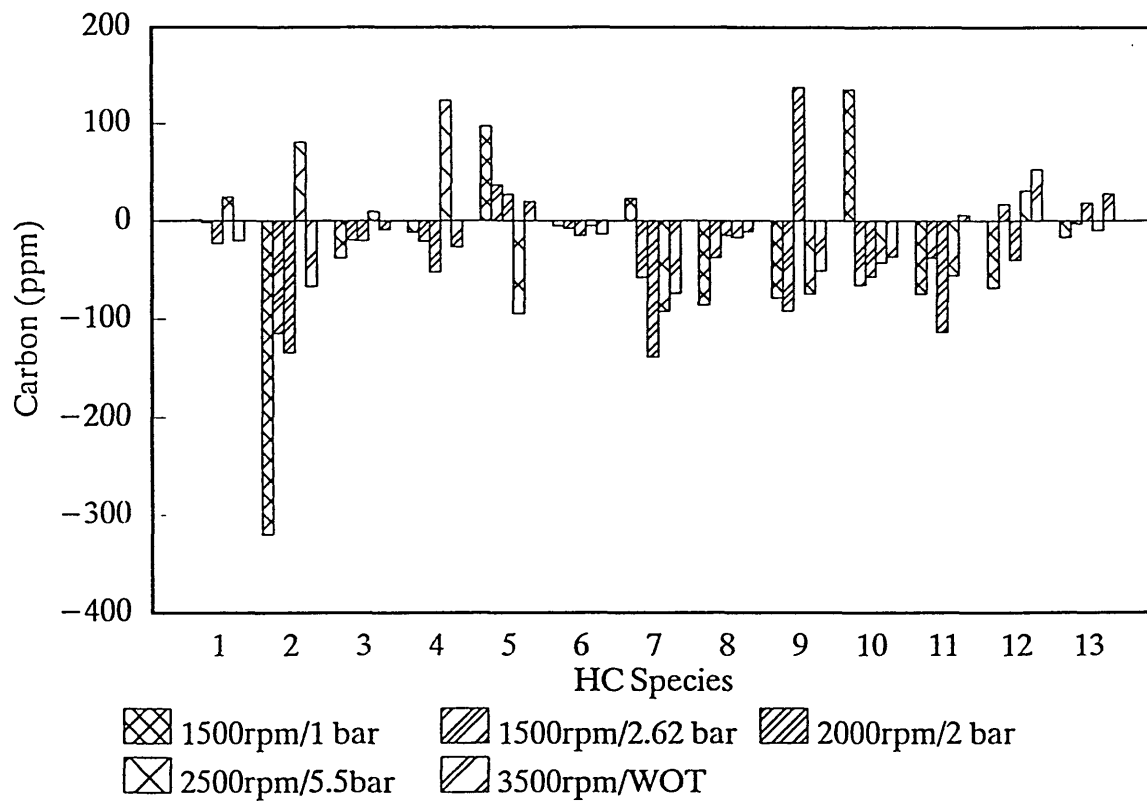


Figure 5.20 Comparison of 13 Species from High Top Ring Pistons against standard build

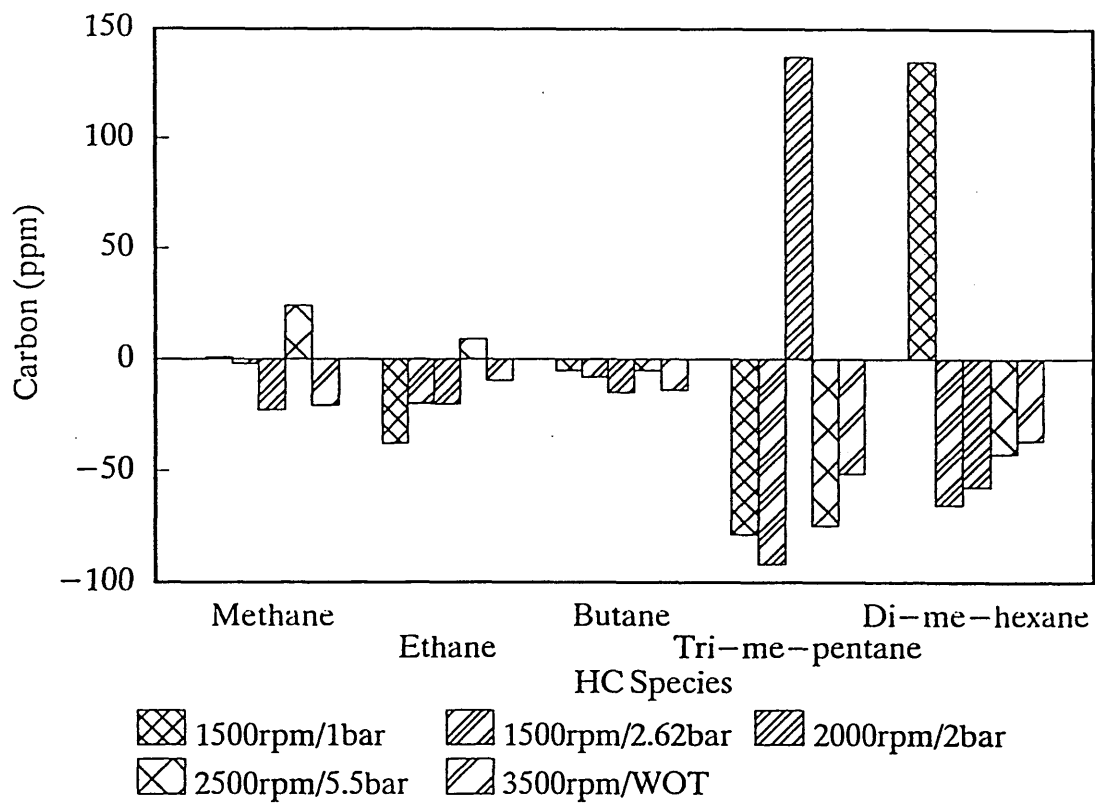


Figure 5.21 Comparison of ALKANES from high top ring piston and standard build

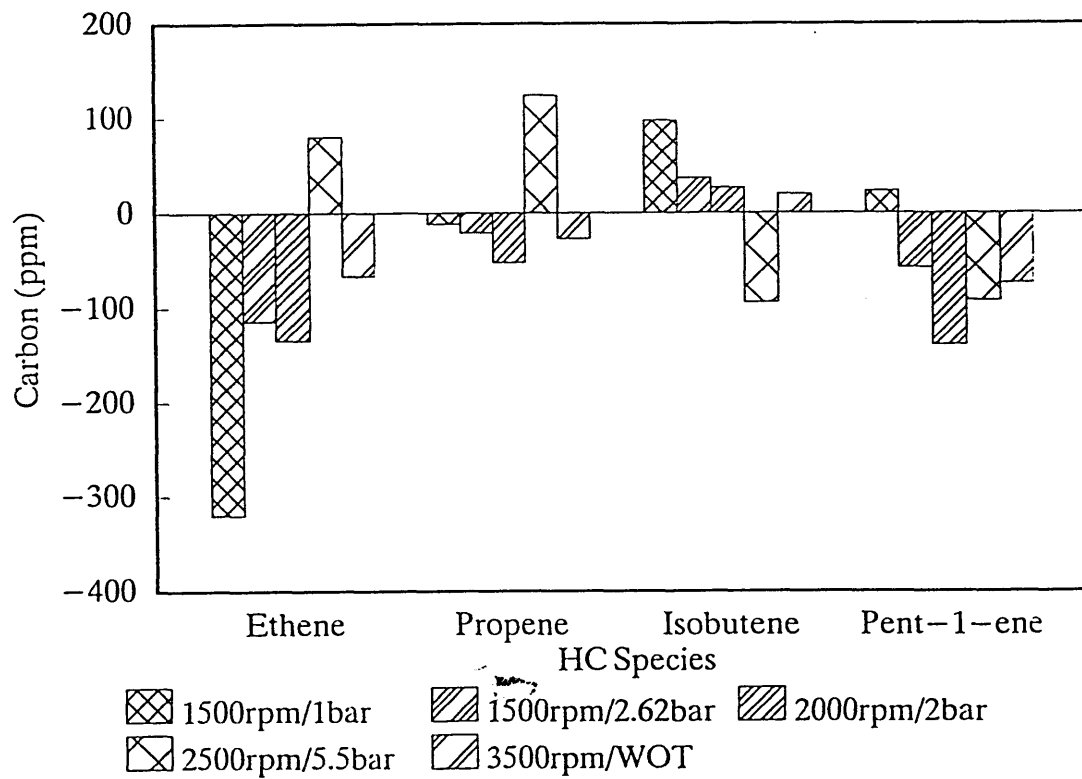


Figure 5.22 Comparison of ALKENES from high top ring pistons and standard build

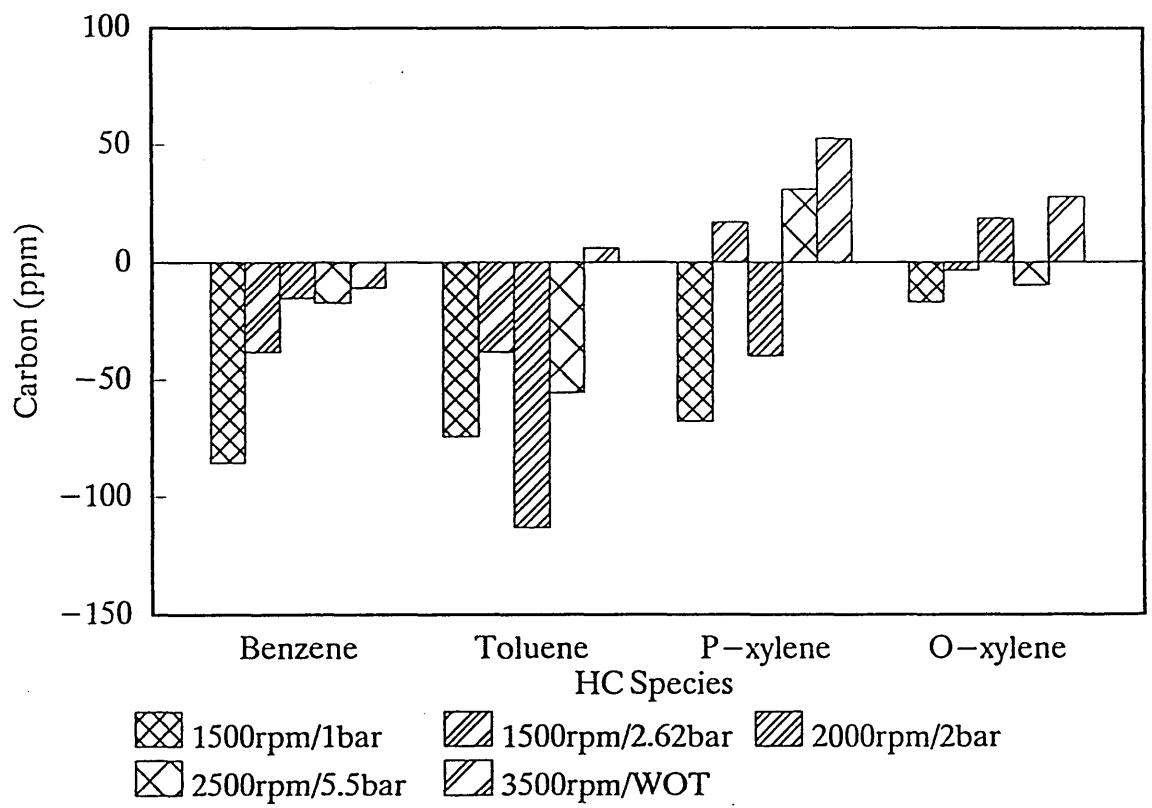


Figure 5.23 Comparison of AROMATICS from high top ring pistons and standard build

5.5. Pressure Balanced 2nd Land Pistons

The pistons manufactured for this test had a large vee groove machined in the second land to increase the 2nd land volume. The concept behind this was to reduce the back flow of gases which flow into this region from the combustion chamber and are composed of unburned mixture.

This effect was observed by Namazian and Heywood (12) in laser sheet photographs. The flow occurs as a jet through the ring gap during the later part of the expansion stroke. This is thought to be a significant contributor to hydrocarbon emissions. Because of its late arrival into the combustion chamber the lower pressure and temperature reduces the rate of oxidation. In addition to emissions the effect contributes to oil consumption, because the high velocity flow picks up oil as it passes through the ring gap. The effect on oil consumption has been modelled by Miyachika (14), who observed that during the exhaust process the pressure in the 2nd land is greater than cylinder pressure. A method of reducing 2nd land pressure is by increasing the 2nd ring gap and raising blow-by flow. An alternative to enlarging the ring gap is to increase the 2nd land volume. Curtis (71) discusses the advantages of enlarging the 2nd land volume to reduce oil consumption in diesel engines by beneficial ring motion and creating a volume for oil accumulation. Any effect on emissions is not mentioned.

During the high pressure part of the cycle, cylinder pressure holds the ring onto the base of the ring groove

and the ring-cylinder interface is sealed by hydrodynamic lubrication of the ring which is able to withstand the combustion pressure. So flow into the 2nd land occurs only through the top ring gap. Increasing the 2nd land volume will reduce the pressure created by storing a similar mass in a larger volume. The larger volume was created by machining a vee groove in the second land, Figure 5.24, avoiding alterations to the ring grooves. The 2nd land volume has been increased by an average of 164% for each piston, Table 5.6. More detailed information on the piston and liner dimensions are given in Appendix 3. Surface finish measurement of the cylinder liner gave similar results to the standard test liner.

Table 5.6 Enlarged 2nd Land Piston and Liner Dimensions

	Dia	Height	Crevice Vol mm ³	% change relative to Standard	
				Land	Including Ring Groove
Top Land	74.45mm	6 mm	381.596	+28.8	+12.7
2nd Land	74.52mm	3.85mm	639.787	+164	+58.4
Liner	74.99mm				

5.5.1. Hydrocarbon Emissions

The hydrocarbon emissions were successfully and repeatably obtained over a series of six runs. Figure 5.25 and 5.26 compares hydrocarbon emissions taken at the

exhaust pipe and exhaust port respectively with those from standard pistons. It can be seen that significant reductions are observed at only two test points 1500rpm 1bar bmep and 2000rpm 2bar bmep. These are just outside the variation limits of plus or minus one standard deviation. There is also no significant change to the hydrocarbon emissions when using trimethyle pentane as a fuel, Figure 5.27.

The blow-by measurement, Figure 5.28, does not follow a consistent trend for all test points.

5.5.2. Gas Chromatography

Substantial changes occur to the profile of HC species. Figure 5.29, is a gas chromatograph plot of a sample taken at 2000 rpm 2 bar bmep. For comparison between standard and enlarged 2nd land piston tests the ppm carbon value for a particular species from the standard build is subtracted from the value obtained from the enlarged 2nd land piston test results. Figure 5.30 compares the 13 selected species for each test point. The positive bars indicate an increase from the standard.

The alkanes from these analyses are plotted in Figure 5.31. The product species are lower than the standard, but show different trends with speed and load. The reductions in methane are greater at high loads whilst ethane reduction is greater at low loads. Fuel species, especially trimethyl pentane, have increased. There are much higher levels at 1500 rpm than any other speed.

The alkenes are plotted in Figure 5.32. The most

notable change is to ethene which has been reduced by 310 ppm at 1500 rpm 1 bar bmep. Isobutene has increased slightly.

Figure 5.33 shows a similar trend for the aromatics. The lighter species, benzene and toluene, being reduced. These are pyrolysis products of heavier aromatic species as well as fuel components.

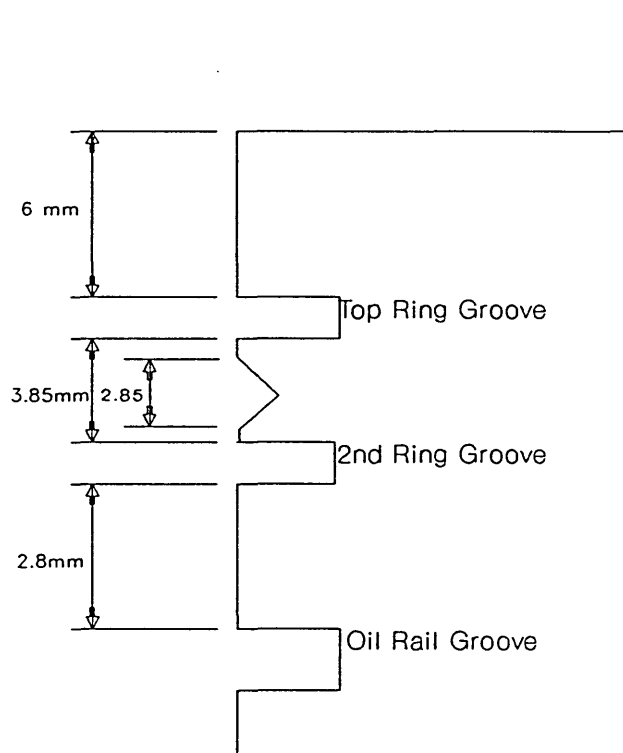


Figure 5.24 Enlarged 2nd Land Piston

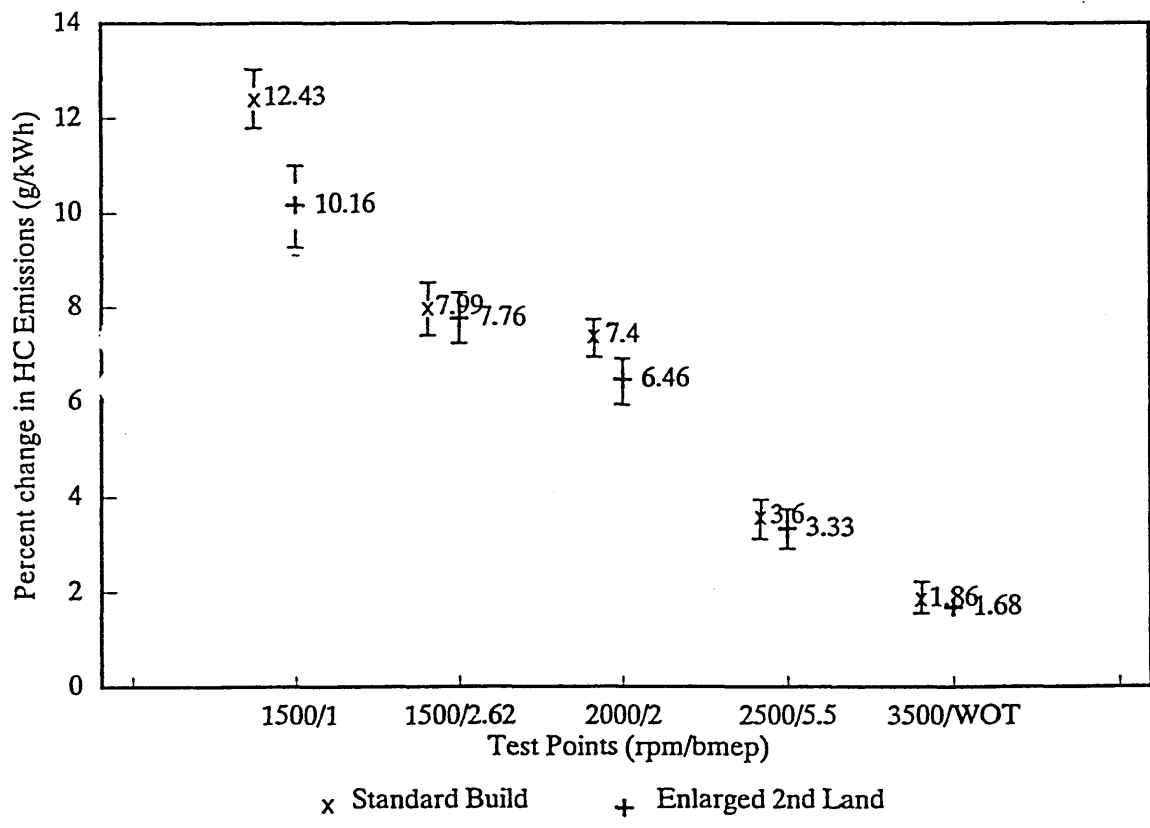


Figure 5.25 Comparison of Hydrocarbon Emissions from Standard and Enlarged 2nd Land Pistons, exhaust Pipe

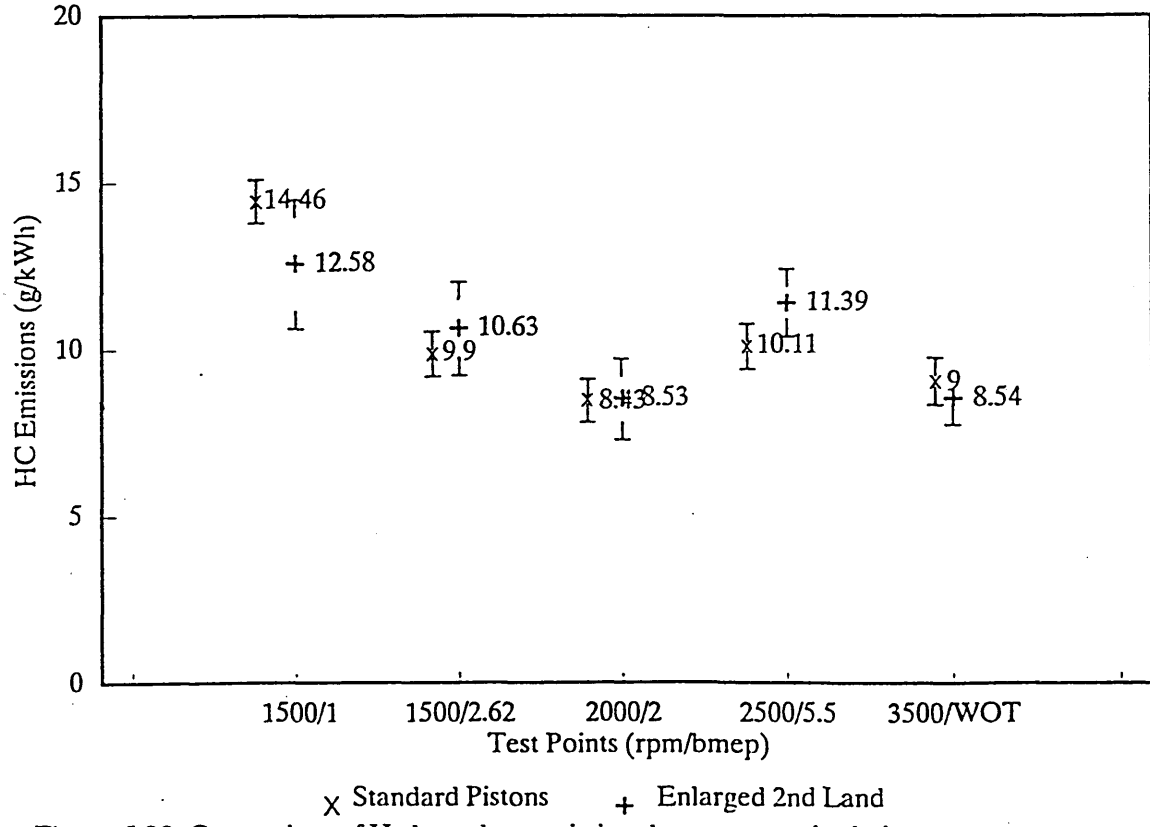


Figure 5.26 Comparison of Hydrocarbon emissions between standard pistons and enlarged 2nd land pistons, samples taken at the exhaust ports.

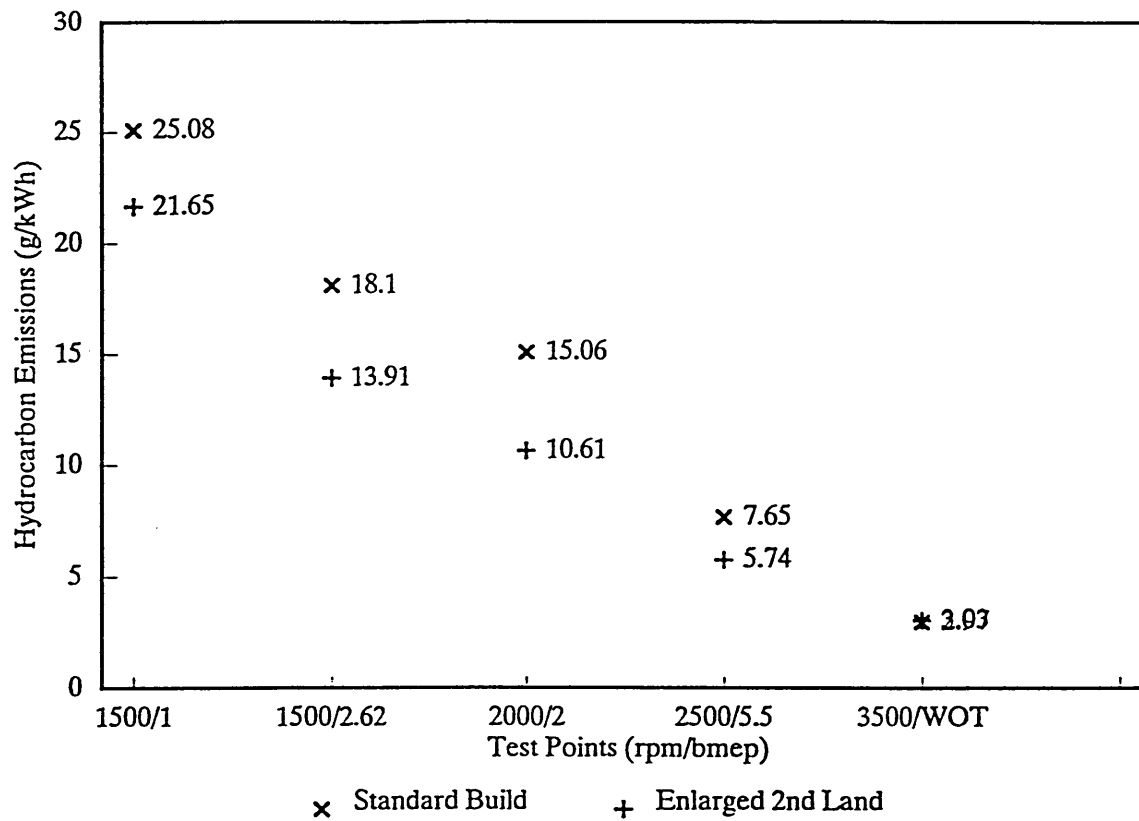


Figure 5.27 Comparison of Hydrocarbon Emissions from standard and Enlarged 2nd Land, Trimethyle Pentane Fuel

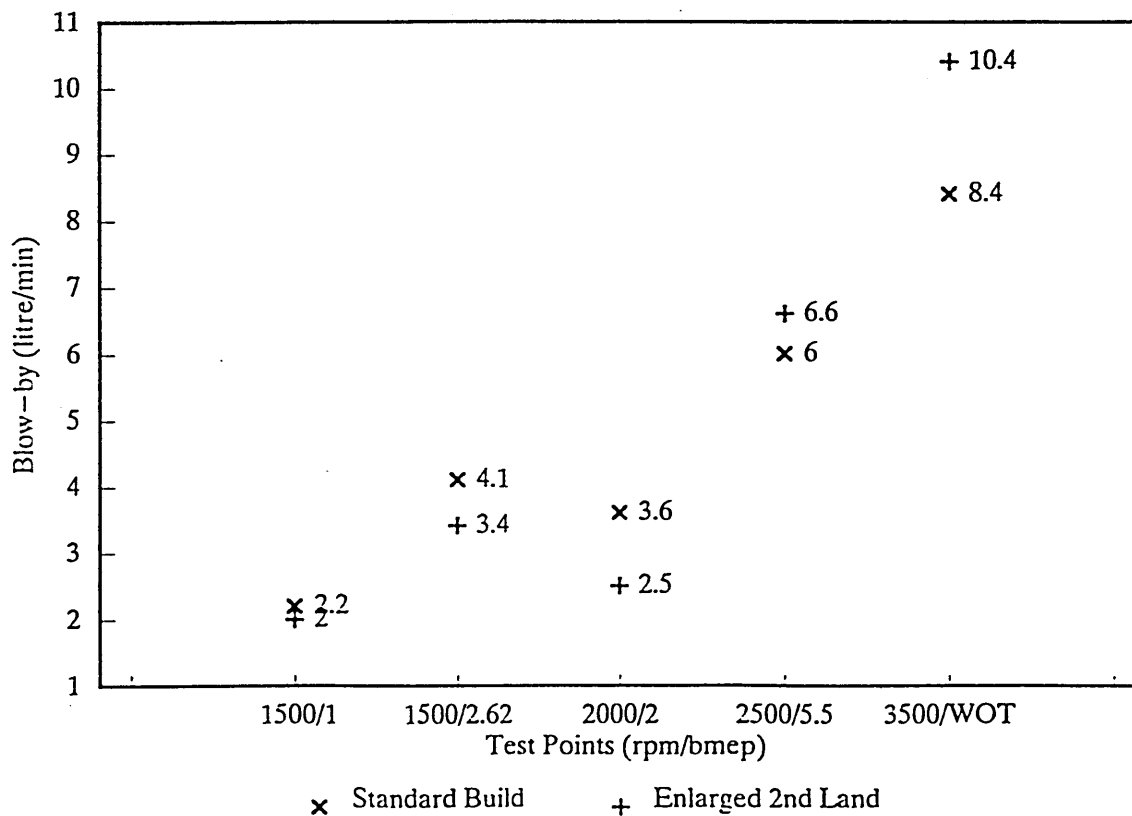


Figure 5.28 Comparison of Blow-by between Standard and Enlarged 2nd Land Pistons

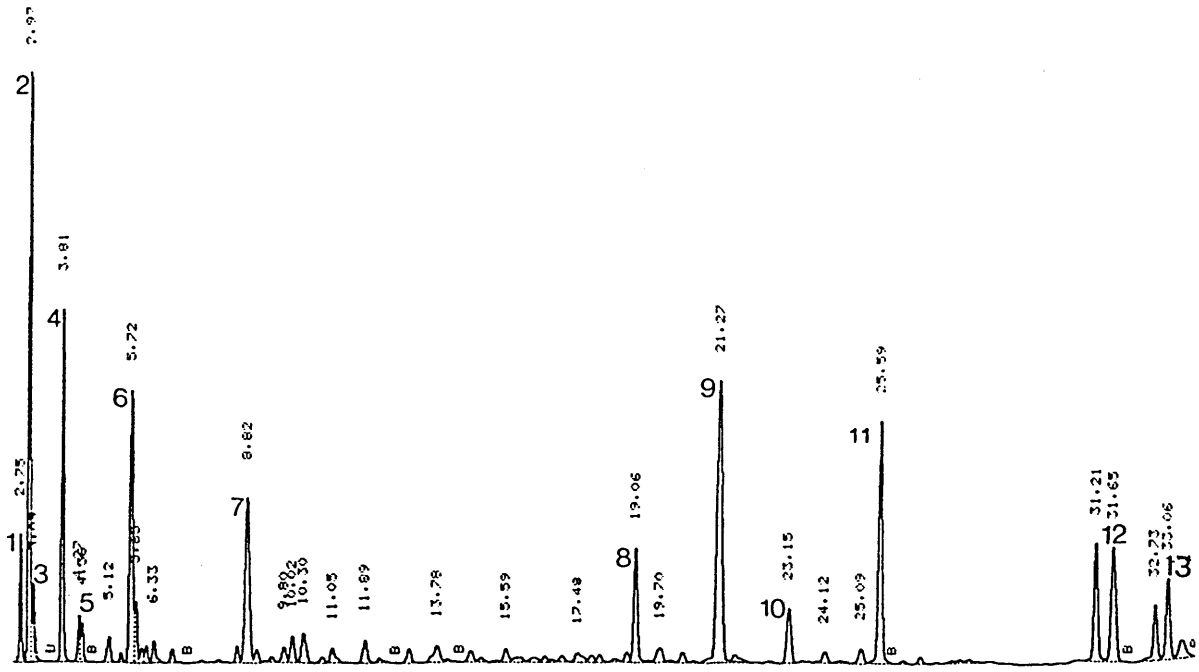


Figure 5.29.a. Gas chromatograph plot from standard pistons, sample taken at 2000 rpm 2 bar bmep

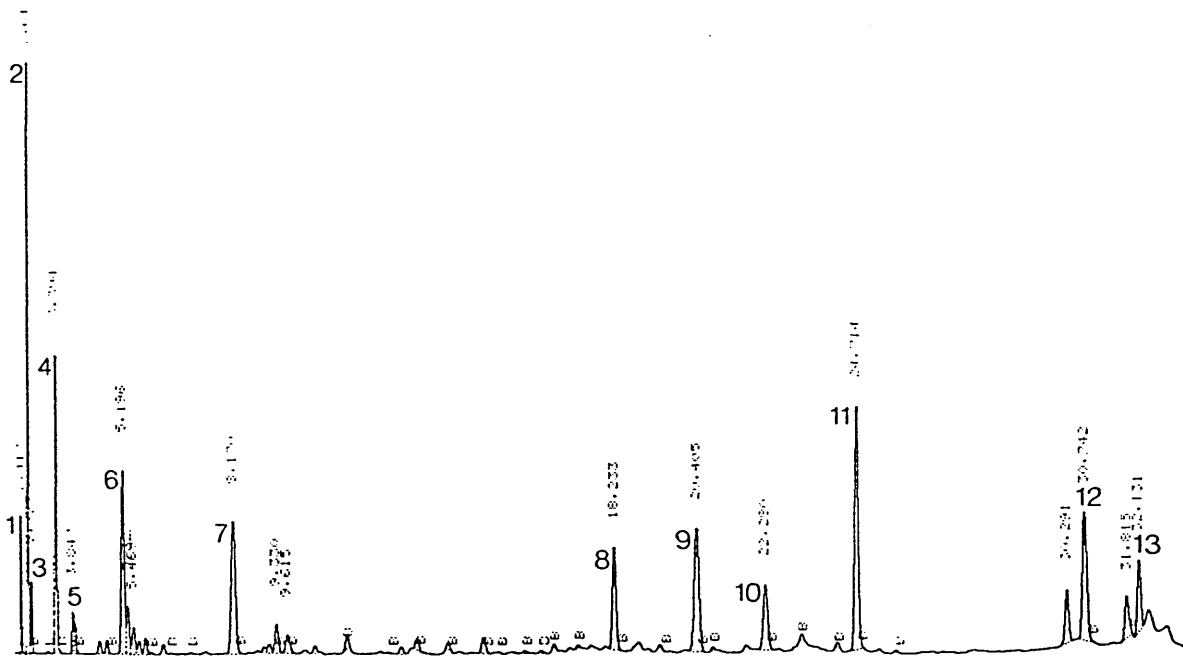


Figure 5.29.b. Gas chromatograph plot from enlarged 2nd land pistons, sample taken at 2000 rpm 2 bar bmep

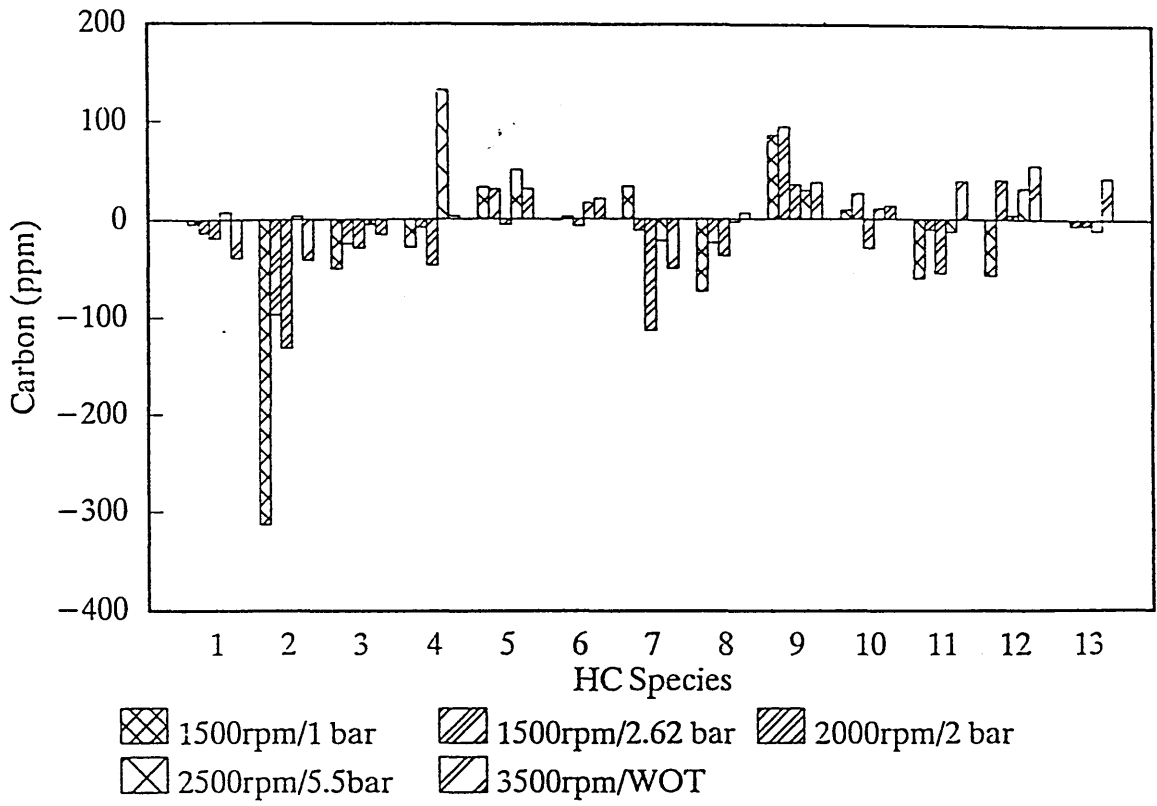


Figure 5.30 Comparison of 13 Species from Enlarged 2nd Land Pistons against standard build

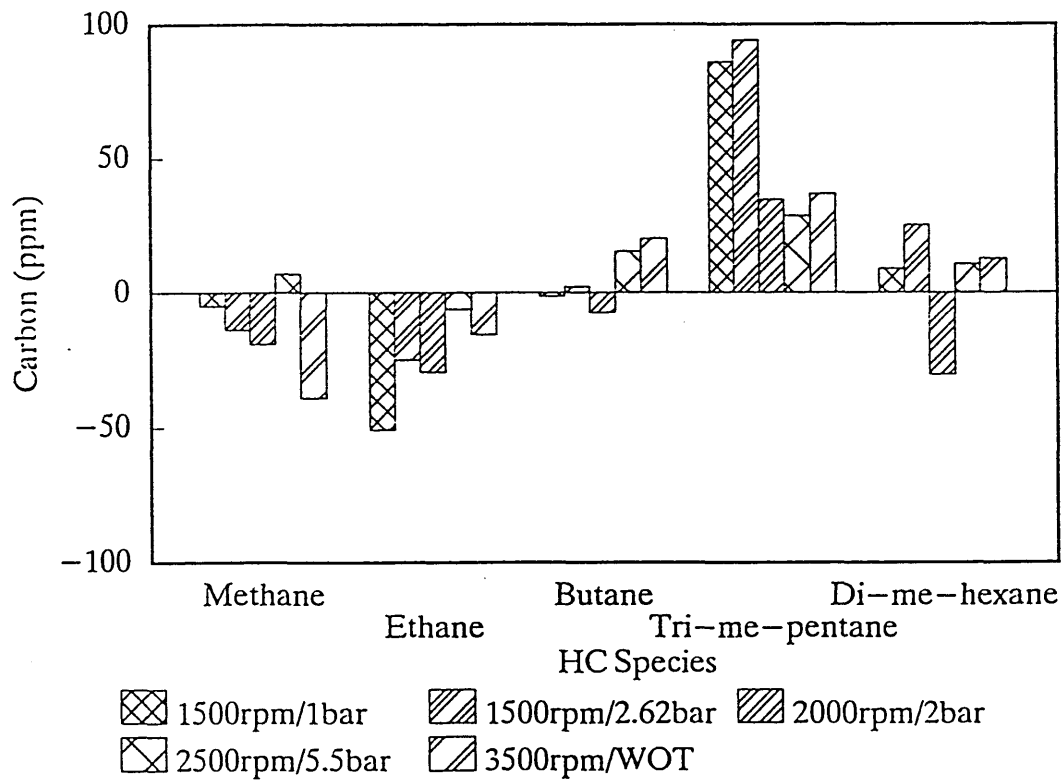


Figure 5.31 Comparison of ALKANES from enlarged 2nd land pistons and standard build

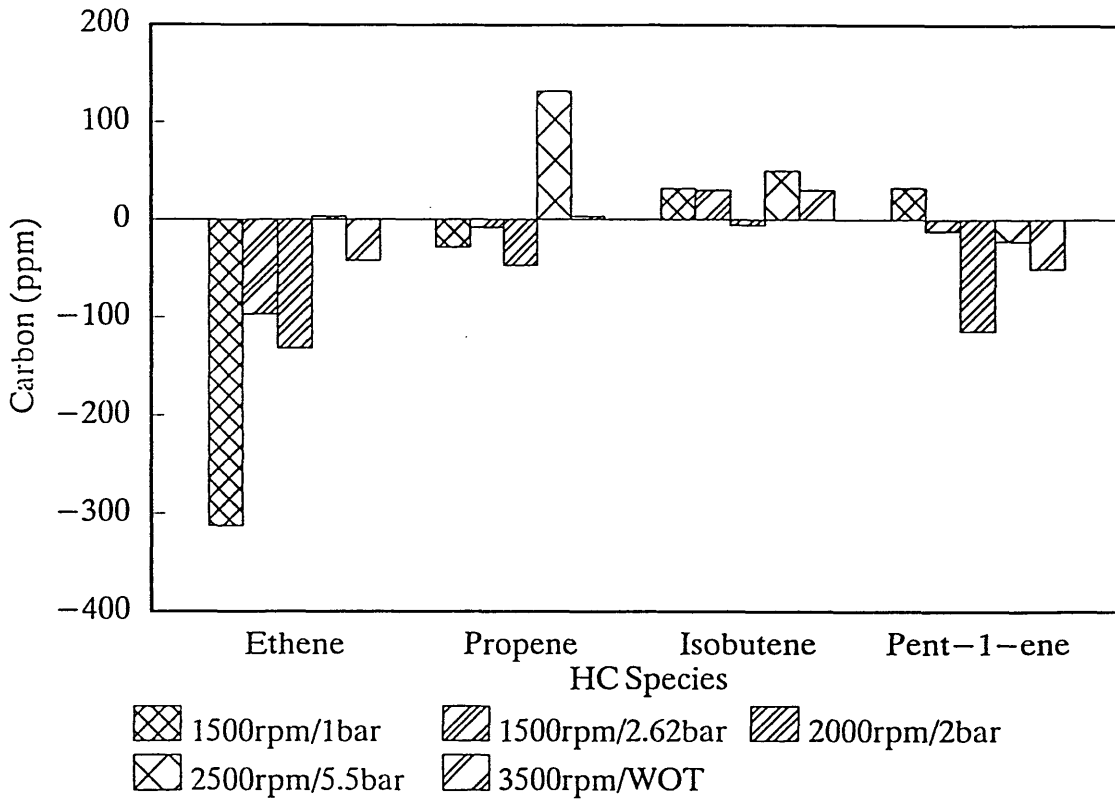


Figure 5.32 Comparison of ALKENES from enlarged 2nd land pistons and standard build

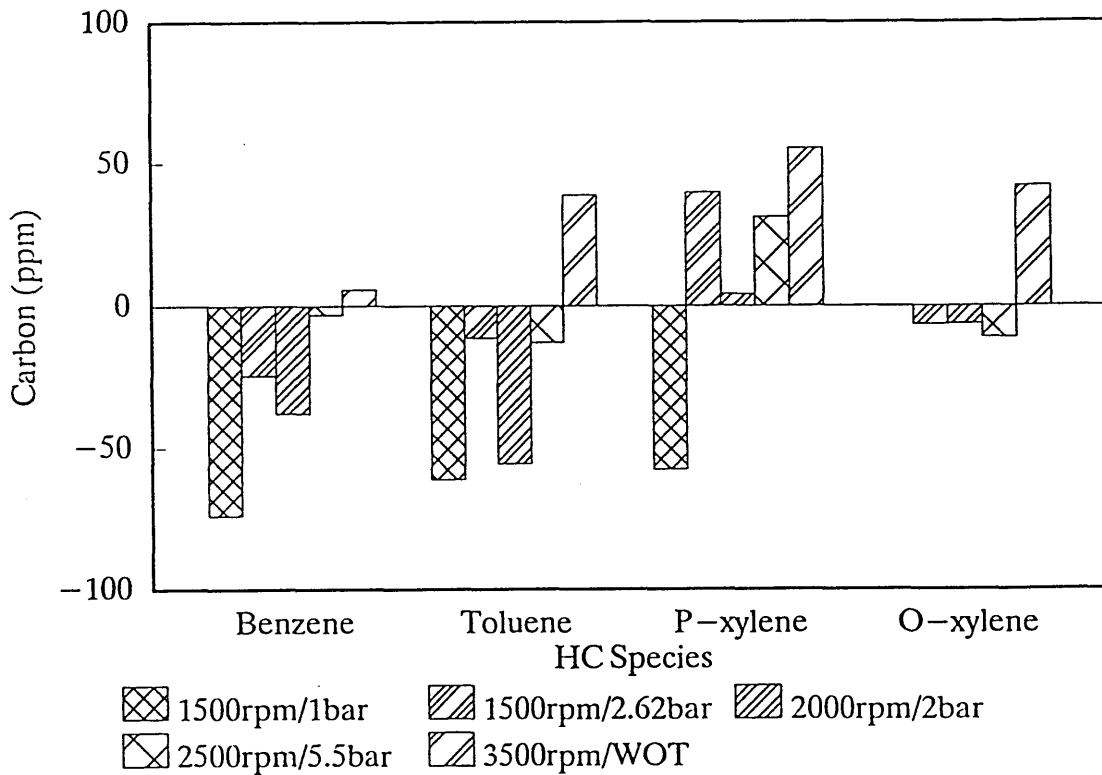


Figure 5.33 Comparison of AROMATICS from enlarged 2nd land pistons and standard build

5.6. Cylinder Liner Surface Finish

The objective of this test was to investigate the effect that cylinder liner surface finish has on hydrocarbon emissions by changing the lubricant thickness. This has been shown to have a direct effect on the absorption and desorption of fuel from these oil layers, refer to Literature survey Chapter 2.

A set of cylinder liners were honed to a smoother surface finish though still keeping the same cross hatch pattern. The surface finish of these smoother liners are compared against the surface traces and bearing area curves of the standard cylinder liners in Figure 5.34.

5.6.1 Defining Oil Layer Thickness

Surface finish controls the oil layer thickness on the cylinder liner. The effects of surface roughness on the lubrication of piston rings and liner were studied by Sandia and Someya (73), who showed that the oil layer is thicker with a rough surface. Because this was a study on lubrication, the oil layers studied were between the ring and liner, but the absorption/desorption effect is due to the oil retained on the liner wall after the passage of the rings. Hegemier and Stewart (74) have also shown that surface finish of the cylinder has an effect on oil consumption, a smoother plateau hone giving lower oil consumption in diesel engines. With respect to emissions a rougher surface with a thicker oil film between ring and cylinder will store more oil in the surface

microstructure and should produce higher hydrocarbon emissions than a smoother surface. The bearing area curve can be used to give an indication of the oil storage area available in the surface finish, definitions of surface finish parameters used are given in Appendix 6.

To quantify the oil layer thickness for different liner surface finishes, the average depth of free space above the bearing area curves within the roughness profile of the material was calculated. This was performed using data obtained from measurement of the surface finish by a Laser Form TalySurf Machine. Each cylinder liner was measured at four points 20mm from the top of the liner; thrust, non thrust and front and back of engine on the neutral axis. The parameter used for this analysis is the TP%. This is the percentage value of the metal in the roughness profile at a specified depth in the profile. A set of Tp% values going down the surface profile was obtained. The free space in the profile is determined by calculating its approximate area by Simpson's Rule. From this and the measurement sampling length the average depth of oil can be found. The following assumptions were made.

a, Oil completely fills the free space in the surface profile.

b, The surface of the oil is flat and parallel with the centre line of the profile.

c, The surface of the oil was taken as the depth of the 2% Tp value.

d, The maximum depth of the oil is taken as the depth of the 98% Tp value.

A typical bearing area curve is shown in Figure 5.35
 The oil occupies the shaded area.

$$\text{Area oil } A_o = \text{Total area} - \text{area metal}$$

$$A_o = D.l - \int l.d(d_t)$$

Where A_o = Area of oil

D = total depth

l = sample length

(d_t) = depth of metal

Data given by surface measuring machine is the T_p value which is the percentage length of metal of the total sample length at a depth d_t .

Thus

$$T_p\% \text{ oil} = 100\% - T_p\% \text{ metal at } d_t$$

$$A_o = \int l_s(1 - T_p/100) d(d_t) \dots \dots \dots [7]$$

The result of these calculations vary slightly for each liner. Table 5.7 sets out the surface parameters for standard and smooth liners and the calculated oil layer thickness. The measured surface data is given in Appendix 3.

The extra honing performed on the cylinder liners had no major effect on the inside diameter. The average liner diameter and dimensions of the pistons are given below in

Table 5.8, and full dimensions are given in Appendix 3.

Table 5.7 Cylinder liner surface finish parameters

Parameter	Standard Liners		Smooth Liners	
	New	Run-in	New	Run-in
Ra μm	0.76	0.25	0.39	0.185
Rk μm	2.28	0.281	0.99	0.3068
Rpk μm	0.748	0.123	0.325	0.136
RvK μm	2.17	1.13	1.44	1.0149
Oil depth μm	1.997	0.224	0.575	0.202

Table 5.8 Piston and Liner Dimensions for Smooth Liner Tests

	Dia	Height	Crevice Vol mm^3	% change relative to Standard	
				top land	including ring groove
Top Land	74.48mm	6 mm	365.246	-23	-8.6
2nd Land	74.52mm	3.85mm	218.241	+9.8	+2.8
Liner	74.98mm				

5.6.2. Hydrocarbon Emissions

In a series of five steady state runs, the results of the hydrocarbon emissions were repeatable with an average variation of 5%. Significant reductions in hydrocarbon

emissions were observed at most test points. Figures 5.36 and 5.37 compare these emissions with those from standard pistons. It can be seen that the largest reductions occur at lower speeds. Hydrocarbon emissions from using trimethyl pentane as fuel shows a similar trend, Figure 5.38.

The blow-by measurement is plotted in Figure 5.39, and again shows little variation from standard.

5.6.3. Gas Chromatography

Substantial changes to the profile of HC species has occurred. Figure 5.40, is a gas chromatograph plot of a sample taken at 2000 rpm 2 bar bmep. For comparison between standard and smooth liner tests the ppm value for a particular species from the standard build is subtracted from the value obtained from the smooth liner test. Figure 5.41 compares the 13 selected species for each test point. The positive bars indicate an increase from the standard. The difference is characterised by a large increase in toluene and large decreases in combustion products.

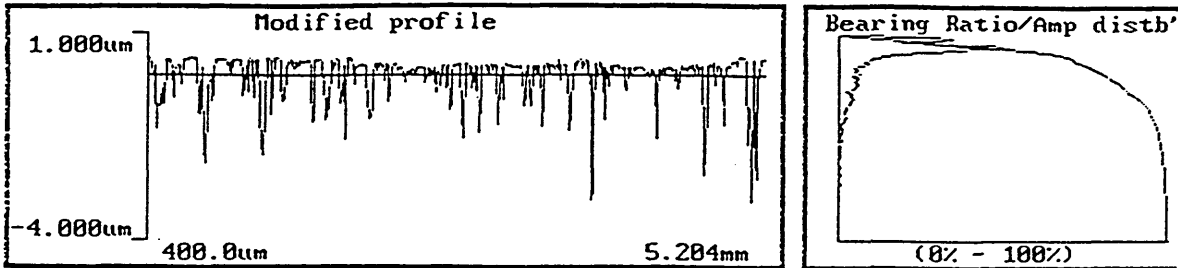
Figure 5.42 plots the alkanes, the products methane and ethane are at much lower levels. Of the fuel species 2,2,4, trimethyl pentane has increased its concentration from the standard and 2,4,dimethyl hexane is only detected at 1500 rpm 1 bar bmep. Butane shows no significant change. Observable are trends in certain species; methane and 2,2,4, trimethyl pentane reduce as speed and load increase.

The alkenes reduce for both products and fuel species, as shown in Figure 5.43. Ethene is an important product as it is formed by the breaking of several different fuel components. Its reduction would indicate a higher level of complete oxidation of fuel.

The levels of the aromatics are plotted in Figure 5.44. This shows the contrast between the large increase in toluene and the small reductions of benzene and the xylenes.

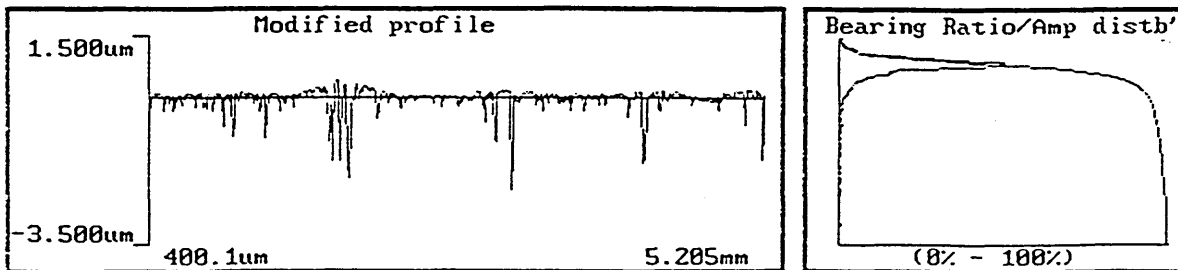
5.6.4. Surface Finish Performance

In addition to the hydrocarbon emissions the performance of the liner must also be assessed. Inspection of the cylinder liner surface finish after the test was completed would give an indication as to the durability of the surface. A visual inspection showed considerable polishing had occurred. The surface measurement normally carried out after the completion of engine tests demonstrated the removal of the honing pattern by bore polishing on the thrust side of the liner. The total running time of the engine for the duration of the test is approximately 80 hours. This would indicate that despite the advantage of reduced hydrocarbon emissions this particular surface finish specification would not be durable for the normal life of a production engine.



Slope	-0.007 deg	Rt4	1.908 um	Rk	0.271 um
Ra	0.313 um	Rt5	3.348 um	Rpk	0.074 um
Rp	0.435 um	Rt6	3.493 um	Rvk	1.180 um
Rv	3.059 um	Rsk	-2.472	Mr1	3.000 %
Rt	3.493 um	S	26.848 um	Mr2	70.000 %
Rt1	2.512 um	RzISO	3.035 um	Sm	65.036 um
Rt2	2.396 um	RzDIN	2.503 um		MORE...
Rt3	1.363 um				

Figure 5.34.a Surface finish data from standard cylinder liners after engine test



Slope	-0.046 deg	Rt4	2.378 um	Rk	0.196 um
Ra	0.146 um	Rt5	1.755 um	Rpk	0.139 um
Rp	0.420 um	Rt6	1.673 um	Rvk	0.589 um
Rv	2.192 um	Rsk	-3.860	Mr1	11.000 %
Rt	2.612 um	S	29.020 um	Mr2	75.000 %
Rt1	1.163 um	RzISO	2.079 um	Sm	52.454 um
Rt2	2.350 um	RzDIN	1.697 um		MORE...
Rt3	0.862 um				

Figure 5.34.b Surface finish data from smooth cylinder liners after engine test

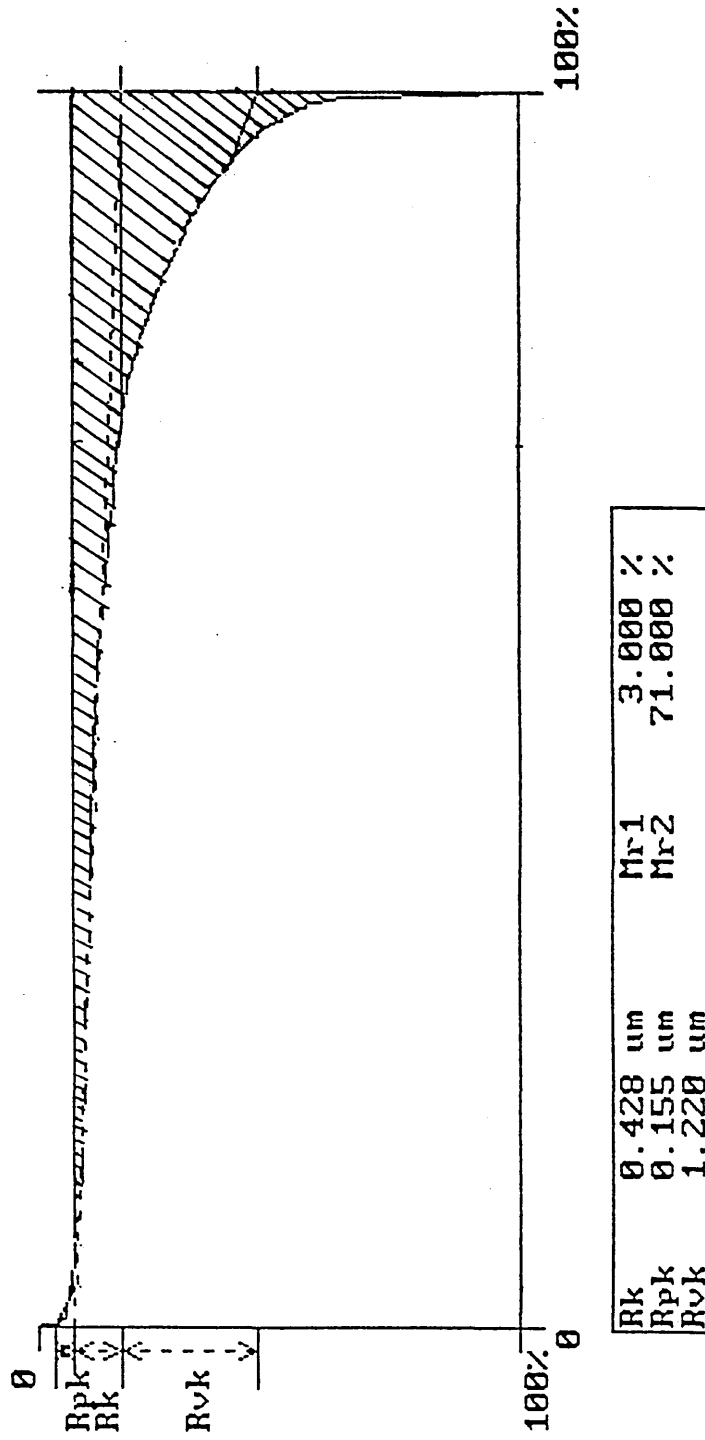


Figure 5.35 Bearing curve showing oil filled area

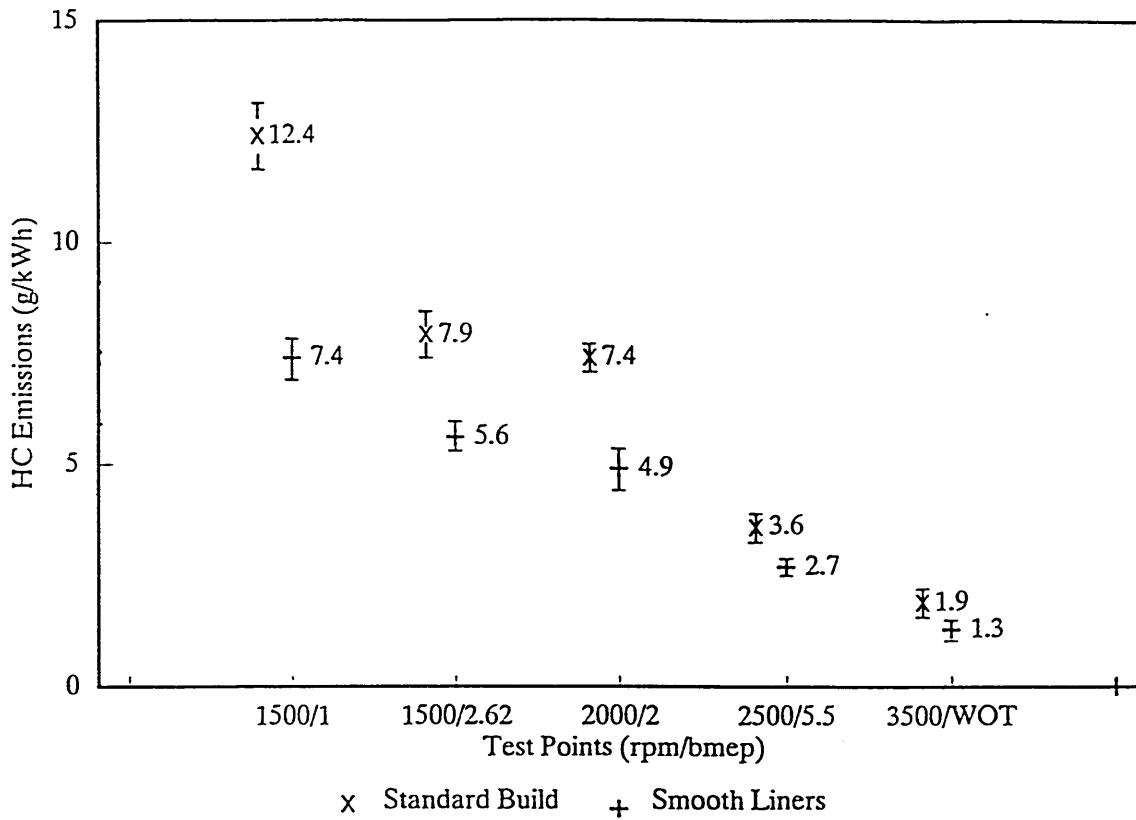


Figure 5.36 Comparison of Hydrocarbon Emissions from standard and smooth liner test, at Exhaust Pipe

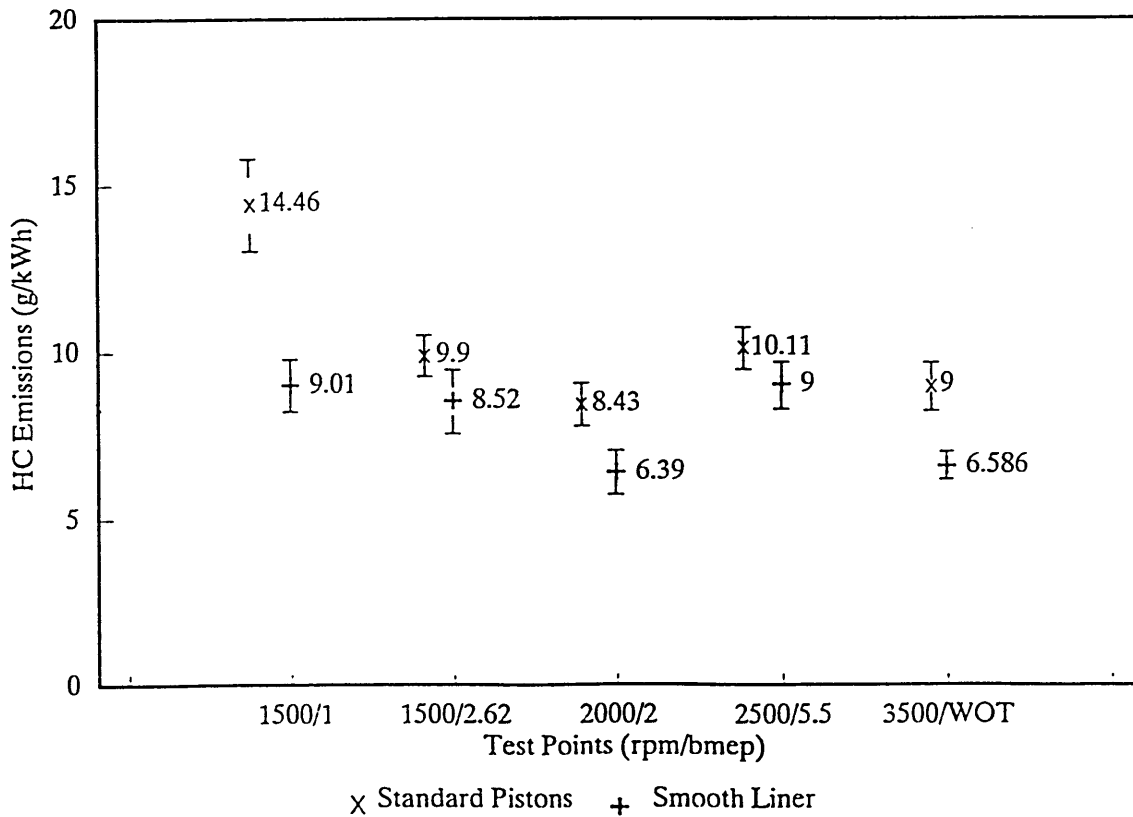


Figure 5.37 Comparison of Hydrocarbon emissions between standard pistons and smooth liners samples taken at the exhaust ports.

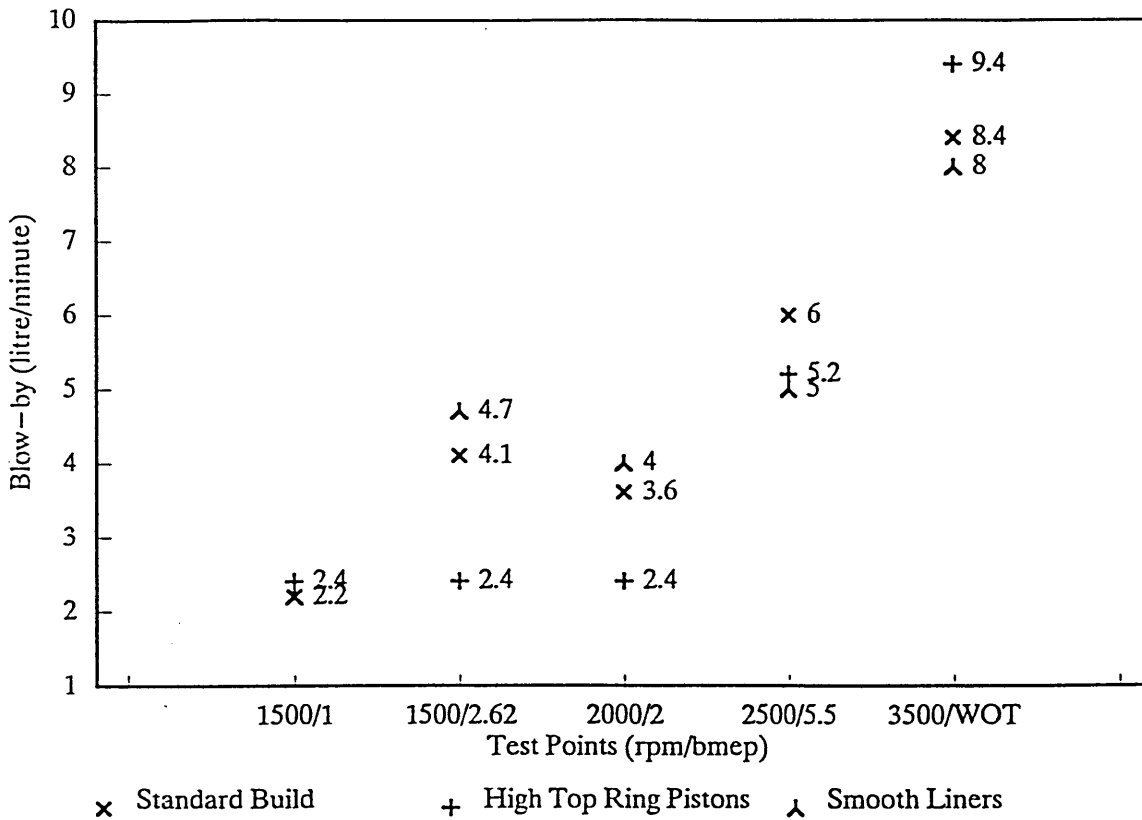


Figure 5.39 Comparison of Blow-by between Standard standard and smooth liner test

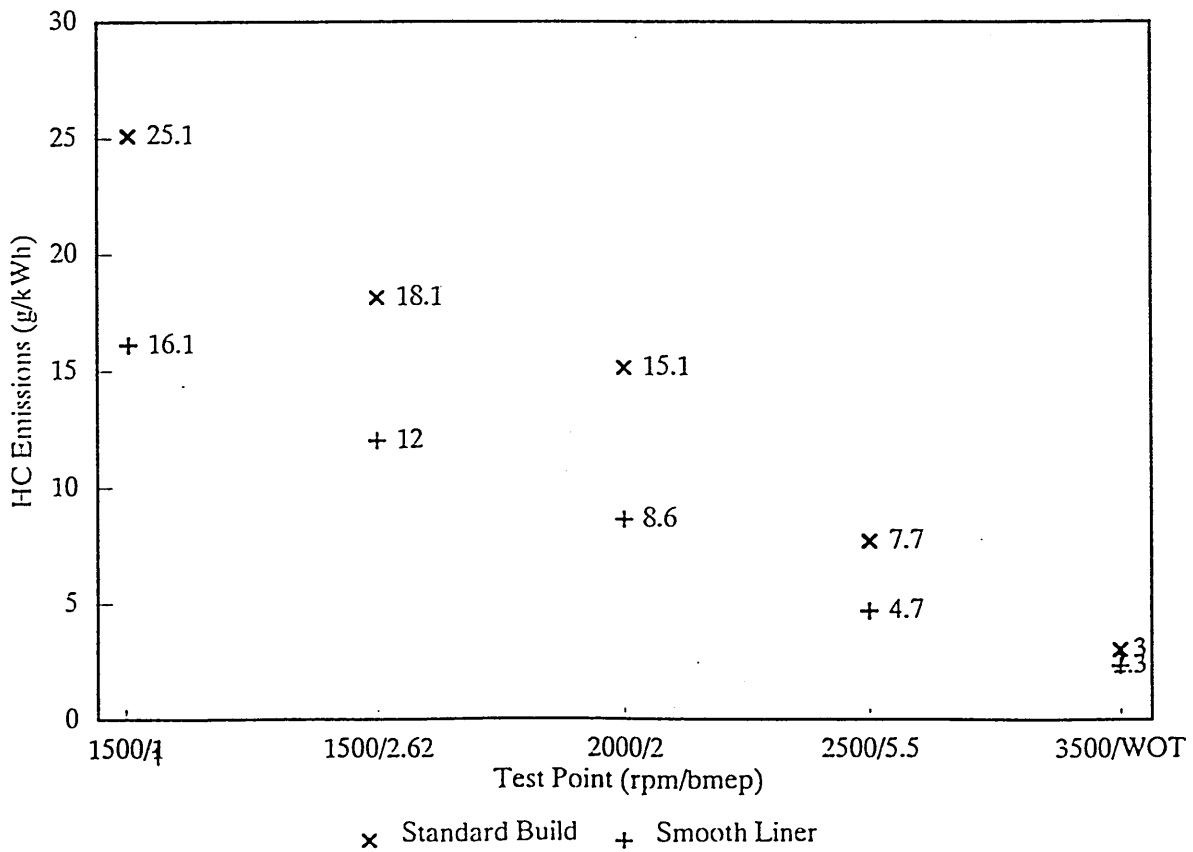


Figure 5.38 Comparison of Hydrocarbon Emissions from standard and smooth liner test, trimethyl pentane fuel

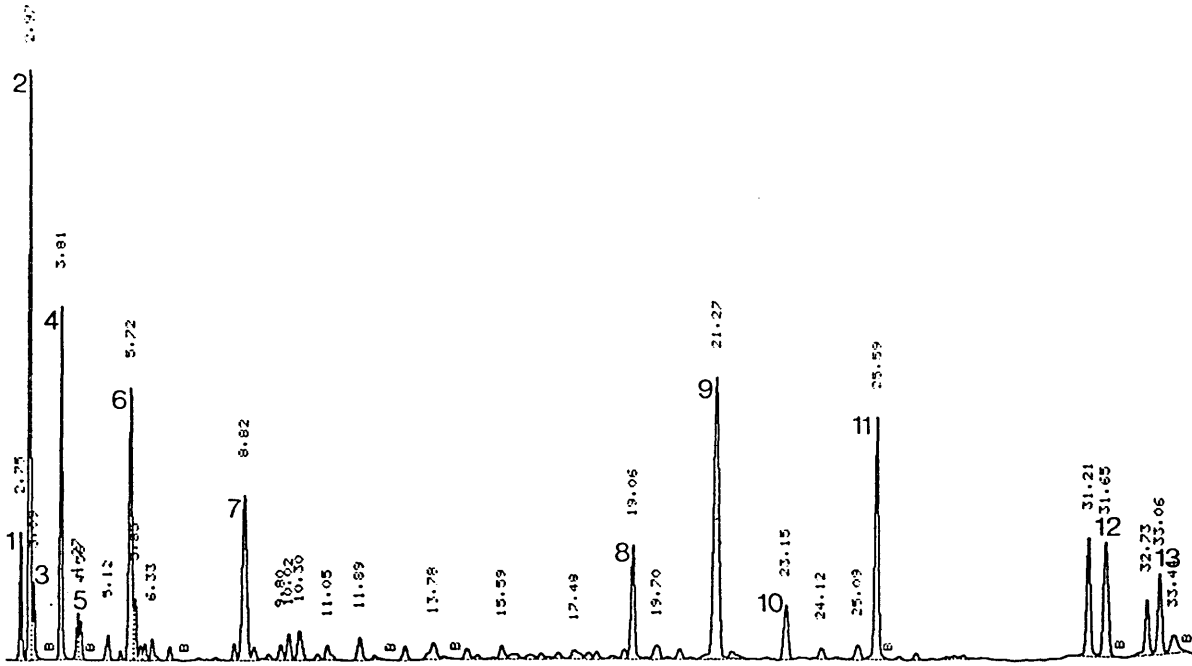


Figure 5.40.b. Gas chromatograph plot from standard pistons, sample taken at 2000 rpm 2 bar bmep

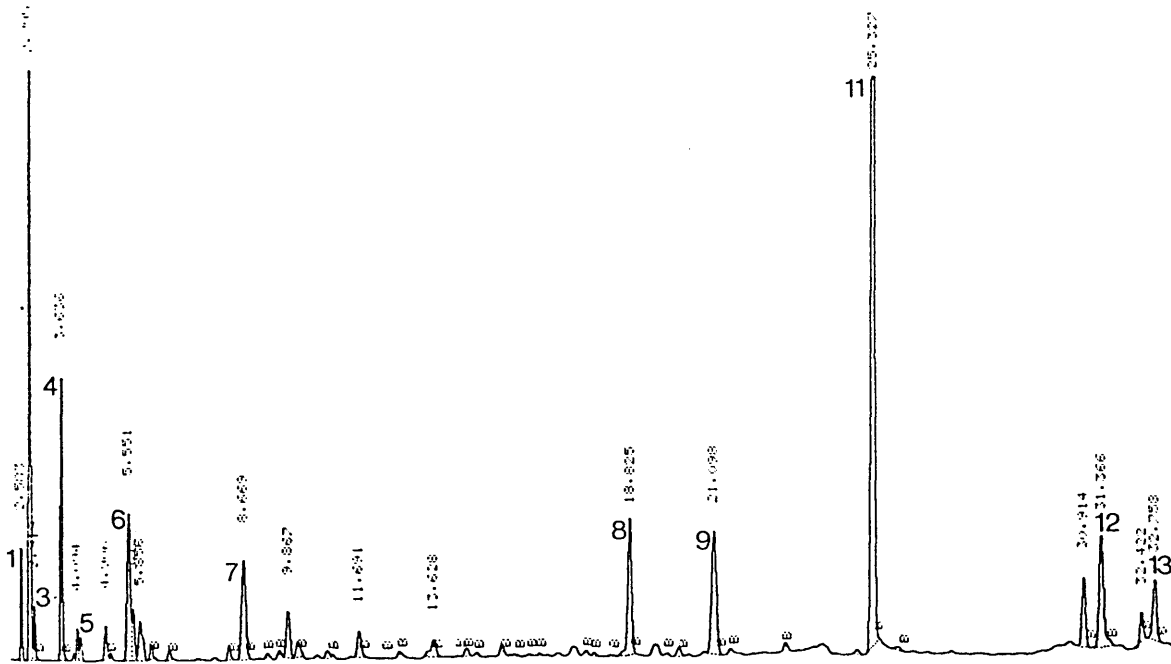


Figure 5.40.a. Gas chromatograph plot from smooth liner, sample taken at 2000 rpm 2 bar bmep

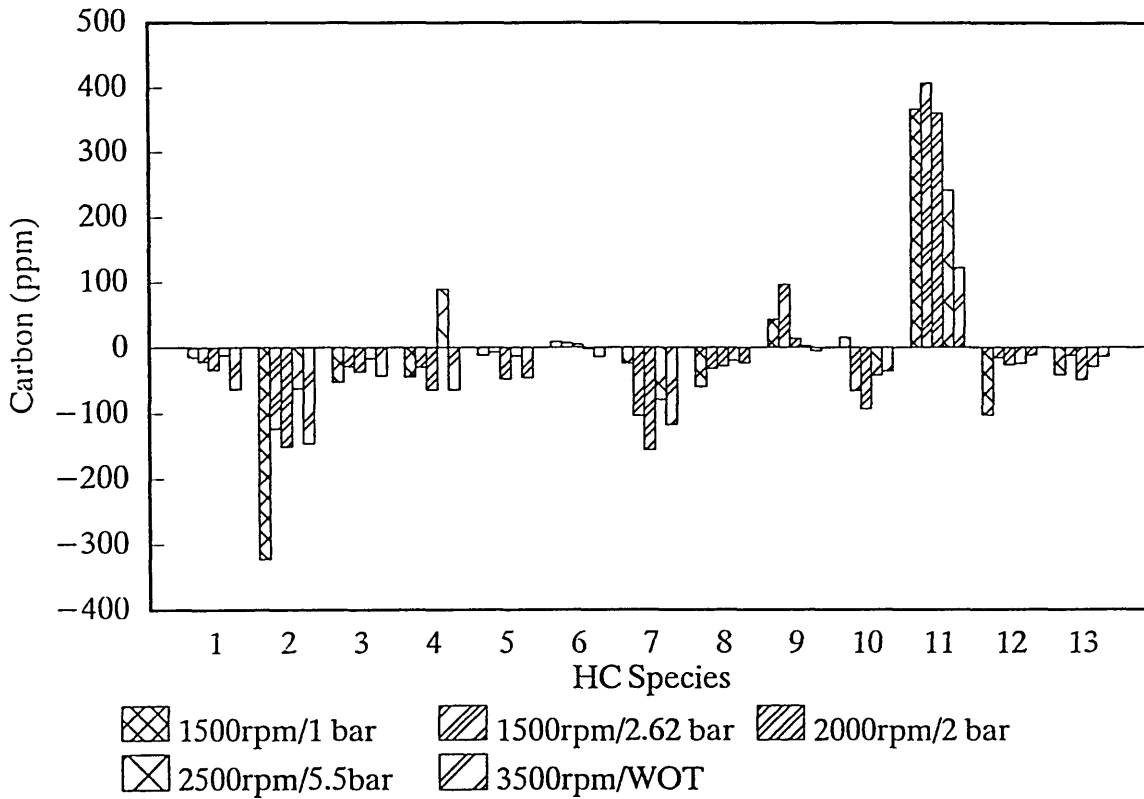


Figure 5.41 Comparison of 13 Species from Smooth Liner Build against standard build

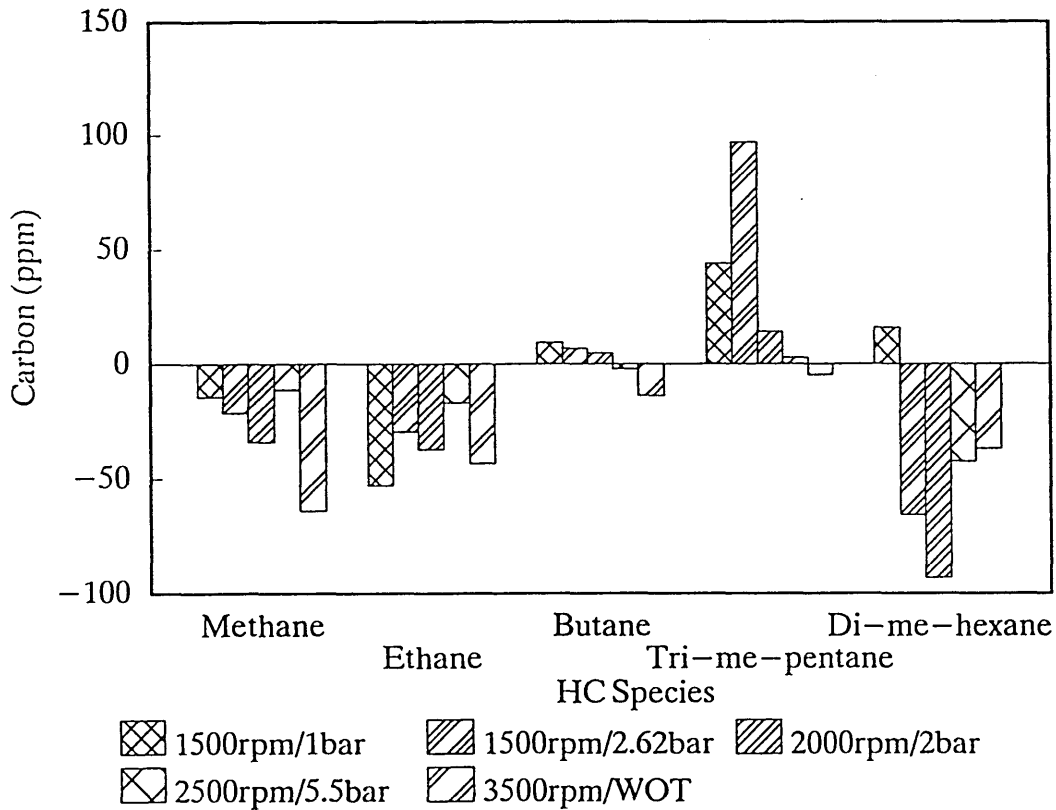


Figure 5.42 Comparison of ALKANES between smooth liner tests and standard

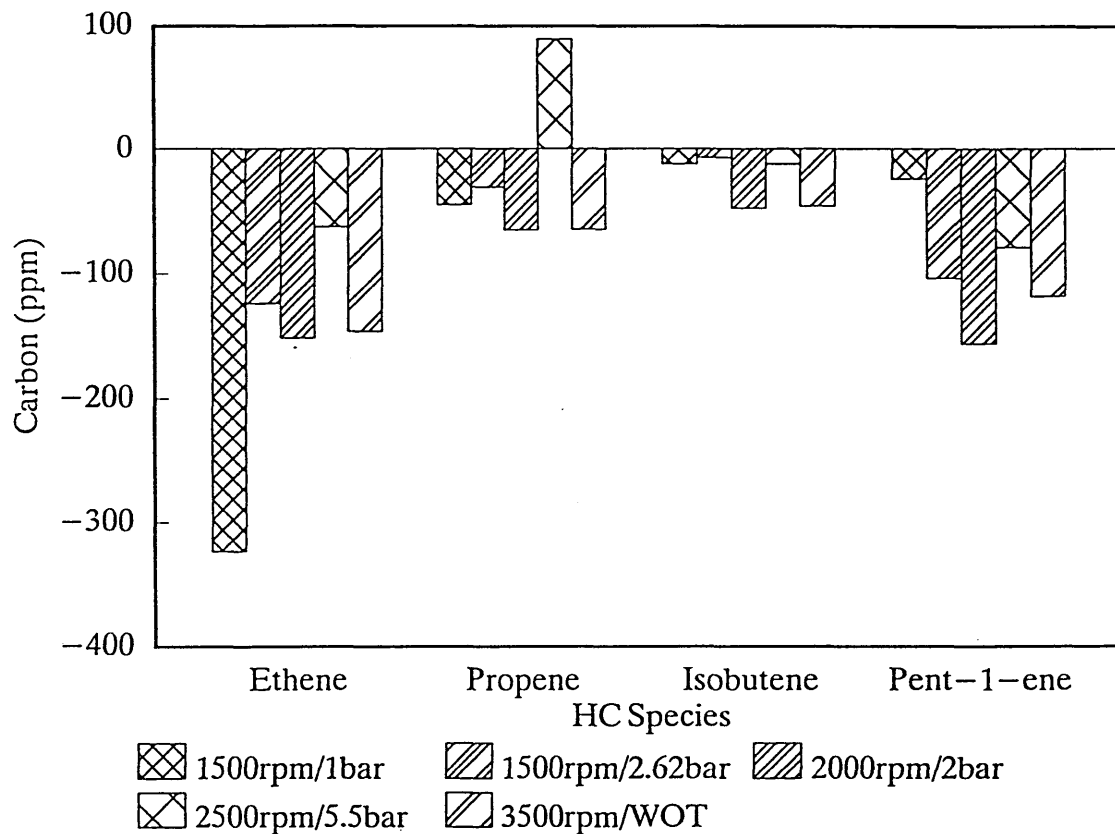


Figure 5.43 Comparison of AKLENES from smooth liner and standard build

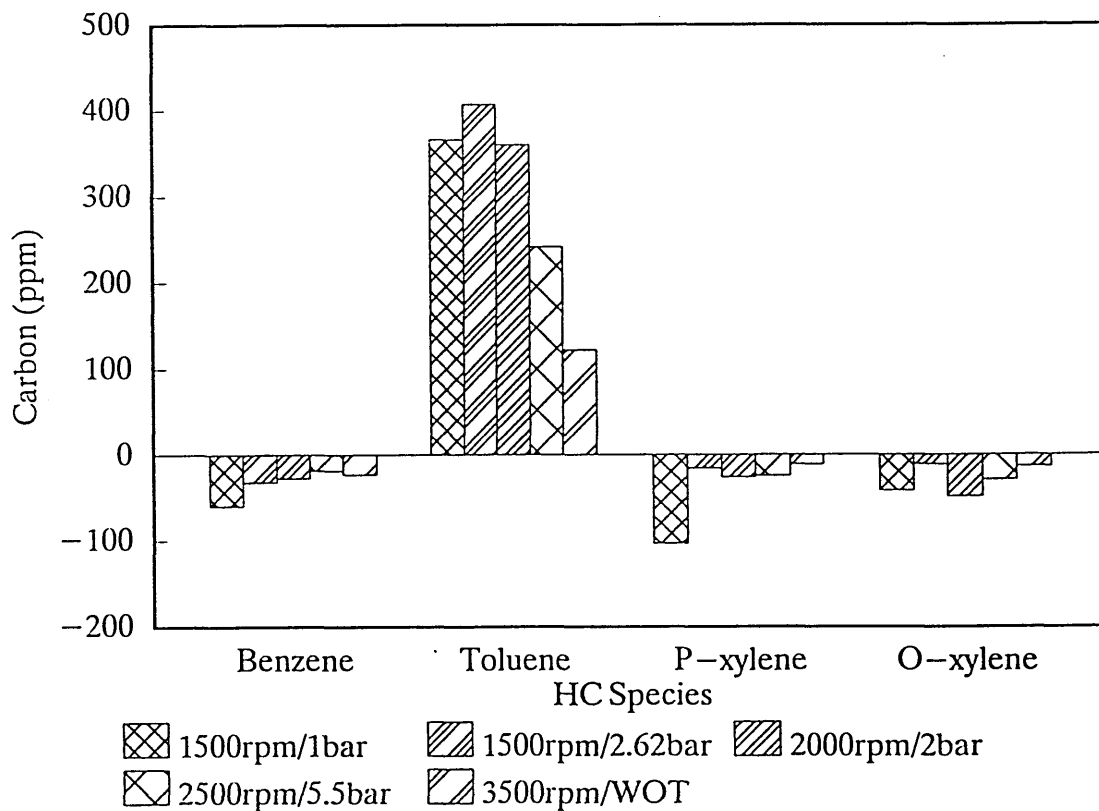


Figure 5.44 Comparison of AROMATICS from smooth liner and standard

5.7. Predictive Calculation Results of Hydrocarbon Emissions

5.7.1. Changes to Crevice Volume for Piston Dimensions used in Experimental Tests

The dimensions from the two engine test where crevice volumes were changed were used as an input to the calculations. These dimensions are given in Table 5.9. The inlet air conditions used in these calculations were obtained from actual test data and piston and liner temperatures have been assumed from previously published data, Furuham (41), and consultation with AE Piston Products Ltd. The input data is tabulated in Appendix 2.

Table 5.9 Piston Dimensions used in Experimental Tests

Piston	Top Land		2nd Land	
	Height	Diameter	Extra Vol.	Diameter
Standard	6 mm	74.5 mm	0	74.44mm
High Top Ring	2.8mm	74.39mm	0	74.53mm
Large 2nd Land	6 mm	74.45mm	0.414cm ³	74.51mm

The results of the calculations indicated that the largest decrease in total crevice flow would occur with the high top ring pistons, Figure 5.45. Although the 2nd land crevice has some influence on the 2nd land flow the major influence on the total flow is the top land volume.

The top ring height also has an influence on the absorption and desorption of fuel in the lubricant, Figure 5.46 indicates that a 2.8mm top land can significantly reduce the mass of fuel being desorbed after combustion.

By combining these calculations with the oxidation model it will indicate the impact of the high top ring on total hydrocarbon emissions. To enable comparison with data from experiment the values have to be normalised against the standard piston results to give a dimensionless emission factor.

$$\text{Emission Factor} = \frac{\text{Emissions from test piston}}{\text{Emissions from standard build}}$$

An emission factor of less than one is a reduction from the standard build. Comparison of calculated values for high top ring pistons against experimental results are shown in Figure 5.47. The calculated predictions give good agreement with experimental results. Both sets of figures show a similar trend of reducing emissions with increasing speed and load, with no significant change at 1500 rpm 1 bar bmep to a normalised level of 0.7 at 3500 rpm wide open throttle.

Changes to the 2nd land crevice volume emissions for predicted and experimental results when normalised are plotted in Figure 5.48. Again the predicted values show good agreement for most test points, except for a higher value at 1500 rpm 1 bar bmep. This is due to the predicted back flow into the combustion chamber, Figure 5.49, which though of a significantly smaller magnitude occurs later in the cycle when oxidation has been reduced.

5.7.2. Cylinder Liner Surface Finish

The oil layer thickness derived from surface measurement of the liners used in experiment were used as inputs to the calculations. The piston dimensions from the smooth liner tests were also slightly different from the standard pistons. The implications for the crevice flow were minimal as displayed in Figure 5.50. The predicted emissions from the thinner oil layer of the smooth liner showed distinct reductions from the standard and comparison with the normalised values of the actual experimental results show good agreement, Figure 5.51. This indicates that the method developed for the assessment of lubricant thickness from surface finish measurements is satisfactory for the prediction of absorption and desorption of fuel in lubricant.

5.8 Study of some Factors Effecting Hydrocarbon Emissions

Having shown that the predictive calculations give good agreement with measured emissions for various designs tested in experiments a study of the relative impact of piston features and cylinder liner finish can be made.

Four features were chosen for the calculations; top land height, oil layer thickness, 2nd land volume and top ring groove depth. The top ring groove was included because this forms part of the total top land volume and could have an impact on hydrocarbon emissions. Each feature had two computer runs with a reduction of 18% and 50%, only one feature being changed per run.

The computer runs were performed at 2000 rpm 2 bar bmep. The results are shown in Figure 5.52 giving percentage reduction of hydrocarbon emissions for each feature. From the graph it can be seen that 2nd land volume and ring groove depth are insignificant at this condition. The most influential source of emissions is the oil layer thickness.

5.9 Summary of Results

5.9.1. Total Hydrocarbon Emissions

Using the normalisation technique described previously the experimental results from the three engine variations are plotted in Figure 5.53. From this it can be seen that significant reductions in emissions were achieved from the high top ring piston test and the smooth liner test. The enlarged 2nd land test only achieved any significant change at 1500 rpm 1.0 bar bmep, at other test points the emissions were similar to the standard test.

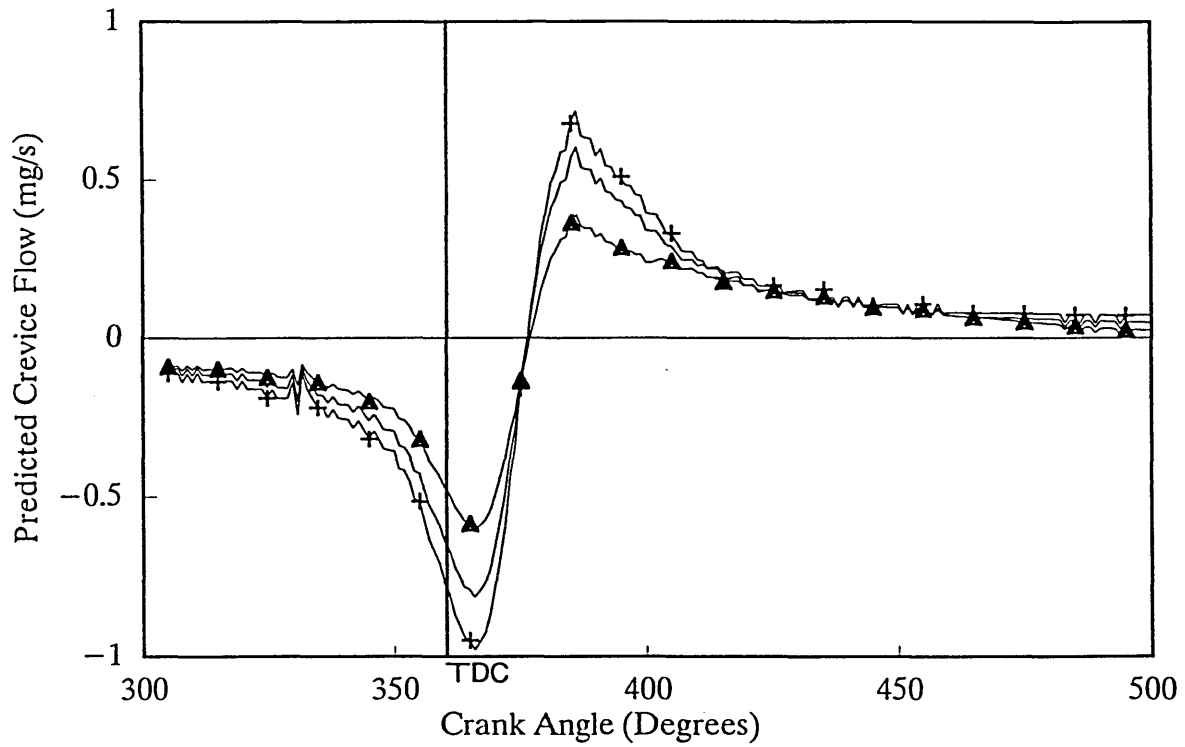
5.9.2. Hydrocarbon Species

To compare hydrocarbon species from each test the concentrations of species within each chemical group were added together across all test points. These summations are plotted in Figure 5.54. This graph shows similar trends to that shown by the total hydrocarbon emissions. The high top ring test shows a reduction in all hydrocarbon species, and

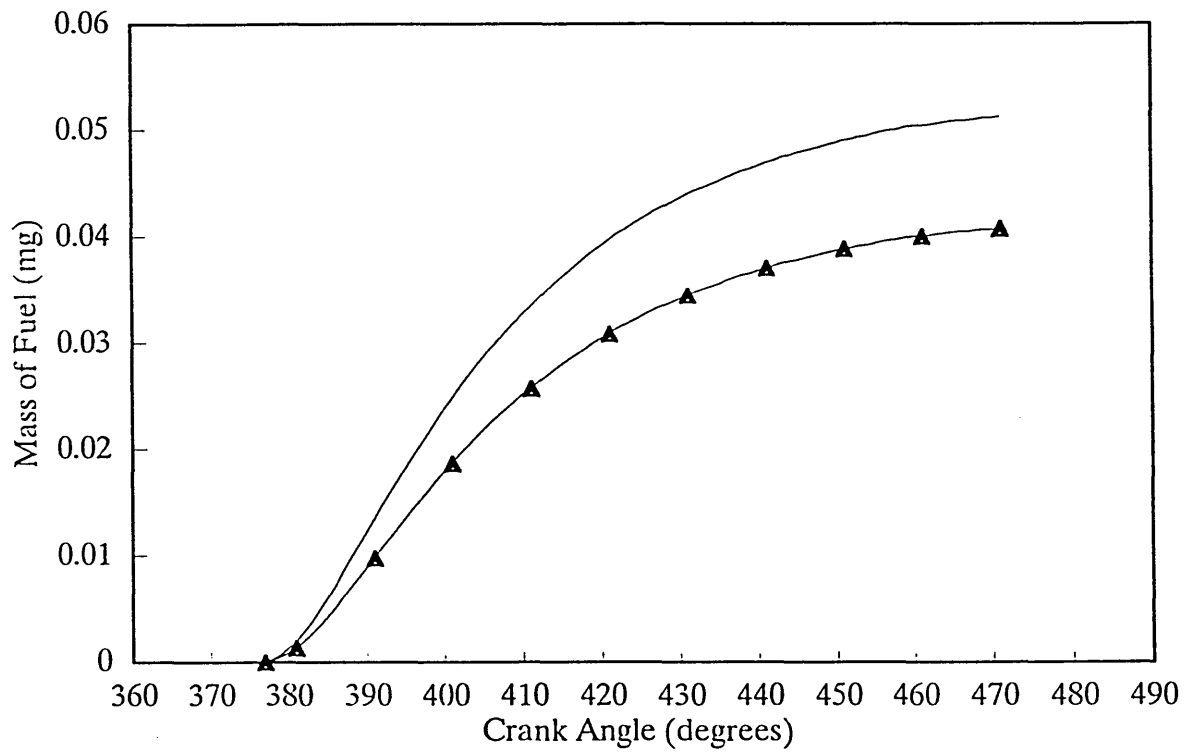
the enlarged 2nd land test shows a slight reduction in alkenes and aromatics. The smooth liner test displays the observed increase in Toluene by a large increase in aromatics while the other species were reduced, bringing the three groups together gives a net decrease in emissions.

5.9.3. Predicted Hydrocarbon changes

The use of the model to predict change in hydrocarbon emissions has shown good correlation to experimental results, Figure 5.55 shows the normalised emissions from each engine variation.



— Standard ▲ High Top Ring Piston + Enlarged 2nd Land
 Figure 5.45 Predicted total crevice flow from high top ring piston and enlarged 2nd land piston at 1500rpm 1bar bmep



— Top Land 6mm ▲ Top Land 2.8mm
 Figure 5.46 Predicted cumulative fuel desorbed from lubricant, Different top land heights at 1500rpm 1bar bmep

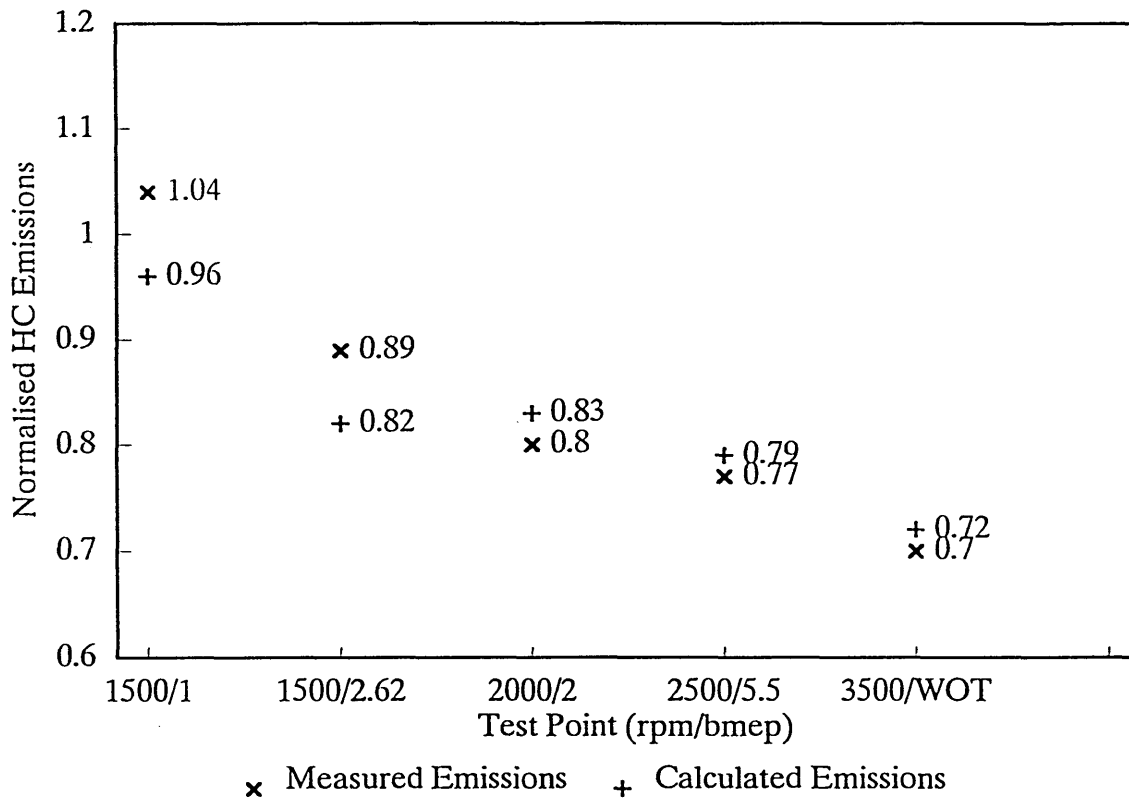


Figure 5.47 Normalised hydrocarbon emissions from high top ring pistons
Comparison between measured and calculated values

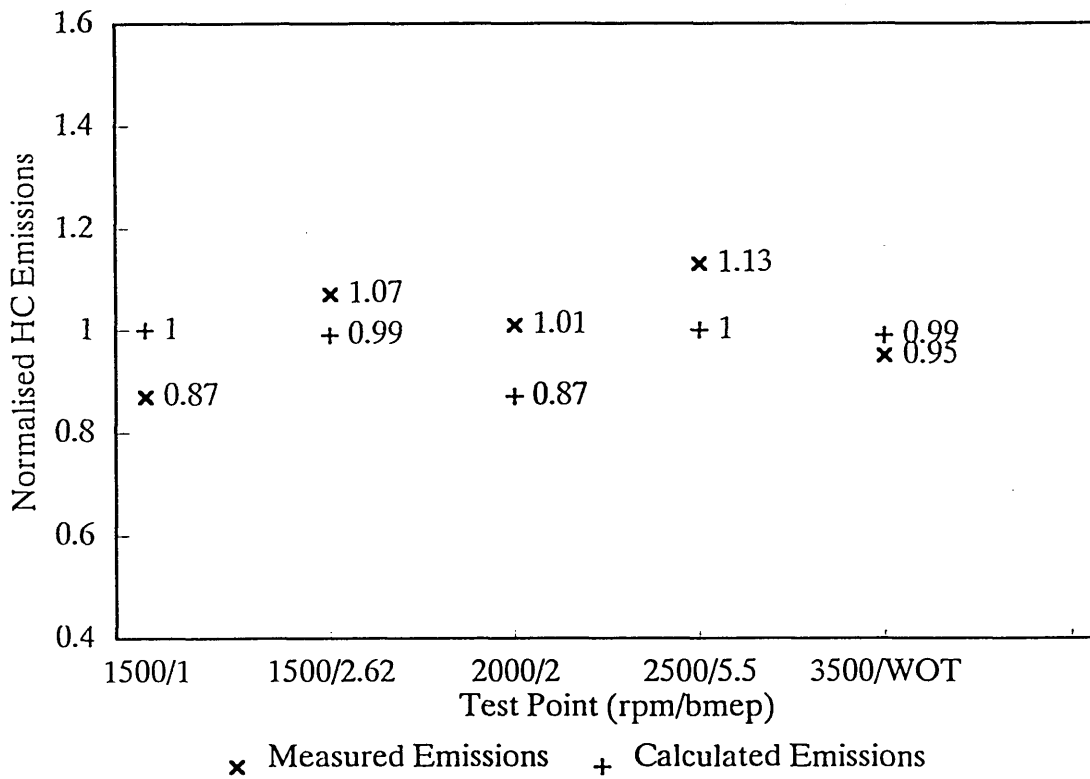
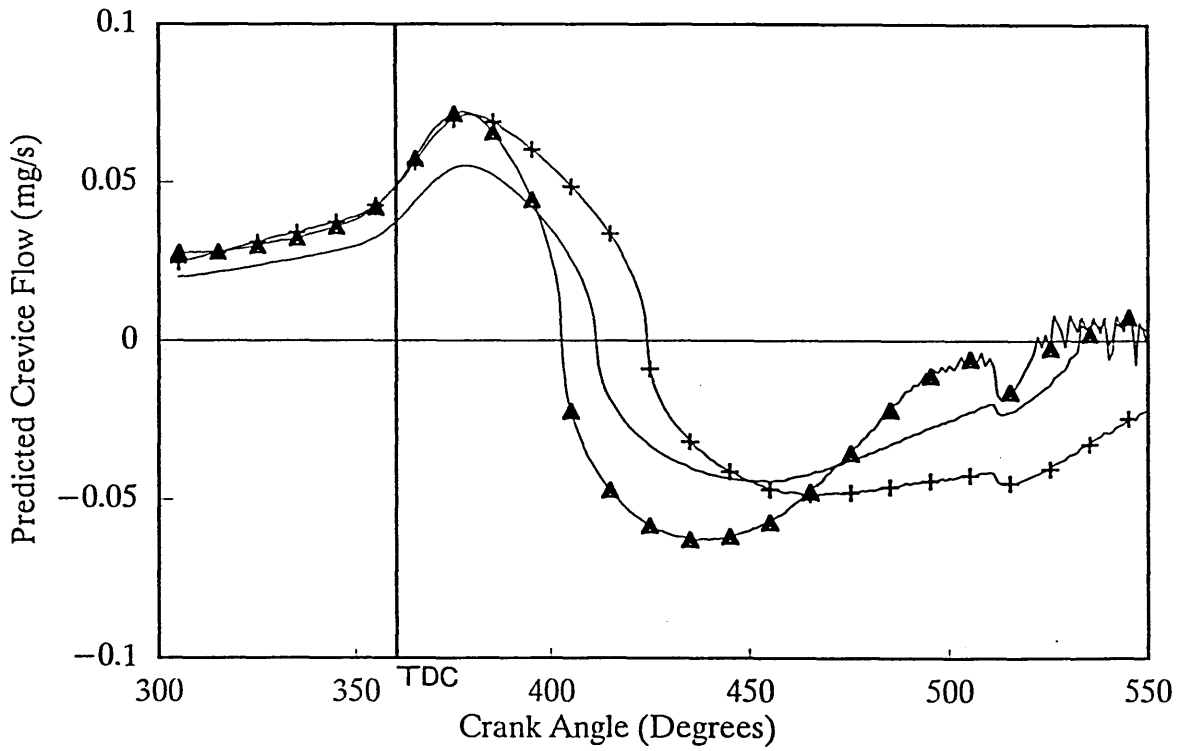
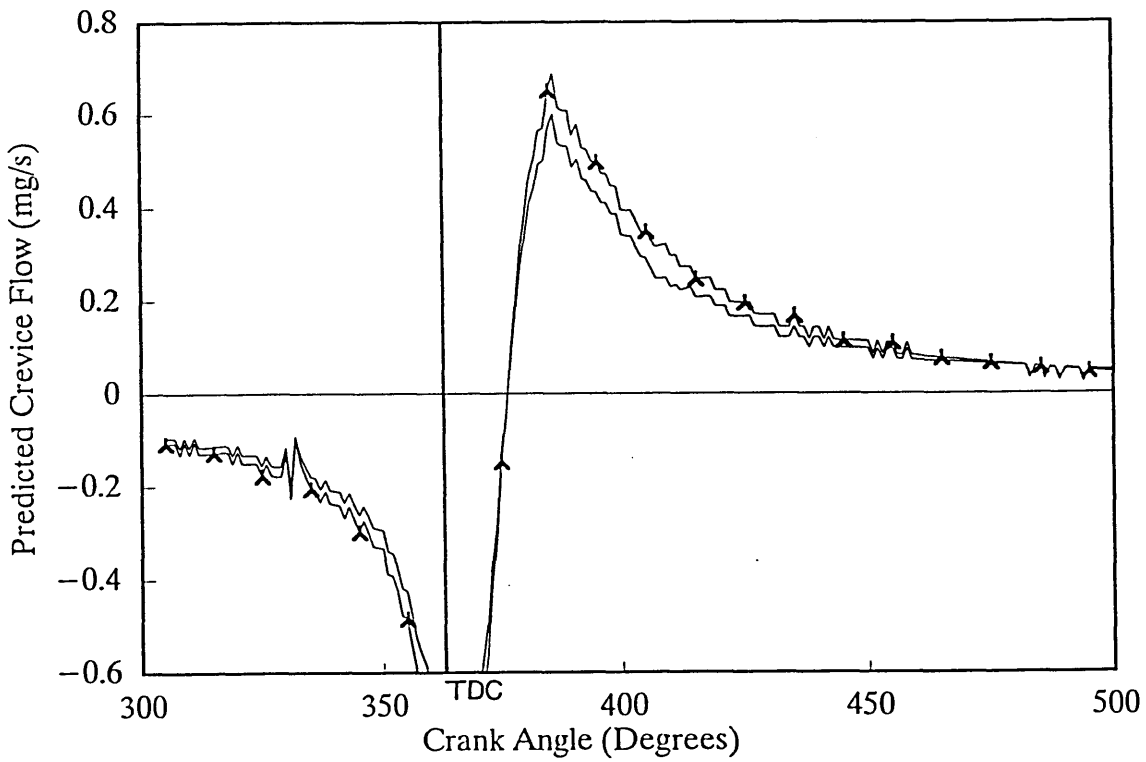


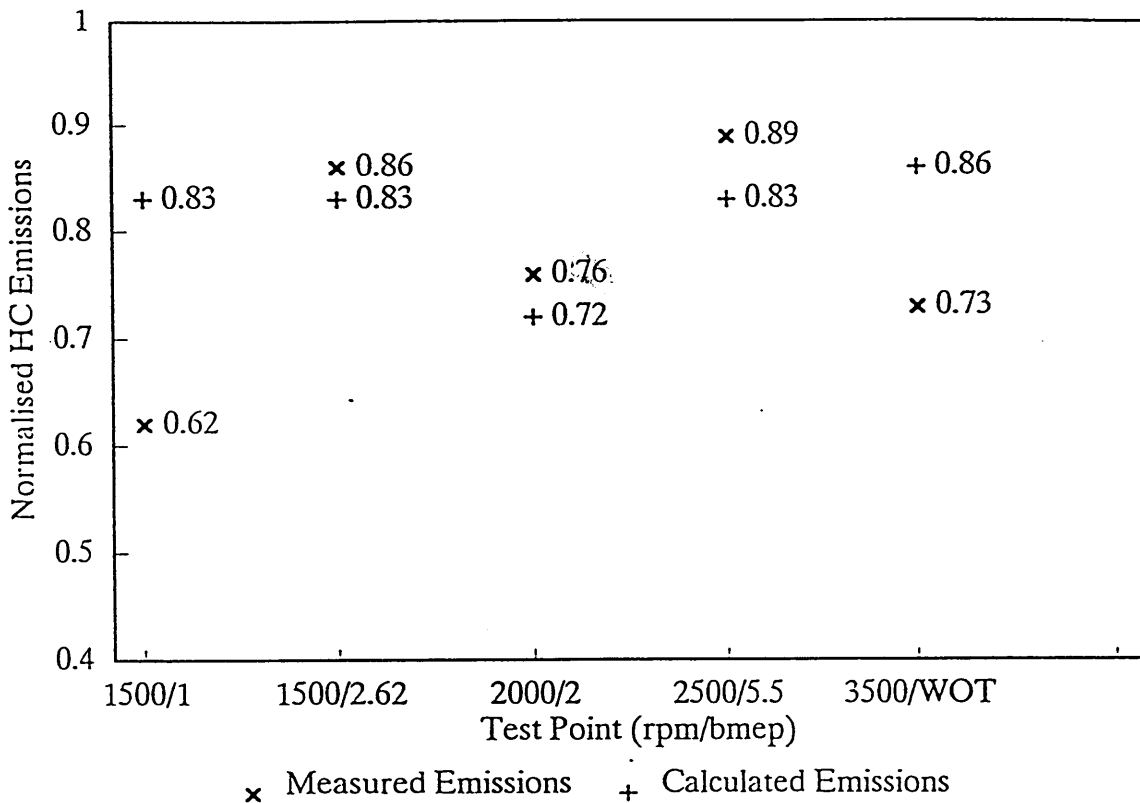
Figure 5.48 Normalised hydrocarbon emissions from enlarged 2nd land piston tests
Comparison between measured and calculated values



— Standard ▲ High Top Ring Piston + Enlarged 2nd Land
 Figure 5.49 Predicted mass flow from 2nd land crevice for high top ring pistons and enlarged 2nd land pistons at 1500rpm 1bar bmep



— Standard ▲ Smooth Liner Piston
 Figure 5.50 Predicted total crevice flow from pistons for smooth liner test at 1500rpm 1bar bmep



x Measured Emissions + Calculated Emissions

Figure 5.51 Normalised hydrocarbon emissions from smooth cylinder liner tests comparison between measured and calculated values

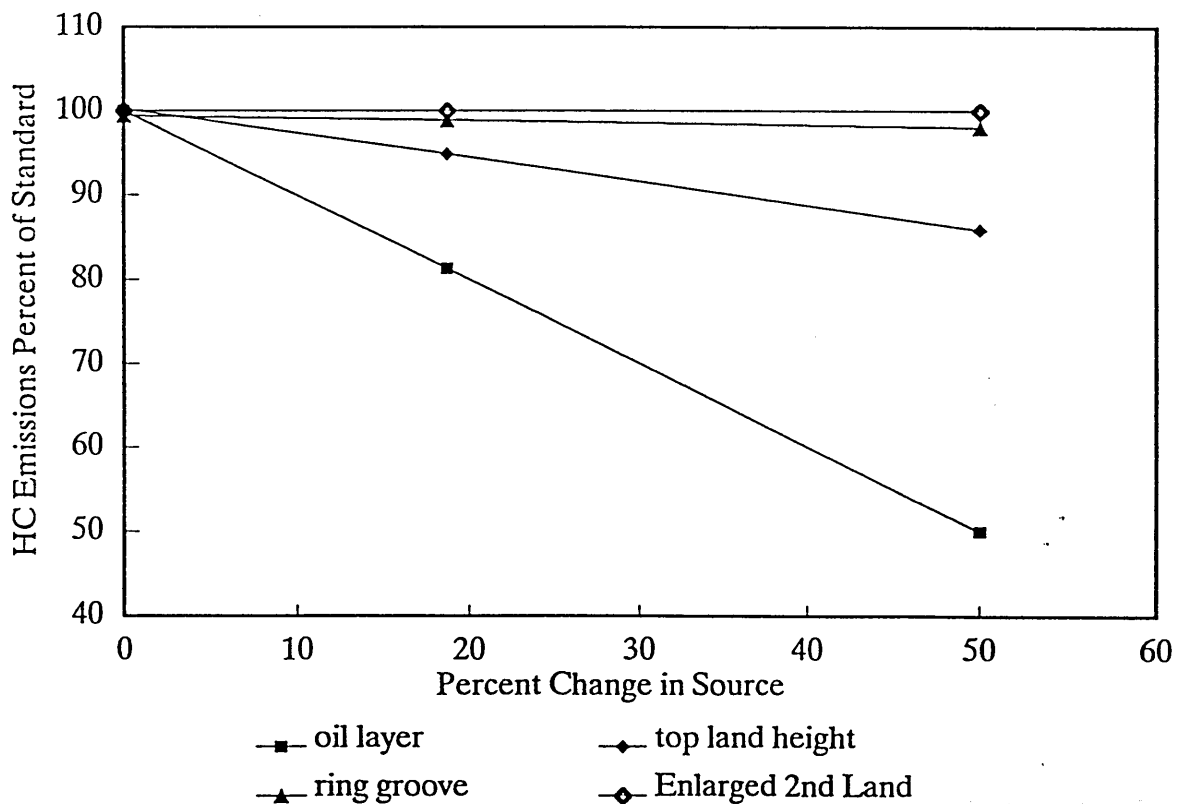


Figure 5.52 Predicted percent change in hydrocarbon emissions at 2000/2bar for percent change in source

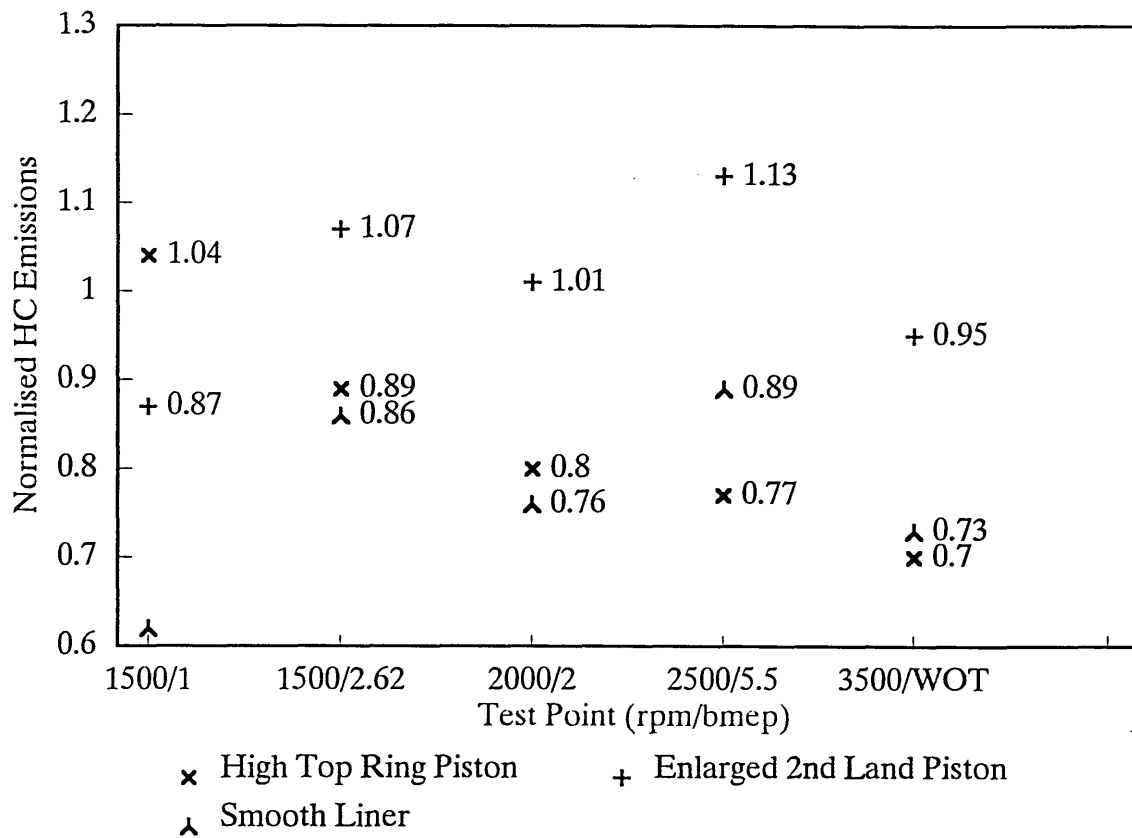


Figure 5.53 Measured normalised hydrocarbon emissions from each engine variation

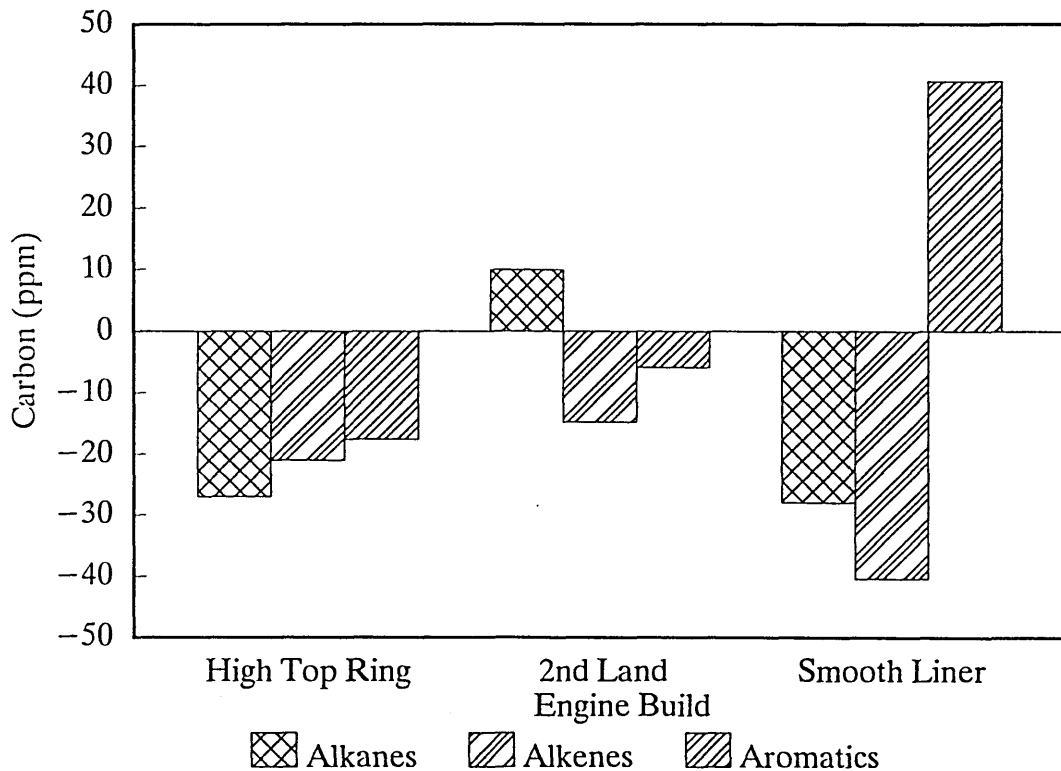


Figure 5.54 Total Alkanes, Alkenes and Aromatics compared against standard build

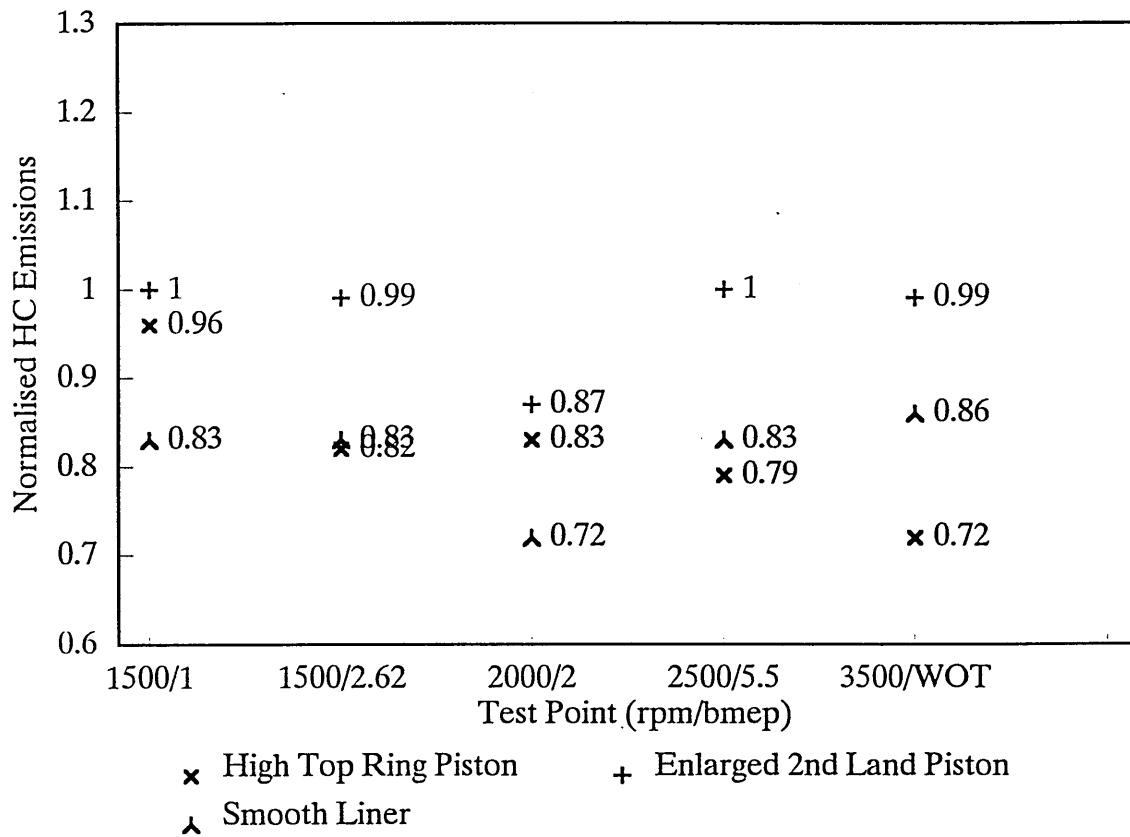


Figure 5.55 Predicted change in normalised Hydrocarbon emissions from each engine variation

6.DISCUSSION

6.1 Introduction

The results from each piston and liner configuration tested have been presented in Chapter 5. These results must be brought together with the results from the theoretical modelling to develop an understanding of the relative contribution to the total hydrocarbon emissions from each source. From this a methodology of controlling emissions can be developed.

6.2. Experimental Results from the Standard Test

6.2.1. Introduction

The standard test will be discussed in detail to review the many other factors affecting the hydrocarbon emissions from the engine, which have been investigated by different researchers. This research has tried to hold these constant to enable a comparison with the piston designs, including air fuel ratio and ignition timing. The results discussed here were observed during the standard and other tests.

6.2.2. Pyrolysis and Oxidation of Emissions in the Exhaust Manifold

The exhaust manifold has a considerable impact on the

hydrocarbon emissions. The hydrocarbon emissions before and after the manifold are plotted in Figure 5.1. This shows that at high speed and load conditions there is a considerable reduction across the manifold. The percentage change in emissions across the manifold is shown in Figure 6.1. The manifold also has a significant effect on the hydrocarbon species which follow a similar trend. At low speed/load conditions there is no significant differences in the gas chromatograph plots before and after the exhaust manifold. However, with higher speed and load a distinct change in the balance in the species occurs. This is readily seen when the engine is fuelled with trimethyle pentane. At 2500 rpm 5.5 bar bmep the unburnt fuel drops from 60% of the total hydrocarbons to 37%. The main product species show an increase of 20%, Table 6.1 shows how the concentration of these species has changed in the exhaust manifold. As this change in species concentration occurs the level of total hydrocarbon emissions has also decreased by 70% at this particular test point. The pyrolysis undergone by trimethyle pentane breaks the structure of this molecule into smaller compounds by breaking the carbon-carbon bonds. This free bond often forms a second bond to the adjacent carbon atom in the chain forming an alkene. Hence the products seen in Table 6.1. Further reactions lead to smaller molecules being formed in addition to complete oxidation occurring at the double bonds reducing the levels of total hydrocarbons. The species analysis for petrol as fuel gives a much more complex result, but the same general trend occurs, with a large increase in pyrolysis products at 2500 rpm 5.5 bar

bmep. At wide open throttle both fuel and products decrease. The percentage change in species is shown in Figure 6.2.

Table 6.1. Unburnt Fuel and Products in Emissions at 2000 rpm 2bar bmep, Fuelled on Trimethyle Pentane

Product Species	Percent Concentration	
	Exhaust Port	Exhaust pipe
Ethylene	2.4%	7.5%
Propylene	4.5%	11.6%
Pent-1-ene	11.8%	23%
Total	18.7%	42.1%
Fuel		
Trimethyl Pentane	60%	37%

The pyrolysis and oxidation of hydrocarbons after combustion is dependent on temperature, residence time and oxygen content, this is stable at 1.4% for an air fuel ratio of 15:1. Table 6.2 shows average exhaust gas temperatures for each test point. The gas temperature at 2500 rpm 5.5 bar bmep is 970 K, combined with the exhaust gas flow rate this gives the correct conditions for high levels of pyrolysis to take place, but insufficient time for full oxidation of the fuel species. This leaves a residue of pyrolysis products. The gas temperature at wide open throttle is high enough for higher levels of pyrolysis and for the oxidation of the products as they

are formed. So the balance between fuel and products is closer to that detected at the exhaust port. An exception to this is an increase of 19% in benzene as a residual of larger aromatic compounds.

Table 6.2 Temperatures at Exhaust ports and pipe

Test Point	Port		Pipe	
	AFR	T (K)	AFR	T (K)
1500/ 1 bar	15	770	15	618
1500/ 2.62	14.9	823	15	688
2000/ 2	15.1	883	15	773
2500/ 5.5	15	970	15	818
3500/ WOT	15.1	1043	15	893

6.2.3. Effect of Single Component Fuel on Hydrocarbon Emissions

The single component fuel was trimethyle pentane which is a branched alkane with eight carbon atoms with the formula C_8H_{18} . The hydrocarbon emissions from this fuel are greater than with petrol across all test points and for each engine build. The trends shown by petrol are also followed by trimethyle pentane. Gas chromatography has shown that 60% of hydrocarbon emissions at the exhaust port are unburned fuel, Table 6.1.

The trimethyle pentane burns slower than a multi-component fuel because it has non of the lighter and more reactive alkenes and aromatics. This leads to peak pressure occurring later and being lower for the same ignition

timing. Thus higher hydrocarbon emissions are due to the poor combustion as the pressure and temperature decrease towards the end of combustion. This would give high levels of unburned fuel as mentioned above.

6.2.4. The effect of different lubricant on emissions

The absorption of fuel in oil has been shown to be a function of the fuel's absorbency in the particular lubricant. This is ideally defined by the Henry Constant as discussed in Chapters 2.3 and 4.2, but this is difficult to quantify for a multi component fuel in a multigrade oil. Tests with another multi grade oil and a synthetic oil gave similar results to the reference lubricant. This test was also carried out during the smooth liner engine test and gave similar results including gas chromatography.

This would indicate that it is the quantity of lubricant present in the combustion chamber rather than the type of lubricant which can control hydrocarbon emissions.

6.3. Comparison of Test Pistons against Standard

6.3.1. High Top Ring Piston

The piston crevice volume is not the only source of hydrocarbon emissions, though at higher speeds it may be the largest due to the higher temperatures and reduced

cycle time for the absorption and desorption of fuel in oil. The volume of the top land was reduced by 35% and achieved a reduction of 25% in hydrocarbon emissions. This could be accepted as a reasonable reduction for the change in volume providing emissions from other sources remained unchanged. However, these are also effected by the change in top ring height.

The modelling, see Chapter 4, suggests that top ring groove flow has a similar timing to the top land and so they would behave as one crevice. The modelling also suggests that changes to top land diameter will affect 2nd land flow. For the high top ring piston the smaller diameter has the effect of increasing this flow. Figure 5.52 shows how the 2nd land flow is affected by this change. The return flow starts approximately 10° earlier than standard and quickly rises to a peak before decreasing rapidly and approaching zero 20° before the standard.

The top land height also has an effect on the absorption of fuel. In this case a reduction in height from 6mm to 2.8mm reduced the area of oil exposed to the unburned fuel by 53% at TDC.

Another change caused by the raising of the piston rings is the effect on piston temperature. The rings are the main route for heat transfer from the piston. An investigation by Furuham (42) has shown that raising the rings can lower the temperature of the piston by approximately 20°C . This also reduces the temperature at the top of the cylinder wall by approximately 3°C . For flow calculations it is assumed that the crevice gas temperature is equal to the piston temperature, this reduces the gas

viscosity. As the mixture flows from the crevices to mix with burnt gases the lower piston temperatures may also effect the rate of oxidation.

The results from this test can now be explained. The reduction in the top land crevice volume is effectively 16%. Combined with the reduction in emissions from desorbed fuel this should have given a reduction at all test points. But at low load the increased 2nd land flow counteracted the reduction, because of the lower level of in-cylinder oxidation. At higher speeds and loads the timing of the second land flow becomes critical. Although the flow is greater than for standard pistons it occurs earlier, and so encounters much higher temperatures leading to its oxidation. Thus at high speeds and loads there is a reduction in emissions from both top and 2nd land crevice volumes and the reduction in the oil area for the absorption and desorbed of fuel. Inspection of Figure 5.11 indicates that this occurs at 2000 rpm, 2bar bmep and higher.

The variations in the hydrocarbon species must be put into the context of the reduced emissions from different sources and the overall reduction in emissions. Most species have been reduced but by differing amounts, rather than a reduction proportional to the change in total hydrocarbon emissions. The balance of the species being emitted are affected by the amount of pyrolysis which occurs. The changes to crevice flow will affect the timing of the mixture returning to the combustion chamber and the conditions of temperature and pressure encountered by the

mixture. These conditions change the rate of pyrolysis and oxidation reactions.

6.3.2. Enlarged 2nd Land Pistons Discussion

The results from this build have only shown a significant reduction in hydrocarbon emissions from two test points despite the increase in 2nd land volume of 162%. At other test points only a slight decrease in emissions was measured which are not seen as significant.

The reduced emissions came from 1500 rpm, 1 bar bmep and 2000 rpm 2 bar bmep. The reductions were due to the change in 2nd land flow. Predictions of this flow, Figure 5.52, indicate that it occurred later in the cycle than for standard pistons, and for a longer duration. The calculations do not take into account piston ring dynamics, Chapter 4.1.

The dynamics of the piston ring and its position within the ring groove has been the subject of many studies. The forces acting on the ring in an axial direction are due to pressure, friction and inertia. During the expansion stroke at low loads the rings move from the bottom to the top of the ring groove. This will allow the 2nd land mixture to be released as blow-by. The predicted reduced pressure in the second land will change the crank angle at which the piston rings lift. As mentioned in Chapter 6.3.1, mixture from the 2nd land undergoes a low level of oxidation at low loads. Reducing this flow will have a significant effect on hydrocarbon emissions.

However, at higher loads the piston rings are more stable so the back flow returns more of the 2nd land mixture to the combustion chamber. This raises the level of hydrocarbon emissions to that of the standard build.

The species profiles given by gas chromatography have shown greater changes. This is due to small changes in the mass flow rate and timing of the 2nd land flow altering the pressure and temperature the species encountered giving different levels of pyrolysis. The reduction in products would indicate that a lower level of pyrolysis is occurring and that the mixture is returning to the combustion chamber later in the cycle, as suggested above.

6.3.3. Smooth Cylinder Liner Discussion

Significant reductions in hydrocarbon emissions have been achieved from this build. The percentage variations from standard are shown in Figure 6.3. Reductions of 40 percent were achieved at 1500 rpm test points. At higher speeds the reduction in hydrocarbon emission levels are marginally lower than those obtained from the high top ring piston tests. Although there were some differences in piston dimensions from the standard, the predicted crevice flow would be similar, Chapter 5.2.

The predicted reduction in oil layer thickness is 17 percent, but the reduction in hydrocarbon emissions are much larger than would be predicted from a direct relationship between lubricant thickness and absorption of fuel. The main differences between actual and predicted results are observed at the lowest and highest speed/load

test points.

The assumption is that the change in oil layer thickness due to surface finish would be the same at any test point. This is the residual oil layer on the liner and not that between piston ring and cylinder. The thickness may be more variable due to oil transportation and viscosity changes with temperature. This will have an impact on an initial assumption that the oil surface would be at the 2% Tp value, for this smoother surface it could be at a lower depth. The oil reservoir measurement, R_{vk} , predicts much smaller reductions in lubricant thickness than the method used in this research.

The reduction of most species observed from standard to smooth liners is in part due to the overall reduction in HC emission levels but some of the reduction in the products could be due to the large increase in toluene. The only significant change to account for the overall decrease in emissions and increase in toluene are the changes to the surface finish. The difference in the calculated oil layer is small, 0.042 micron, for the worn liners. Absorption and desorption processes are very sensitive to changes in oil thickness. Dent and Lakshminarayanan (4) indicated a rapid decrease in emissions with reducing oil layer thickness.

The following is a possible mechanism for the increase in toluene:

The various components of the fuel are not absorbed into the oil evenly, some species being more readily absorbed. The controlling factor is cylinder pressure, the

more soluble species being absorbed at lower pressures. If the oil layer is reduced then the oil may become saturated and unable to absorb other species. The species not absorbed would be burnt or oxidised while the species emerging from the oil later in the cycle would escape oxidation. The concentration of aromatics in Hydrocarbon emissions in the standard test is higher than in the fuel, possibly due to their absorption in oil. The reduced oil layer in smooth liner tests must then be selecting toluene which is more soluble than other aromatics due its molecular weight and structure.

To observe if the oil absorbed toluene more easily than other aromatics, samples of oil were taken from the engine during operation. These were heated to a temperature of 80°C, this is below the boiling point of the normal constituents of the lubricant. Vapour was withdrawn from above the oil then injected into the gas chromatograph. The results were compared against samples from fresh lubricant. Vapour from fresh oil showed no significant levels of lighter fuel hydrocarbons, but samples of used oil show an increased presence of hydrocarbon species, especially toluene. Figure 6.4 compares gas chromatograph plots of oil vapour from standard and smooth liner tests. Both samples were taken from the engine operating at 3500 rpm wide open throttle. From these plots it can be seen that toluene is a major component of fuel vapour absorbed by the oil. The toluene peak is much greater from the smooth liner. Toluene comprises 10% of the vapour from standard and 40% from the smooth liner tests. This is (in) approximately the same proportion as the emissions, and

suggests that the increase in toluene is due to its being preferentially absorbed by the lubricating oil.

The decreasing trend of toluene with increasing speed and load, Figure 5.48, is also consistent with its being absorbed into the oil. As the absorption and desorption effect reduces with increase in speed, its contribution to total hydrocarbon emissions decreases.

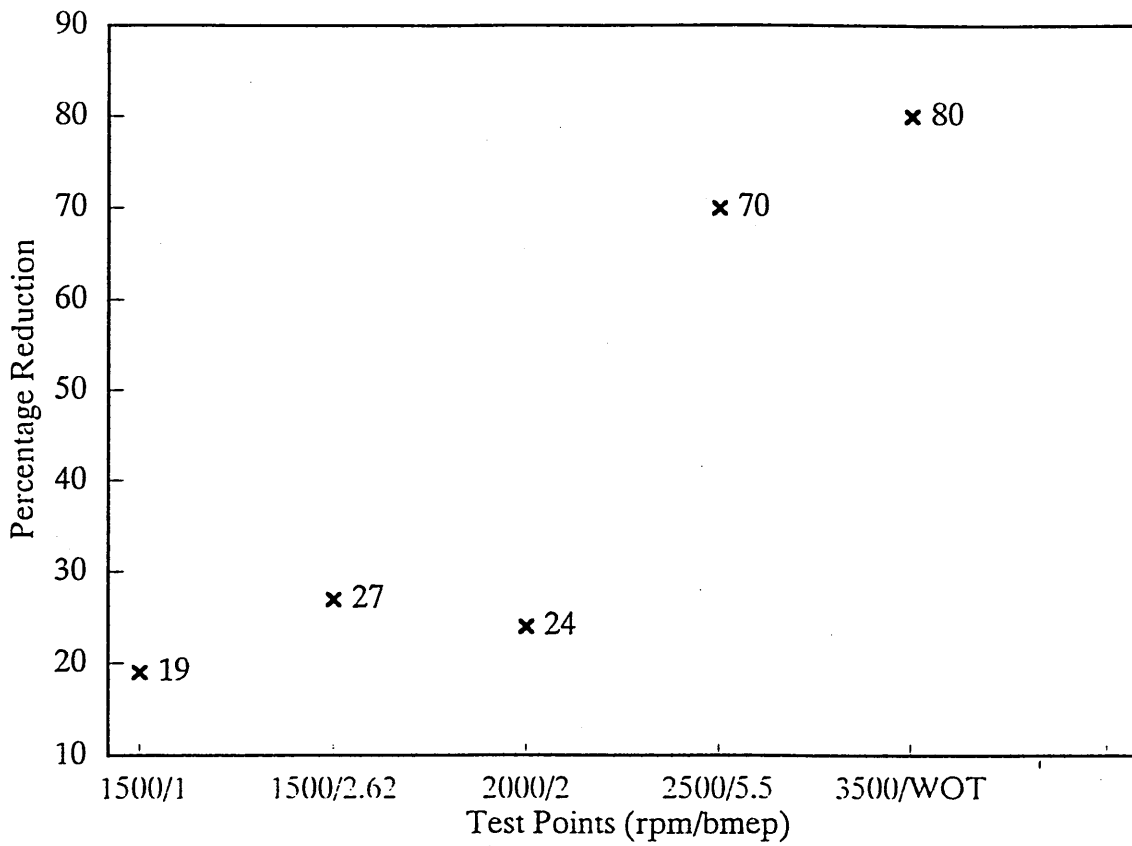


Figure 6.1 Percentage reduction in hydrocarbon emissions across the exhaust manifold

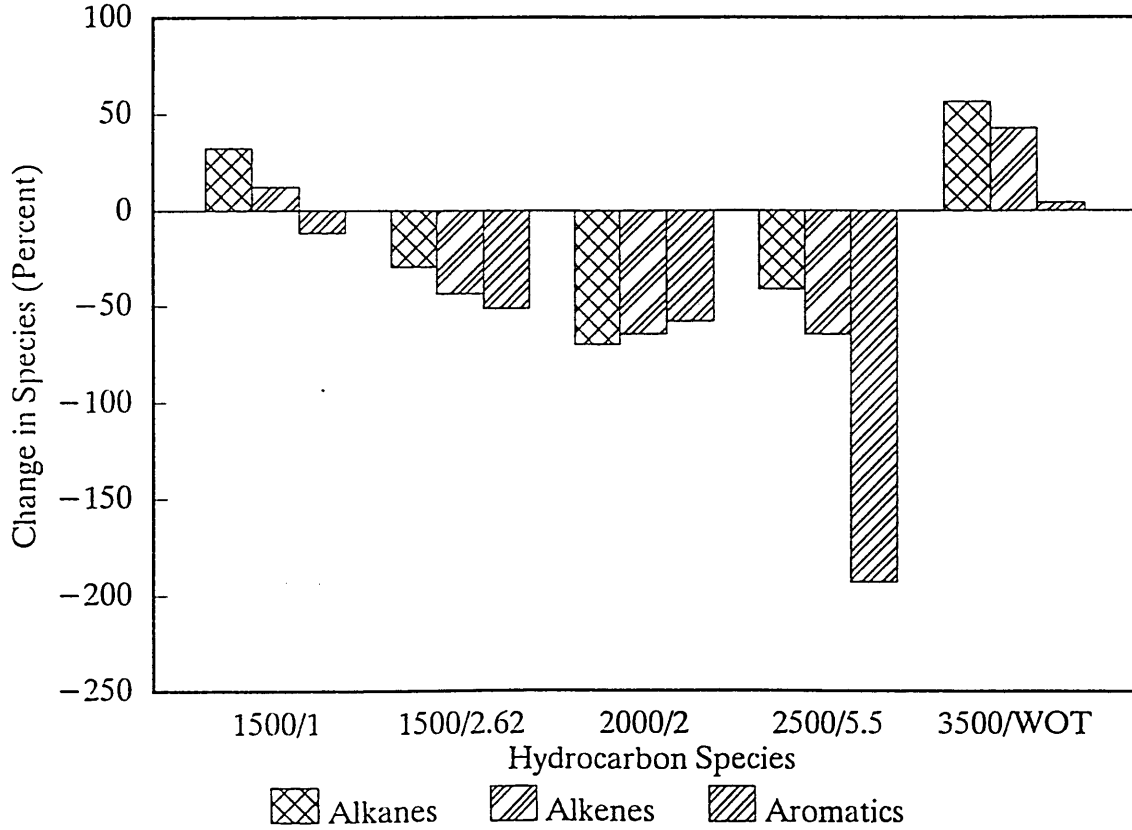


Figure 6.2 Percentage change in HC species across the exhaust manifold

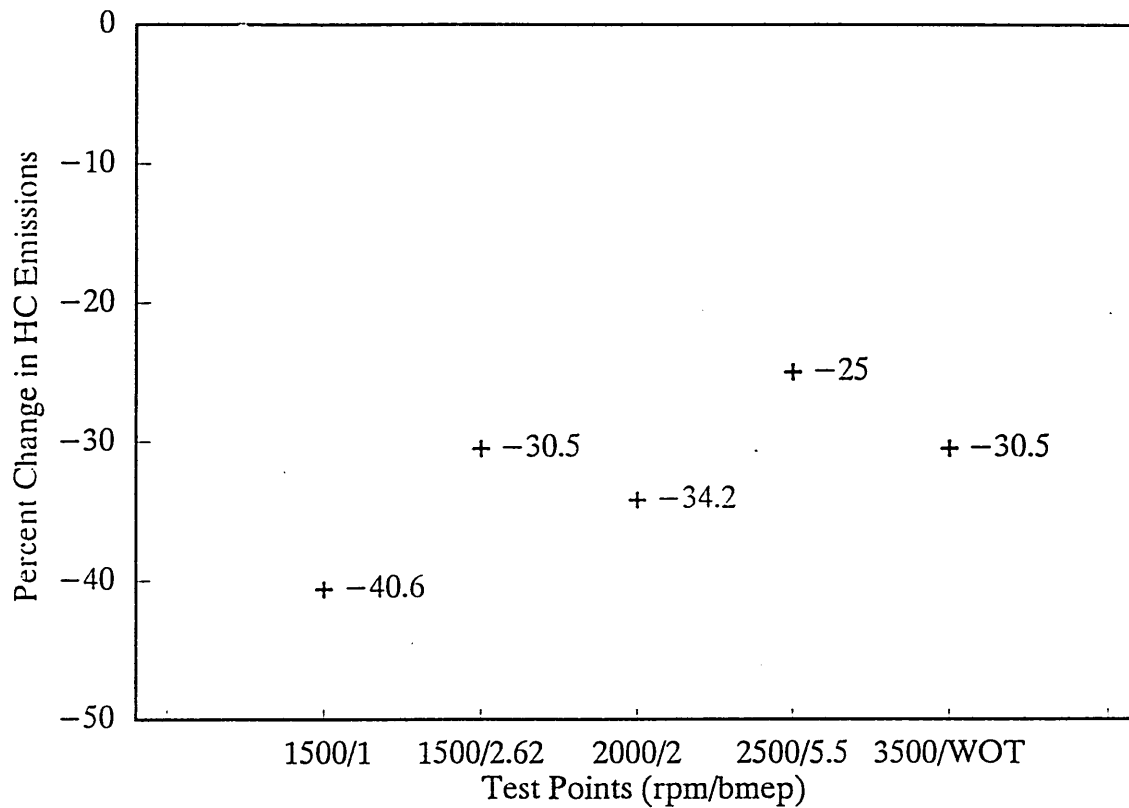
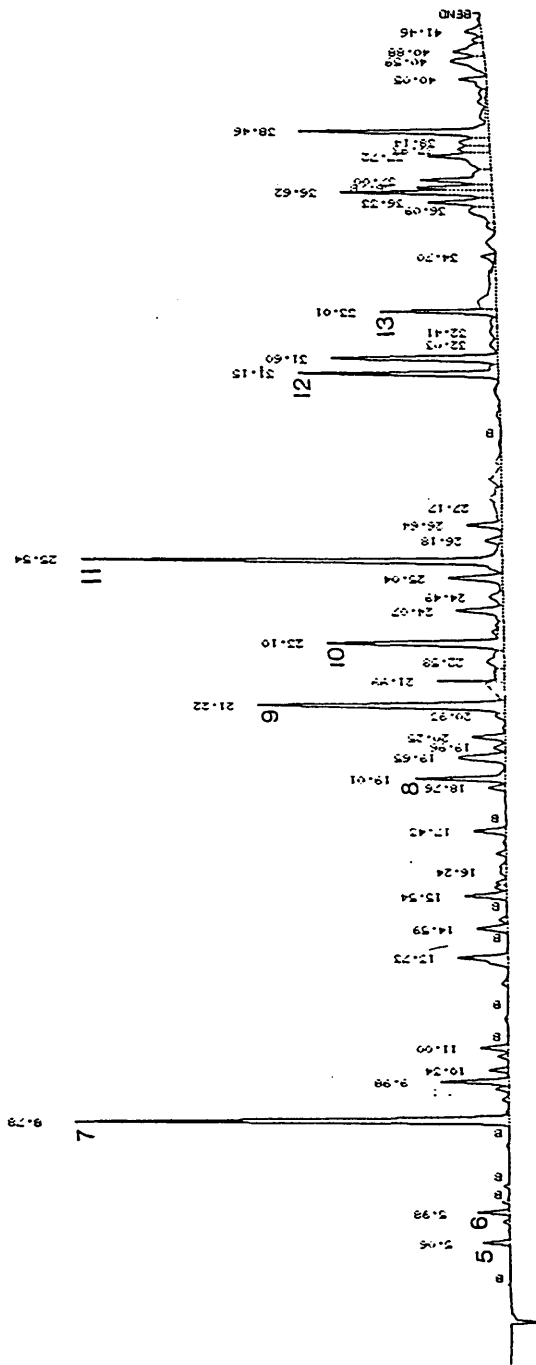


Figure 6.3 Percentage change in hydrocarbon emissions from standard to smooth liner test



6.4. Methods of Reducing Hydrocarbon Emissions

The results show that the two successful methods of controlling hydrocarbon emissions were top land crevice volume and cylinder liner surface finish. Both these methods have limits to their effectiveness.

6.4.1. Top Land Crevice Volume

The theoretical work has shown two aspects to reducing hydrocarbon emissions from crevice volumes, reducing top land height and reducing clearance between piston and cylinder.

In addition to reducing the top land volume raising the top piston ring reduces the area of oil exposed for the absorption of fuel. However, the reduction of top land height is limited by its strength to withstand the top ring inertia forces. Various researchers have used pistons with minimum top lands, or L shaped piston rings, but these were usually operated for short duration tests, Wentworth (5) and UKEEC (54). The minimum top land height can be reduced by improvements to material strength of piston and reduction of top ring mass. The 2.8 mm top land in the experiment performed in this research was the safe minimum for the particular piston specification.

Reducing the clearance between piston and cylinder is limited by the different coefficients of expansion of the aluminium alloy piston and the cast iron cylinder liner. The clearance at the engine's maximum operating temperature must be adequate to avoid seizure. This will give larger

clearance at lower operating conditions.

6.4.2. Cylinder Liner Surface Finish

The requirement for a thin lubricant layer to reduce absorbed fuel emissions must be balanced with the need for adequate lubrication. The plateau honing of the cylinder liner has been developed to give a high surface metal area as a bearing surface and to have regular grooves as a lubricant reservoir. A polished surface will not retain oil and the engine would either have high oil consumption or a piston could seize due to inadequate lubrication. The liners used in experiment were found to be polished on the thrust side by the tests completion. Considerable research will be required to identify a compromise between engine durability and lubricant thickness for low emissions.

6.5. Optimum Piston and Liner Design

The ideal piston for low hydrocarbon emissions would have the minimum top land height and maximum diameter, and the cylinder liner surface finish should be very smooth to minimise retained oil. However, taking the above discussion into consideration an optimum set of piston and cylinder liner dimensions were identified Table 6.3, and Figure 6.5 is a sketch of this piston. The main features of these pistons are a small top land with the minimum clearance between piston and cylinder and a larger 2nd land diameter. To allow for adequate lubrication the oil layer specified was thicker than the smooth liner test. These were used as

inputs into the computer model.

The calculations gave considerably lower 2nd land pressures than the standard, Figure 6.6 shows the effect this has on 2nd land flow. The magnitude of the flow back into the chamber is slightly reduced. The top land flow is also reduced, Figure 6.7. The optimum crevices show approximately 75% reduction in flow. The impact on total crevice flow is demonstrated in Figure 6.8.

Plotting the predicted normalised emissions for the ideal and optimum piston against other engine builds, Figure 6.9, it can be seen that the predicted change in emissions are very low for the ideal piston. The optimum piston achieves emissions lower than any test. This demonstrates the potential to reduce hydrocarbon emissions by tightening component specification even after the compromises for component durability and other requirements.

Table 6.3 Piston Dimensions for Minimum Emissions

Piston	Top Land		2nd Land	
	Height	Diameter	Extra Vol.	Diameter
Ideal	1.0 mm	74.8 mm	0	74.75mm
Optimum	2.5 mm	74.65mm	0	74.55mm
Ideal Oil Layer	0.15 μm			
Optimum Oil Layer	0.225 μm			

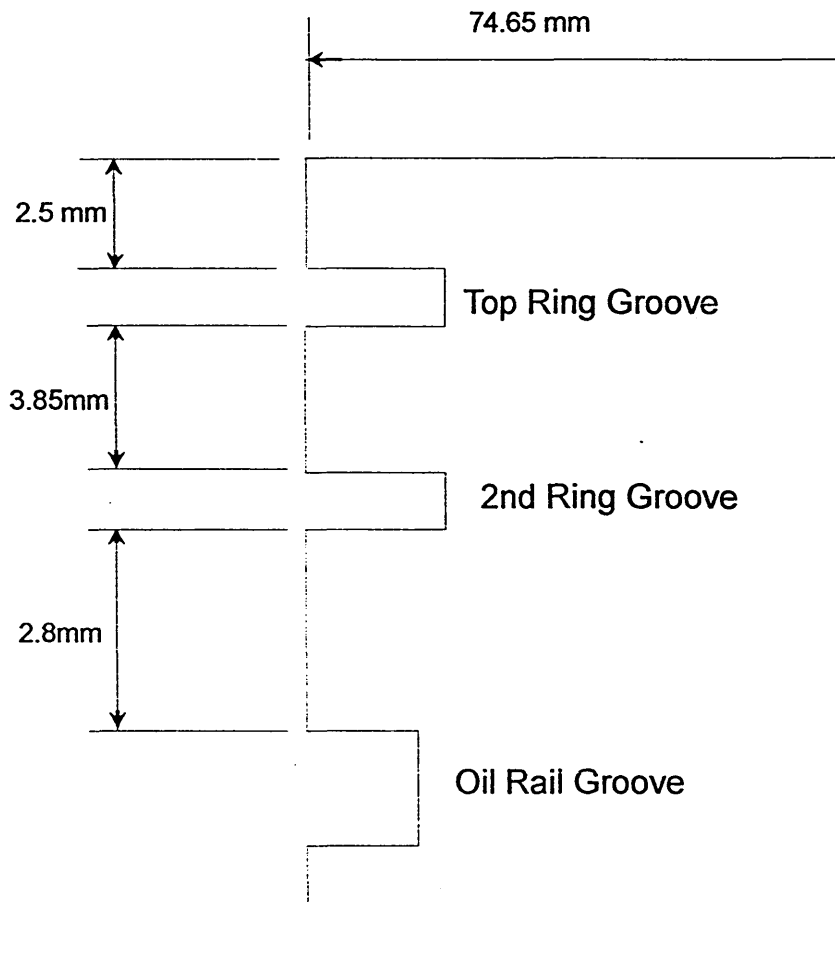


Figure 6.5 Sketch of optimum piston showing dimensions

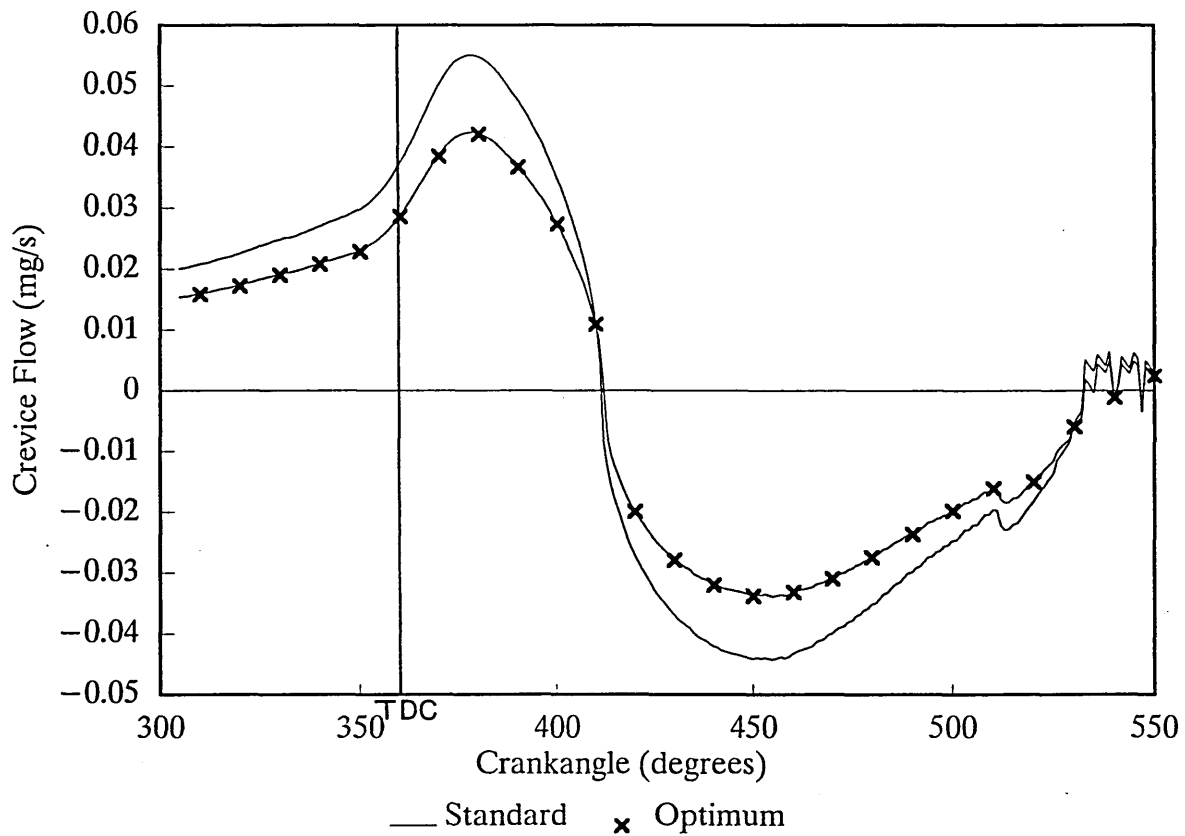


Figure 6.6 Predicted 2nd land crevice flow from optimum piston at 1500rpm 1 bar bmep

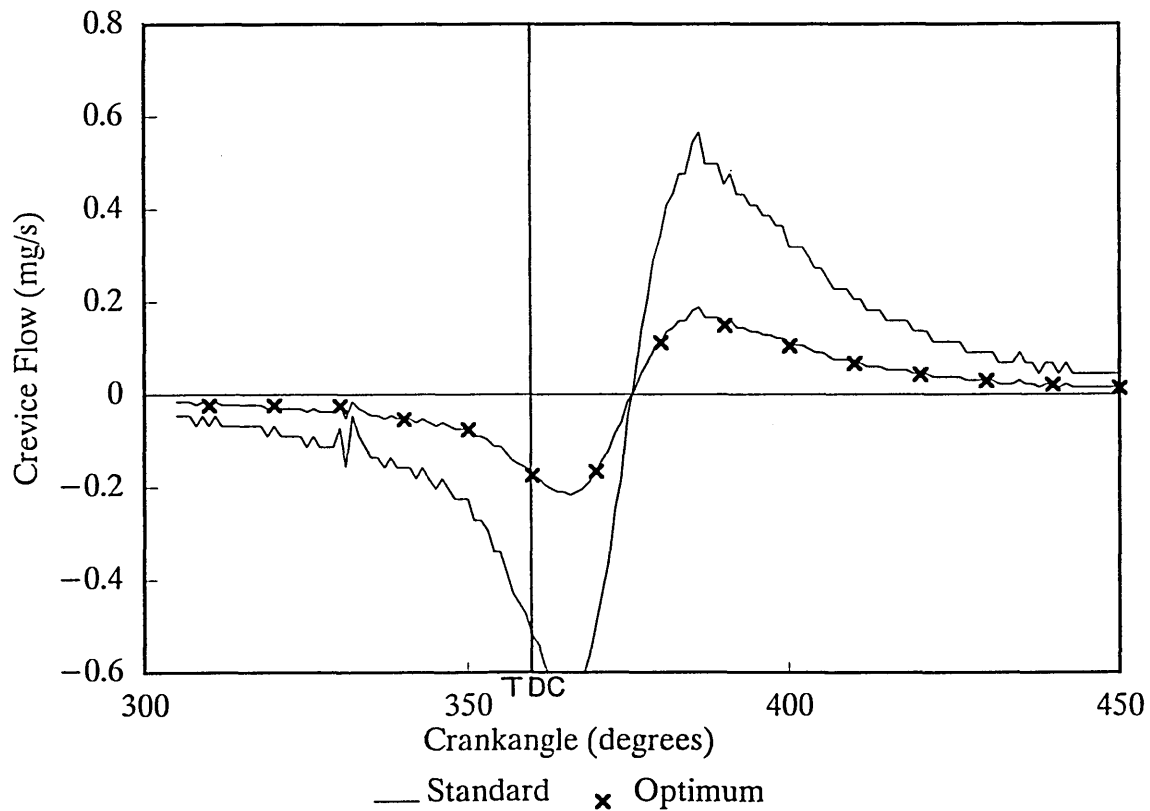


Figure 6.7 Predicted top land crevice flow from optimum piston at 1500rpm 1bar bmep

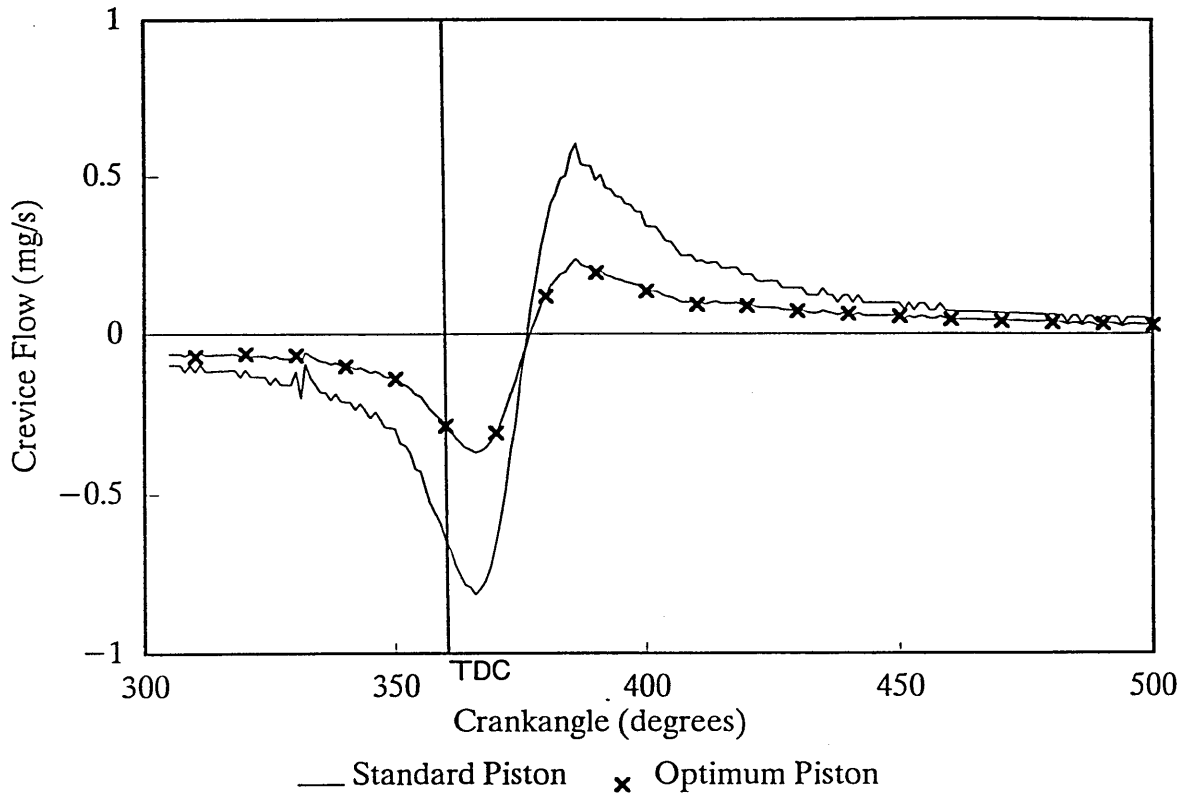


Figure 6.8 Predicted total flow from Piston Crevices for Optimum Piston Dimensions at 1500rpm 1bar bmep

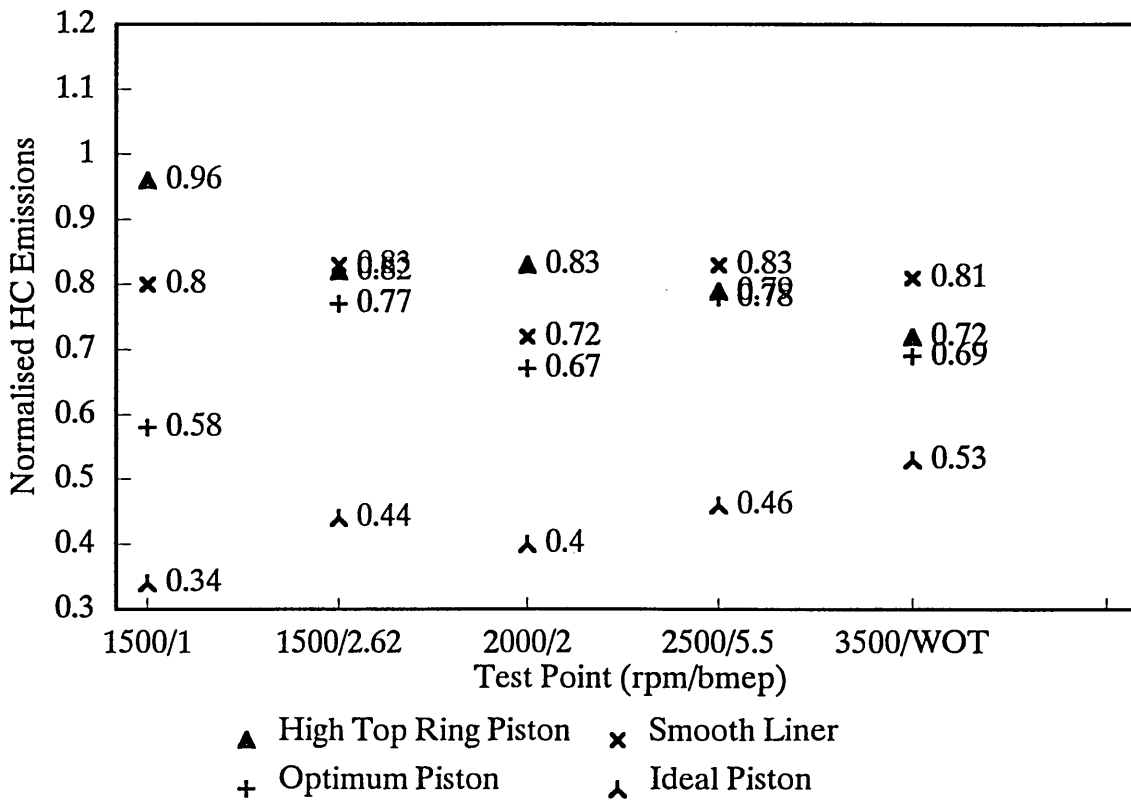


Figure 6.9 Predicted normalised hydrocarbon emissions from Optimum and ideal piston designs compared against tested piston variants

7. CONCLUSION

7.1. Introduction

These conclusions will assess the two main aspects of this research, experimental including gas chromatography and modelling. The two sections will then be combined to indicate the piston design considerations for reduced hydrocarbon emissions.

7.2.1 Experimental

The results obtained from the tests showed that piston crevice volumes and lubricant thickness can influence hydrocarbons and by careful design reduce these emissions. The link between the change in design and emissions was not directly proportional, by changing one aspect of the design to reduce emissions from one source, will affect emissions from other formation mechanisms. This was evident in the high top ring tests, where both 2nd land crevice flow and absorption were effected by the changes in piston design. The change in hydrocarbon emissions from a particular design also varied with speed and load. The normalised emissions from each design variation has shown that the largest reduction in emissions was gained from the smooth cylinder liner, especially at low speed low load conditions. The reduction in emissions was greater than would have

been predicted from the change in oil layers and is probably due to the lubricant layer being thinner than predicted, because the surface of the lubricant is lower in the surface profile at certain speeds and loads than was assumed in calculations.

The enlarged 2nd land test gave only small reductions in emissions. Although the magnitude of 2nd land flow was reduced it is the timing of this flow that has a greater effect on the total hydrocarbon emissions.

7.2.2. Gas Chromatography

The analysis of hydrocarbon species from each engine test has shown that the balance of these species is sensitive to the design changes. It was observed that each hydrocarbon compound is affected differently, some increased in concentration despite an overall decrease in emissions. For the analysis thirteen species were identified, these were divided into three groups, Alkanes, Alkenes and Aromatics. The largest change in the species distribution was observed from the smooth liner test. The thinner oil layer appeared to be saturated by toluene and so other species were not absorbed due to them being less soluble in the lubricant.

7.3. Modelling

The results from the modelling gives an excellent correlation with experimental results and predicted similar trends with changes in piston and cylinder liner

configuration. The average error between predicted and measured hydrocarbon emissions is 9%. The closest results are obtained at the middle range of speeds and loads.

The simplification of 2nd land crevice flow has enabled some prediction of the effects of volume changes in this region. It has been demonstrated in the experimental work that changes to the volume of this region has only a small effect on the total hydrocarbon emissions, but when combined with other changes it can have a significant effect at certain conditions.

To enable the prediction of directly comparable results would require a considerably more complex model.

7.4. Piston Features for reducing Hydrocarbon Emissions

The feature of piston design dominant as a control of hydrocarbon emissions is the top land. In addition to affecting the mass of fuel stored in the top land the dimensions also affect 2nd land crevice flow and fuel absorption into oil. These effects are dependent on speed and load, it has been shown that at certain conditions 2nd land crevice flow can significantly effect hydrocarbon emissions, by altering the time that mixture returns to the combustion chamber and thus the rate of oxidation experienced by the mixture.

The use of a smoother cylinder liner can be effective in reducing the quantity of oil present for the absorption and desorption process and this has been shown to be effective in reducing hydrocarbon emissions. Also

absorption of fuel into the lubricant is dependent on the time available for diffusion through the oil. The amount of fuel a lubricant will absorb is also affected by the lubricant temperature. Emissions from this source will be greater when low speed and load give longer cycle times for diffusion and lower lubricant temperatures.

8. RECOMMENDATIONS FOR FUTURE WORK

8.1 Pistons for Low Hydrocarbon Emissions

To further the understanding of the contribution of each source of emissions to the total both the experimental and modelling could be extended.

The piston crevices should continue to be an area of development. Improved material selection could strengthen piston top lands to allow higher top rings. The temperature variations of pistons and liners at different operating conditions should be further investigated. This could result in closer running clearances between piston and cylinder.

The reduction in hydrocarbon emissions achieved by reducing the thickness of oil layers can be extended by investigating surface finish and lubricant retention on a surface and how this may satisfy the lubrication requirements of piston rings.

The piston ring design could be improved to reduce the oil required by the ring and in conjunction with a smooth cylinder liner would reduce emissions and prevent the polishing of the bore observed after the experiment. Material selection could also contribute as ceramic and composite materials continue to be developed.

8.2 Extending the Predictive Model

The model which has been developed has made several

assumptions to enable it to run with the data available. It has been shown that it is capable of predicting the trends encountered for different piston designs, but it could be improved and extended to predict levels of hydrocarbon emissions at the exhaust port.

The model has assumed cold piston dimensions for calculation of crevice volumes. This could be improved with accurate prediction of piston and cylinder temperatures for the piston design changes. From this the modelling of their dimensions at these temperatures would give the crevice volumes. Also an accurate method of predicting oxidation and the extension of the model to predict oxidation which occurs in the exhaust port. The modelling of oxidation has been discussed by Heywood (73) and it was shown that actual levels of oxidation are prone to considerable variability not predicted by these models.

The cold starting of engines has been identified by many researches as a period when hydrocarbon emissions are very high. The contribution of crevice volumes and oil layers at low engine temperatures and poor combustion conditions has not been identified.

9 ACKNOWLEDGEMENTS

I would like to thank the following people for their help and support throughout this research.

Prof. D.H.Tidmarsh	Director of Studies
Dr P.Foss	Second supervisor
Dr B.L.Ruddy	Second supervisor
E.Hartley	Industrial Advisor

I would also like to thank Dr D.Leathard for his advice on chemical analysis.

Science and Engineering Research Council, for funding Award Number 90554982.

AE Piston Products Ltd for contribution of financial aid and equipment.

I Wish also to thank P.Kisby, D.Allen, R.Wilkinson and all of the technicians in the School of Engineering who have assisted me in this research.

REFERENCES

1 Cragg,C: Cleaning up motor car pollution, new fuels and technology. Financial business information. ISBN 1 85334 158 4. 1992.

2 Daniel,W.A: Flame quench at the walls of an internal combustion engine. Proceedings of the 6th international symposium on combustion. 1957.

3 Daniel,W.A. Wentworth,J.T: Exhaust gas hydrocarbons, Genesis and Exodus. 1962. SAE 486B.

4 Tabaszynski,R.J: Time resolved measurement of the HC massflow rate in the exhaust of an SI engine. SAE Transactions. 1972. SAE 720112.

5 Wentworth,J.T: Piston and ring variables affect exhaust emissions. SAE. 680109

6 Wentworth,J.T: Effect of top compression ring profile on oil consumption and blow-by with the sealed ring orifice design. SAE. 820089.

7 Wiess,P. Keck,J.C: Fast sampling valve measurements of HC,s in the cylinder of a CFR engine. SAE 810149.

8 Lorusso,J.A. Kaiser,E.W. Lavoie,G.A: Quench layer contribution to exhaust hydrocarbons from a spark ignited engine. Combustion Science and Technology. 1981. Vol.25. p121-125.

9 Heywood, J.B. Keck, J.C: Sources of unburned hydrocarbon from homogeneous charge auto engines. Sandia report. 1983. SAND83-8241.

10 Haskell, W.W. Legate, C.E: Exhaust hydrocarbon emissions from gasoline engines - surface phenomena. SAE. 720255.

11 Namazian, M. Heywood, J.B: Schlieren visualisations of the flow and density fields in the cylinder of an SI engine. SAE 800044.

12 Namazian, M and Heywood, J.B: Flow in the piston-cylinder-ring crevices of an SI engine and its effect on HC emissions, efficiency and power. SAE. 820088.

13 Panesar, A. Brown, P.G. Woods, W.A: The results of recent experiments on unburnt hydrocarbons. Combustion in Engines, Technology and Application. IMechE.1988. C45/88.

14 Miyachika, M: An analytical evaluation method for lubrication oil consumption. Proceedings IMechE, 1991. Vol 205 No D1. pp 31-39

15 Kue, T.W. Seenau, M.C. Theobald, M.A. and Jones, J.D: Calculation of flow in the piston-cylinder-ring crevices of a homogenous charge engine and comparison with experiment. SAE 890838.

16 Reitz, R.D. and Kue, T.W: Modeling of HC emissions due to crevice flows in premixed-charge engines. SAE 892085.

17 Hymas,G.J. Girgulis,V.J. Brown,P.G. and Woods,W.A:
Post flame release of hydrocarbons in a spark ignited
engine. Proceedings International Conference, Combustion in
Engines. Technology, Applications and the Environment
IMEchE. 1992.

18 Kaiser,E.W. Adamczyk,G.A. Lavoie,G.A: The effect
of oil layers on the HC emissions generated during closed
vessel combustion. Combustion Institute. 18th Symposium on
Combustion, 1981. p 1881-1890.

19 Kaiser,E.W. Rothschild,W.G. Lavoie,G.A: The effect
of fuel and operating variables on hydrocarbon species
distribution in the exhaust from a multi cylinder engine.
Combustion Science and Technology. 1983. Vol 32. pp 245-
265.

20 Adamczyk, A.A: Rothschild,W.G. Kaiser,E.W: The
effect of fuel and oil structure on hydrocarbon emissions
from oil layers during closed vessel combustion. Combustion
Science and Technology. 1985. Vol 44. pp 113-124.

21 Adamczyk,A.A. and Kack,R.A: The effect of oil
layers on hydrocarbon emissions: Low solubility oils.
Combustion Science and Technology. 1984. Vol. 36. pp 227-
234.

22 Ishizawa,S and Takagi,Y: A study of hydrocarbon
emissions from a spark ignition engine (the influence of
fuel absorbed into cylinder lubricating oil film). JSME.
International Journal. 1987. Vol.30. No.260. pp 310-317.

23 Yates,D.A: The compact high-speed gas sampling valve for an internal combustion engine. ImechE. 1987. pp 35-42

24 Yates,D.A: Hydrocarbon sampling from the combustion chamber of a lean burn engine. Conference proceedings Vehicle Emissions and European Air Quality. ImechE. 1987. C332/87. pp 221-227.

25 Schramm,J and Sorenson,S.C: Effects of lubricating oil on hydrocarbon emissions in an S.I. engine. SAE 89062.

26 Carrier,G. Fendell,F. Feldman,P: Cyclic absorption /desorption of gas in a liquid wall film Combustion Science and Technology. 1981. Vol.25. pp9-19.

27 Dent,J.C. and Lakshminarayanan,P.A: A model for absorption and desorption of fuel vapour by cylinder lubricating oil film and its contribution to HC emissions. SAE. No 830652.

28 Korematsu,K: Effects of fuel absorbed in oil film on unburnt hydrocarbon emissions from spark ignition engines. Japanese Society of Mechanical Engineers. 1990. Vol. 33. No.3 pp 606-614.

29 Korematsu,K: Effects of fuel absorbed in oil film on unburnt hydrocarbon emissions from spark ignition engines. (Influence of oil added on piston crown on total hydrocarbon concentration in exhaust gas). Japanese Society of Mechanical Engineers. 1991. Vol. 34. No.3 pp 362-368.

30 Gatellier,B. Trapy,J. Herrier,D. Quelin,J.M. and Galliot,F. Hydrocarbon emissions of SI engines as influenced by fuel absorption-desorption in oil films. SAE 920095.

31 Rassweiler,G.M. and Withrow,L: Motion pictures of engine flames correlated with pressure cards. SAE 800131 (first presented in 1938).

32 Stone,C.R. and Green-Armytage,D.I: Comparison of methods for the calculation of mass fraction burnt from engine pressure time diagrams. Proceedings IMechE. 1987. Vol 201. No D1. pp 61-67.

33 Lavoie,G.A. Blumberg,P.N: A fundamental model for predicting fuel consumption, NOx and HC emissions of the conventional spark ignited engine. Combustion Science and Technology. 1980 Vol. 21 pp 225-258.

34 Schramm,J and Sorenson,S.C: A model for hydrocarbon emissions from S.I. engines. SAE 902169.

35 Bascunana,J.L. Skibinski,J. and Weaver,E.E: Rates of exhaust gas reactions. SAE 770639.

36 Caton,J.A. and Heywood,J.B: Models for heat transfer, mixing and hydrocarbon oxidation in a exhaust port of a spark ignited engine. SAE 800290.

37 Bennet, J. Girgis, N.S. Kokabi, M. and Yates, D.A.: Species concentration changes in gas sampled from the exhaust port and combustion chamber of a spark ignited engine: Cyclic dispersion and fuel-in-lubricant solubility effects. Conference Proceedings IMechE 1990. C394/046. pp 61-69.

38 Crouch, A.R. Gilbert, I.P. and Norris, R.D. Gasoline engine efficiency-design solutions. Conference Proceedings. FISITA. IMechE. 1992. Vol 1. C389/188. pp 271-280.

39 Kamp, H and Essig, G: Piston design for low emission engines. Conference Proceedings, World wide engine emission standards and how to meet them. IMechE. 1991. pp 221-243.

40 Gupta, A.K. and Jiang, L: The effect of piston geometry on combustion and emissions. Conference Proceedings, Winter Annual Meeting of American Society of Mechanical Engineers. ASME. 1991. pp 109-119.

41 Furuhashi, S. Kojima, M. Enomoto, Y. and Yamaguchi, Y: Some studies on two ring pistons in an automobile turbocharged gasoline engine. SAE 840183.

42 Furuhashi, S. Hiruhama, M. Takamatsu, T. and Shin, K: Development of a two ring piston with low friction and small compression height without increase in blow-by, overheat and oil consumption. Proceedings International Conference, Combustion Engines. Reduction of Friction and wear. IMechE. 1985. C63/85. pp 43-49.

43 Frank,R.M. and Heywood,J.B: The effect of piston temperature on hydrocarbon emissions from a spark-ignited directinjection engine. SAE 910558.

44 Douaud, A. deSoete,G. Henalt,C: Experimental analysis of the initiation and development of part load combustions in an SI engine. SAE 1983. paper 830338.

45 Benjamin, S.F. Haynes,C.D. Tidmarsh,D.H: Lean burn engines for low exhaust emissions. IMechE. 1986. C320/86.

46 Benjamin,S.F: The development of GTL barrel swirl combustion system with application to four valve spark ignition engines. Combustion in Engines Technology and Applications. IMechE. 1988/3 C54/88.

47 deBoer,C.D. Johns,R.JR. Grigg,D.W. Train,B.M. Denbrath,I. Linns,J.R: Refinement with performance and economy for 4 valve automotive engines. Automotive power systems. Environment and Conservation. IMechE. 1990-9 C394/053. p147-155.

48 Fraidl,G.K. Mikulic,L.A. Quissek,F: Development strategies for low emission high performance 4 valve engines. Journal IMechE. 1990. Vol.4. No.D1. p59-65.

49 Hu,Z. Vafidis,C. Whielaw,J.H. Chapman,J. and Head,R.A: Correlation between in-cylinder flow, performance and emissions characteristics of a Rover pentroof four valve engine. Proceedings International Conference, Combustion in Engines. Technology, Applications and the Environment IMechE. 1992. C448/026. pp. 157..164.

50 Stone, C.R. Sorrel, A.J. Biddulph, T.W. and Marshall, R.A: Analysis of spark-ignition engine performance after a cold start, with thermal and cyclic measurements. Proceedings International Conference, Automotive Power Systems, Environment and Conservation. IMechE. 1990. C394/007. pp 181-193.

51 Andrews, G.E. Harris, J.R. and Ounzain, A: Experimental methods for investigating the transient heating and emissions of an SI engine during the warm-up period. Conference Proceedings Experimental methods in Engine Research and Development. IMechE. 1988. pp101-108.

52 Andrews, G.E. Harris, J.R. and Ounzain, A: The role of cooling water and lubricating oil temperature on transient emissions during SI engine warm-up. Conference Proceedings, New developments in power train and chassis engineering. IMechE. 1989. C382/015. pp37-49.

53 Sorrel, A.J. and Stone, C.R: Spark ignition engine performance during warm-up. SAE 890567.

54 Kaplan, J.A. and Heywood, J.B: Modelling the spark ignition engine warm-up process to predict component temperature and hydrocarbon emissions. SAE 910302.

55 United Kingdom Engine Emissions Consortium. Boam, D.J. Finlay, I.C. Biddulph, T.W. Ma, T. Lee, R. Richardson, S. Bloomfield, J. Green, J.A. Wallace, S. Woods, W.A. and Brown, P. The sources of unburnt hydrocarbon emissions from spark ignited engines during cold start and

warmup. Proceedings International Conference, Combustion in Engines, Technology, Applications and the Environment. IMechE 1992. C448/064. pp 57-72.

56 Brown,P.G. and Woods,W.A: Measurements of unburnt hydrocarbons in a spark ignited combustion engine during the warm-up period. SAE 922233.

57 Bailey,J.C. Schmidle,B.W. Williams,M.L: Hydrocarbon speciation in motor vehicle exhaust and its significance for air quality. IMechE. 1987.Paper C327/87. pp177-185.

58 Daniel,W.A: Engine variable effects on exhaust hydrocarbon composition. SAE 670124.

59 Dempster,N.M. Shore,P.R: An investigation into the production of hydrocarbon emissions from a gasoline engine tested on chemically defined fuels. SAE 900354.

60 Koehl,W.J. Benson,J.D. Burns,V. Gorse,R.A. hochhauser,A.M. and Reuter,R.M: Effects of gasoline composition and properties on vehicle emissions: A review of prior studies-Auto/oil air quality improvement research program. SAE 912321

61 Ninomiya,J.S. and Biggers,B: Effects of toluene content in fuel on aromatic emissions in the exhaust. Journal of air pollution control. 1970. Vol. 20 No 9. pp 609-611.

62 Shore,P.R. Humphries,D.T. and Haddad,O: Speciated hydrocarbon emissions from aromatic, olefinic and paraffinic model fuels. SAE 930373.

63 Booth, M. McArragher, J.S. and Marriott, J.M: The influence of motor vehicle emission control legislation on future fuel quality. Fourth International Symposium on the performance evaluation of automotive fuels and lubricants. CEC. Birmingham ICC. United Kingdom. 5-7 May 1993.

64 Kowalewicz, A: Methanol as a fuel for spark ignited engines: a review and analysis. Proceedings IMechE 1993. Vol 207 Part D. pp 43-52.

65 Wallace, S Junday, J. Jones, D.A. and Watson, M.D: Performance and durability evaluation of a natural gas/gasoline light commercial vehicle. Fourth International Symposium on the performance evaluation of automotive fuels and lubricants. CEC. Birmingham ICC. United Kingdom. 5-7 May 1993.

66 Jaaskelainen, H.E. and Wallace, J.S: Performance and emissions of a natural gas fueled 16 valve DOHC four cylinder engine. SAE 930380.

67 Wallace, S and May, J. Private communication.

68 Matukuma, A. Retention indices of alkanes through C_{10} and alkenes through C_8 and relation between boiling points and retention data. Gas Chromatography 1968. Proceedings of the seventh international conference on gas chromatography. The Institute of Petroleum. 1968. pp 55-75.

69 Chappelow, C.C. and Prausnitz, J.M: Solubilities of gases in high boiling hydrocarbon solvents. AIChE Journal. 1974. Vol 20, No 6. pp 1097-1104.

70 Heywood, J.B.: Internal Combustion Engine Fundamentals. McGraw-Hill. 1988. ISBN 0-07-100499-8.

71 Curtis, J.M.: Piston ring dynamics and its influence on the power cylinder performance. SAE 810935.

72 Sigworth, H.W. Myers, P.S. and Uyehara, O.A.: The disappearance of ethylene, propylene, n-butane and 1-butane in spark ignition engine exhaust. SAE 810935.

73 Sandia, S. and Someya, T.: The effect of surface roughness on lubrication between a piston ring and a cylinder liner. IMechE conference on Tribology Friction, lubrication and Wear, 1987, paper C223/87, pp. 135-143.

74 Hegemier, T. and Stewart, M.: Some effects of liner finish on diesel engine operating characteristics. SAE 930716.

75 Spindt, R.S. Air-fuel ratios from exhaust gas analysis. SAE transactions 1965. SAE 650507.

APPENDIX 1 CALCULATIONS

Engine Performance Parameters

$$\text{Brake Mean Effective Pressure (bmep)} = \frac{4\pi T}{nAl} = K T \quad \text{Nm}^2$$

$$\text{Where } K = \text{constant} = \frac{4\pi}{nAl}$$

$$\text{for Rover K16 engine } K = \frac{4\pi}{4\pi \cdot 0.0375^2 \cdot 0.079}$$

$$K = 9.0014 \times 10^3$$

$$\text{Specific Fuel Consumption (sfc)} = \frac{\text{fuel flow rate}}{\text{brake power}} \quad \text{g/kWh}$$

$$\text{sfc} = \frac{m_f}{B_p} \quad \text{g/kWh}$$

$$\text{Brake Thermal Efficiency} = \frac{\text{brake power}}{m_f Q_{\text{net}}}$$

Calculations for air fuel ratio and specific emissions

Air Fuel ratio

The method for calculating air fuel ratio from the exhaust gas analysis was developed by Spindt (72). The formula used for the air fuel ratio is;

$$\text{AFR} = \left(1 + \frac{3(\text{HC})}{(\text{CO}) + (\text{CO}_2)} \right)^{-1} \left[\frac{11.492}{(1 + \text{H/C})} \left((\text{CO}_2) + \frac{1}{2}(\text{CO}) + (\text{O}_2) \right) + \frac{119.807 (\text{CO}_2)}{3.5(\text{CO}_2) + (\text{CO})} \frac{1}{(1 + \text{C/H})} \right]$$

Where () = % Concentration
 H/C = Hydrogen carbon ratio

Brake Specific Emissions Based on Spindt AFR and SFC

Carbon Monoxide

$$\begin{aligned} \text{CO (G/kWh)} &= \frac{\text{CO}\%}{100} \times K \times \text{AFR} \times \text{SFC} \times \frac{\text{CO density}}{\text{inlet air density}} \\ &= \frac{\text{CO}\%}{100} \times K \times \text{AFR} \times \text{SFC} \times \frac{1.164 \times R \times T_a}{P_a} \end{aligned}$$

Nitric Oxide

$$\begin{aligned} \text{NOx (g/kWh)} &= \frac{\text{NO(ppm)}}{10^6} \times K \times \text{AFR} \times \text{sfc} \times \frac{\text{NOx density} \times H}{\text{inlet air density}} \\ &= \frac{\text{NO(ppm)}}{10^6} \times K \times \text{AFR} \times \text{sfc} \times \frac{1.912 \times R \times T_a \times H}{P_a} \end{aligned}$$

Hydrocarbons

$$\begin{aligned} \text{HC (g/kWh)} &= \frac{\text{HC(ppm)}}{10^6} \times K \times \text{AFR} \times \text{sfc} \times \frac{\text{HC density}}{\text{inlet air density}} \\ &= \frac{\text{HC(ppm)}}{10^6} \times K \times \text{AFR} \times \text{sfc} \times \frac{0.577 \times R \times T_a}{P_a} \end{aligned}$$

Where

AFR = air/fuel ratio based on Spindt

FC = Specific fuel consumption g/kWh

R = gas constant for air = 287.1 j/kg K

P_a = inlet air pressure N/m²

T_a = inlet air temperature, K

K = 0.93, Conversion factor from inlet air volume to exhaust gas volume after passing through a water trap.

H = Humidity corection factor = $\frac{1}{(1 - 0.0047)} (h - 75)$

h = absolute humidity

$$h = \frac{43.478 \cdot R \times P_d}{(P_b - (P_d \times R/100))}$$

P_d = Saturated vapour pressure, mbar at ambient dry bulb temperature.

P_b = Ambient air pressure, mbar

Defining Constants required for Combustion Analysis

Molecular Weights and Air Fuel Ratio

The Hydrocarbon fuel is specified as C_aH_b

Carbon/Hydrogen Ratio = $Y = b/a$

For the reference fuel CEC RF-08-A-85, the C/H by mass is 7.48:1

$$\text{Mol Ratio } Y = \frac{\text{No atoms} \times \text{Mol weight Carbon}}{\text{No atoms} \times \text{Mol weight hydrogen}} = \frac{1 \times 12.011}{7.48 \times 1.008}$$

$$Y = 1.593$$

Most petrols have 8 carbon atoms, thus; $a = 8$

$$\text{and } b = a \times Y = 8 \times 1.593 = 12.744$$

The fuel can be written as $C_8H_{12.744}$

The stoichiometric air fuel ratio AFR_s is given by;

$$AFR_s = \frac{\text{mass of air to react with one carbon atom} + \text{hydrogen}}{\text{Mol weight carbon} + (\text{Mol weight hydrogen} \times Y)}$$

$$AFR_s = \frac{34.56 (4 + Y)}{12.011 + 1.008Y}$$

The tests carried out in this research were at 15:1 AFR

$$\text{The equivalence ratio } \phi = \frac{F/A_{s-}}{F/A_{act}} = \frac{14.2}{15} = 0.947$$

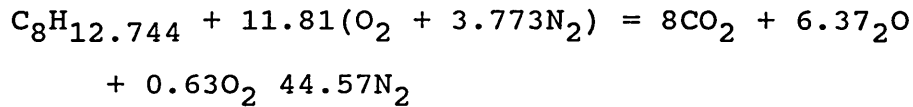
Excess air = 105%

Mol wt. air \approx 28.96

Mol weight of fuel RF-08-A-85

$$\text{Mol}_F = 12.011 \times 8 + 1.008 \times 12.744 = 108.934$$

The Combustion Equation



1 Mol of fuel Requires the following number of Mols of air for combustion at 15:1 air/fuel ratio and will produce the given number of product Mols.

$$1 + 11.81(1 + 3.744) = 8 + 6.37 + 0.63 + 44.57$$

$$1 \text{ Mol}_f + 56.38 \text{ Mol}_{\text{air}} = 59.566 \text{ Mol}_p$$

Mol weights of reactants and products M_r and M_p

$$M_r = \frac{1}{n} \cdot \sum n_i M_i$$

and

$$M_p = \frac{1}{n} \cdot \sum n_i M_i$$

Where n = Number of Mols

M = Mol weight

For AFR 15:1

$$M_r = \frac{1}{57.38} (108.93 + 56.38 \times 28.96)$$

$$M_r = 30.35$$

$$M_p = \frac{1}{59.566} (352.08 + 114.79 + 20.16 + 1248.41)$$

$$M_p = 29.132$$

Gas Constants

Universal gas constant $R_o = 8.314 \text{ kJ/kg.K}$

$$R = \frac{R_o}{M}$$

$$R_r = \frac{R_o}{M_r} = \frac{8314}{30.35} = 273.9 \text{ J/kg.K}$$

$$R_p = \frac{R_o}{M_p} = \frac{8314}{29.132} = 285.4 \text{ J/kg.K}$$

Defining gamma

The value of gamma varies with gas temperature and with different mixture of gases between burnt and unburnt. The fuel and equivalence ratio also affect gamma, due its definition by the ratio of specific heats;

$$\gamma = \frac{C_p}{C_v}$$

Using values for gamma from standard tables for air and regression a function for gamma against temperature was found.

$$\gamma = -6.21 \times 10^{-12} \cdot T^3 + 5.2645 \times 10^{-8} \cdot T^2 - 1.557 \times 10^{-4} \cdot T + 1.447$$

This does not allow for differences due to the mixture of fuel and air or when this is burnt later in the cycle. However it was shown by Rassweiler and Withrow (30) that the value gamma has only a small effect on the predictions of burn rate.

Appendix 2 Conditions for Calculation of Oxidation

Speed/Load	Build	Temperatures °C			Man Dep.Hg	Oil Depth um
		Piston	Liner	Inlet		
1500/1bar	Std	277	140	58.7	525	0.244
1500/1bar	HTRP	252	140	"	"	0.238
1500/1bar	Smth	277	140	"	"	0.202
1500/1bar	2nd	277	140	"	"	0.244
1500/1bar	Opt	277	145	"	"	0.235
1500/2.62	Std	287	150	56	410	0.244
1500/2.62	HTRP	267	145	"	"	0.238
1500/2.62	Smth	287	150	"	"	0.202
1500/2.62	2nd	287	150	"	"	0.244
1500/2.62	Opt	267	145	"	"	0.235
2000/2bar	Std	287	150	54.7	465	0.244
2000/2bar	HTRP	267	145	"	"	0.238
2000/2bar	Smth	287	150	"	"	0.202
2000/2bar	2nd	287	150	"	"	0.244
2000/2bar	Opt	267	145	"	"	0.235
2500/5.5	Std	297	155	47.5	245	0.244
2500/5.5	HTRP	277	150	"	"	0.238
2500/5.5	Smth	297	155	"	"	0.202
2500/5.5	2nd	297	155	"	"	0.244
2500/5.5	Opt	277	150	"	"	0.235
3500/WOT	Std	307	165	46.4	23	0.244
3500/WOT	HTRP	287	160	"	"	0.238
3500/WOT	Smth	307	165	"	"	0.202
3500/WOT	2nd	307	165	"	"	0.244
3500/WOT	Opt	287	160	"	"	0.235

APPENDIX 2 Listing of Combined Programme to Predict
Hydrocarbon Emissions

```

5  CLS 0

5  CLS 0
10 DEFSNG A-Z
20 REM make an array called A!
30 DIM A(4, 471)
40 REM Combined model for crevice & abs/des emissions and Oxidation
50 PRINT " "
60 REM Model to Calculate Top Land Crevice flow and Gas Temperature
70 REM Version 1 leakage to 2nd land and ring groove 13/06/93
80 PRINT "A Combined Model for Emissions and Oxidation"
90 PRINT "Calculations for Top Land Crevice Flow."
100 PRINT " "
110 REM define constants, all are suffix C
120 CONST CX = 12, CY = 2, CZ = 6
130 REM crank shaft throw = r and con rod length = L
140 CONST r = .0395, L = .1315
150 REM define mol Wt of mixture = Mr
160 REM Univ. gas const = Ro kJ/kg
170 CONST Mr = 30.35, Ro = 8.314, Pi = 3.1415927#
180 CONST ratio = 9.5
190 REM Enter variables
200 PRINT " To calculate the crevice flow some values are required."
210 PRINT " "
215 INPUT "Enter Test Point Identification " , test$
217 INPUT "Test Description, Piston Type etc. " , runs$
218 INPUT "Enter Computer Simulation Run " , testno$
220 INPUT "Engine speed, rpm " , n
230 INPUT "Enter top land height, m " , h
240 INPUT "Enter piston Dia, m " , D
250 INPUT "Piston 2nd Land Dia, m " , D2
260 INPUT "Additional 2nd Land Vol m^2 " , land
270 INPUT "Then cylinder dia, m " , dc
280 INPUT "Manifold Depression, mm Hg " , Hg
290 INPUT "Temperature of inlet air, Deg C " , Ta
300 INPUT "Ambient air pressure, mbar " , Pamb
310 INPUT "Piston Temperature K " , Tp
320 INPUT "Cylinder Wall Temperature Deg C " , Tc
330 INPUT "Predicted Liner Oil layer um " , O
340 INPUT "Mix Ratio, Crevice Flow, 0 < x < 1 " , Xmix
350 PRINT " "
360 PRINT "Are these values correct ? Answer 1 if yes, 2 if no"
370 INPUT ans
380 IF ans = 1 THEN
390 GOTO 430
400 ELSE
410 GOTO 210
420 END IF
430 REM Calculate sub functions, Ma mass air in chamber.
440 Md = Pamb * 100 - (13600 * 9.81 * Hg / 1000)
450 REM ring groove clearance volumes and initial mass
460 REM DEFINE TEMP VALUE OF Tp and CRANK ANGLE x.
470 P1 = 100000
480 REM piston ring dimensions
490 CONST Ring1T = .001196
500 CONST Ring1W = .0029
510 CONST Ring2W = .0029
520 CONST L2nd = .00325
530 CONST RGD = .0672, RG1T = .00124, RG2T = .00154
540 REM 2nd land vol
550 C21a = Pi * (dc ^ 2 - D2 ^ 2) / 4
560 REM Land = C21v * L2nd * 1.6
570 C21v = C21a * L2nd + land
580 REM volume behind rings Rvol1 & Rvol2
590 Rvol1 = (dc - 2 * Ring1W - RGD) * Pi * RGD * RG1T
600 Rvol2 = (dc - 2 * Ring2W - RGD) * Pi * RGD * RG2T

```

```

610 REM total 2nd land volume
620 REM Vol2 = C2lv + Rvol2
630 Vol2 = C2lv
640 REM initial mass in crevice volumes
650 mo2 = Md * Rvol1 / ((Ro / Mr) * 1000 * Tp)
660 mo3 = P1 * C2lv / ((Ro / Mr) * 1000 * Tp)
670 mo4 = P1 * Rvol2 / ((Ro / Mr) * 1000 * Tp)
680 REM initial mass in total 2nd land volume M2i
690 REM M2i = mo3 + mo4
700 M2i = mo3
710 Arg2 = Ring2E * Ring2W
720 REM define constants for ring groove flow, viscosity of gas, mu
730 REM top ring side clearance ht, area normal to flow, Af
740 mu = 3.3E-07 * Tp ^ .7
750 ht = RG1T - Ring1T
760 Af = ht * Pi * D
770 Crg = .2 * ht ^ 2 * Af / (24 * Ring1W * mu * (Ro / Mr) * Tp * 1000)
780 REM area of piston = A
790 CONST ringgap = .00041, Cd = .86
800 A = (Pi * D ^ 2) / 4
810 A2 = ringgap * (dc - D) / 2
820 K = A2 / A
830 REM ring end gap
840 REM define constants to calculate gamma
850 CONST Aga = -6.214E-12, Bga = 5.26449E-08, Cga = -.000155656#
860 CONST Dga = 1.44722
870 CONST Dga1 = 1.51, Dga2 = 1.4
880 Inlet = 225 * Pi / 180
890 Vsw = A * .079
900 CE1 = SQR(L ^ 2 / r ^ 2 - (SIN(Inlet)) ^ 2)
910 Vsl = A * r * ((1 - COS(Inlet)) + L / r - CE1)
920 Vcyl = Vsl + Vsw / ratio
930 Tg1 = Ta + 273
940 Ma = Md * Vcyl / ((Ro / Mr) * 1000 * Tg1)
950 REM Calculate sub functions
960 w = n * Pi * 2 / 60
970 REM top land crevice volume, CA + ring groove volume Rvol1
980 CA = Pi / 4 * (dc ^ 2 - D ^ 2) * h
990 CK = CX * n * h
1000 REM constant values for crevice mass flow rate
1010 CJ = Mr * CA * CZ * n / (Ro * 1000 * Tp)
1020 P2nd = P1
1030 Prg = Md
1040 PV1 = .0003
1050 nt1 = -.0004
1060 OPEN "i", #1, "C:\qbasic\data\io35C32.dat"
1070 FOR i = 1 TO 470
1080 INPUT #1, b$
1090 deg = VAL(LEFT$(b$, 3))
1100 rad = deg * Pi / 180
1110 xs = LEN(b$)
1120 P = VAL(MID$(b$, 4, xs))
1130 IF P = 0 THEN
1140 GOTO 1990
1150 ELSEIF deg < 160 THEN
1160 GOTO 1990
1170 ELSE
1180 P2 = P * 100000
1190 END IF
1200 dp = P2 - P1
1210 dpp = P2 + P1
1220 dp3 = P2 - P3
1230 REM Piston Displacement = PX, Velocity = PC
1240 REM Vol Displacement by Piston = PV
1250 CE1 = L ^ 2 / r ^ 2 - (SIN(rad)) ^ 2
1260 CE = SQR(CE1)

```

```

1270 PX = r * ((1 - COS(rad)) + L / r - CE)
1280 PC1 = .5 * SIN(2 * rad) / CE
1290 PC = w * r * (SIN(rad) + PC1)
1300 PV = PX * A
1310 Vol = PV + Vsw / ratio
1320 REM calcs for gas temperature.
1330 IF P1 / P2 = 1 THEN
1340     nt = nt1
1350     ELSE
1360     nt = LOG(P1 / P2)
1370 END IF
1380 nb = LOG(Vol / PV1)
1390 IF P < 4.5 THEN
1400     nu = 1.3
1410     ELSE
1420     nu = (nt * 1.1) / nb
1430 END IF
1440 ni = (nu - 1) / nu
1450 dT = (((P2 / P1) ^ ni) - 1) * Tg1
1460 Tg2 = Tg1 + dT
1470 P3 = P1
1480 P1 = P2
1490 m1 = m
1500 PV1 = Vol
1510 Tg1 = Tg2
1520 REM PRINT deg, P, dp
1530 IF deg < 305 THEN
1540     GOTO 1990
1550     ELSEIF P < 1.3 THEN
1560     GOTO 1990
1570     ELSE
1580     GOTO 1590
1590 END IF
1600 Rho = P2 * Mr / (Tg2 * Ro * 1000)
1610 REM Crevice mass Flow = m, Units of mass flow g/s.
1620 REM Calc crevice flow velocity = Cv
1630 IF dp = 0 THEN
1640     m = -1 * CJ * dp3
1650     Cv = CK * dp3 / dpp
1660     ELSE
1670     m = -1 * CJ * dp
1680     Cv = CK * dp / dpp
1690 END IF
1700 REM allow for leakage into 2nd land
1710 dp2nd = P2 - P2nd
1720 IF Prg <= P3 THEN
1730     Dpsq = Prg ^ 2 - P3 ^ 2
1740     mrg = Crg * Dpsq
1750     ELSE
1760     Dpsq = Prg ^ 2 - P3 ^ 2
1770     mrg = Crg * Dpsq * -1
1780 END IF
1790 SQ1 = (2 * dp2nd) / (Rho * (1 - K ^ 2))
1800 IF dp2nd < 0 THEN
1810     SQ1 = -1 * SQ1
1820     ELSE
1830     SQ1 = SQ1
1840     END IF
1850 SQ = SQR(SQ1)
1860 IF P2nd <= P2 THEN
1870     mq = Cd * A2 * SQ
1880     ELSE
1890     mq = Cd * A2 * SQ * -1
1900 END IF
1910 REM mass in 2nd land volume and pressure + Ring groove data
1920 M2i = M2i + mq / (n * 6)

```

```

1930     mo2 = mo2 + mrg / (n * 6)
1940     P2nd = M2i * Ro / Mr * 1000 * Tp / Vol2
1950     Prg = mo2 * Ro / Mr * 1000 * Tp / Rvol1
1960     mrg = mrg / 10
1970     actm = m - mq - mrg
1980     Rv = Cv - PC
1995     PRINT " "
2000     PRINT deg, Tg2, actm
2010     REM read data to array A!
2020     REM CREVICE FLOW, READ IN 3rd AND 4th COLUMN
2030     IF deg <= 375 THEN
2040         GOTO 1990
2050     ELSE
2060         A(3, i) = actm
2070         A(4, i) = Tg2
2080     END IF
2090     REM A(4, i), A(3, i)
2100 NEXT i
2110 CLOSE #1 -
2120 REM next section calculates absorpion/deorpion
2130 PRINT " "
2140 PRINT "This next section calculates absorpion effects"
2150 REM define mol Wt of oil and fuel Mo & Mf
2160 REM mol fraction fuel in air = Molf
2170 CONST Mo = 550, Mf = 108.934, Molf = .01743
2180 REM Oil density = Od
2190 CONST Od = 857, Am1 = -.0001972
2200 CONST c1 = 1.1304, Am2 = -.432
2210 Tw = Tc + 273
2220 Oc = O / 1000000
2230 REM approximate Henry Constant, Units Pascal
2240 loghc = -1.82 + .0125 * (Tw - 300)
2250 Hcats = (10 ^ loghc)
2260 Hc = Hcats * 101.3
2270 REM Calculate Cm = (Cmax - Cmin), for speed variation
2280 Cm = n * Am1 + c1
2290 REM initial value of P1
2300 P1 = 400000
2310 PRINT " "
2320 PRINT "Henry Constant =", Hc
2330 PRINT "Value of Cm =", Cm
2340 PRINT " ";
2350     OPEN "i", #2, "c:\qbasic\data\io35C32.dat "
2360 FOR i = 1 TO 470
2370     INPUT #2, b$
2380     deg = VAL(LEFT$(b$, 3))
2390     rad = deg * Pi / 180
2400     xs = LEN(b$)
2410     P = VAL(MID$(b$, 4, xs))
2420     IF P <= 1.3 THEN
2430         GOTO 2910
2440     ELSEIF deg < 305 THEN
2450         GOTO 2910
2460     ELSE
2470         P2 = P * 100000
2480     END IF
2490     REM P2 = current cylinder pressure N/m^2
2500     REM Calcs to piston displacement from TDC, Y
2510     CE = SQR(L ^ 2 / r ^ 2 - (SIN(rad)) ^ 2)
2520     Y = r * ((1 - COS(rad)) + L / r - CE)
2530     REM calc y/S and dY
2540     Ys = Y / (2 * r)
2550     IF deg = 375 THEN
2570         dY = Y + h
2580     ELSE
2590         dY = Y - Y1

```

```

2600     END IF
2610     REM calc Ceq with values of Henry Constant, Hc.
2620     Ceq = (Mf * P2) * Molf / (Mo * Hc)
2630     REM Calculate Cmax - Cmin, approx values
2640     Cmy = Cm + Am2 * Ys
2650     dmf = Cmy * Pi * D * Oc * Od * Ceq * dY * 1000
2660     REM Units of dmf are mgram.
2670     mftot = mftot + dmf
2680     Y1 = Y
2690     IF deg <= 375 THEN
2700         P375 = P2
2710         ELSE
2720         Pdif = P1 - P2
2730     END IF
2740     IF P375 = P2 THEN
2750         GOTO 2910
2760     ELSE
2770         Pratio = Pdif / P375
2780     END IF.
2790     P1 = P2
2800     REM mass of fuel release per degree
2810     dm = Pratio * mftot
2820     PRINT deg, Pratio, dm
2830     REM read data to array A!
2840     A(1, i) = deg
2850     A(2, i) = dm
2860     REM A(1, i), A(2, i)
2870 NEXT i
2880 CLOSE #2
2890 PRINT "*****"
2900 PRINT "Cumulative mass of fuel emitted, mg, = ", mftot
2910 PRINT "*****"
2920 PRINT " "
2930 PRINT "This next section calculates Oxidation effects"
2940 PRINT " "
2950 PRINT "Calculations for Oxidation of Crevice HC's"
2960 CONST Mp = 29.132
2970 CONST Molu = 57.38, Molb = 59.57, molfuel = 108.9, O2 = 1.4
2980 IF n = 1500 THEN
2990     finish = 385
3000     ELSEIF n = 2000 THEN
3010     finish = 390
3020     ELSEIF n >= 2500 THEN
3030     finish = 380
3040 END IF
3050 REM *****
3060 REM Calculate sub functions
3070 REM Sudden freezing Temperature. Tsf
3080 log1 = O2 * 100 * Md / Pamb
3090 bot = .02 * LOG(log1)
3100 Tsf = 1320 / (1 + bot)
3110 REM *****
3120 PRINT " "
3130 PRINT " Temporary values of intermediate calcs."
3140 PRINT " "
3150 PRINT "Md ="; Md, "Vcyl ="; Vcyl,
3160 PRINT " "
3170 xHCi = 1 / (Molu + Xmix * Molb)
3180 xO2i = 11.81 / (Molu + Xmix * Molb)
3190 xHCab = 1 / (1 + Xmix * .8 * Molb)
3200 Mt = Molu * Xmix + Molb * (1 - Xmix)
3210 PRINT "xHCi ="; xHCi, "xHCab ="; xHCab
3220 Rt = Ro / Mt
3230 FOR i = 380 TO 465
3240     Tg = A(4, i)
3250     REM combustion gas temperatures

```

```

3260     Tm = (Xmix * Tg + Tp) / (Xmix + 1)
3270     REM Crevice Mass Flow Rate
3280     Ms = A(3, i)
3290     IF Ms <= .000001 THEN
3300         GOTO 3830
3310     ELSE
3320         mc = Ms / (n * 6)
3330     END IF
3340     REM define desorbed fuel and crank angle
3350     deg = A(1, i)
3360     dm = A(2, i)
3370     REM *****
3380     REM Define new Mol Fractions
3390     REM *****
3400     xHct2 = (mc * xHCi + mctot * xHCrl + xHCab * dm) / (mc + mctot + dm)
3410     REM *****
3420     REM calculate Change in HC Concentration
3430     IF finsh >= deg THEN
3440         dxHC = xHct2
3450     ELSEIF Tm > Tsf THEN
3460         dxHC = xHct2
3470     ELSE
3480         dxHC = xHct2 * .5
3490     END IF
3500     xHCr = xHct2 - dxHC
3510     mctot = mctot + mc + dm
3520     dxHctot = dxHctot + dxHC
3530     xHCrl = xHCr
3540     PRINT " "
3550     PRINT deg, Tm, Tsf, dxHC
3560     REM OPEN "a", #5, "c:\qbasic\data\oxid20c1.dat"
3570     REM PRINT #5, deg, Tm, dxHC, dxHctot
3580     REM CLOSE #5
3590 NEXT i
3600 mHC = molfuel * xHCr * mctot * (Xmix + 1) / (Xmix * Molb)
3610 PRINT "*****"
3620 PRINT "mass of unburnt fuel, mHC =", mHC
3630 PRINT "*****"
3640 PRINT "Temperature sudden freezing, Tsf ="; Tsf
3650 PRINT "*****"
3660 PRINT "Mass of Air Initially in Cylinder ="; Ma
3670 PRINT "*****"
3680     OPEN "a", #6, "c:\qbasic\data\OPT-run1.dat"
3690     PRINT #6, test$, runs$, testno$, mHC
3700     CLOSE #6
4000 END

```

Listing of Program to Calculate Piston Crevice Flow

```

5 CLS 0
10 REM Version 1 leakage to 2nd land and ring groove 13/06/93
20 PRINT " "
30 REM Model to Calculate Top Land Crevice flow and Gas Temperature
40 PRINT "calculations for top land crevice flow."
50 PRINT " "
60 REM define constants, all are suffix C
70 DEFSNG A-Z
80 CONST CX = 12, CY = 2, CZ = 6
90 REM crank shaft throw = r and con rod length = L
100 CONST r = .0395, L = .1315
110 REM define mol Wt of mixture = Mr
120 REM Univ. gas const = Ro kJ/kg
130 CONST Mr = 30.35, Ro = 8.314, Pi = 3.1415927#
135 CONST ratio = 9.5
140 REM Enter variables
150 PRINT " To calculate the crevice flow some values are required."
160 PRINT " "
170 INPUT "Engine speed, rpm ", n
180 INPUT "Enter top land height, m ", h
190 INPUT "Enter piston Dia, m ", D
195 INPUT "Piston 2nd Land Dia, m ", D2
196 INPUT "Additional 2nd Land Vol cm^3 ", Land
200 INPUT "Then cylinder dia, m ", dc
205 INPUT "Manifold Depression, mm Hg ", Hg
210 INPUT "Temperature of inlet air, Deg C ", Ta
230 INPUT "Ambient air pressure, mbar ", Pamb
233 PRINT " "
234 PRINT "Are these values correct ? Answer 1 if yes, 2 if no"
INPUT ans
IF ans = 1 THEN
GOTO 240
ELSE
GOTO 150
END IF
240 REM Calculate sub functions, Ma mass air in chamber.
250 Md = Pamb * 100 - (13600 * 9.81 * Hg / 1000)
260 REM ring groove clearance volumes and initial mass
270 REM DEFINE TEMP VALUE OF Tp and CRANK ANGLE x.
280 CONST Tp = 550
285 P1 = 100000
286 REM piston ring dimensions
288 CONST Ring1T = .001196
290 CONST Ring1W = .0029
300 CONST Ring2W = .0029
310 CONST L2nd = .00385
315 CONST RGD = .0672, RG1T = .00124, RG2T = .00154
320 REM 2nd land vol
330 C2la = Pi * (dc ^ 2 - D2 ^ 2) / 4
334 REM Land = C2lv * L2nd * 1.6
340 C2lv = C2la * L2nd + (Land / 1000000)
360 REM volume behind rings Rvol1 & Rvol2
370 Rvol1 = (dc - 2 * Ring1W - RGD) * Pi * RGD * RG1T
380 Rvol2 = (dc - 2 * Ring2W - RGD) * Pi * RGD * RG2T
390 REM total 2nd land volume
400 REM Vol2 = C2lv + Rvol2
Vol2 = C2lv
410 REM initial mass in crevice volumes
420 mo2 = Md * Rvol1 / ((Ro / Mr) * 1000 * Tp)
430 mo3 = P1 * C2lv / ((Ro / Mr) * 1000 * Tp)
440 mo4 = P1 * Rvol2 / ((Ro / Mr) * 1000 * Tp)
450 REM initial mass in total 2nd land volume M2i
460 REM M2i = mo3 + mo4
M2i = mo3
470 Arg2 = Ring2E * Ring2W
473 REM define constants for ring groove flow, viscosity of gas, mu

```

```

474 REM top ring side clearance ht, area normal to flow, Af
475 mu = 3.3E-07 * Tp ^ .7
476 ht = RG1T - Ring1T
    Af = ht * Pi * D
    Crg = .2 * ht ^ 2 * Af / (24 * Ring1W * mu * (Ro / Mr) * Tp * 1000)
480 REM area of piston = A
490 CONST ringgap = .00041, Cd = .86
500 A = (Pi * D ^ 2) / 4
510 A2 = ringgap * (dc - D) / 2
520 K = A2 / A
530 REM ring end gap
540 REM define constants to calculate gamma
550 CONST Aga = -6.214E-12, Bga = 5.26449E-08, Cga = -.000155656#
560 CONST Dga = 1.44722
570 CONST Dga1 = 1.51, Dga2 = 1.4
580 Inlet = 225 * Pi / 180
590 Vsw = A * .079
600 CE1 = SQR(L ^ 2 / r ^ 2 - (SIN(Inlet)) ^ 2)
610 Vs1 = A * r * ((1 - COS(Inlet)) + L / r - CE1)
620 Vcyl = Vs1 + Vsw / ratio
630 Tg1 = Ta + 273
640 Ma = Md * Vcyl / ((Ro / Mr) * 1000 * Tg1)
650 REM Calculate sub functions
660 w = n * Pi * 2 / 60
665 REM top land crevice volume, CA + ring groove volume Rvol1
670 CA = Pi / 4 * (dc ^ 2 - D ^ 2) * h
680 CK = CX * n * h
690 REM constant values for crevice mass flow rate
700 CJ = Mr * CA * CZ * n / (Ro * 1000 * Tp)
710 P2nd = P1
715 Prg = Md
720 PV1 = .0003
730 nt1 = -.0004
740 OPEN "i", #2, "C:\qbasic\data\p15132.dat"
750 FOR i = 1 TO 650
760 INPUT #2, A$
770 b$ = A$
780 deg = VAL(LEFT$(b$, 3))
790 RAD = deg * Pi / 180
800 xs = LEN(A$)
810 P = VAL(MID$(A$, 4, xs))
820 IF P = 0 THEN
830 GOTO 1660
840 ELSE
850 P2 = P * 100000
860 END IF
870 dp = P2 - P1
880 dpp = P2 + P1
890 dp3 = P2 - P3
960 REM Piston Displacement = PX, Velocity = PC
970 REM Vol Displacement by Piston = PV
980 CE1 = L ^ 2 / r ^ 2 - (SIN(RAD)) ^ 2
990 CE = SQR(CE1)
1000 PX = r * ((1 - COS(RAD)) + L / r - CE)
1010 PC1 = .5 * SIN(2 * RAD) / CE
1020 PC = w * r * (SIN(RAD) + PC1)
1030 PV = PX * A
1040 Vol = PV + Vsw / ratio
1050 REM calcs for gas temperature.
1060 IF P1 / P2 = 1 THEN
1070 nt = nt1
1080 ELSE
1090 nt = LOG(P1 / P2)
1100 END IF
1110 nb = LOG(Vol / PV1)
1120 IF P < 4.5 THEN

```

```

1130         nu = 1.3
1140         ELSE
1150         nu = (nt * 1.1) / nb
1160     END IF
1170     ni = (nu - 1) / nu
1180     dT = (((P2 / P1) ^ ni) - 1) * Tg1
1190     Tg2 = Tg1 + dT
1200     P3 = P1
1210     P1 = P2
1220     m1 = m
1230     PV1 = Vol
1240     Tg1 = Tg2
1250     REM PRINT deg, P, dp
1260     IF deg < 305 THEN
1270         GOTO 1660
1280         ELSEIF P < 1.2 THEN
1290         GOTO 1660
1300         ELSE
1310         GOTO 1330
1320     END IF
1330     Rho = P2 * Mr / (Tg2 * Ro * 1000)
1340     REM Crevice mass Flow = m, Units of mass flow g/s.
1345     REM Calc crevice flow velocity = Cv
1350     IF dp = 0 THEN
1360         m = -1 * CJ * dp3
1363         Cv = CK * dp3 / dpp
1380         ELSE
1390         m = -1 * CJ * dp
1393         Cv = CK * dp / dpp
1400     END IF
1410     REM allow for leakage into 2nd land
1420     dp2nd = P2 - P2nd
1430     IF Prg <= P3 THEN
1430         Dpsq = P3 ^ 2 - Prg ^ 2
1430         mrg = Crg * Dpsq
1430         ELSE
1430         Dpsq = Prg ^ 2 - P3 ^ 2
1430         mrg = Crg * Dpsq * -1
1440     END IF
1440     SQ1 = (2 * dp2nd) / (Rho * (1 - K ^ 2))
1450     IF dp2nd < 0 THEN
1460         SQ1 = -1 * SQ1
1470         ELSE
1480         SQ1 = SQ1
1490         END IF
1500     SQ = SQR(SQ1)
1510     IF P2nd <= P2 THEN
1513         mq = Cd * A2 * SQ
1515         ELSE
1520         mq = Cd * A2 * SQ * -1
1525     END IF
1530     REM mass in 2nd land volume and pressure + Ring groove data
1540     M2i = M2i + mq / (n * 6)
1545     mo2 = mo2 + mrg / (n * 6)
1550     P2nd = M2i * Ro / Mr * 1000 * Tp / Vol2
1550     Prg = mo2 * Ro / Mr * 1000 * Tp / Rvol1
1550     mrg = mrg / 10
1560     actm = m - mq - mrg
1570     Rv = Cv - PC
1580     PRINT " "
1590     PRINT deg, P2, Prg
1600         OPEN "a", #4, "c:\qbasic\data\flo15L16.dat"
1610         PRINT #4, deg, P2, P2nd, Prg
1620         CLOSE #4
1630         OPEN "a", #5, "c:\qbasic\data\mas15L16.dat"
1640         PRINT #5, deg, m, mq, mrg, actm

```

Listing of Programme to Calculate Fuel Absorbed in
Oil Layers

```

5  REM Version      05/06/93
10 CLS 0
20 PRINT "      "
30 REM sub function of model, Absorption/desorption.
40 PRINT "Calculations for Mass of Fuel Emitted from Oil"
45 PRINT "Due to the absorption/desorption effect"
50 PRINT "resolved for Crank Angle Through Engine Cycle"
60 PRINT "      "
70 REM define constants
80  DEFSNG A-Z
90  REM crank shaft throw = r, con rod length = L, Piston Dia = dp
100  CONST r = .0395, l = .1315, dP = .075
110  REM define mol Wt of mixture, oil and fuel Mr, Mo & Mf
120  REM Univ. gas const = Ro  kJ/kg, mol fraction fuel in air = Molf
130  CONST Mr = 30.35, Ro = 8.314
140  CONST Mo = 550, Mf = 108.934, Molf = .01743
150  REM Oil density = Od
160  CONST Od = 857, Pi = 3.1415927#, m1 = -.0001972
170  CONST c1 = 1.1304, m2 = -.432
180 REM Enter variables
190 PRINT " To calculate the Absorption effect some values are required."
200 PRINT " Please enter the following;"
210 PRINT "      "
220 INPUT "Engine speed,          rpm  ", n
230 INPUT "Predicted Liner Oil layer  um  ", O
240 INPUT "Cylinder Wall Temperature degrees C  ", Tc
250 INPUT "Piston Top Land Height      m  ", h
260 Tw = Tc + 273
270 Oc = O / 1000000
280 REM approximate Henry Constant, Units Pascal
290 loghc = -1.82 + .0125 * (Tw - 300)
300 Hcats = (10 ^ loghc)
310 Hc = Hcats * 101.3
320 REM Calculate Cm = (Cmax - Cmin), for speed variation
330 Cm = n * m1 + c1
340 REM initial value of P1
350 P1 = 400000
360 PRINT "      "
370 PRINT "Henry Constant =", Hc
375 PRINT "Value of Cm = ", Cm
380 PRINT "      "
390      OPEN "i", 2, "c:\qbasic\data\p15l32.dat"
400 FOR i = 1 TO 724
410      INPUT #2, a$
420      b$ = a$
430      deg = VAL(LEFT$(b$, 3))
440      rad = deg * Pi / 180
450      xs = LEN(a$)
460      P = VAL(MID$(a$, 4, xs))
470      IF P <= 1.2 THEN
480          GOTO 910
490      ELSEIF deg < 365 THEN
500          GOTO 910
510      ELSE
520          P2 = P * 100000
530      END IF
540      REM P2 = current cylinder pressure N/m^2
550      REM Calcs to piston displacement from TDC, Y
560      CE = SQR(1 ^ 2 / r ^ 2 - (SIN(rad)) ^ 2)
570      Y = r * ((1 - COS(rad)) + l / r - CE)
580      REM calc y/S and dY
590      Ys = Y / (2 * r)
600      IF deg = 375 THEN
610          dY = Y + h

```

```

620         ELSE
630             dY = Y - Y1
640         END IF
650         REM calc Ceq with values of Henry Constant, Hc.
660         Ceq = (Mf * P2) * Molf / (Mo * Hc)
670         REM Calculate Cmax - Cmin, approx values
680         Cmy = Cm + m2 * Ys
690         dmf = Cmy * Pi * dP * Oc * Od * Ceq * dY * 1000
700         REM Units of dmf are mgram.
710         mftot = mftot + dmf
720         Y1 = Y
730         PRINT "    "
740         IF deg <= 375 THEN
750             P375 = P2
760         ELSE
770             Pdif = P1 - P2
780         END IF
790         IF P375 = P2 THEN
800             -GOTO 910
810         ELSE
820             Pratio = Pdif / P375
830         END IF
840         P1 = P2
850         REM mass of fuel release per degree
860         dm = Pratio * mftot
870         fueltot = fueltot + dm
880         PRINT deg, Pratio, dm
890         OPEN "a", #5, "c:\qbasic\data\des25xs4.dat"
900         PRINT #5, deg, dm, fueltot
910         CLOSE #5
920     NEXT i
930     CLOSE 2
940     PRINT "*****"
950     PRINT "Cumulative mass of fuel emitted, mg, = ", mftot
960     PRINT "*****"
990     END

```

Listing of Combustion Analysis Programme

```

10 CLS 0
20 PRINT "      "
30 REM sub function of model Temperature and Heat Release.
40 PRINT "Calculations for Temperature and Heat Release"
50 PRINT "resolved for Crank Angle Through Engine Cycle"
60 PRINT "      "
70 REM define constants, all are suffix H
80 DEFSNG A-Z
90   REM crank shaft throw = r and con rod length = L
100  CONST r = .0395, L = .1315
110  REM define mol Wt of mixture = Mr
120  REM Univ. gas const = Ro  kJ/kg
130  CONST Mr = 30.35, Ro = 8.314, Pi = 3.1415927#
131  REM define constants to calculate gamma
132  CONST Ag = -6.214E-12, Bg = 5.26449E-08, Cg = -.000155656#
133  CONST Dg = 1.44722
134  CONST Dg1 = 1.51, Dg2 = 1.4
140 REM Enter variables
150 PRINT " To calculate the Heat Release some values are required."
160 PRINT " Please enter the following;"
170 PRINT "      "
180 INPUT "Engine speed,          rpm      ", n
190 INPUT "Piston Diameter          m        ", D
200 INPUT "Manifold Depression,      mm Hg   ", Hg
210 INPUT "Temperature of inlet air, Deg C ", Ta
220 INPUT "Compresion Ratio,            ", ratio
230 INPUT "Ambient air pressure,      mbar    ", Pamb
240 REM Calculate sub functions, Ma  mass air in chamber.
250 Md = Pamb * 100 - (13600 * 9.81 * Hg / 1000)
260 Inlet = 225 * Pi / 180
270 Vsw = (Pi * D ^ 2 * .079) / 4
280 CE1 = SQR(L ^ 2 / r ^ 2 - (SIN(Inlet)) ^ 2)
290 Vsl = (Pi / 4) * D ^ 2 * r * ((1 - COS(Inlet)) + L / r - CE1)
300 Vcyl = Vsl + Vsw / ratio
310 Tg1 = Ta + 273
320 Ma = Md * Vcyl / ((Ro / Mr) * 1000 * Tg1)
330 PRINT "      "
340 PRINT " Temporary values of intermediate calcs."
350 PRINT "      "
360 PRINT "Md ="; Md, "Vcyl ="; Vcyl,
370 PRINT "Ma = "; Ma
380 PRINT "      "
390 P1 = 110000
400 PV1 = .0003
410 ntl = -.0004
420   OPEN "i", 2, "c:\qbasic\data\p35c32.dat"
430 FOR i = 1 TO 719
440   INPUT #2, A$
450   B$ = A$
460   deg = VAL(LEFT$(B$, 3))
470   rad = deg * Pi / 180
480   xs = LEN(A$)
490   P = VAL(MID$(A$, 4, xs))
500   IF deg < 280 THEN
510     GOTO 1200
520   ELSE
530     P2 = P * 100000
540   END IF
550   REM P2 = current cylinder pressure N/m^2
560   dp = P2 - P1
570   dpp = P2 + P1
580   REM Calcs to define volume
590   CE = SQR(L ^ 2 / r ^ 2 - (SIN(rad)) ^ 2)
600   PV = Pi / 4 * D ^ 2 * r * ((1 - COS(rad)) + L / r - CE)
610   Vol = PV + Vsw / ratio
620   REM calcs for gas temperature.

```

```

640     IF P1 / P2 = 1 THEN
650         nt = nt1
660     ELSE
670         nt = LOG(P1 / P2)
680     END IF
690     nb = LOG(Vol / PV1)
700     IF P < 4.5 THEN
710         nu = 1.3
720     ELSE
730         nu = (nt * 1.1) / nb
740     END IF
750     ni = (nu - 1) / nu
760     dT = (((P2 / P1) ^ ni) - 1) * Tg1
770     Tg2 = Tg1 + dT
780     REM calcs for heat release
790     REM define gamma
840     gamma = Ag * Tg2 ^ 3 + Bg * Tg2 / 2 + Cg * Tg2 + Dg
930     dQa = dp * (Vol + PV1) / 2
940     dQb = gamma * (Vol - PV1) * dpp / 2
950     REM heat release per crank angle dQ
955     REM ignition timing A = 341, B = 332 C=337, D & E = 340, F = 345
960     IF dp = 0 THEN
970         dQ = 0
980     ELSEIF deg < 345 THEN
990         dQ = 0
1000    ELSEIF deg > 400 THEN
1005        dQ = 0
1007    ELSE
1010        dQ = (dQa + dQb) / (gamma - 1)
1020    END IF
1030    IF dQ < 0 THEN
1040        dQtot = dQtot
1050    ELSE
1060        dQtot = dQtot + dQ
1070    END IF
1080    P1 = P2
1090    PV1 = Vol
1100    nt1 = nt
1110    Tg1 = Tg2
1120    PRINT " "
1130    PRINT deg, P, Tg2, dQtot
1140        OPEN "a", #3, "c:\qbasic\data\heat35r4.dat"
1150        PRINT #3, deg, P, Tg2, dQ
1160        CLOSE #3
1170        OPEN "a", #4, "c:\qbasic\data\dq35r-4.dat"
1180        PRINT #4, deg, dQtot
1190        CLOSE #4
1200 NEXT i
1210 CLOSE 2
1220 REM Calculations for theoretical heat release
1230 REM mass of fuel inducted = mf
1240 mf = Ma / 16
1250 Qf = 42787000
1260 Qind = Qf * mf
1270     OPEN "i", #4, "c:\qbasic\data\dq35r-4.dat"
1280 FOR i = 1 TO 500
1290     INPUT #4, A$
1300     B$ = A$
1310     deg = VAL(LEFT$(B$, 8))
1320     xs = LEN(A$)
1330     dQ1 = VAL(MID$(A$, 10, xs))
1340     REM calculate mass fraction burnt as %
1350     IF dQ1 = 0 THEN
1360         GOTO 1460
1370     ELSEIF dQtot - dQ1 < .00001 THEN
1380         GOTO 1460

```

```

1390         ELSE
1400         xburn = (dQ1 / dQtot) * 100
1410     END IF
1420     PRINT deg, dQ1, dQtot, xburn
1430     OPEN "a", #5, "c:\qbasic\data\burn35r4.dat"
1440         PRINT #5, deg, dQ1, xburn
1450     CLOSE #5
1460     NEXT i
1470 CLOSE #4
1480 PRINT "Qind =", Qind, "dQtot =", dQtot, "Ma =", Ma
1490 END

```

**Listing of Programme to Calculate Oxidation of
In-Cylinder Hydrocarbon**

```

5 REM 24/05/93
10 CLS 0
20 PRINT " "
30 REM OXIDATION MODEL
40 PRINT "Calculations for Oxidation of Crevice HC's"
50 PRINT "resolved for Crank Angle Through Engine Cycle"
60 PRINT " "
70 REM define constants, all are suffix H
80 DEFSNG A-Z
90 REM MAKE A 2 X 200 ARRAY CALLED A!
100 DIM A!(4, 200)
110 REM crank shaft throw = r and con rod length = L
120 CONST r = .0395, L = .1315
130 REM define mol Wt of mixture = Mr and Mp
140 REM Univ. gas const = Ro kJ/kg
150 CONST Mr = 30.35, Mp = 29.132, Ro = 8.314
160 CONST Molu = 57.38, Molb = 59.57, Molf = 108.9, O2 = 1.4
170 REM Enter variables
180 PRINT " To calculate the oxidation some values are required."
190 PRINT " Please enter the following;"
200 PRINT " "
210 INPUT "Engine speed, rpm ", N
220 INPUT "Piston Diameter m ", D
230 INPUT "Manifold Depression, mm Hg ", Hg
240 INPUT "Temperature of inlet air, Deg C ", Ta
250 INPUT "Compression Ratio, ", ratio
260 INPUT "Ambient air pressure, mbar ", Pamb
270 INPUT "Mix Ratio, Crevice Flow, 0 < x < 1 ", Xmix
280 INPUT "Piston Temperature K ", Tp
290 REM *****
300 REM Calculate sub functions, Ma mass air in chamber.
310 Md = Pamb * 100 - (13600 * 9.81 * Hg / 1000)
320 Inlet = 225 * 3.142 / 180
330 Vsw = (3.142 * D ^ 2 * .079) / 4
340 CE1 = SQR(L ^ 2 / r ^ 2 - (SIN(Inlet)) ^ 2)
350 Vsl = (3.142 / 4) * D ^ 2 * r * ((1 - COS(Inlet)) + L / r - CE1)
360 Vcyl = Vsl + Vsw / ratio
370 Tg1 = Ta + 273
380 Ma = Md * Vcyl / ((Ro / Mr) * 1000 * Tg1)
381 REM Sudden freezing Temperature. Tsf
382 log1 = O2 * 100 * Md / Pamb
383 bot = .02 * LOG(log1)
384 Tsf = 1320 / (1 + bot)
390 REM *****
400 PRINT " "
410 PRINT " Temporary values of intermediate calcs."

```

```

420 PRINT " "
430 PRINT "Md ="; Md, "Vcyl ="; Vcyl,
440 PRINT "Ma = "; Ma, "Tsf ="; Tsf
450 PRINT " "
460 xHCi = 1 / (Molu + Xmix * Molb)
470 xO2i = 11.81 / (Molu + Xmix * Molb)
480 Mt = Molu * Xmix + Molb * (1 - Xmix)
490 Rt = Ro / Mt
500 OPEN "i", #3, "c:\qbasic\data\des20rs1.dat"
510 FOR i = 1 TO 100
520 INPUT #3, m$
530 N$ = m$
540 deg = VAL(LEFT$(N$, 8))
550 REM FROM ABSORPTION MODEL NUMBER FIRST COLUMN
560 A!(1, i) = deg
570 REM A!(1, i)
580 xs = LEN(m$)
590 dm = VAL(MID$(m$, 10, xs))
600 REM NUMBER SECOND COLUMN
610 A!(2, i) = dm
620 REM T A!(2, i)
630 NEXT i
640 CLOSE #3
650 OPEN "i", #4, "c:\qbasic\data\2mas20-3.dat"
660 FOR i = 1 TO 100
670 INPUT #4, m$
680 N$ = m$
690 deg = VAL(LEFT$(N$, 9))
700 zs = LEN(m$)
710 Tg = VAL(MID$(m$, 10, 12))
720 Ms = VAL(RIGHT$(m$, 8))
730 REM CREVICE FLOW, READ IN 3rd AND 4 COLUMN
740 A!(3, i) = Ms
750 A!(4, i) = Tg
760 REM A!(4, i), A!(3, i)
770 NEXT i
780 CLOSE #4
790 REM Mass Crevice Flow per deg Crank Angle
800 FOR i = 1 TO 100
810 Tg = A!(4, i)
820 REM combustion gas temperatures
830 Tm = (Xmix * Tg + Tp) / (Xmix + 1)
840 REM Crevice Mass Flow Rate
850 Ms = A!(3, i)
860 IF Ms <= .0001 THEN
870 GOTO 1190
880 ELSE
890 mc = Ms / (N * 6)
900 END IF
910 REM define desorbed fuel and crank angle
920 deg = A!(1, i)
930 dm = A!(2, i)
940 REM *****
950 REM Define new Mol Fractions
960 REM *****
970 xHct2 = (mc * xHCi + mctot * xHCr1 + dm) / (mc + mctot)
980 REM *****
990 REM calculate Change in HC Concentration
1000 IF Tm > Tsf THEN
1010 dxHC = xHct2
1020 ELSE
1030 dxHC = xHct2 * .5
1040 END IF
1050 xHCr = xHct2 - dxHC
1060 mctot = mctot + mc
1080 dxHctot = dxHctot + dxHC

```

```
1090     xHCr1 = xHCr
1100     PRINT " "
1110     PRINT deg, Ms, Tm, dxHC
1130         OPEN "a", #5, "c:\qbasic\data\oxid20c4.dat"
1140         PRINT #5, deg, Tm, dxHC, dxHCtot
1150         CLOSE #5
1190 NEXT i
1210 mHC = Molf * xHCr * mctot * (Xmix + 1) / (Xmix * Molb)
1220 PRINT "*****"
1230 PRINT "mass of unburnt fuel =", mHC
1240 PRINT "*****"

1500 END
```

APPENDIX 3 TABLES OF PISTON AND CYLINDER DIMENSIONS

Table A 1 Standard Pistons

Table A 2 High Top Ring Pistons

Table A 3 Enlarged 2nd Land Pistons

Table A 4 Pistons accompanying Smooth Liner

Table A 5 Predicted Oil Layer Thickness

Table A 6 Compiled Average Dimensions from above

tables

APPENDIX 3

TABLE A 1

STANDARD PISTON DIAMETERS AND CREVICE VOLUMES

PISTON 1	DIAMETER (mm)	HEIGHT (mm)	LINER (mm)	VOLUME (mm ³)
TOP LAND				
TOP	74.616	6	74.976	296.079
BOTTOM	74.498			
2nd LAND	74.441	3.85		241.718

PISTON 2	DIAMETER	HEIGHT	LINER	VOLUME
TOP LAND				
TOP	74.618	6	74.976	294.666
BOTTOM	74.5			
2nd LAND	74.443	3.85		240.817

PISTON 3	DIAMETER	HEIGHT	LINER	VOLUME
TOP LAND				
TOP	74.617	6	74.98	297.861
BOTTOM	74.5			
2nd LAND	74.445	3.85		241.73

PISTON 4	DIAMETER	HEIGHT	LINER	VOLUME
TOP LAND				
TOP	74.617	6	74.978	296.793
BOTTOM	74.499			
2nd LAND	74.44	3.85		243.07

	STANDARD PISTONS AND LINERS CLEARANCE VOLUME			VOLUME INCLUDING RING GROOVE
	MAX	MIN	AVERAGE	
TOP LAND	297.861	294.666	296.35	800.07
2nd LAND	243.07	240.817	241.834	850.67

APPENDIX 3

TABLE A 2

HIGH TOP RING PISTON DIAMETERS AND CREVICE VOLUMES

PISTON 1	DIAMETER (mm)	HEIGHT (mm)	LINER (mm)	VOLUME (mm ³)
TOP LAND				
TOP	74.3794	2.8	74.978	196.613
BOTTOM	74.3794			
2nd LAND	74.5365	3.85		199.599

PISTON 2	DIAMETER	HEIGHT	LINER	VOLUME
TOP LAND				
TOP	74.3947	2.8	74.98	192.268
BOTTOM				
2nd LAND	74.5356	3.85		200.916

PISTON 3	DIAMETER	HEIGHT	LINER	VOLUME
TOP LAND				
TOP	74.396	2.8	74.978	191.181
BOTTOM				
2nd LAND	74.5305	3.85		202.306

PISTON 4	DIAMETER	HEIGHT	LINER	VOLUME
TOP LAND				
TOP	74.4035	2.8	74.978	188.726
BOTTOM				
2nd LAND	74.5336	3.85		200.908

	HIGH TOP RING PISTONS AND LINERS CLEARANCE VOLUME			VOLUME INCLUDING RING GROOVE
	MAX	MIN	AVERAGE	
TOP LAND	196.613	188.726	192.197	695.917
2nd LAND	202.306	199.599	200.93225	809.773

TABLE A 3

ENLARGED 2ND LAND PISTONS DIAMETERS AND CREVICE VOLUMES

PISTON 1

	DIAMETER (mm)	HEIGHT (mm)	LINER (mm)	VOLUME (mm ³)
TOP LAND				
TOP	74.42	6	74.9845	379.504
BOTTOM	74.475			
2nd LAND	74.522	3.85		637.521

PISTON 2

	DIAMETER	HEIGHT	LINER	VOLUME
TOP LAND				
TOP	74.42	6	74.9836	381.691
BOTTOM	74.467			
2nd LAND	74.51	3.85		628.409

PISTON 3

	DIAMETER	HEIGHT	LINER	VOLUME
TOP LAND				
TOP	74.425	6	74.9867	380.01
BOTTOM	74.473			
2nd LAND	74.51	3.85		620.451

PISTON 4

	DIAMETER	HEIGHT	LINER	VOLUME
TOP LAND				
TOP	74.415	6	74.9885	385.179
BOTTOM	74.472			
2nd LAND	74.51	3.85		672.765

	ENLARGED 2nd LAND PISTONS AND LINERS CLEARANCE VOLUME			VOLUME INCLUDING RING GROOVE
	MAX	MIN	AVERAGE	
TOP LAND	385.179	379.504	381.596	885.316
2nd LAND	672.765	620.451	639.7865	1248.6275

APPENDIX 3

TABLE A 4

PISTONS AND SMOOTH LINER DIAMETERS AND CREVICE VOLUMES

PISTON 1	DIAMETER (mm)	HEIGHT (mm)	LINER (mm)	VOLUME (mm ³)
TOP LAND				
TOP	74.477	6	74.997	367.552
BOTTOM	74.477			
2nd LAND	74.52	3.85		215.654

PISTON 2	DIAMETER	HEIGHT	LINER	VOLUME
TOP LAND				
TOP	74.476	6	74.997	368.258
BOTTOM	74.476			
2nd LAND	74.51	3.85		220.162

PISTON 3	DIAMETER	HEIGHT	LINER	VOLUME
TOP LAND				
TOP	74.486	6	74.991	356.921
BOTTOM	74.486			
2nd LAND	74.51	3.85		217.44

PISTON 4	DIAMETER	HEIGHT	LINER	VOLUME
TOP LAND				
TOP	74.475	6	74.996	368.254
BOTTOM	74.475			
2nd LAND	74.51	3.85		219.708

	SMOOTH LINER CLEARANCE VOLUME			VOLUME INCLUDING RING GROOVE
	MAX	MIN	AVERAGE	
TOP LAND	368.258	356.921	365.246	868.966
2nd LAND	220.162	215.654	218.241	827.082

APPENDIX 3

Table A 5

Average Values

Liner		Oil Depth um	Rk um	Rpk um	Rvk um
Standard	New	1.9972	2.186	0.8018	2.4265
	Old	0.2437	0.2814	0.1233	1.1297
High Top Ring	New	1.647	2.2415	0.8268	1.8283
	Old	0.2376	0.32	0.066	1.262
Enlarged 2nd Land	New	1.234	2.2806	0.7484	2.1696
	Old	0.2482	0.2943	0.1723	1.1103
Smooth Liners	New	0.5751	0.9925	0.3255	1.4428
	Old	0.2019	0.3068	0.136	1.0149

APPENDIX 3 PISTON DIMENSIONS

TABLE OF PISTON AND LINER DIAMETERS FOR EACH BUILD

STANDARD PISTON

	DIAMETER (mm)	HEIGHT (mm)	LINER (mm)	VOLUME (mm ³)
TOP LAND	74.55	6	74.98	296.1
2nd LAND	74.44	3.85		241.7

HIGH TOP RING PISTON

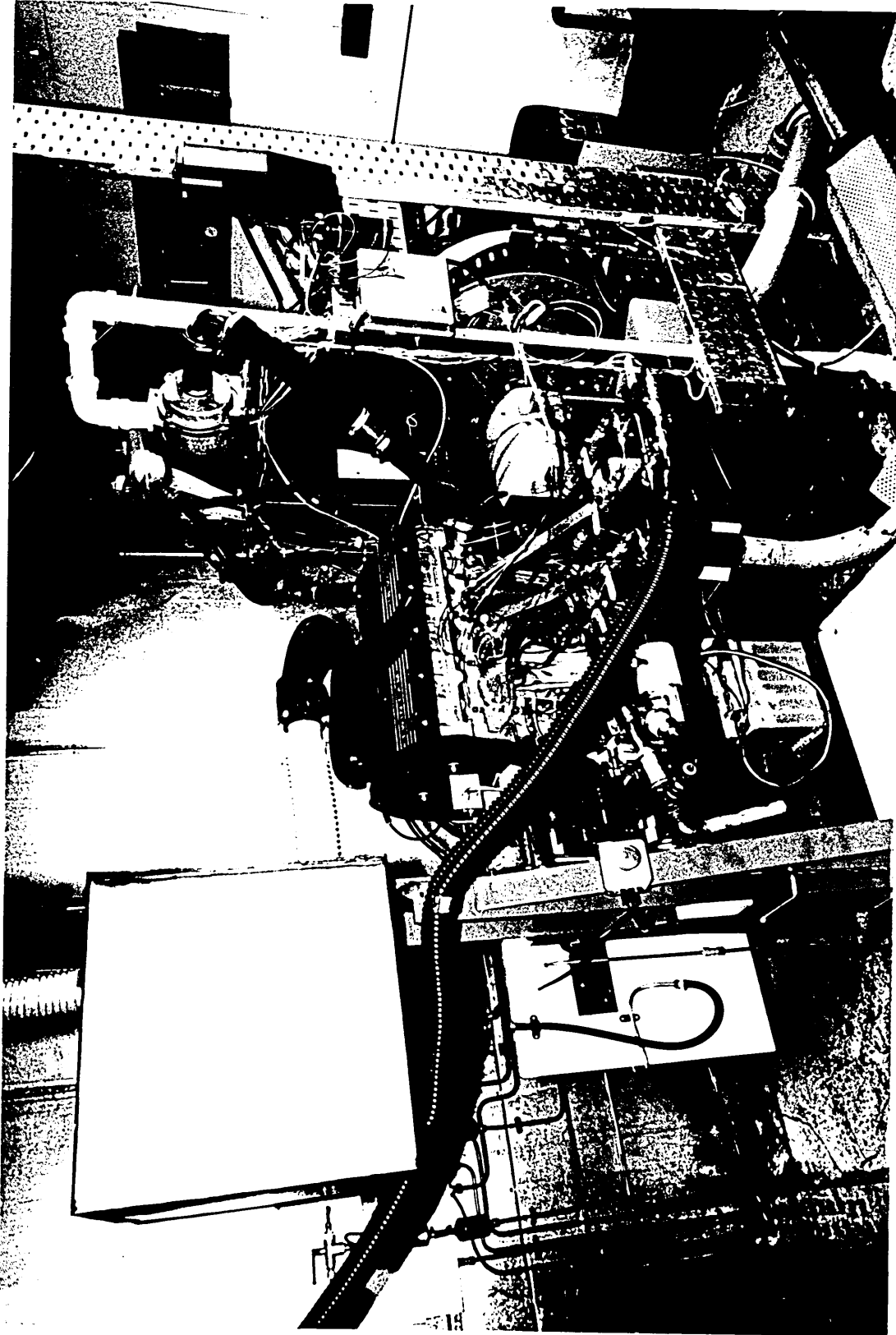
	DIAMETER	HEIGHT	LINER	VOLUME
TOP LAND	74.38	2.8	74.98	196.6
2nd LAND	74.54	3.85		199.6

ENLARGED 2ND LAND PISTONS

	DIAMETER	HEIGHT	LINER	VOLUME
TOP LAND	74.42	6	74.98	379.5
2nd LAND	74.52	3.85		637.5

PISTONS AND SMOOTH LINER

	DIAMETER	HEIGHT	LINER	VOLUME
TOP LAND	74.48	6	74.997	367.6
2nd LAND	74.52	3.85		215.7



Photograph of Engine in Test Cell

Analysis sheets supplied with reference fuel, trimethyle pentane and oil.

19th Amendment issue
**CEC REFERENCE OR STANDARDISATION
 OILS DATA SHEET**

NUMBER: RL-139/4
SHEET ISSUE DATE: AUGUST 19
SUPERSEDES: APRIL 1990

PURPOSE:

HIGH PERFORMANCE REFERENCE OIL TO ASSESS CONTROL OF "BLACK SLUDGE"
 THE DB M102E BENCH ENGINE TEST.

CHARACTERISTICS:

SAE GRADE.....	10W/30	
DENSITY AT 15 °C (ASTM D1298/IP160).....	0.857	G/ML
FLASH POINT (ASTM D93/IP34).....	223	°C
POUR POINT (ASTM D97/IP15).....	-39	°C
VISCOSITY AT 100 °C (ASTM D445/IP71)....	12.09	MM ² /S
VISCOSITY AT 40 °C (ASTM D445/IP71)....	78.9	MM ² /S
VISCOSITY AT -20 °C (ASTM D2602).....	2220	MPAS
VI (ASTM D2270/IP226).....		
TBN (PERCHLORIC) (IP 276 ASTM D2896)...	9.5	MG KOH/G
TAN (ASTM D664/IP 177).....	2.08	MG KOH/G
SULPHATED ASH (ASTM D874/IP163).....	0.98	% MASS
ELEMENTAL ANALYSIS:-		% MASS
ZINC.....	0.097	% MASS
PHOSPHORUS.....	0.136	% MASS
CALCIUM.....	0.213	% MASS
BARIUM.....	-	% MASS
MAGNESIUM.....	0.027	% MASS
NITROGEN.....	-	% MASS
OTHER.....	-	% MASS

COMPOSITION:

PART SYNTHETIC BASE OIL WITH API S6/CD PERFORMANCE PACKAGE AND
 VISCOSITY INDEX IMPROVER.

ORIGINATED BY:

DKA WORKING GROUP "MOTOREN" PROBIM M102E ZUR VERHINDERUNG VON
 SCHAMMBILDUNG IN OTTOMOTREN

HISTORY:

WIDELY EVALUATED AS A GOOD REFERENCE OIL BY KST

AVAILABLE FROM:

H. KRUGER, WEST GERMANY
 SILKOLENE LUBRICANTS PLC, BELPER, DERBYS, UK.

DATA SHEET PREPARED BY: I. R. TAYLOR (REF: 13001423/80112-88)



Öffentlich bestellte und vereidigte Chemiker
(Handelschemiker) der Handelskammer Hamburg
Analysen · Gutachten · Beratung

Fintelmann und Meyer · Postfach 5004 63 · D · 2000 Hamburg 50

Haltermann GmbH
Frau Noffz
Postfach 93 01 66
2102 HAMBURG 93

B21

Gur ref. : Pi
Your ref. : Noffz

Hamburg, 31/10/92

Analysis Certificate No. 40626

Ref. : 1 sample CEC RF 08-A-85
marked : CEC RF 08-A-85
Shore Tank 131
drawn by us on 20.10.1992
at the plant of Haltermann, Wilhelmsburg
received on : 20.10.1992 in 4 x 1 l bottle and 2 x 1/2 l bottle
Seal : none

CEC REFERENCE FUEL RF-08-A-85:

Knocking characteristic Octane number RON-CFR (ASTM D 2699)	98.2	*
Knocking characteristic Octane number MON-CFR (ASTM D 2700)	88.2	*
Density at 15 °C (ASTM D 1298)	0.7502	kg/l
Vapor pressure (Reid method) (ASTM D 323)	0.61	bar
Distillation (ASTM D 86)		
- initial boiling point at	31	°C
- 10 % v/v at	52	°C
- 50 % v/v at	109	°C
- 90 % v/v at	171	°C
- final boiling point at	198	°C
- residue	1.0	% v/v
Hydrocarbon types by fluorescent indicator adsorption (ASTM D 1319)		
- Olefines	6.7	% v/v
- Aromatics	31.7	% v/v
- Saturates	61.6	% v/v
Carbon/hydrogen ratio (Ultimate analysis)	7.14 : 1	



Öffentlich bestellte und vereidigte Chemiker
(Handelschemiker) der Handelskammer Hamburg
Analysen · Gutachten · Beratung

Fintelmann und Meyer · Postfach 50 04 63 · D · 2000 Hamburg 50

Analysis Certificate No. 40626 - 2 -

Oxidation stability		
Induction period (ASTM D 525)	> 960	min
Existent gum (ASTM D 381)	0.6	mg/100 ml
Sulfur by the Wickbold method (DIN EN 41)	37	mg/kg
Lead (ASTM D 3237)	0.0042	g/l
Phosphorus (ASTM D 3231)	< 0.2	mg/l
Copper corrosion (ASTM D 130)	1 a	
Methyl-tert-butylether (GC-FID)	< 0.05	% m/m

*The CFR-motor is succesfully regularly checked in cooperative test programmes.



Dr. E.-Ch. FINTELMANN u. Dr. H.-M. MEYER
der vereidigte handelschemiker

Johann Wollersheim (GmbH & Co.)
Werk Wilhelmshurg
Labor

Signature *Signature*



PHILLIPS 66 COMPANY

BARTLESVILLE, OKLAHOMA 74004
PHONE: 918 661-6600 TWX 910 841-2560 TLX 49-2455

SPECIALTY CHEMICALS

2, 2, 4-TRIMETHYLPENTANE

ISOOCTANE

ASTM Grade

<u>Property</u>	<u>Typical Value</u>	<u>Specification</u>	<u>Test Method</u>
Composition, Wt%			ASTM D 2268
2,2,4-Trimethylpentane	99.95	99.75 Min.	
Normal Heptane	0.01	0.10 Max.	
Other C ₈ 's	0.04		
Lead Content, g/gal.	0.000	0.002 Max.	ASTM D 3237 Mod.
Nonvolatile matter, mg/100 ml	0.16		ASTM D 381
Sulfur content, ppm	<1		ASTM D 3120

Notice: The information contained herein is, to the best of our knowledge and belief, accurate. Since the conditions of handling and use are beyond our control we make no guarantee of results. We assume no liability for damages or penalties resulting from use or reliance on the above information or recommendations, nor are these to be taken as a license to operate under, or recommendations to infringe, any patent.

Reissued
August, 1989
0145BB
EJH/RC

Appendix 6

Definitions of Surface Finish Parameters

The parameters for the bearing curve are Rpk, Rk, Rvk, Mr1, Mr2 and Tp. These are illustrated in Figure A1.

Rpk

This is the reduced peak height and is defined as the top portion of the surface which will be worn away in the early life of the engine.

Rk

This is the depth of the roughness core profile it forms the long term running surface for the cylinder liner.

Rvk

Defined as the reduced trough depth and gives a measure of the oil retaining capability of the surface.

Mr1

Determines the line of intersection coinciding with the upper limit of the roughness core profile as a percentage.

Mr2

The intersection coinciding with the lower limit of the roughness core profile as a percentage.

Tp %

This is the bearing curve ratio and defines the percentage of metal at a fixed depth in the profile.

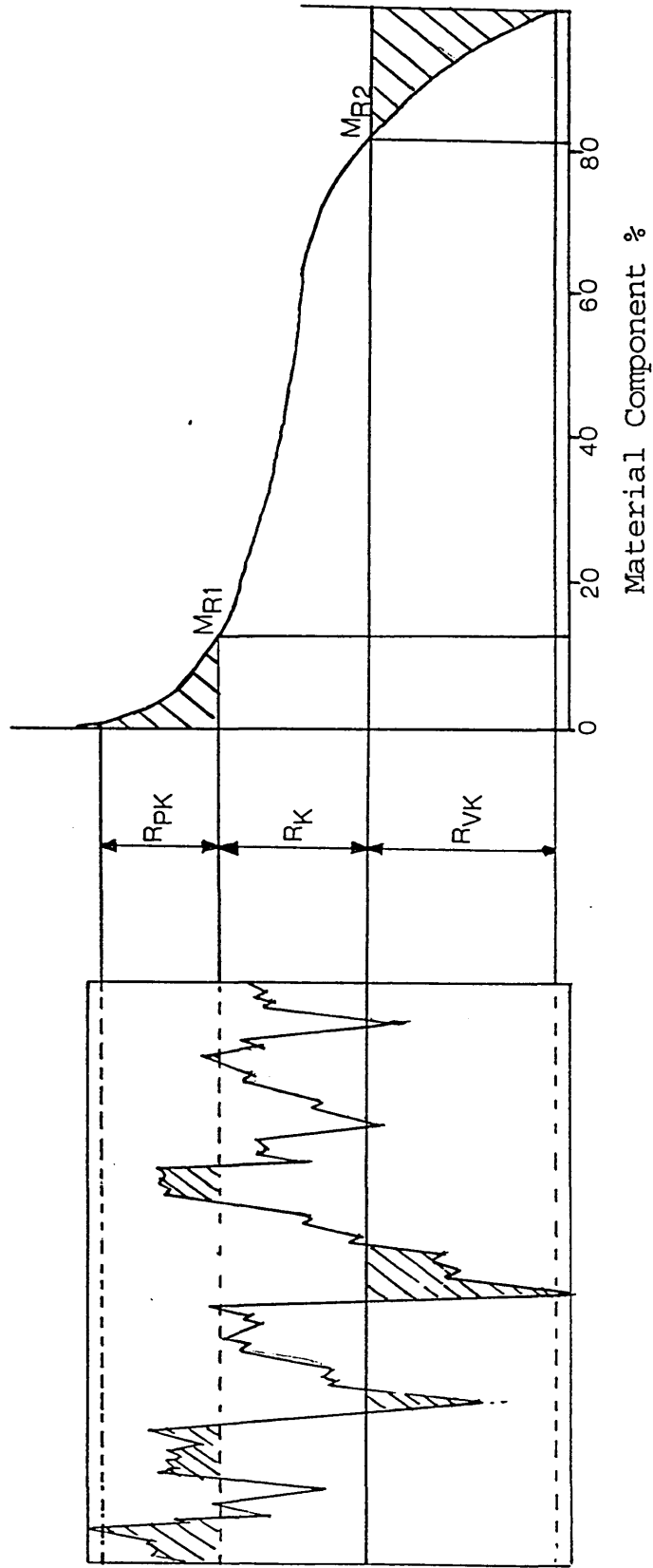


Figure A 1 Sketch showing surface finish parameters

A Comparison of Hydrocarbon Emissions from Different Piston Designs in an SI Engine

Michael Willcock, David H. Tidmarsh, and Peter Foss
Sheffield Hallam University

David Bates
AE Piston Products Ltd.

The appearance of the ISSN code at the bottom of this page indicates SAE's consent that copies of the paper may be made for personal or internal use of specific clients. This consent is given on the condition, however, that the copier pay a \$5.00 per article copy fee through the Copyright Clearance Center, Inc. Operations Center, 27 Congress St., Salem, MA 01970 for copying beyond that permitted by Sections 107 or 108 of the U.S. Copyright Law. This consent does not extend to other kinds of copying such as copying for general distribution, for advertising or promotional purposes, for creating new collective works, or for resale.

SAE routinely stocks printed papers for a period of three years following date of publication. Direct your orders to SAE Customer Sales and Satisfaction Department.

Quantity reprint rates can be obtained from the Customer Sales and Satisfaction Department.

To request permission to reprint a technical paper or permission to use copyrighted SAE publications in other works, contact the SAE Publications Group.



GLOBAL MOBILITY DATABASE

All SAE papers, standards, and selected books are abstracted and indexed in the SAE Global Mobility Database.

No part of this publication may be reproduced in any form, in an electronic retrieval system or otherwise, without the prior written permission of the publisher.

ISSN 0148-7191

Copyright 1993 Society of Automotive Engineers, Inc.

Positions and opinions advanced in this paper are those of the author(s) and not necessarily those of SAE. The author is solely responsible for the content of the paper. A process is available by which discussions will be printed with the paper if it is published in SAE transactions. For permission to publish this paper in full or in part, contact the SAE Publications Group.

Persons wishing to submit papers to be considered for presentation or publication through SAE should send the manuscript or a 300 word abstract of a proposed manuscript to: Secretary, Engineering Activity Board, SAE.

Printed in USA

A Comparison of Hydrocarbon Emissions from Different Piston Designs in an SI Engine

Michael Willcock, David H. Tidmarsh, and Peter Foss
Sheffield Hallam University

David Bates
AE Piston Products Ltd.

ABSTRACT

The total hydrocarbon emissions and the distribution of hydrocarbon species from the emissions of two different piston and cylinder liner designs;

- 1 reduced top land height,
- 2 smoother cylinder bore,

were compared with a standard production Rover K16 spark ignited engine. Reductions in total HC emissions were achieved for both designs. The variations between the relative quantities of a selection of the most significant species were investigated for each design, considerable differences were observed between these design changes.

INTRODUCTION

Reduction of exhaust pollutants from automotive vehicles continues to be an important area of research for the automotive industry. Despite the use of catalytic converters reduction of emissions at source is still an essential for the future internal combustion engine. Although current legislation deals with only the total amount of hydrocarbon emissions, there is considerable interest in the speciation of the hydrocarbons. Gas chromatography has frequently been used to identify hydrocarbon species, to observe whether emissions are unburnt fuel or combustion products, and their variability with engine conditions, Kaiser et al [1].

The origins of hydrocarbon emissions have been well reported by many researchers and are from three main sources.

1. Unburned mixture from crevice volumes, mainly from piston top land.
2. Fuel is absorbed into oil layers

during compression and is released during expansion.

3. Quenching of bulk gases, this mostly due to poor combustion.

This paper investigates the impact of piston design on total hydrocarbon emissions and the distribution of a selection of hydrocarbon species. Current gas chromatography techniques have identified more than 30 species in the exhaust emissions. However, the impact of design changes can be best demonstrated by restricting this number to the most significant species present. The piston designs investigated were chosen to achieve a reduction in hydrocarbon emissions, but which could be readily adopted for commercial production rather than purely for research. There has been no attempt to alter the combustion chamber design.

EQUIPMENT

The engine used throughout this research was a 1.4 litre 16 valve unit with wet liners and multi point fuel injection. The engine control unit could be adjusted to maintain accurate control of operating conditions, described in Table 1. The engine was coupled to a Schenk eddy-current dynamometer. During tests CO, CO₂, O₂, HC and NO_x were measured. Hydrocarbon emissions were measured by NDIR in propane units. Regular calibration ensured the accuracy of the analysing equipment, including feeding calibration gases into the sample line at the engine. The sample line includes sampling points at the exhaust port of each cylinder and the exhaust pipe immediately below the manifold, the sample being passed through a heated line to the analysers. Thermocouples were used to monitor exhaust gas temperatures at the sampling points and to measure the coolant and

oil temperatures. Air and fuel flow to the engine were measured. A record of the engine operating conditions was kept enabled consistent conditions at the test points to be achieved to an accuracy of 5%. The results discussed here are the statistical mean of several tests. Throughout this research the tests were repeated taking samples from each test point on different days these gave consistent and repeatable results.

Table 1 Test Points

Speed(RPM)	BMEP(bar)
950	0.2
1500	1.0
1500	2.62
2000	2.0
2500	5.5
3500	Wide Open Throttle

Air fuel ratio at all points 15:1
Ignition timing adjusted to give peak pressure at 12 ATDC

The lubricating oil used is a CEC reference oil (RL 139/4) of viscosity 10W/30. The fuel is a reference unleaded petrol CEC RF-08-A-85, with knocking characteristic Octane numbers of RON 97.1, MON 87.4.

GAS CHROMATOGRAPHY - The sample was carried to the gas chromatograph through a heated sample line without being diluted or filtered. A Perkin Elmer 8600 gas chromatograph was used with a wall coated open tubular column, the stationary phase being CP-Sil-5 CB, the column length 50m and the inside diameter 0.32 mm. This equipment gave good resolution of a wide range of hydrocarbons from C1 to C9. The method used is described in Table 2.

Table 2 Gas Chromatograph Method

Temperature Programme
Temperature 1 = 30 (deg C)
Iso time = 2 minutes
Ramp 1 = 4 (deg C/minute)
Temperature 2 = 200 (deg C)
Injector Temperature 100 (deg C)
Detector Temperature 250 (deg C)
Carrier Gas Helium
Flow Rate 1 (ml/minute) at 20 deg C
Injector Automatic sampling valve,
0.1 ml sample loop
Detection Flame Ionisation Detector

From emission samples taken from the standard engine build and with the gas chromatograph method described above

a selection of 13 species were chosen and identified with calibration gases. These species were a selection of products and fuel components representative of the main types of species alkanes, alkenes and aromatics. They accounted for approximately 75% of the area of the gas chromatograph trace. These are named and listed in Table 3. It can be observed from Figure 1, gas chromatograph plots from unleaded gasoline and emissions, that there is a significant reduction in the number of peaks detected in the emissions compared to the fuel. Unburned fuel species do not survive the combustion process in equal proportions. Some C1 to C3 hydrocarbons are not present in gasoline but, are products of incomplete combustion. Many components of fuel are not detected in the emissions. Dempster and Shore [7], identified a greater part of the hydrocarbon emissions as combustion products.

Table 3 Major hydrocarbon species from emissions

Peak	Name
1	Methane
2	Ethene (ethylene)
3	Ethane
4	Propene (propylene)
5	Isobutene
6	Butane
7	pent-1-ene
8	Benzene
9	2,2,4, trimethyl pentane
10	2,4, dimethyl hexane
11	Toluene
12	P-Xylene and M-Xylene
13	O-Xylene

The flame ionisation detector connected to the gas chromatograph gives an output proportional to the carbon atoms present. Using calibration gas mixtures of known concentration allows the parts per million (ppm) concentration of carbon to be calculated. The amount of a particular compound is found by dividing the carbon atoms detected by the number of atoms in that compound.

PISTON DESIGNS

Two different piston and liner configurations were compared against emission readings taken from standard piston and liners for this particular engine. Before installation piston and liner dimensions were measured to give an accurate assessment of the crevice

Table 4 Cylinder liner surface finish parameters

Parameter	A Standard Liners		B Smooth Liners	
	New	Run-in	New	Run-in
Ra	0.76	0.25	0.39	0.185
Rk	2.28	0.281	0.99	0.3068
Rpk	0.748	0.123	0.325	0.136
RvK	2.17	1.13	1.44	1.0149
Oil depth	1.997	0.244	0.575	0.202

volumes. The liner surface finish was also measured. The engine was subjected to twenty hours running-in before testing commenced to ensure conformity of pistons, rings and liners. New pistons and liners are fitted for each configuration.

1. Reducing top land crevice volume-The effect that the top land has on hydrocarbon emissions is well reported. Namazian and Heywood [2] showed that the reduction in emissions was directly proportional to the top land crevice volume. Also in a series of tests Wentworth [3] used a piston and ring configuration to completely seal off the piston crevice volume, achieving significant reductions in emissions. However it is the objective of this research to produce practical designs suitable for use in modern automotive engines.

A set of pistons was manufactured with higher 1st and 2nd rings. Detailed measurement of pistons and liners indicated that the top land crevice volume was reduced by 35%. The top ring groove was treated as a separate crevice. The 2nd land crevice was similar to the standard pistons.

2. Cylinder liner Surface finish-For the next test the cylinder liners were honed to a smoother surface finish though still keeping the same cross hatch pattern. The reasoning for this is set out below. A new set of standard pistons were used. The absorption of fuel by the lubricating oil film is affected by many variables, Dent and Lakshminarayanan (4) showed that oil layer thickness can have a considerable effect on emissions. The model developed by Korematsu (5) showed that the mass of fuel emitted from the oil was directly proportional to the oil layer thickness.

The effects of surface roughness on the lubrication of piston rings and liner were studied by Sandia and Someya (6), who showed that the oil layer is thicker with a rough surface. However, because this was a study on lubrication these oil layers were between the ring and liner. The interest for the absorption/desorption effect is due to the oil retained on the liner wall after the passage of the rings. On a rougher surface with a thicker oil film between ring and cylinder more oil will be stored in the surface microstructure and should produce higher hydrocarbon emissions than a smoother surface. The bearing area curve can be used to give an indication of the oil storage area available in the surface finish. Figure 2 compares the surface traces and bearing area curves of the standard piston liners and the smoother liners produced for this test.

To quantify the oil layer thickness for different liner surface finishes the free space above the bearing area curves within the roughness profile of the material was calculated. This was performed using a set of T_p values going down the surface profile, determining its area by Simpson's Rule for approximate integration. From this the average depth of free space can be found. The following assumptions were made.

Oil completely fills the surface profile.

The surface of the oil was taken as the depth of the 2% T_p value.

The surface of the oil is flat and parallel with the centre line of the profile.

The maximum depth of the oil is taken as the depth of the 98% T_p value.

The result of these calculations vary slightly for each liner. Table 4 sets out the surface parameters for each

set of liners and the calculated oil layer thickness.

RESULTS AND DISCUSSION

The results from the high top ring piston show reductions in hydrocarbon emissions at most test points, Figure 3 is a comparison against standard pistons. From this it can be seen that the greatest reductions occur at the higher speeds and loads. At speeds above 2000 rpm reduction of total hydrocarbon emissions of over 25% were achieved. These reductions are consistent with the reduction in crevice volume being a larger source of hydrocarbon emissions at higher speeds and loads. The gas chromatography results indicated that the reduction in emissions were not uniform for all hydrocarbon species, Figure 4 is a plot taken at 2000 rpm 2 bar bmep. For comparison between standard and high top ring pistons the ppm value for a particular species from the standard build is subtracted from the value from the high top ring piston. Figure 5 compares the species at each test point. Positive bars show an increase from the standard.

For further comparison the details of the speciation require closer inspection. The three main groups of compounds will be treated separately, these are; Alkanes, Alkenes and Aromatics.

The differences in Alkanes are plotted in Figure 6. All have been reduced in concentration, the reduction being greater for the fuel species, 2,2,4 trimethyl pentane, 2,4, dimethyl hexane. Note that at some test points trimethyl pentane was not detected and that apart from the anomaly at 1500 rpm 1 bar bmep, 2,4, dimethyl hexane was not detected from the high top ring pistons. Also note that there was a decrease in 2,4, dimethyl hexane in the standard emissions as speed and load increased. Methane and ethane were reduced by a lesser amount.

The Alkenes, Figure 7, have also been reduced, particular Pent-1-ene and ethene.

The aromatics indicate an increasing trend with higher loads although at low load there is a decrease in emissions. At higher loads there is a significant increase in the xylenes. Both benzene and toluene produce a lesser proportion of emissions than for standard pistons, Figure 8.

The variations in each of these species must be put into the context of the overall reduction in emissions. Most

species have been reduced but by differing amounts, rather than a reduction proportional to the change in the crevice volume. This reduction shows that either a much larger proportion of fuel species are being fully oxidised, or emissions are being reduced from another source. However, the emissions were reduced by only 25%, less at lower speeds and loads, Figure 8, indicates that the xylenes increased their proportion of total emissions, thus compensating for the reduction of the lighter species.

An increase in oxidation could occur if the crevice mixture returned to the cylinder earlier in the engine cycle. However, observation of flow models indicated that though the mass flow rate was reduced, the peak flow occurred at similar points in the engine cycle. Also the percentage of total crevice mass returned to the cylinder per degree crank angle were the same. However, the changes in piston design will have changed the temperature profile of the piston. Furuhashi et al (8) achieved a significant cooling effect by raising the piston rings. The geometry of the top land has also been altered and this will affect the crevice flow. Temperature and geometry affects require further investigation.

The changed top land height could also affect the absorption of fuel into the oil. Measurements of oil consumption indicated a decrease due to the changes in the piston ring configuration. This could result in less oil above the top ring on the cylinder wall. The area of oil exposed is also reduced by raising the rings.

LINER SURFACE FINISH-The total HC emissions from these tests when compared against the standard, Figure 9, show significant reduction in total HC emissions. These reductions are greater at lower speeds and loads, consistent with reducing the contribution of the absorption and desorption effect to total hydrocarbon emissions. It was observed by Dent and Lakshminarayanan (4) that this effect decreased as speed and load increased.

Substantial changes to the profile of HC species has occurred. Figure 10, is a gas chromatograph plot of a sample taken at 2000 rpm 2 bar bmep. For comparison between standard and smooth liner tests the ppm value for a particular species from the standard build is subtracted from the value obtained from the smooth liner test. Figure 11 compares the 13 selected species for each test point. The

positive bars indicate an increase from the standard. The difference is characterised by a large increase in toluene and large decreases in combustion products.

Figure 12 plots the alkanes in more detail. The products methane and ethane are at much lower levels. Of the fuel species 2,2,4, trimethyl pentane has increased its concentration from the standard and 2,4, dimethyl hexane is only detected at 1500 rpm 1 bar bmeq. Butane shows no significant change. Observable are trends in certain species; methane and 2,2,4, trimethyl pentane reduce as speed and load increase.

The alkenes reduce for both products and fuel species, as shown in Figure 13. Ethene is an important product as it is formed by the breaking of several different fuel components. Its reduction would indicate a higher level of complete oxidation of fuel. The levels of the aromatics are plotted in Figure 14. This shows the contrast between the large increase in toluene and the small reductions of benzene and the xylenes.

The reduction of most species observed from standard to smooth liners is in part due to the overall reduction in HC emission levels but some of the reduction in the products could be due to the increase in toluene. The only significant change to account for the overall decrease in emissions and increase in toluene are the changes to the surface finish. The difference in the calculated oil layer is small, 0.042 micron, for the worn liners. Absorption and desorption processes are very sensitive to changes in oil thickness. Dent and Lakshminarayanan (4) indicated a rapid decrease in emissions with reducing oil layer thickness.

The following is a possible mechanism for the increase in toluene:

The various components of the fuel are not absorbed into the oil evenly, some species being more readily absorbed. The controlling factor is cylinder pressure, the more soluble species being absorbed at lower pressures. If the oil layer is reduced then the oil may become saturated and unable to absorb other species. The species not absorbed would be burnt or oxidised while the species emerging from the oil later in the cycle would escape oxidation. The concentration of aromatics in Hydrocarbon emissions in the standard tests are higher than in the fuel, possibly due to their absorption in oil. The reduced oil layer

in smooth liner tests must then be selecting Toluene which is more soluble than other aromatics due its molecular weight and structure.

To observe if the oil absorbed toluene more easily than other aromatics, samples of oil were taken from the engine during operation. These were heated to a temperature of 80 deg C. Vapour was withdrawn from above the oil then injected into the gas chromatograph. The results were compared against vapour from fresh lubricant. Fresh oil showed no significant levels of hydrocarbon, but as the tests progressed the G.C. trace shows an increased presence of hydrocarbon species, especially toluene. Figure 15 compares gas chromatograph plots of oil vapour from standard and smooth liner tests. Both samples were taken from the engine operating at 3500 rpm wide open throttle. From these plots it can be seen that toluene is a major component of fuel vapour absorbed by the oil. The toluene peak is much greater from the smooth liner. Toluene comprises 10% of the vapour from standard and 40% from the smooth liner tests. This is approximately the same proportion as the emissions, and suggests that the increase in toluene is due to its being preferentially absorbed by the lubricating oil.

The decreasing trend of toluene with increasing speed and load, Figure 14, also is consistent with its being absorbed into the oil. As the absorption and desorption effect reduces with increase in speed, its contribution to total hydrocarbon emissions decreases.

CONCLUSION

It has been demonstrated that the design and manufacturing specification of pistons and liners can not only affect the total hydrocarbon emissions but individual hydrocarbon species, both in the unburned fuel and the products of combustion.

High top ring pistons achieved a reduction in overall hydrocarbon emissions and significant changes in hydrocarbon species plotted by gas chromatography. The proportion of combustion products and lighter fuel components have been reduced. Results showed that the reduction in emissions were more complex. Absorption and desorption of fuel in lubricating oil was affected by the reduction of top land height and oil consumption.

The results from tests on smooth cylinder liners also indicated reduced

total hydrocarbon emissions. Gas chromatography identified a large increase in one particular compound, toluene. Further investigation showed this to be due its preferential absorption in lubricating oil relative to other fuel species.

Changes to the speciation in both tests produced more of the heavier harmful emissions. However, with further research it will be possible to design piston and liner configurations to achieve lower total hydrocarbon emissions and to control the amounts of harmful hydrocarbon species.

ACKNOWLEDGEMENT

The authors wish to thank Dr D. Leathard, Sheffield Hallam University, for his advice and assistance, and SERC and AE piston Products Ltd for funding and supply of equipment for this research.

REFERENCES

- 1 Kaiser, E.W. Rothschild, W.G. and Lavoie, G.A: The effect of fuel and operating variables on hydrocarbon emission species distributions in the exhaust from a multicylinder engine. Combustion Science and Technology. 1983, Vol.32, pp 245-265.
- 2 Namazian, M and Heywood, J.B: Flow in the piston-cylinder-ring crevices of an SI engine and its effect on HC emissions, efficiency and power. SAE 820088.
- 3 Wentworth, J.T: Piston and ring variables affect exhaust emissions. SAE 680109
- 4 Dent, J.C. and Lakshminarayanan, P.A: A model for absorption and desorption of fuel vapour by cylinder lubricating oil film and its contribution to HC emissions. SAE. 830652.
- 5 Korematsu, K: Effects of fuel absorbed in oil film on unburnt hydrocarbon emissions from spark ignition engines. Japanese Society of Mechanical Engineers. 1990. Vol. 33. No 30. pp 606-614.
- 6 Sandia, S. and Someya, T: The effect of surface roughness on lubrication between a piston ring and a cylinder liner. IMechE conference on Tribology Friction, lubrication and Wear, 1987, paper C223/87, pp. 135-143.
- 7 Dempster, N.M. Shore, P.R: An investigation into the production of hydrocarbon emissions from a gasoline engine tested on chemically defined fuels. SAE 900354.
- 8 Furuhashi, S. Kojima, M. Enomoto, Y. and Yamaguchi, Y: Some studies on two-ring-pistons in automobile turbocharged gasoline engines. SAE 840183.

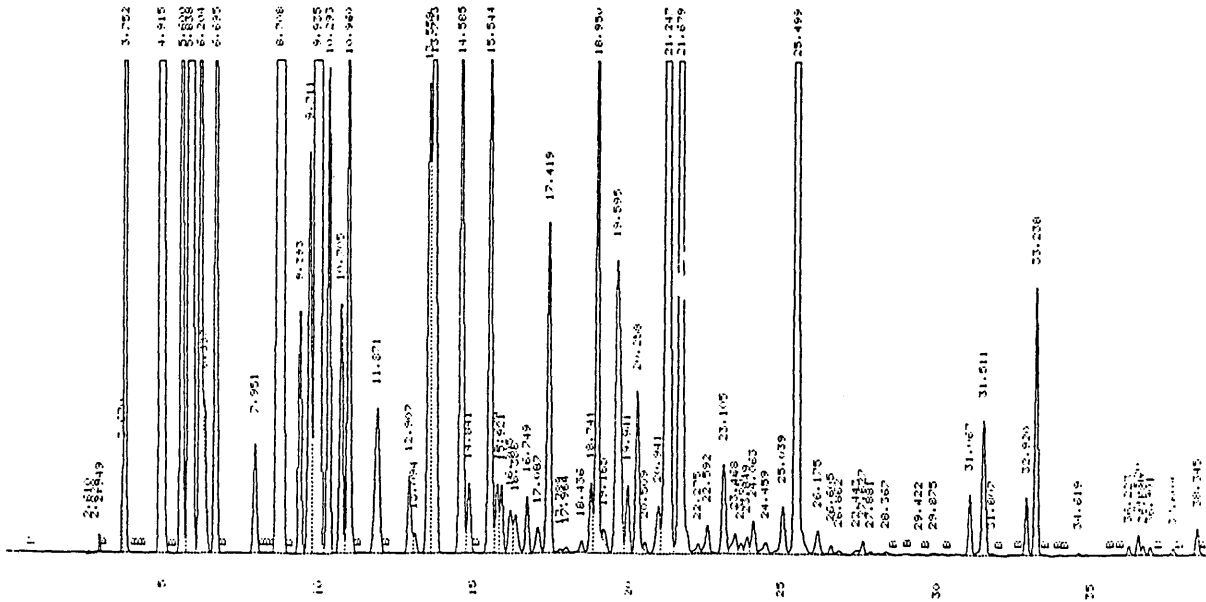


Figure 1, a, Gas chromatography plot of reference fuel

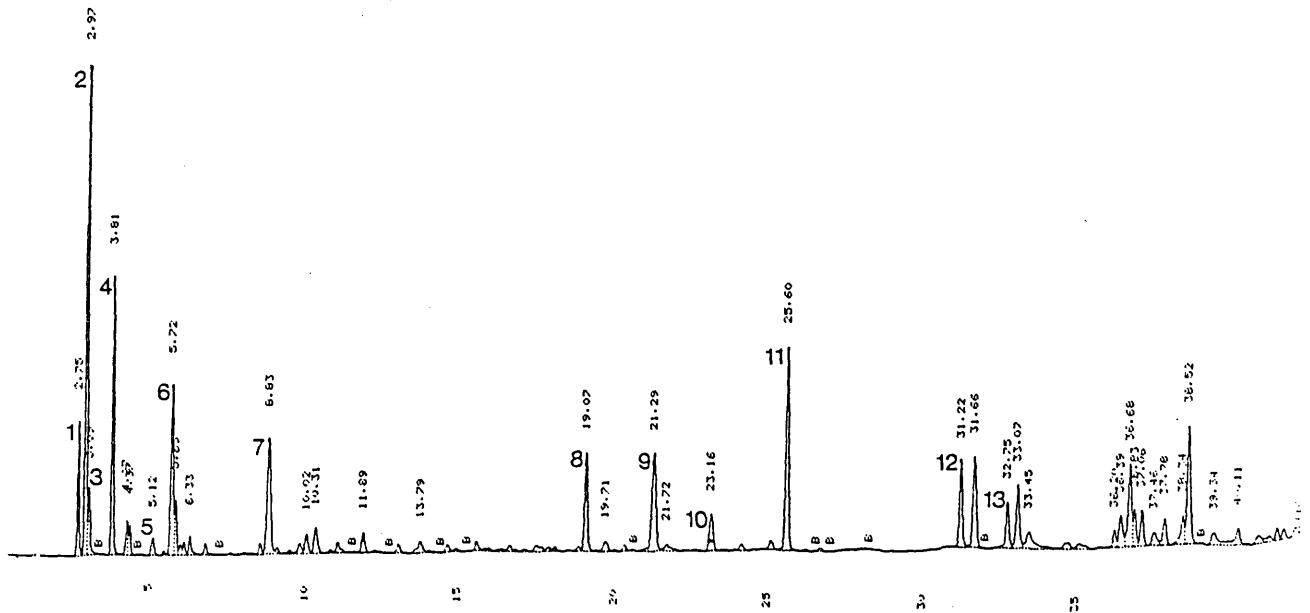


Figure 1, b, GC plot of emissions at 2500 rpm 5.5 bar bmep using standard pistons

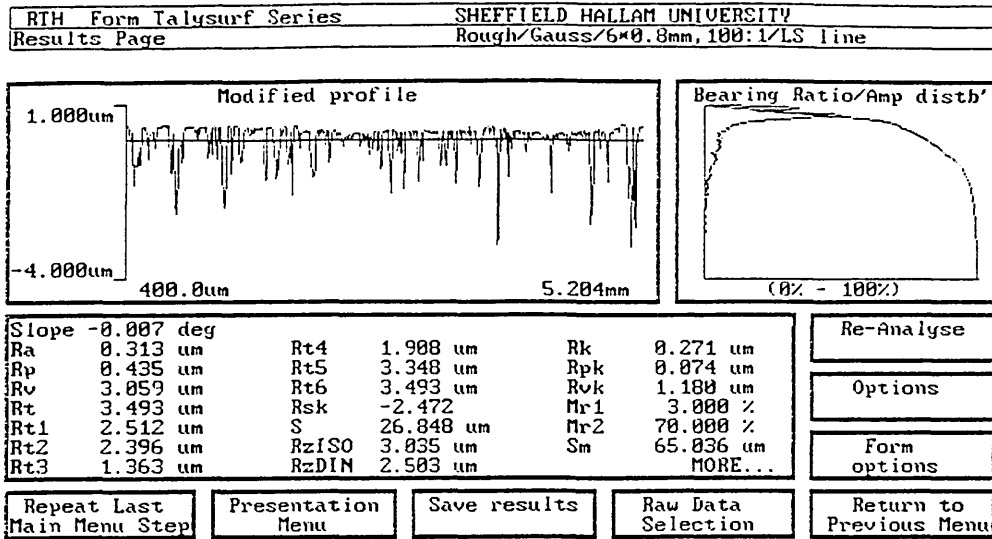


Figure 2, a, Surface finish data from standard cylinder liners

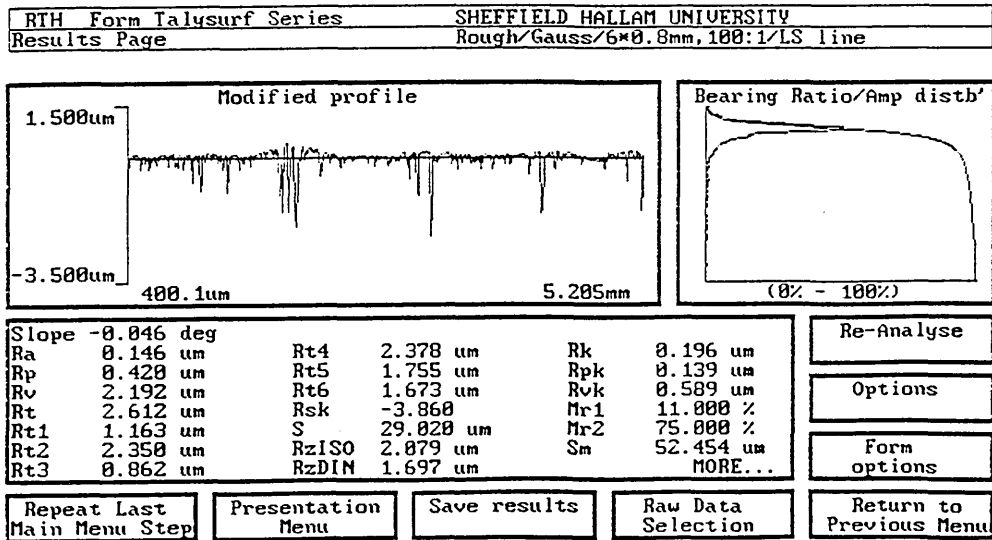


Figure 2, b, Surface finish data from smooth cylinder liners

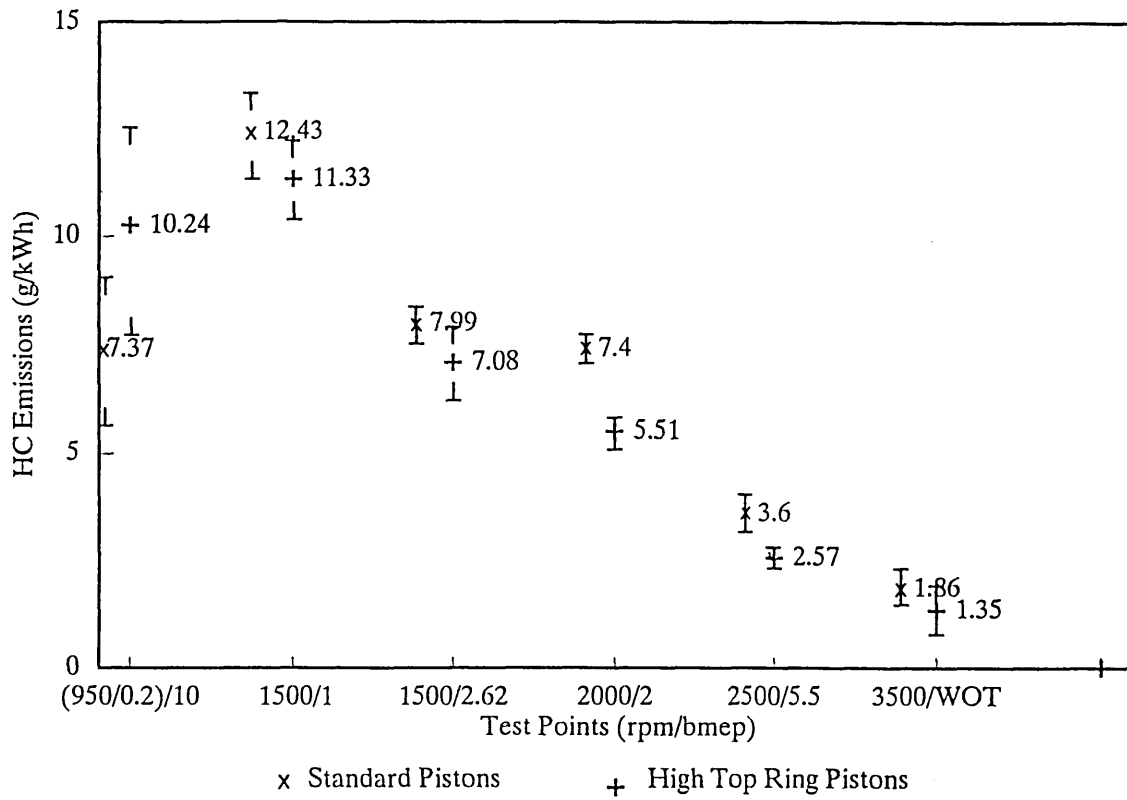


Figure 3 Hydrocarbon emissions, comparison between Standard pistons and high top ring pistons

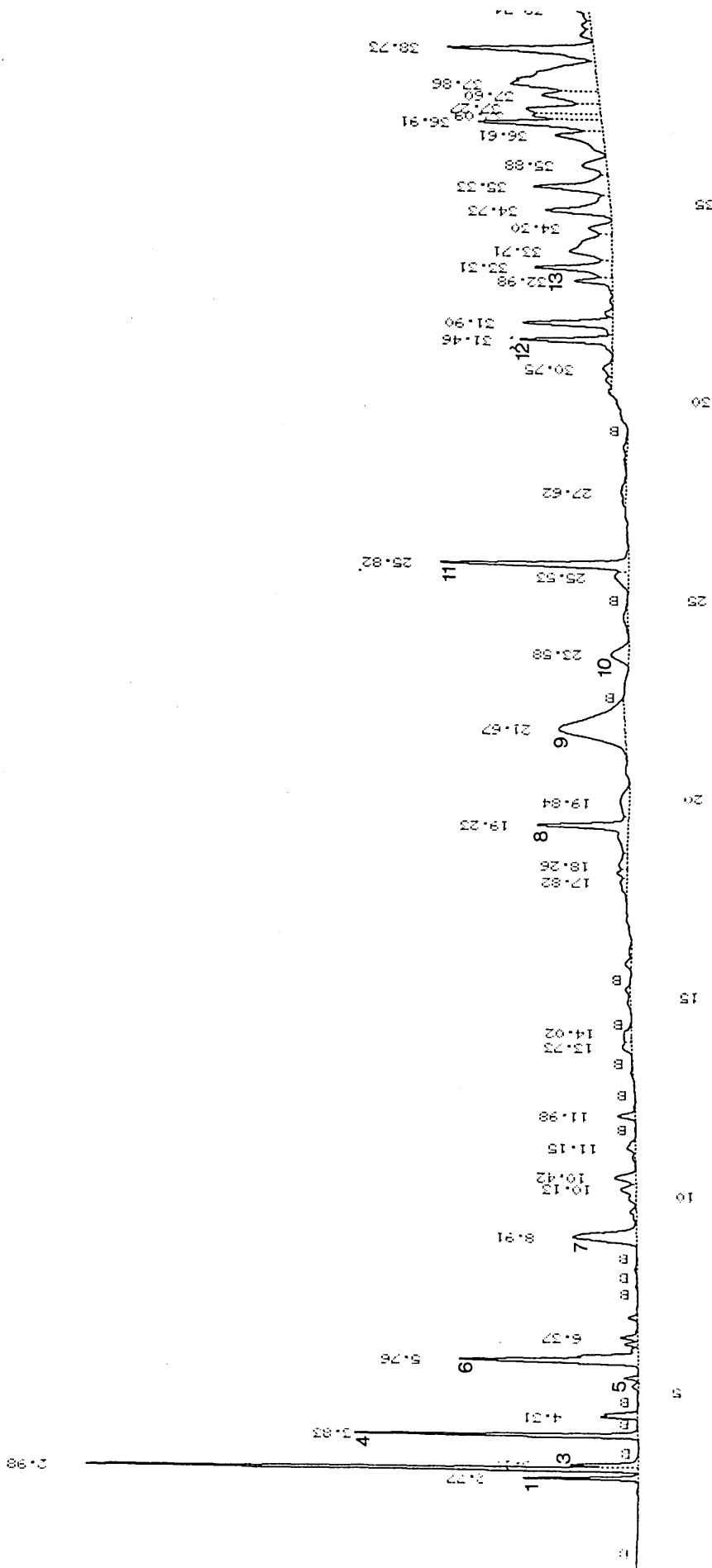


Figure 4 Gas chromatograph plot from high top ring piston tests sample taken at 2000 rpm 2 bar bmep

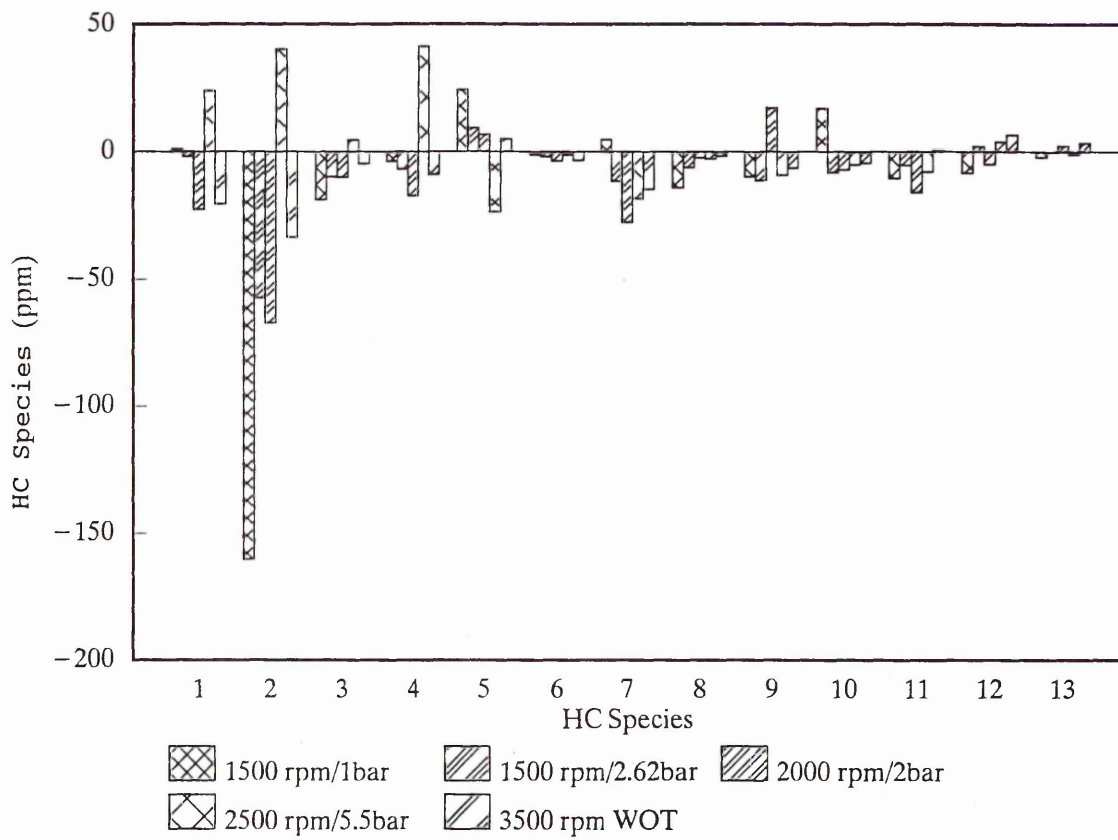


Figure 5 Comparison of HC species, difference between standard and high top ring pistons

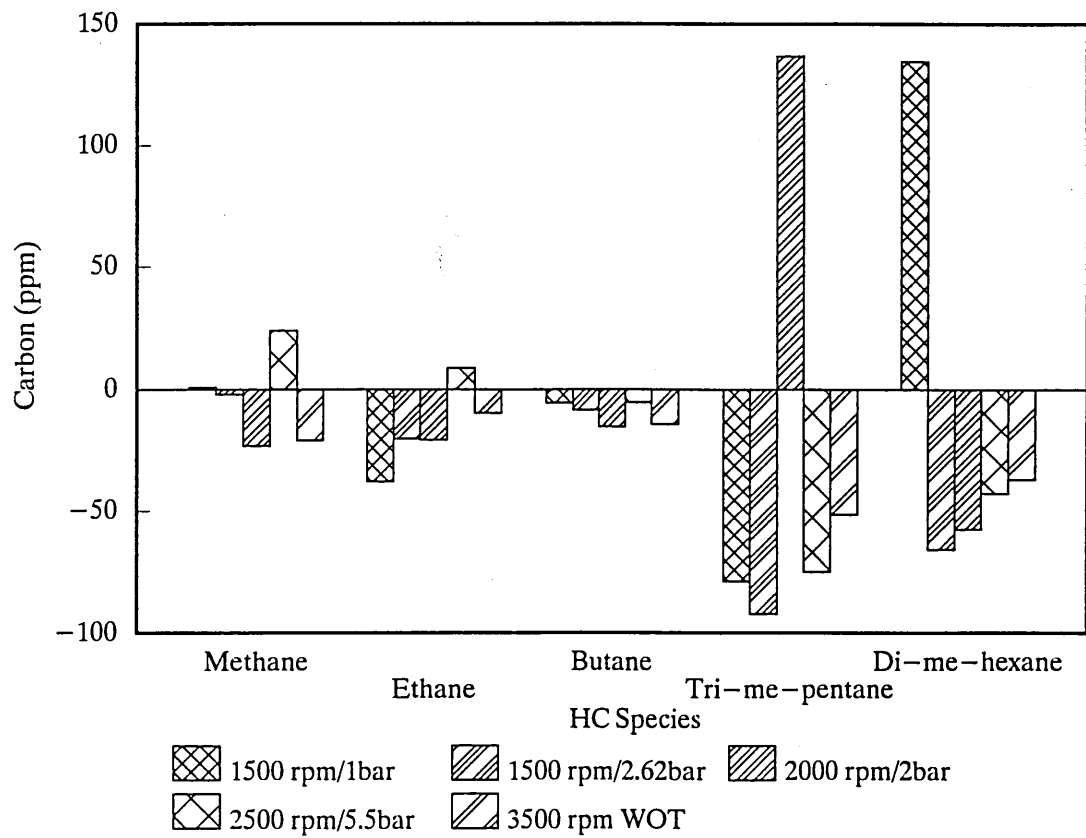


Figure 6 Comparison of Alkanes, difference between standard and high top ring pistons

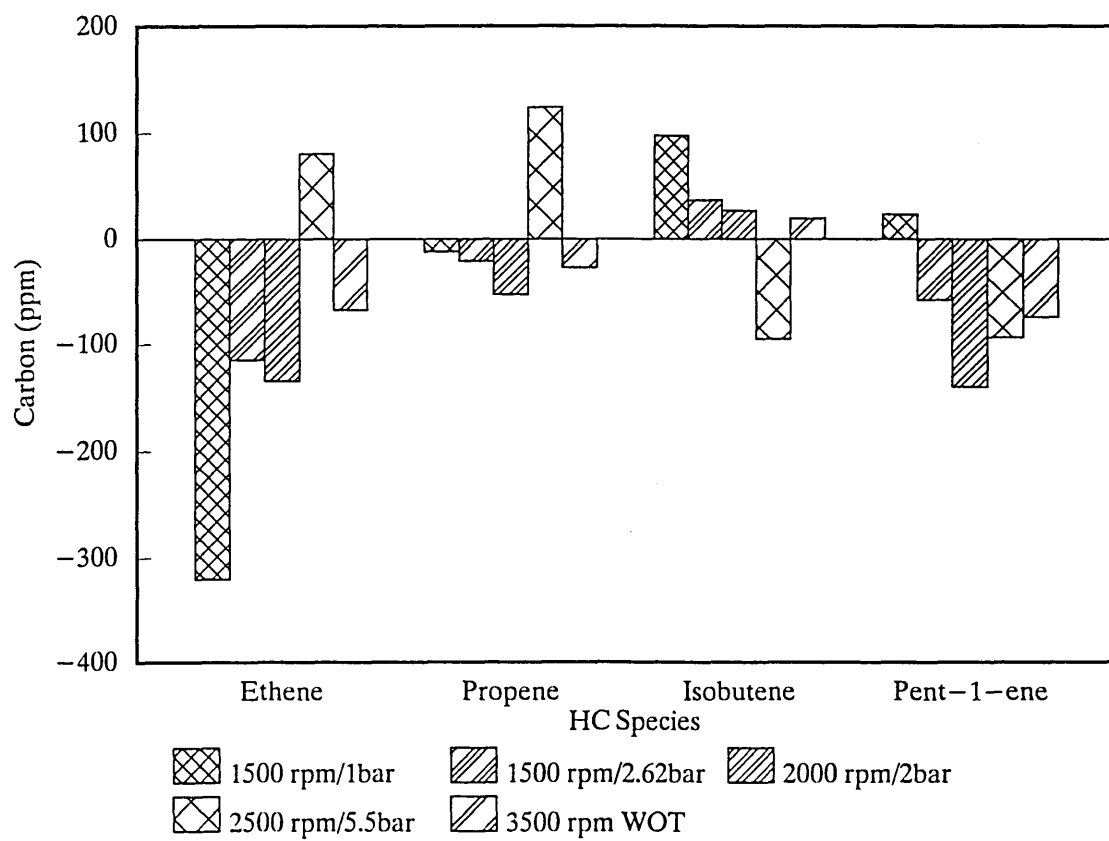


Figure 7 Comparison of Alkenes, difference between standard and high top ring pistons

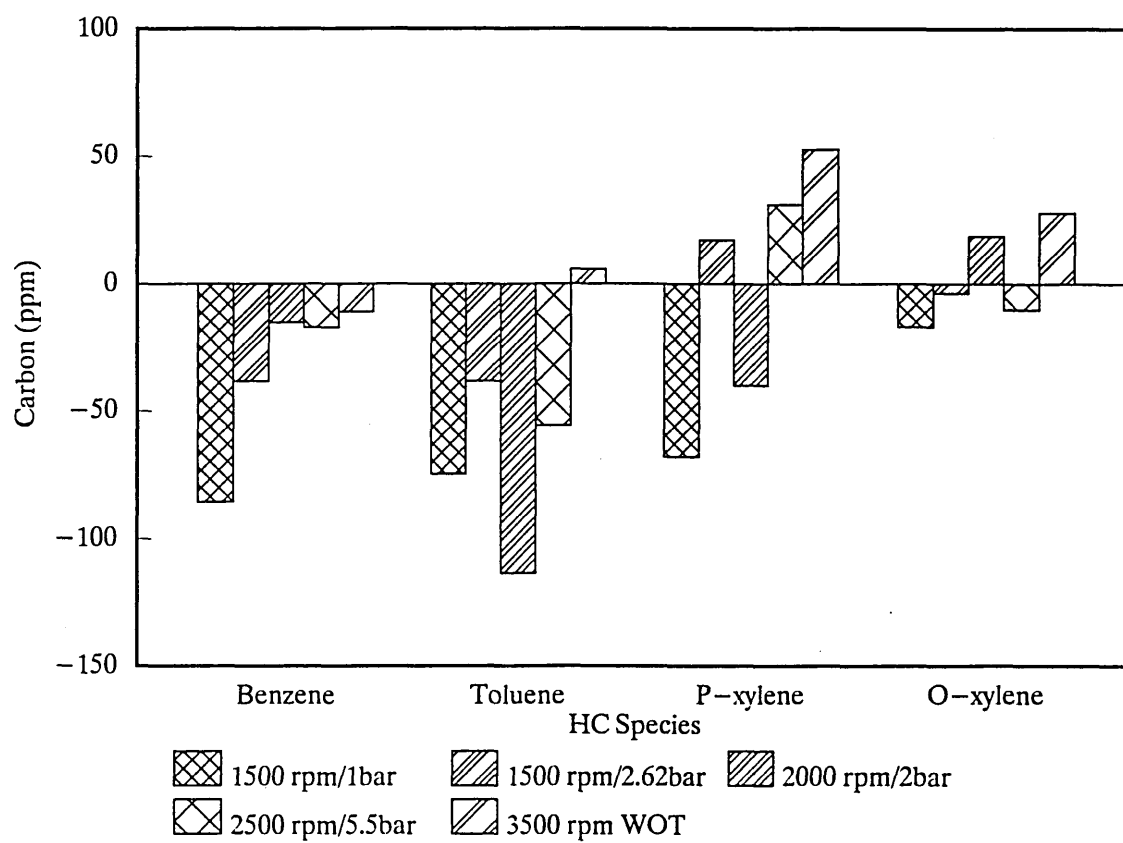


Figure 8 Comparison of Aromatics, difference between standard and high top ring pistons

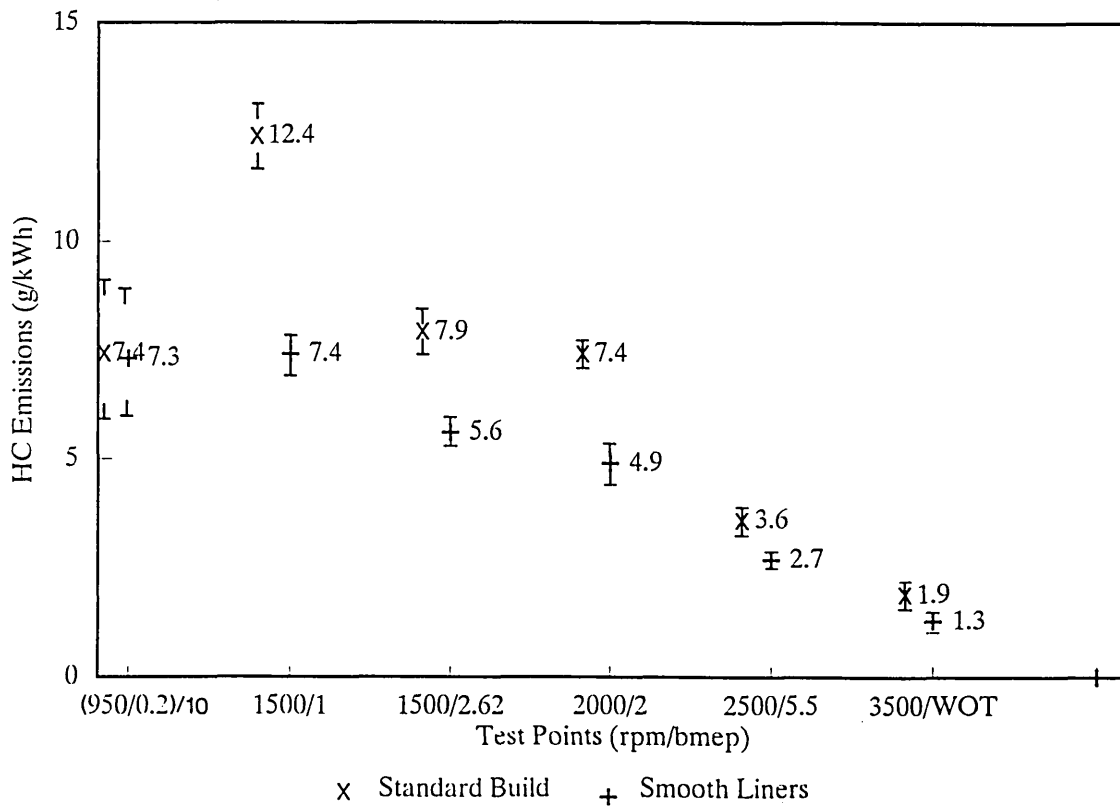


Figure 9 Hydrocarbon emissions, comparison between Standard build and smooth liners

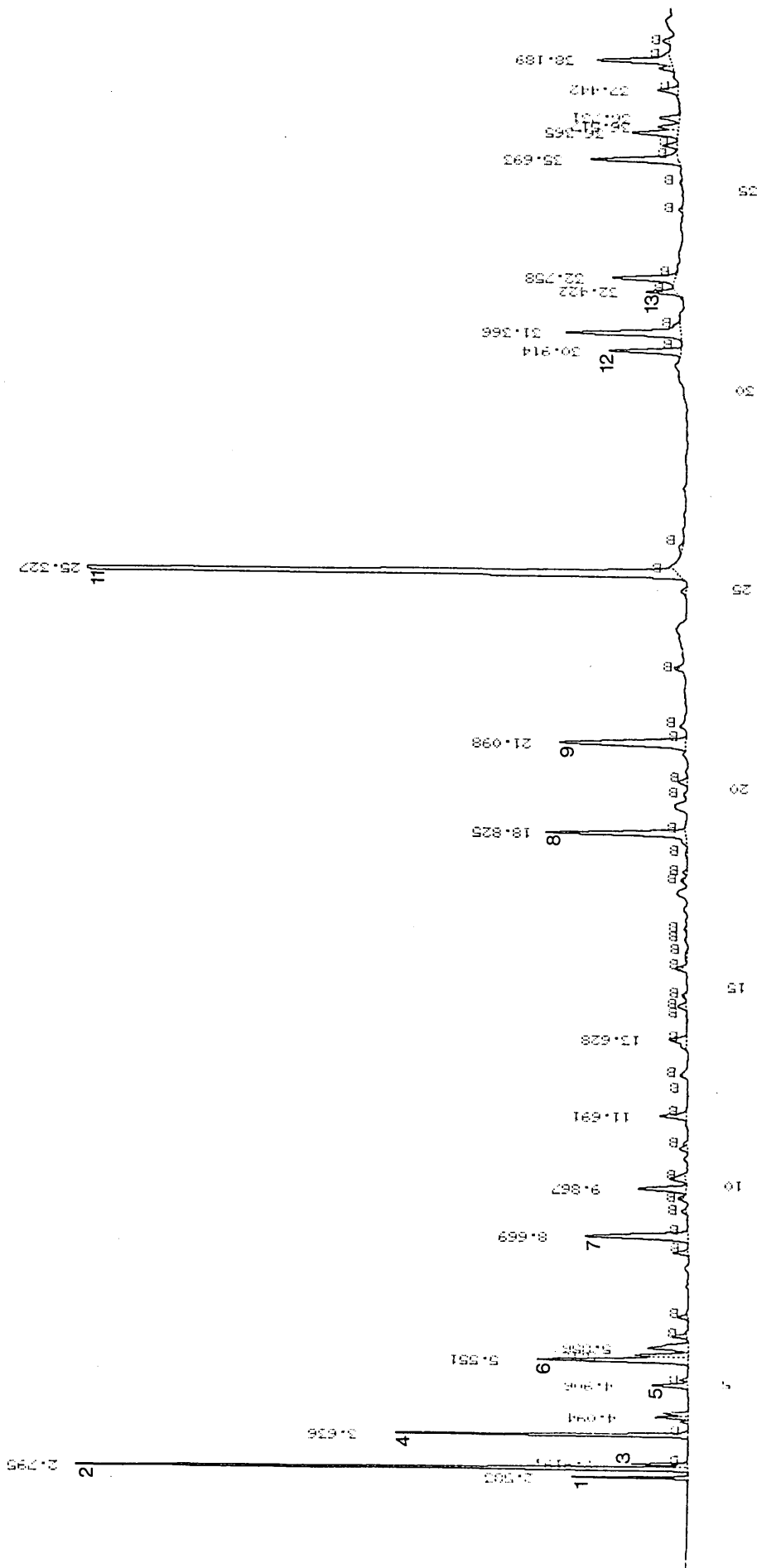


Figure 10 Gas chromatograph plot from smooth liner tests sample taken at 2000 rpm 2 bar bmeq

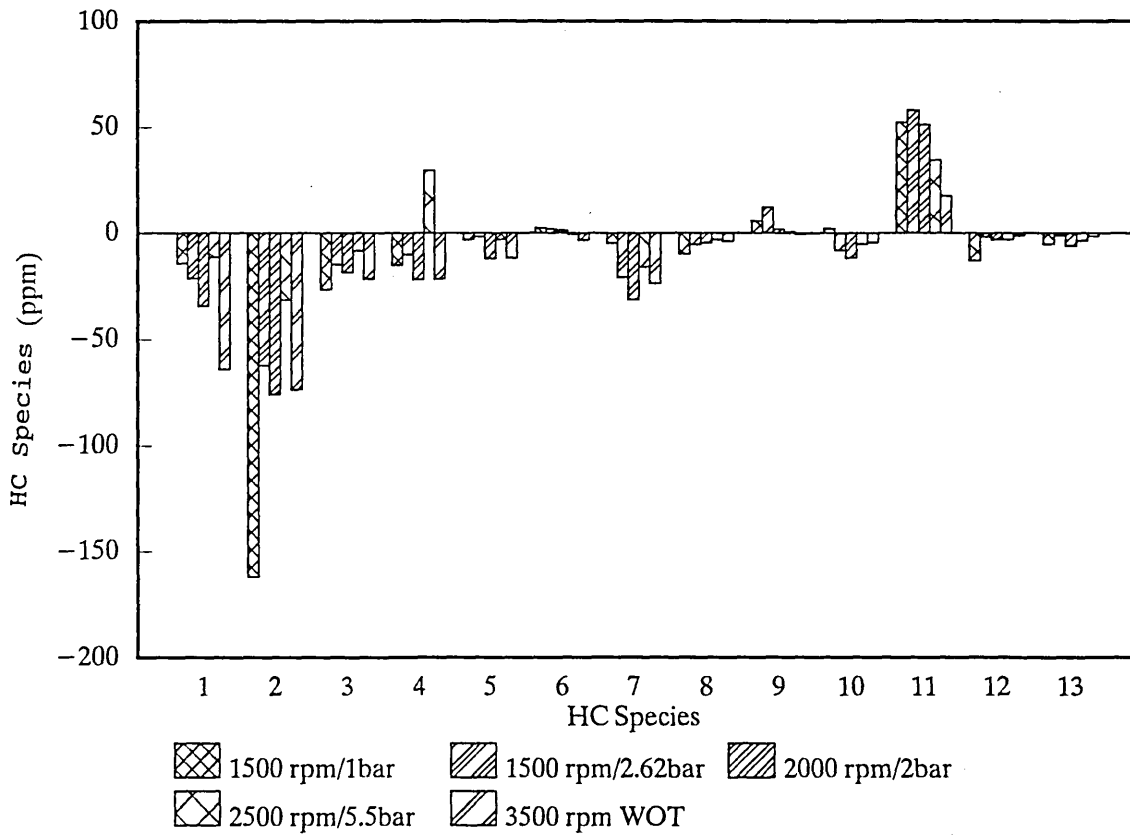


Figure 11 Comparison of HC species, difference between standard and smooth liner

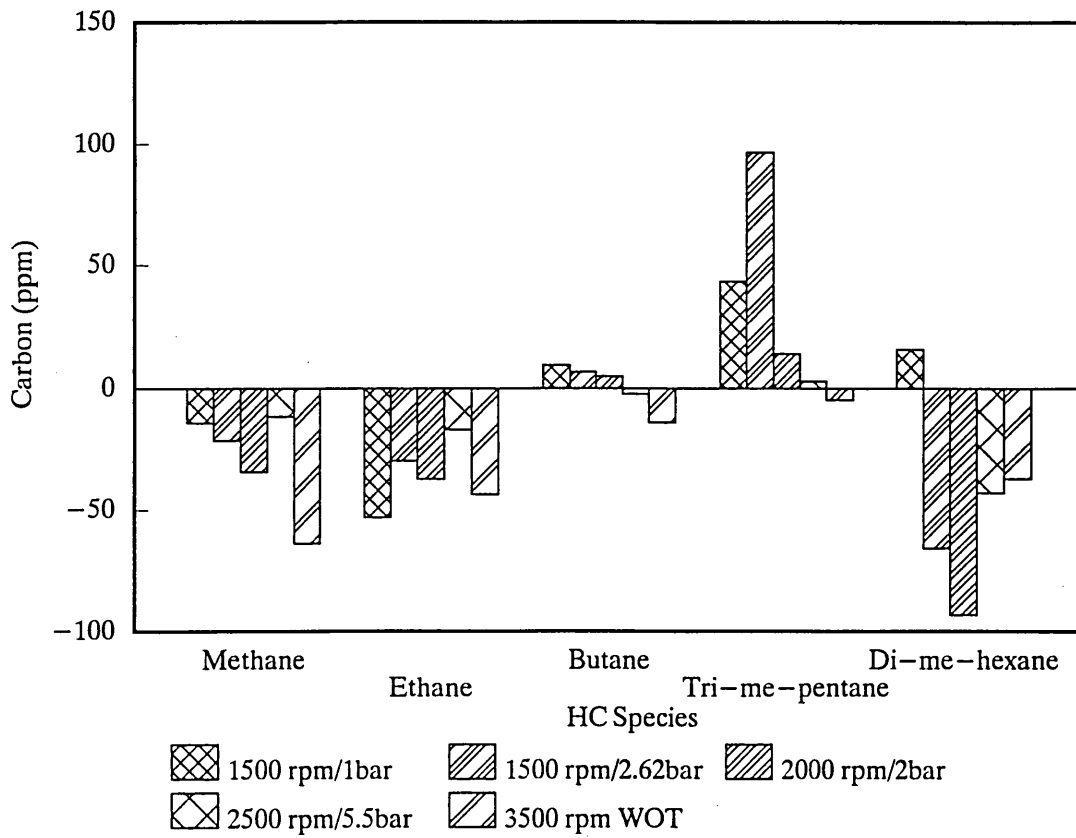


Figure 12 Comparison of Alkanes, difference between standard and smooth liner

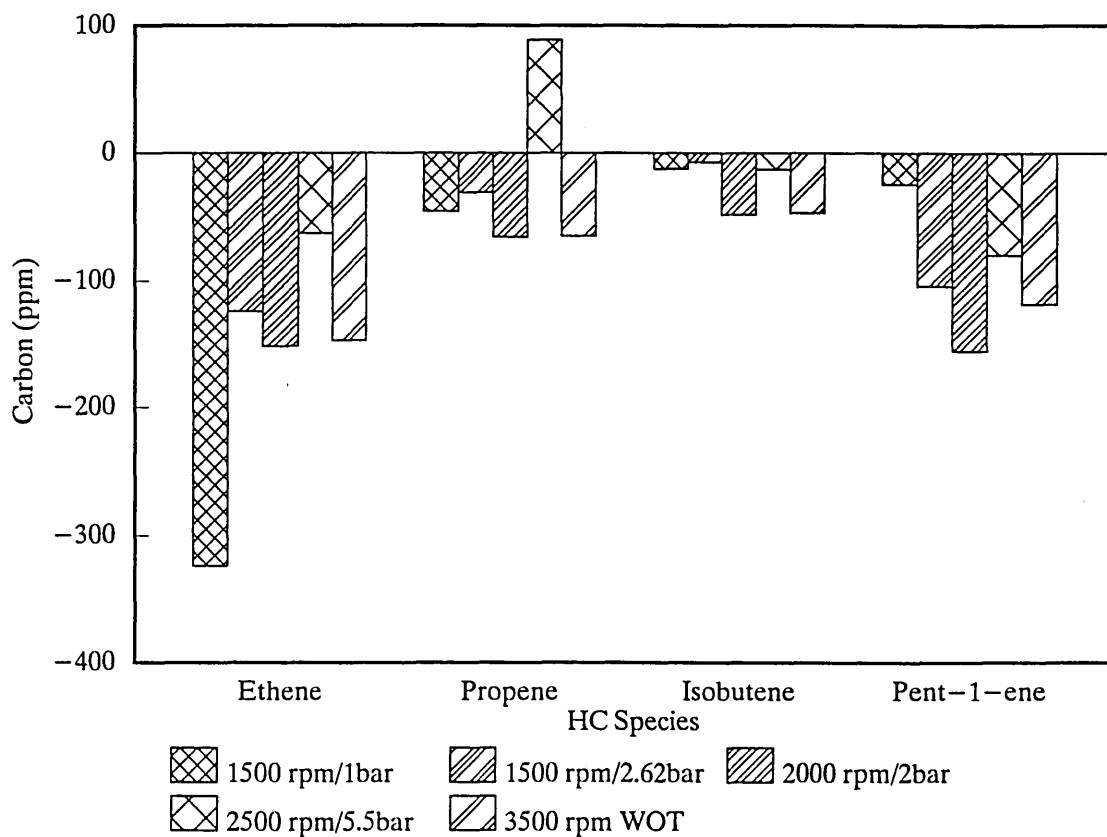


Figure 13 Comparison of Alkenes, difference between standard and smooth liner

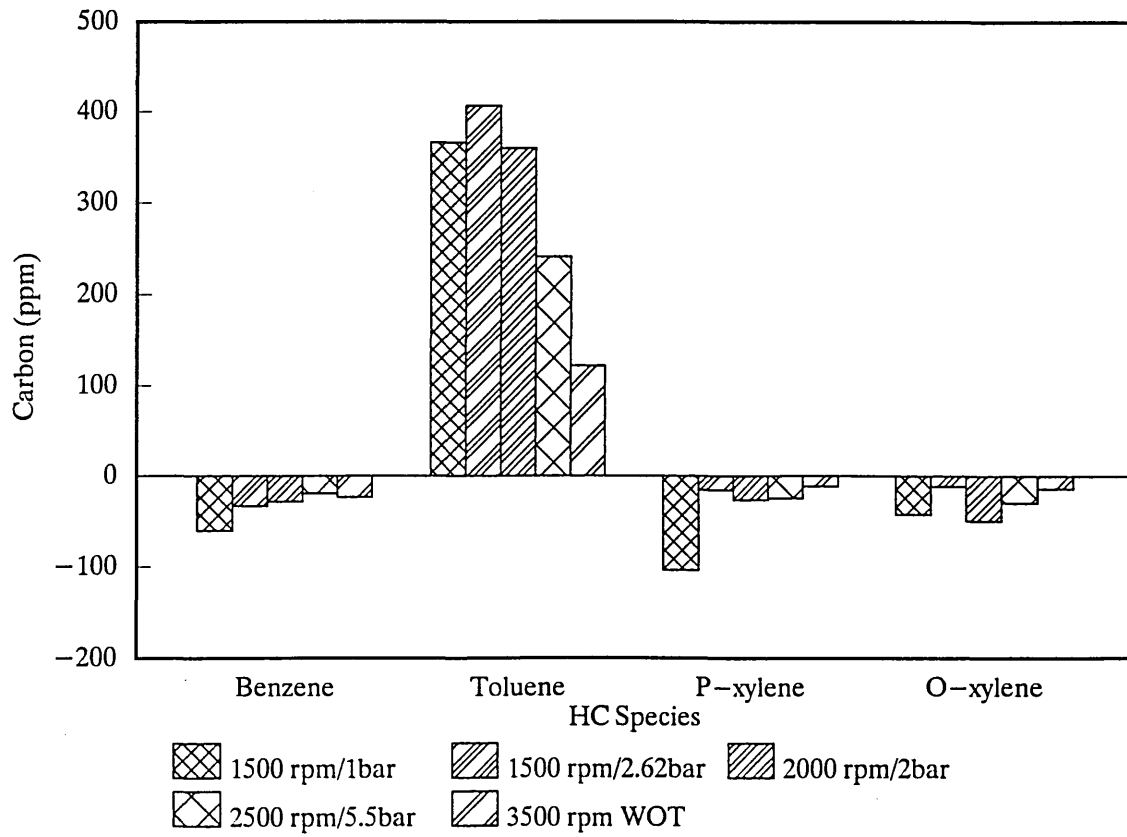
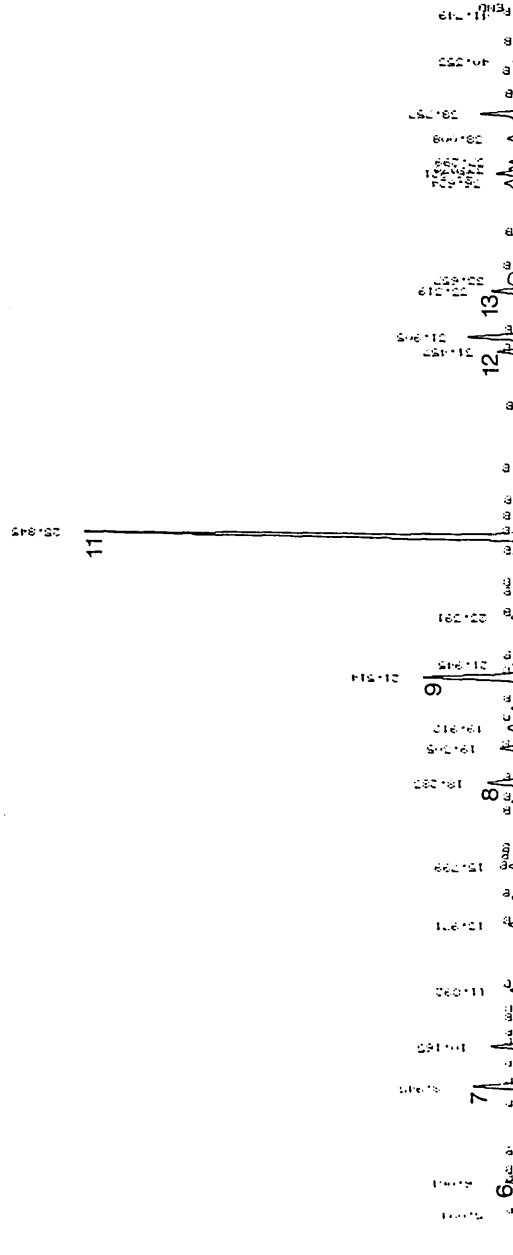
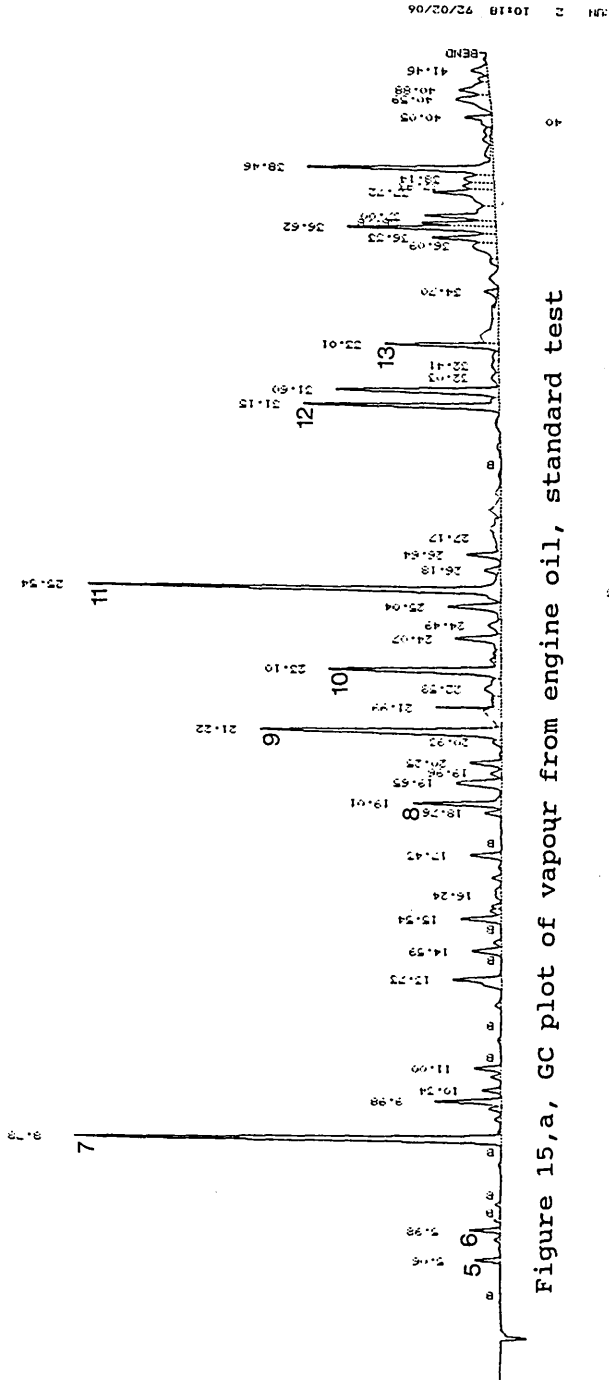


Figure 14 Comparison of Aromatics, difference between standard and smooth liner



Towards quality of testing

**An Evaluation of Cylinder Liner Finish and Synthetic Oil
on Exhaust Hydrocarbon Species from an SI Engine**

by

M Willcock, D H Tidmarsh and P Foss (Sheffield Hallam University)

Fourth
International
Symposium
on the
performance
evaluation
of automotive
fuels and
lubricants

5 - 7 May, 1993

International
Convention
Centre
Birmingham
United Kingdom

An Evaluation of Cylinder Liner Finish and Synthetic Oil on Exhaust Hydrocarbon Species from an SI Engine

ABSTRACT

With the continuing emphasis on reducing emissions from automotive engine this paper investigates the effect of cylinder lubrication on hydrocarbon emissions. It is shown that the use of current formulas of synthetic oil has little effect on total emissions. However, more positive results were obtained using cylinder surface finish to control oil layers in the combustion chamber. Studies of the hydrocarbon species in the emissions showed significant differences due to surface finish profiles.

RÉSUMÉ

Parallèlement à la pression constante exercée pour réduire les émissions à l'échappement des moteurs, cet exposé examine l'influence de la lubrification des cylindres sur les émissions d'hydrocarbures. Il est démontré que l'utilisation des formules courantes d'huiles synthétiques n'a que peu d'effet sur les émissions totales. Toutefois des résultats plus positifs ont été obtenus en prenant pour paramètre l'état de surface des chemises pour contrôler la couche d'huile dans la chambre de combustion. L'étude des espèces émises dans les hydrocarbures imbrûlés a mis en évidence des différences significatives liées au profil de rugosité des surfaces des chemises.

INTRODUCTION

Increasing legislation for the reduction of vehicle emissions requires all aspects of emissions control to be continually reassessed. The specification of components and materials within the engine can be useful in controlling emissions.

The absorption of fuel by the lubrication oil on the cylinder walls during compression and combustion, and its subsequent desorption, has been recognised as a major source of hydrocarbon emissions. There are many variables which impact on the amount of fuel that the oil will absorb, such as engine speed, engine temperature, oil film thickness and viscosity. Adamczyk et al (1) and (2) tried various oils with a mixture fuels in a closed combustion chamber. It was found that

unburnt fuel was the principal effluent after combustion and that fuel/oil combinations had a significant effect on HC emissions.

An investigation by Schramm and Sorenson (3) observed that different oils varied the emissions due to differences in the fuels solubility into different oils. Dent and Lakshminarayanan (4) showed that lubricating oil film thickness also has a considerable effect on hydrocarbon emissions. The model developed by Korematsu (5) showed that the mass of fuel emitted from the oil was directly proportional to the oil layer thickness.

This paper investigates the effect of oil film thickness on hydrocarbon emissions for a reference oil and a fully synthetic lubricant and the distribution of a selection of hydrocarbon species. Gas chromatography is used to

identify hydrocarbon species and also to observe whether emissions are unburnt fuel or combustion products. Current gas chromatography techniques have identified more than 30 species. However, to illustrate the effects of oil and surface finish effects a selection of the most significant species were chosen.

EQUIPMENT

The engine used throughout this research was a 1.4 litre 16 valve unit with wet liners and multi point fuel injection. The engine control unit could be adjusted to maintain accurate control of operating conditions, given in Table 1. The engine was coupled to a Schenk eddy-current dynamometer. During tests CO, CO₂, O₂, HC and NO_x were measured. Hydrocarbon emissions were measured by NDIR in propane units. Regular calibration ensured the accuracy of the analysing equipment, including feeding calibration gases into the sample line at the engine. The sample line includes sampling points at the exhaust port of each cylinder and in the exhaust pipe immediately below the manifold, the sample being passed through a heated line to the analysers. Thermocouples were used to monitor exhaust gas temperatures at the sampling points and to measure the coolant and oil temperatures. Air and fuel flows to the engine were measured. A record of the engine operating conditions was kept enabling consistent conditions at the test points to be achieved to an accuracy of 5%. The results discussed here are the statistical mean of several tests. Throughout this research the tests were repeated taking samples from each test point on different days. These were found to be consistent and repeatable.

The standard lubricating oil used is a CEC reference oil (RL 139/4) of viscosity 10W/30. The fuel is a reference unleaded petrol CEC RF-08-A-85, with knocking characteristic Octane numbers of RON 97.1, MON 87.4.

GAS CHROMATOGRAPHY, COMPARISON OF HYDROCARBON SPECIES FROM FUEL AND ENGINE EMISSIONS

The sample was carried to the gas chromatograph through a heated sample line without being diluted or filtered. A Perkin Elmer 8600 gas chromatograph was used with a wall coated open tubular column, the stationary phase being CP-Sil-5 CB, the column length 50m and the inside diameter 0.32 mm. This equipment gave good resolution of a wide range of hydrocarbons from C1 to C9. The method used is described in Table 2.

From emission samples taken from the standard engine build and with the gas chromatograph method described above a selection of 13 species were chosen and identified with calibration gases. These species were a selection of products and fuel components representative of the main types of species alkanes, alkenes and aromatics. They accounted for approximately 75% of the area of the gas chromatograph trace. These are named and listed in Table 3. It can be observed from Figure 1, gas chromatograph plots from unleaded gasoline and emissions, that there is a significant reduction in the number of peaks detected in the emissions compared to the fuel. Unburned fuel species do not survive the combustion process in equal proportions. Some C1 to C3 hydrocarbons are not present in gasoline but, are products of incomplete combustion. Many components of fuel are not detected in the emissions. Dempster and Shore (6), identified a greater part of the hydrocarbon emissions as combustion products.

The flame ionisation detector connected to the gas chromatograph gives an output proportional to the carbon atoms present. Using calibration gas mixtures of known concentration allows the parts per million (ppm) concentration of carbon to be calculated. The amount of a particular compound is found by dividing the carbon atoms detected by the number of atoms in that

compound.

CYLINDER LINER SURFACE FINISH

For the next test the cylinder liners were honed to a smoother surface finish though still keeping the same cross hatch pattern. The reasoning for this is set out below. A new set of standard pistons were used.

The effects of surface roughness on the lubrication of piston rings and liner were studied by Sandia and Someya (7), who showed that the oil layer is thicker with a rough surface. However, because this was a study on lubrication, the oil layers studied were between the ring and liner, but the absorption/desorption effect is due to the oil retained on the liner wall after the passage of the rings. On a rougher surface with a thicker oil film between ring and cylinder more oil will be stored in the surface microstructure and should produce higher hydrocarbon emissions than a smoother surface. The bearing area curve can be used to give an indication of the oil storage area available in the surface finish. Figure 2 compares the surface traces and bearing area curves for standard piston liners and the smoother liners produced for this test.

To quantify the oil layer thickness for different liner surface finishes, the average depth of free space above the bearing area curves within the roughness profile of the material was calculated. This was performed using a set of T_p values going down the surface profile, determining its approximate area by Simpson's Rule. The following assumptions were made.

- a) Oil completely fills the surface profile.
- b) The surface of the oil is flat and parallel with the centre line of the profile.
- c) The surface of the oil was taken as the depth of the 2% T_p value.
- d) The maximum depth of the oil is taken as the depth of the 98% T_p value.

The result of these calculations vary slightly for each liner. Table 4 sets out the surface parameters for each set of liners and the calculated oil layer thickness.

RESULTS AND DISCUSSION

The total hydrocarbon emissions from smooth liner tests when compared against the standard show significant reduction in hydrocarbon emissions, see Figure 3. These reductions are greater at lower speeds and loads, consistent with reducing the contribution of the absorption and desorption effect to total hydrocarbon emissions. It was observed by Dent and Lakshminarayanan (4) that the absorption of fuel decreased as speed and load increased, due to increases in oil temperature and the shorter cycle time.

Hydrocarbon emissions from different lubricants from standard and smooth liner tests are shown Figure 4. Substantial changes to the profile of hydrocarbon species have occurred between the smooth liner tests and standard. Figure 5 is a gas chromatograph plot of a sample taken at 2000 rpm 2 bar bmep from the smooth liner tests. To compare standard and smooth liner tests the ppm value for a particular species from the standard build is subtracted from the value obtained from the smooth liner test. Positive values indicate an increase from the standard, Figure 6 compares the 13 selected species for each test point. The difference is characterised by a large increase in toluene and large decreases in combustion products.

The alkanes are plotted in Figure 7 as parts per million of carbon. Between the standard and smooth liner tests, the products methane and ethane have decreased considerably. Of the fuel species 2,2,4, trimethyl pentane has increased its concentration from the standard and 2,4, dimethyl hexane is not detected. Butane shows no significant change. Observable are trends in certain species; methane and 2,2,4, trimethyl pentane reduce as speed and load increase. Between the different lubricants there is a slight reduction for each species from synthetic oil, both from

the standard build and smooth liners.

The alkenes reduce for both products and fuel species, as shown in Figure 8. This again indicates similar trends to the alkanes of reductions between the reference and synthetic oils and also the reduced levels between standard and smooth liners. In particular ethene has been reduced significantly. This is an important product as it is formed by the breaking of several different fuel components. Its reduction would indicate a higher level of complete oxidation of fuel from the smooth liner tests. Pent-1-ene also shows significant reductions.

The levels of the aromatics are plotted in Figure 9. This shows the contrast between the large increase in toluene and the small reductions of benzene and the xylenes. Synthetic oil has reduced most of the aromatics except from o-xylene which has increased.

The reduction of most species observed from standard to smooth liners is in part due to the overall reduction in HC emission levels but some of the reduction in the products could be due to the increase in toluene. The only significant change to account for the overall decrease in emissions and increase in toluene are the changes to the surface finish. The difference in the calculated oil layer is small, 0.042 micron, for the worn liners. Absorption and desorption processes are very sensitive to changes in oil thickness. Dent and Lakshminarayanan (4) indicated a rapid decrease in emissions with reducing oil layer thickness. The following is a possible mechanism for the increase in toluene emitted from the smooth liner tests.

The various components of the fuel are not absorbed into the oil evenly, some species being more readily absorbed. The controlling factor is cylinder pressure, the more soluble species being absorbed at lower pressures. If the oil layer is reduced then the oil may become saturated and unable to absorb other species. Species not absorbed would be burnt or oxidised while the species emerging from the oil later in the cycle would escape

oxidation. The concentration of aromatics in hydrocarbon emissions in the standard tests are higher than in the fuel, possibly due to their absorption in oil. The reduced oil layer in smooth liner tests must then be selecting Toluene which is more soluble than other aromatics due its molecular weight and structure.

To observe if the oil absorbed toluene more easily than other aromatics, samples of oil were taken from the engine during operation. These were heated to a temperature of 80 deg C. Vapour was withdrawn from above the oil then injected into the gas chromatograph. The results were compared against vapour from fresh lubricant. Fresh oil showed no significant levels of hydrocarbon, but as the tests progressed the G.C. trace shows an increased presence of hydrocarbon species, especially toluene. Figure 10 compares gas chromatograph plots of oil vapour from standard and smooth liner tests. Both samples were taken from the engine operating at 3500 rpm wide open throttle. From these plots it can be seen that toluene is a major component of fuel vapour absorbed by the oil. Toluene comprises 10% of the vapour from standard and 40% from the smooth liner tests. This is approximately the same proportion as the emissions, and suggests that the increase in toluene is due to its being preferentially absorbed by the lubricating oil.

The results from tests on smooth cylinder liners also indicated reduced total hydrocarbon emissions. Gas chromatography identified a large increase in one particular compound, toluene. Further investigation showed this to be due its preferential absorption in lubricating oil relative to other fuel species.

CONCLUSIONS

The results from these tests indicate that the hydrocarbon emissions are affected more by the amount of oil present than the use of this particular synthetic oil.

The reductions achieved from the smooth liner tests were in the lower speed and load range of

the engine, which is of importance for reducing hydrocarbon emissions within urban areas. However, at the end of the test the bore showed significant signs of wear and a compromise between hydrocarbon emissions and durability must be made.

The changes in specification observed indicate that, with further research the specification of surface finish can be chosen to reduce emissions and alter the balance between each hydrocarbon species.

ACKNOWLEDGEMENTS

The authors wish to thank Dr D Leathard, School of Science, Sheffield Hallam University, for his advice and assistance. Also SERC and AE Piston Products Ltd for funding and supply of equipment for this research.

REFERENCES

1. Adamczyk, A.A: Rothschild, W.G. Kaiser, E.W: The effect of fuel and oil structure on hydrocarbon emissions from oil layers during closed vessel combustion. Combustion Science and Technology. 1985. Vol 44. pp 113-124.
2. Adamczyk, A.A. and Kack, R.A: The effect of oil layers on hydrocarbon emissions: Low solubility oils. Combustion Science and Technology. 1984. Vol. 36. pp 227-234.
3. Schramm, J and Sorenson, S.C: Effects of lubricating oil on hydrocarbon emissions in an S.I. engine. 1989. SAE 89062.
4. Dent, J.C. and Lakshminarayanan, P.A: A model for absorption and desorption of fuel vapour by cylinder lubricating oil film and its contribution to HC emissions. SAE. 1983. No 830652.
5. Korematsu, K: Effects of fuel absorbed in oil film on unburnt hydrocarbon emissions from spark ignition engines. Japanese Society of Mechanical Engineers. 1990. Vol. 33. No 30. pp 606-614.
6. Dempster, N.M. Shore, P.R: An investigation into the production of hydrocarbon emissions from a gasoline engine tested on chemically defined fuels. 1990. SAE paper 900354.
7. Sandia, S. and Someya, T: The effect of surface roughness on lubrication between a piston ring and a cylinder liner. IMechE Conference on Tribology Friction, lubrication and Wear, 1987, paper C223/87, pp. 135-143.

Tables

- | | |
|---------|--|
| Table 1 | Test Points |
| Table 2 | Gas Chromatograph Method |
| Table 3 | Major Hydrocarbon Species from Emissions |
| Table 4 | Cylinder Line Surface Finish Parameters |

Figures

- | | |
|--------|--|
| Fig 1a | Gas Chromatography Plot of Reference Fuel |
| Fig 1b | GC Plot of Emissions at 2500 rpm 5.5 bar bmep Using Standard Pistons |
| Fig 2a | Surface Finish Data from Standard Cylinder Liners |
| Fig 2b | Surface Finish Data from Smooth Cylinder Liners |
| Fig 3 | Hydrocarbon Emissions, Comparison Between Standard Build and Smooth Liners |

Fig 4a Comparison of HC Emissions with Different Lubricants

Fig 4b A Comparison of Hydrocarbon Emissions for Different Lubricating Oils from Smooth Liner Tests

Fig 5 Gas Chromatograph Plot From Smooth Liner Tests Sample Taken at 2000 rpm 2 bar bmep

Fig 6 Comparison of HC Species, Difference Between Standard and Smooth Liner

Fig 7 Hydrocarbon Species (Alkanes), Comparison of Reference Oil and Synthetic Oil at 2000 rpm 2 bar bmep

Fig 8 Hydrocarbon Species (Alkenes), Comparison of reference oil and synthetic Oil at 2000 rpm 2 bar bmep

Fig 9 Hydrocarbon Species Comparison of Reference Oil and Synthetic Oil at 2000 rpm 2 bar bmep

Fig 10a GC Plot of Vapour From Engine Oil, Standard Test

Fig 10b GC Plot of Vapour From Engine Oil, Smooth Liner Test

TABLE 1

Test Points

Speed (RPM)	BMEP (bar)
950	0.2
1500	1.0
1500	2.62
2000	2.0
2500	5.5
3500	Wide Open Throttle

Air Fuel ratio at all points 15:1

Ignition timing adjusted to give peak pressure at 12 deg ATDC

TABLE 2**Gas Chromatograph Method****Temperature Programme**

Temperature 1	=	30°C
ISO time	=	2 minutes
Ramp 1	=	4°C/minute
Temperature 2	=	200°C

Injector Temperature	100°C
Detector Temperature	250°C
Carrier Gas	Helium
Flow Rate	1 ml/minute at 20°C
Injector	Automatic sample valve, 0.1 ml sample loop
Detection	Flame Ionisation Detector

TABLE 3**Major Hydrocarbon Species from Emissions**

Peak	Name
1	Methane
2	Ethene (ethylene)
3	Ethane
4	Propene (propylene)
5	Isobutene
6	Butane
7	pent-1-ene
8	Benzene
9	2,2,4, trimethyl pentane
10	2,4, dimethyl hexane
11	Toluene
12	P-Xylene and M-Xylene
13	O-Xylene

TABLE 4**Cylinder Liner Surface Finish Parameters**

Parameter	Standard Liners		Smooth Liners	
	New	Run-in	New	Run-in
Ra (μm)	0.76	0.25	0.39	0.185
Rk (μm)	2.28	0.281	0.99	0.3068
Rpk (μm)	0.748	0.123	0.325	0.136
RvK (μm)	2.17	1.13	1.44	1.0149
Oil depth (μm)	1.997	0.224	0.575	0.202

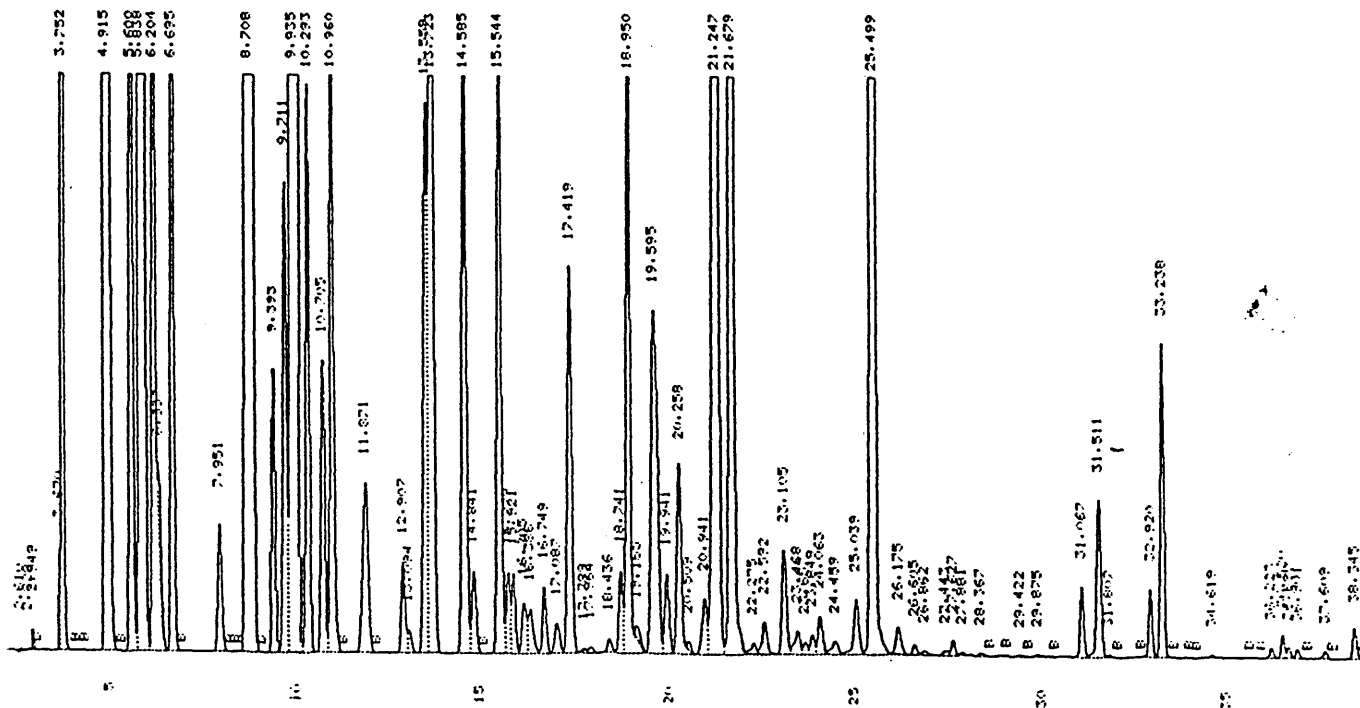


Figure 1, a, Gas chromatography plot of reference fuel

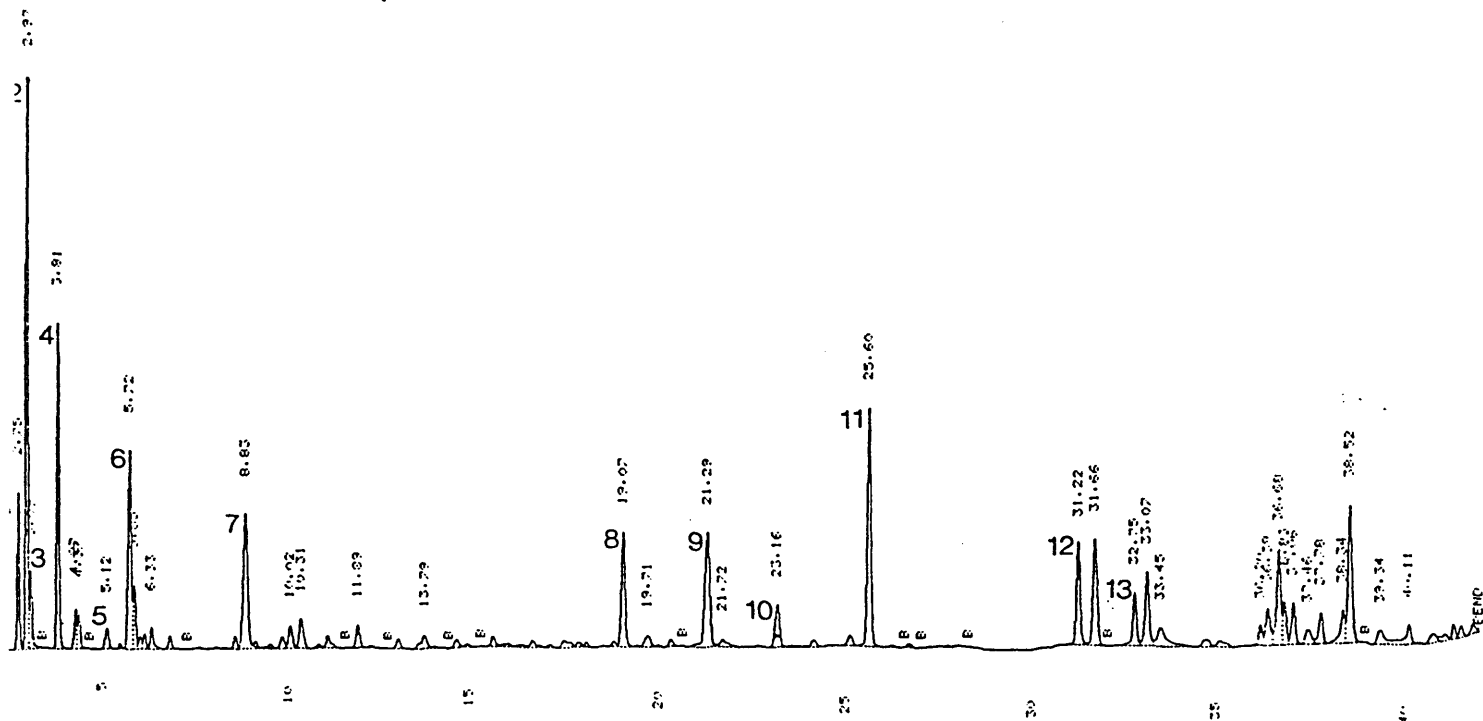


Figure 1, b, GC plot of emissions at 2500 rpm 5.5 bar bmep using standard pistons

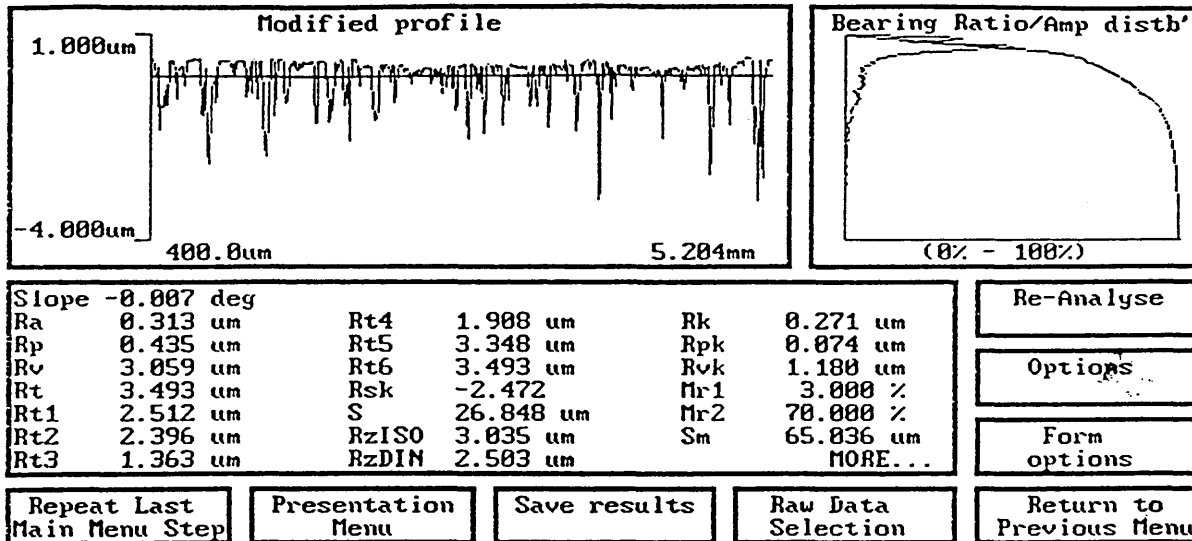


Figure 2, a, Surface finish data from standard cylinder liners

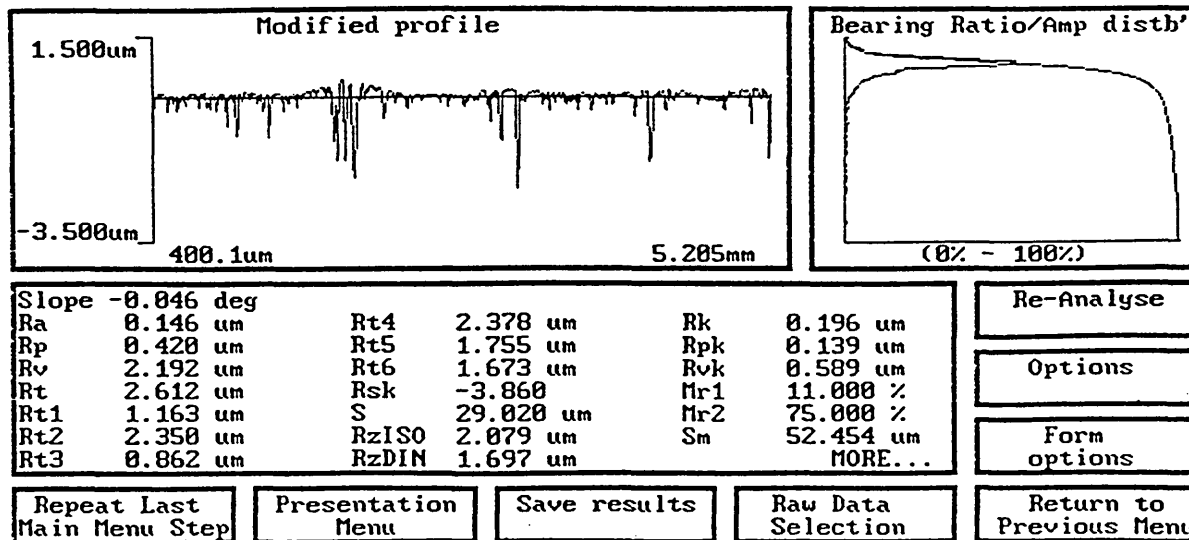
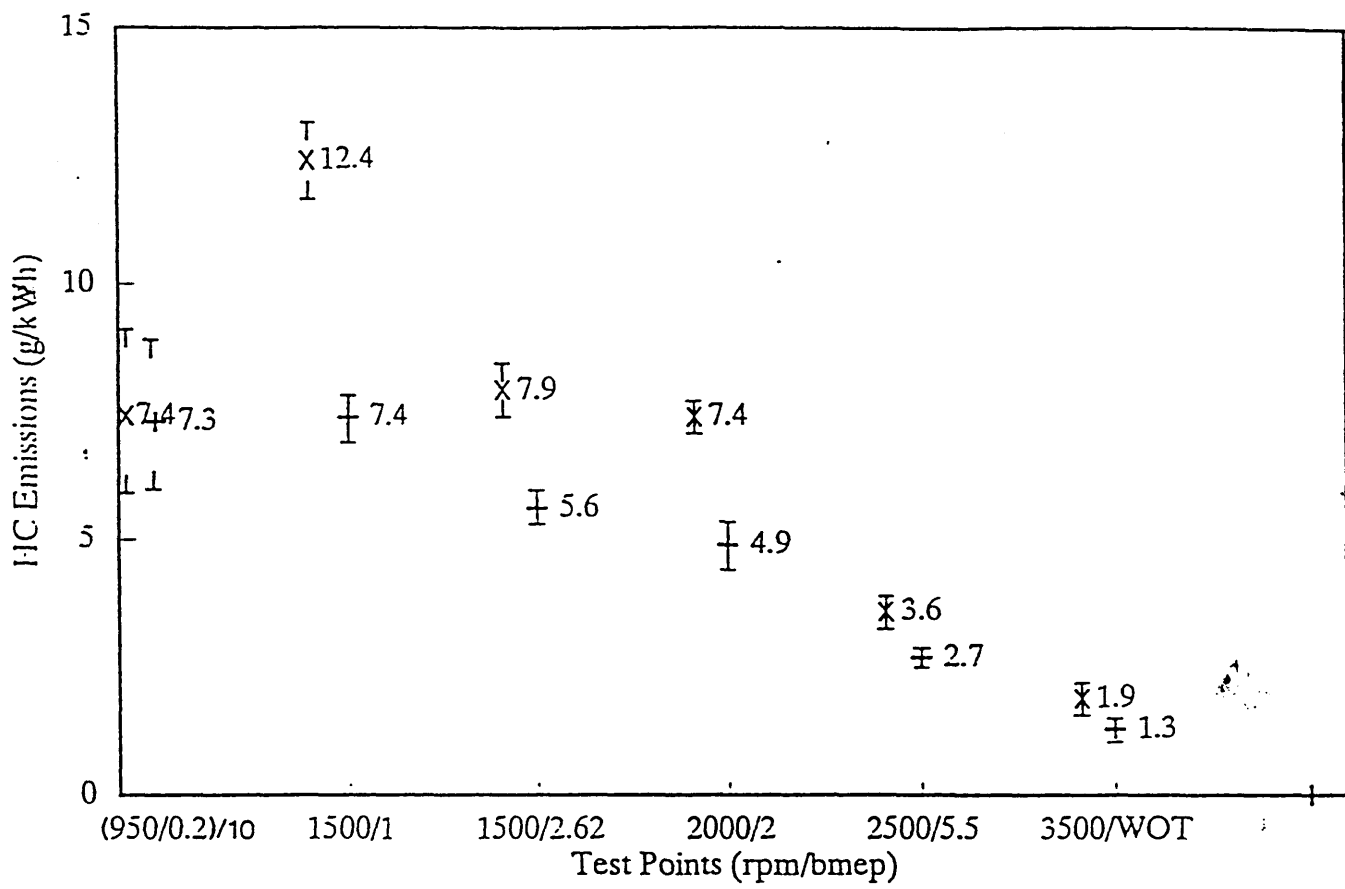


Figure 2, b, Surface finish data from smooth cylinder liners



x Standard Build + Smooth Liners

Figure 3 Hydrocarbon emissions, comparison between Standard build and smooth liners

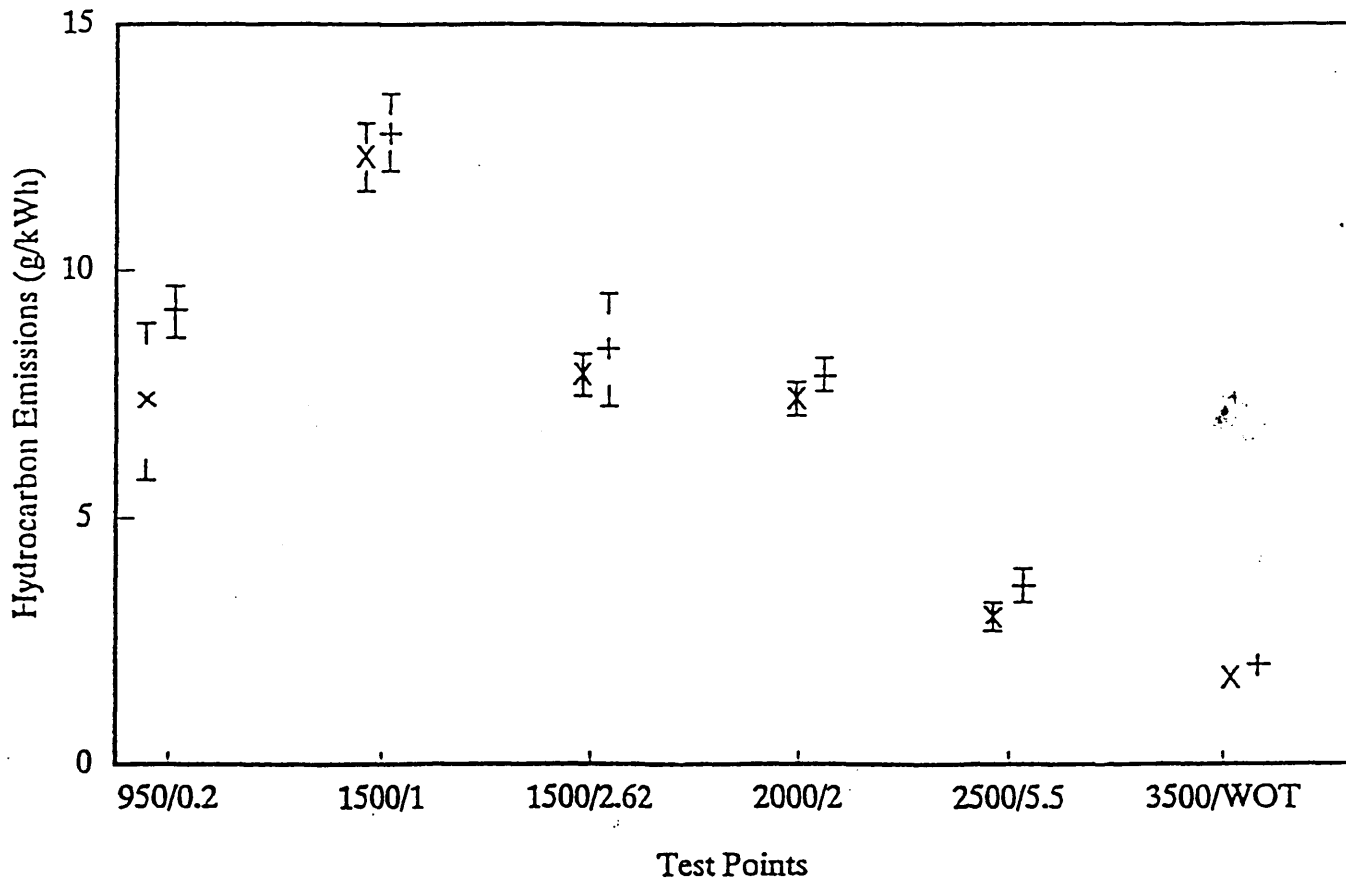
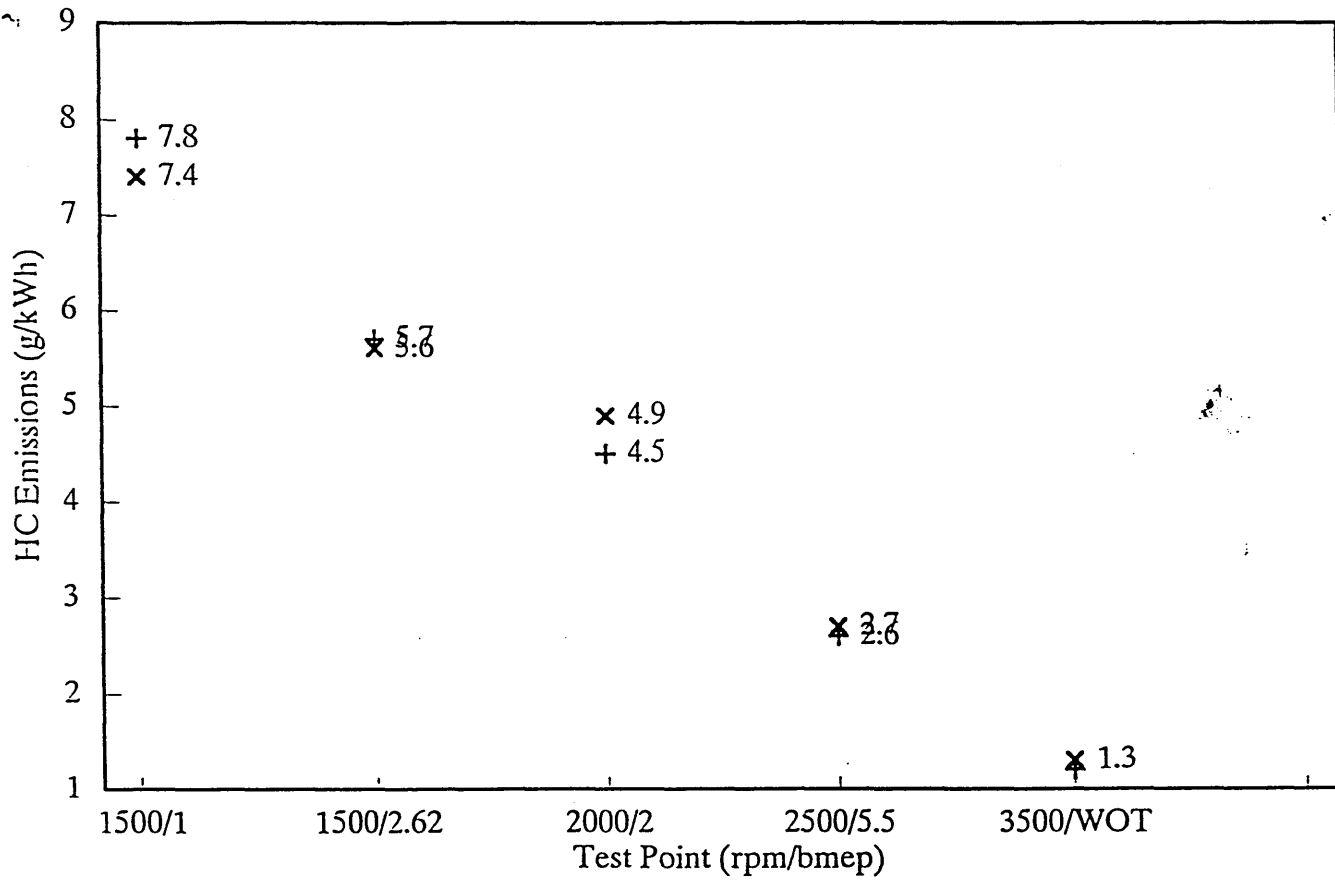


Figure 4 a x Reference Oil + Synthetic Oil
 Comparison of HC Emissions with Different Lubricants



x Reference Oil + Synthetic Oil

Figure 4.b A comparison of hydrocarbon emissions for different lubricating oils from smooth liner tests

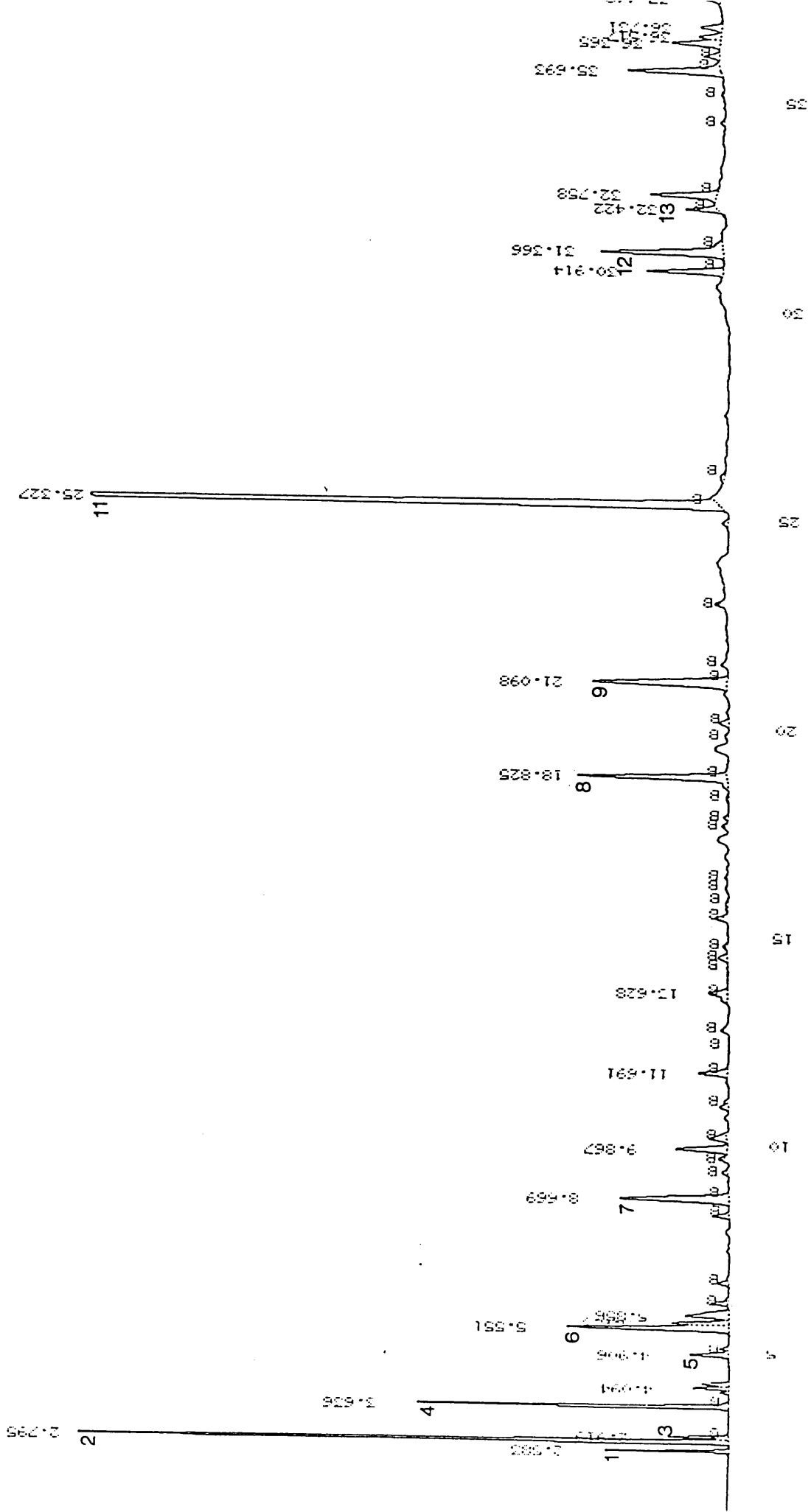


Figure 5 Gas chromatograph plot from smooth liner tests sample taken at 2000 rpm 2 bar bmep

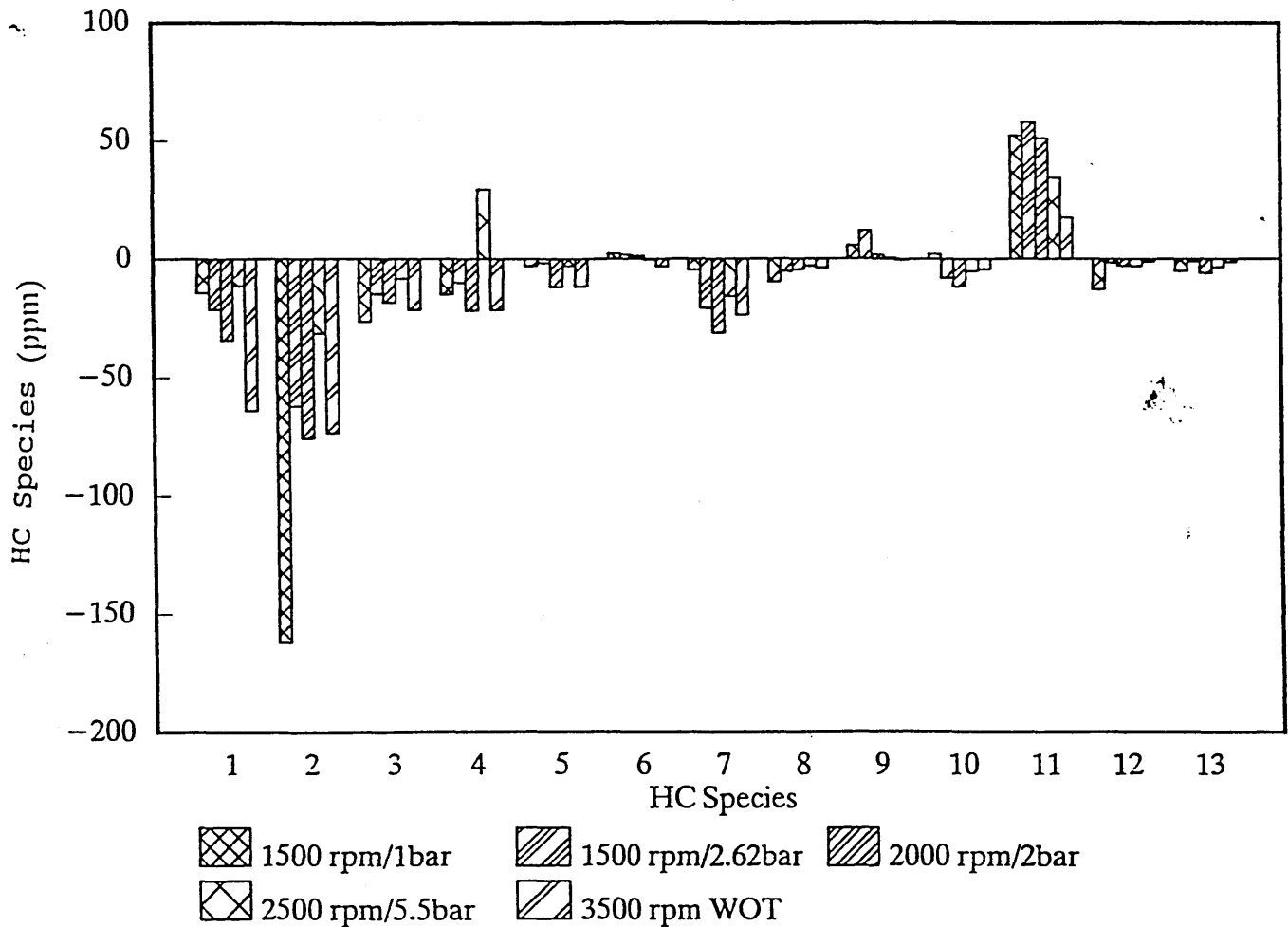


Figure 6 Comparison of HC species, difference between standard and smooth liner

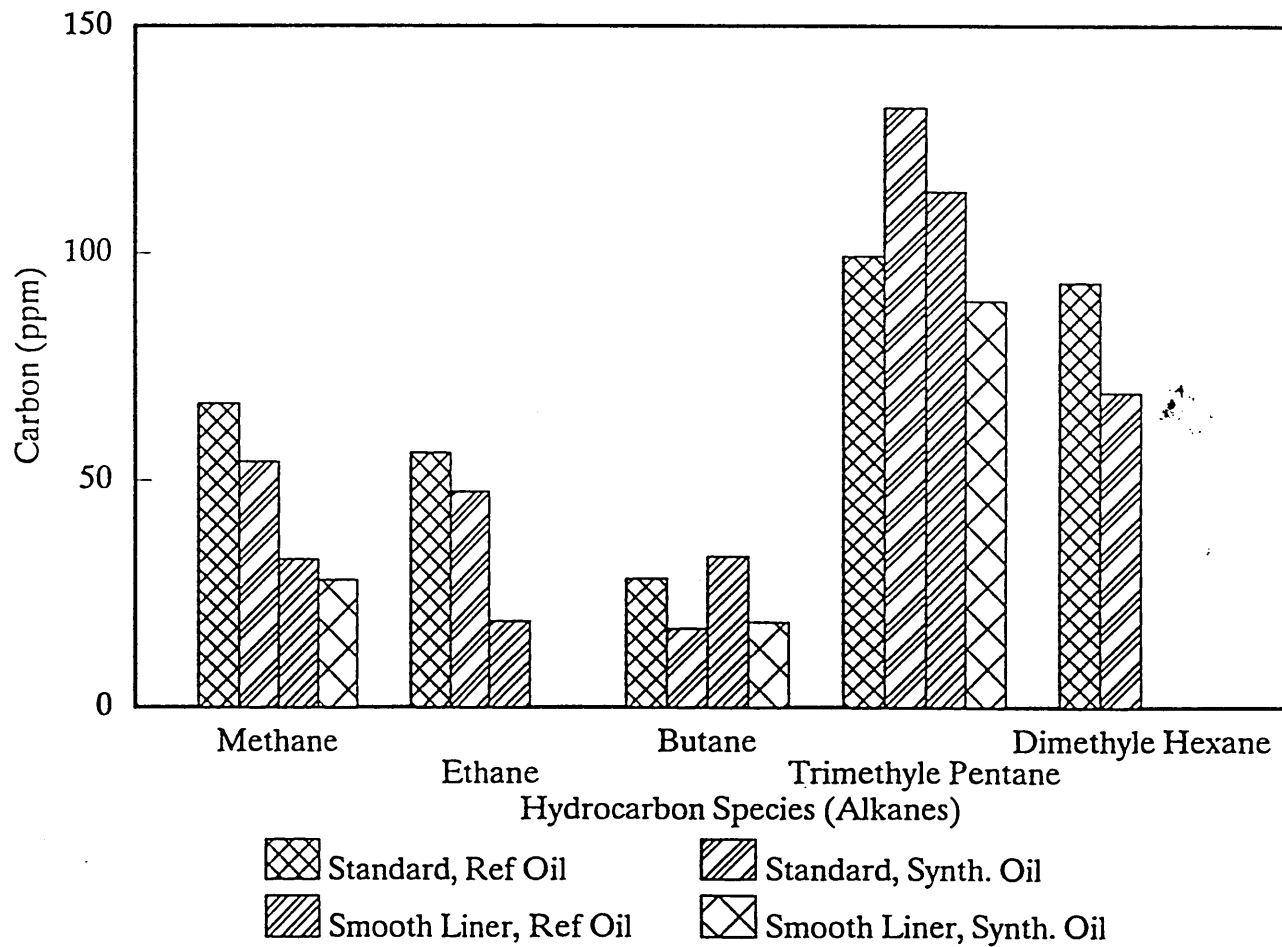


Figure 7 Hydrocarbon species (Alkanes), comparison of reference oil and synthetic oil at 2000 rpm 2 bar bmep

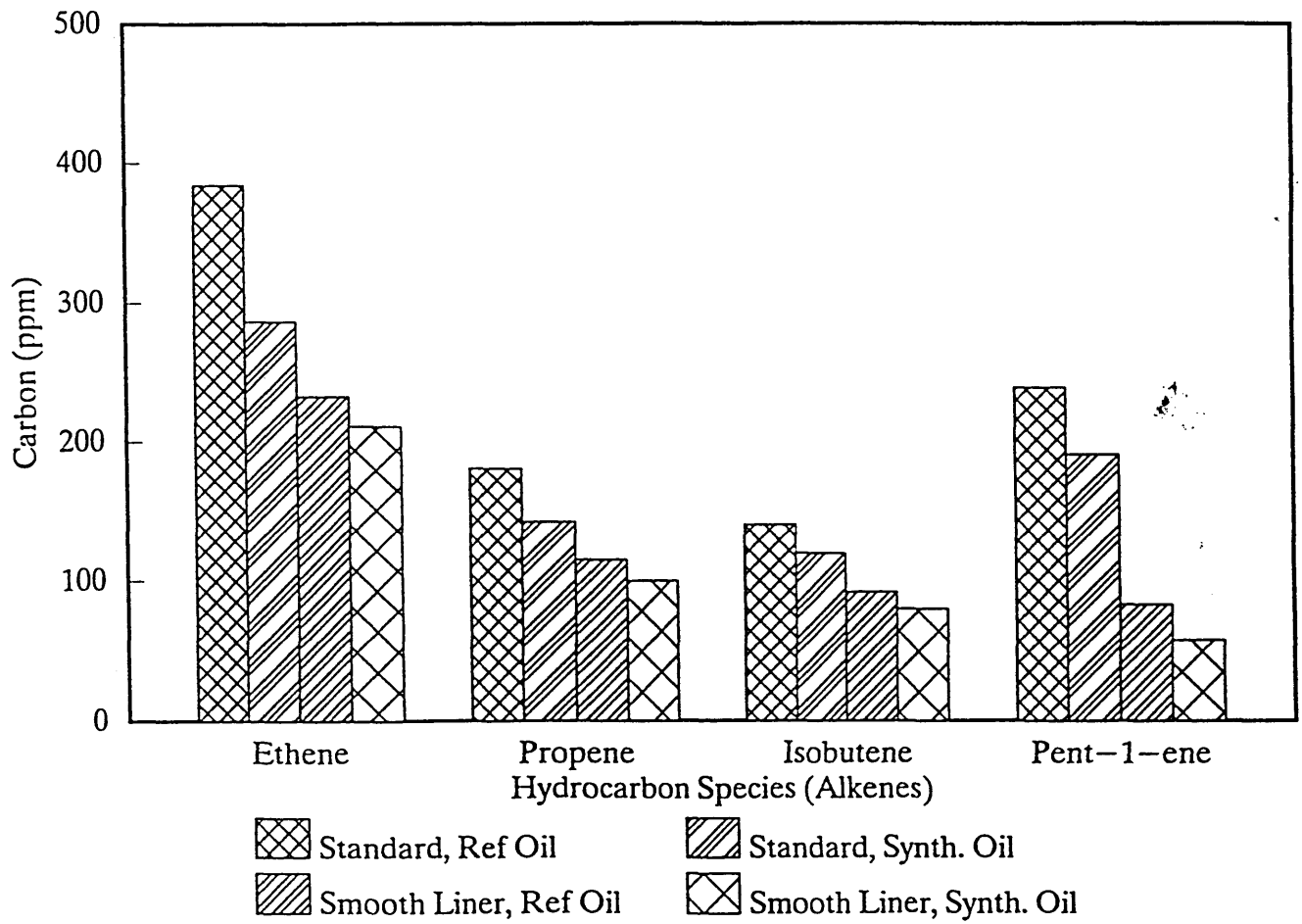


Figure 8 Hydrocarbon species (Alkenes), comparison of reference oil and synthetic oil at 2000 rpm 2 bar bmep

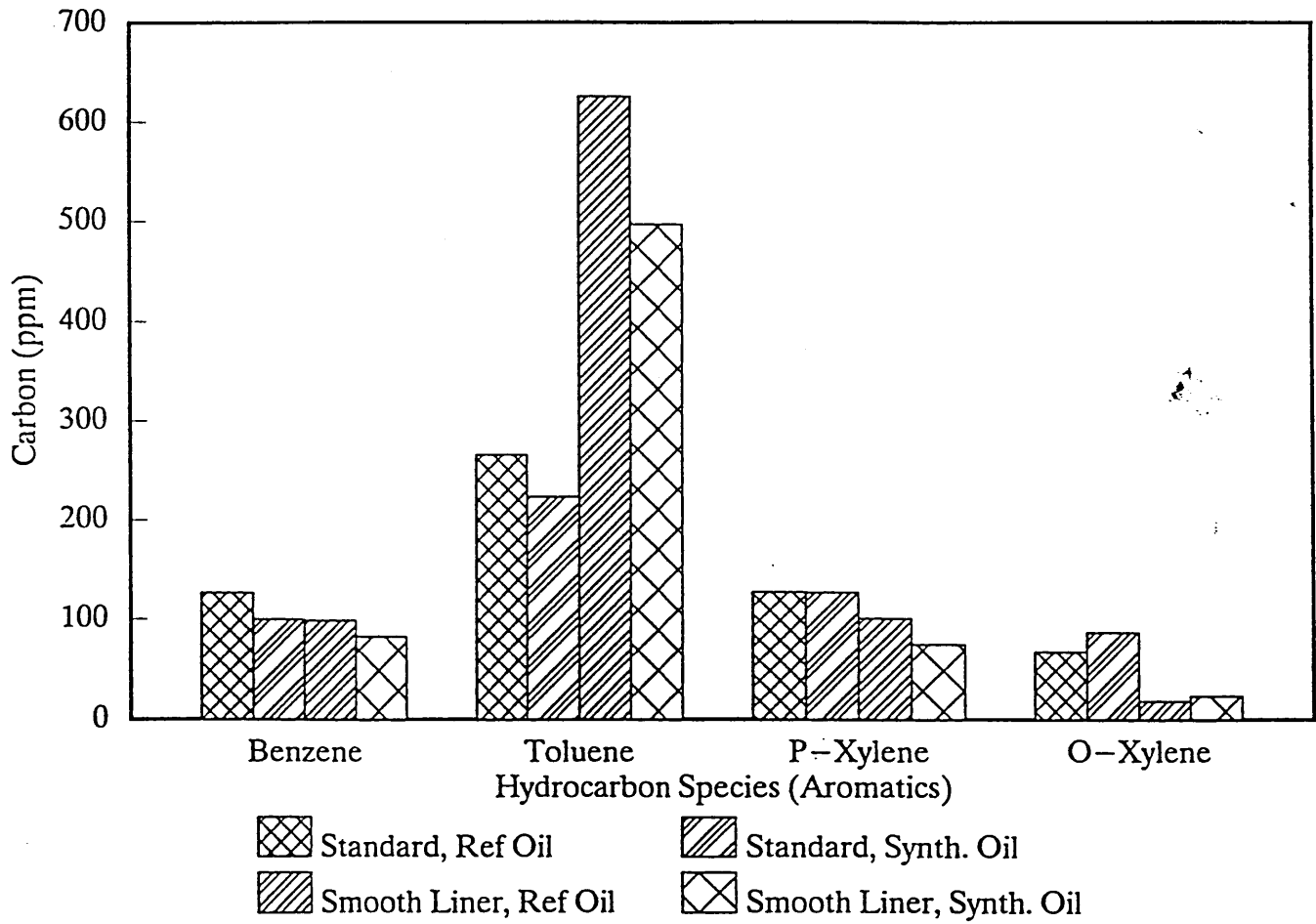


Figure 9 Hydrocarbon species comparison of reference oil and synthetic oil at 2000 rpm 2 bar bmep

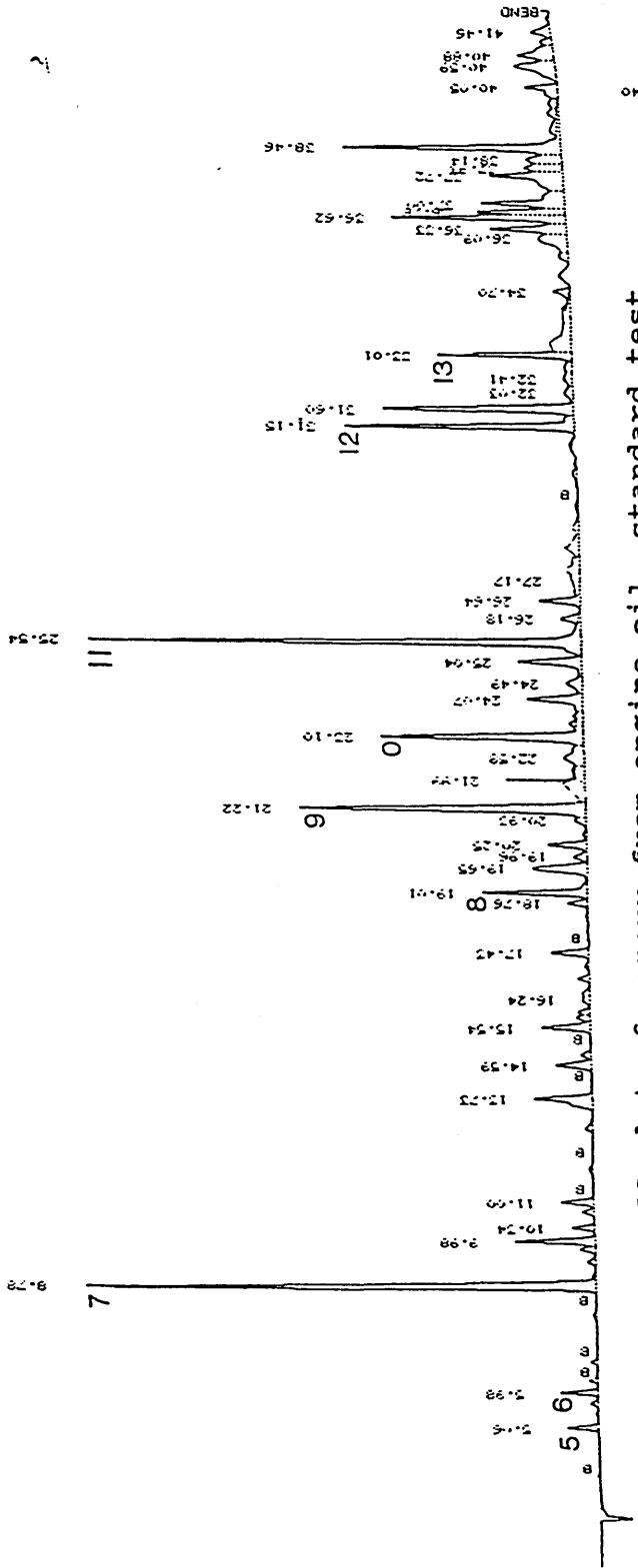


Figure 10, a, GC plot of vapour from engine oil, standard test

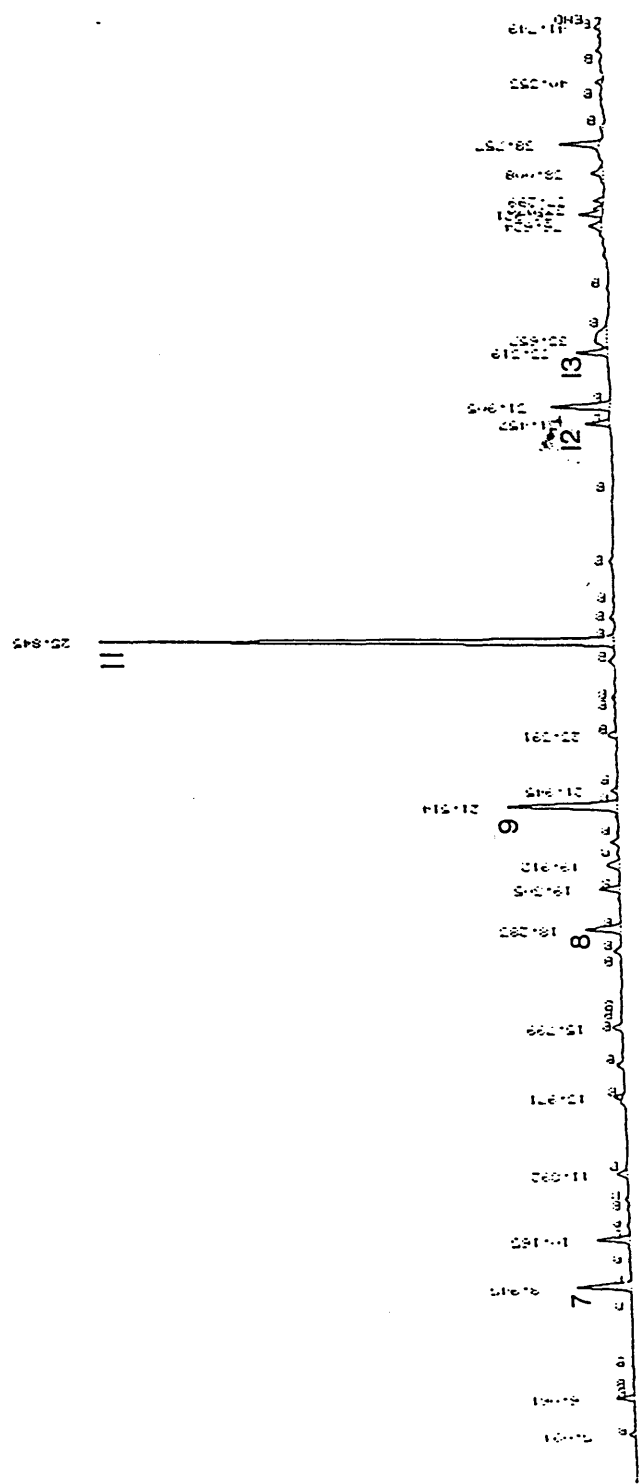


Figure 10, b, GC plot of vapour from engine oil, smooth liner test

An Investigation into the Degradation and Oxidation of Certain Hydrocarbon Species in the Exhaust Manifold of an SI Engine

by M Willcock, BEng and E D Hartley, BA, AE Piston Products Ltd

P Foss, BSc, MSc, PhD, MRAS, Sheffield Hallam University, and

D Tidmarsh, PhD, BSc, CEng, FIMechE, University of Central England

SYNOPSIS The after treatment of engine exhaust gases to reduce emissions has become the major form of controlling vehicle emissions in the 1990's. However, it has also been observed that the exhaust manifold can substantially reduce the level of hydrocarbon emissions. In this study of certain hydrocarbon species in the exhaust emissions it is shown that the manifold can change the overall mix of species. Reducing levels of unburnt fuel and often increasing the products of pyrolysis.

1 INTRODUCTION

The effects of recent legislation for the control of vehicle emissions has meant that catalytic converters are being fitted to all new cars. However this cannot be the final solution to vehicle emissions, and research is continuing to reduce engine out emissions. An aspect of this is the oxidation of hydrocarbon species across the exhaust manifold. After the main combustion event the residual hydrocarbons continue undergoing reactions in the cylinder, exhaust port and exhaust pipe.

There are many variables which control these reactions Sigworth et al (1) observed that the oxidation rate is strongly effected by oxygen concentration and gas temperature, residence time at high temperatures is also important. The reaction rate was observed to increase rapidly as oxygen concentration increased above 1%. The effect this had on particular hydrocarbon species was observed by Bascunana et al (2) species up to C4 were injected into the flow of exhaust gas. It was observed that in addition to complete oxidation, the breaking up of larger species into C2 and C3 species also occurred. This type of research was performed with specially designed reactors under controlled conditions.

Recent European legislation insisting on the use of catalytic converters and the current development of reformulated

fuels is generating interest in the impact that hydrocarbon species has on the catalyst efficiency. After the catalyst has reached its operating temperature their effectiveness is dependent on the reactivity of hydrocarbon species fed to them. Kojima et al (3) observed the effect of different catalyst configurations on hydrocarbon emissions. The HC species most easily oxidised were the Alkenes followed by aromatics and lastly alkanes.

The reduction of Hydrocarbon emissions across the exhaust manifold was observed during engine tests, so an investigation of the change in speciation was instigated. The objective of this paper is to comment on observed changes in hydrocarbon emission levels and speciation as the exhaust flows through the manifold. This is part of an ongoing project investigating hydrocarbon speciation changes in engine operation and configurations.

2 EQUIPMENT

The engine used throughout this research was a 1.4 litre 16 valve unit with wet liners. The throttle body fuel (TBI) injection system and manifold was altered to multi point fuel injection. The engine control unit could be adjusted to maintain accurate control of operating conditions, given in Table 1. The engine was coupled to a Schenk eddy-current dynamometer. During tests

CO, CO₂, CH₄, HC and NOx were measured. Hydrocarbon emissions were measured by NDIR in propane units. Regular calibration ensured the accuracy of the analysing equipment, including feeding calibration gases into the sample line at the engine. The sample line includes sampling points at the exhaust port of each cylinder and in the exhaust pipe immediately below the manifold, the sample being passed through a heated line to the analysers.

Thermocouples were used to monitor exhaust gas temperatures at the sampling points and to measure the coolant and oil temperatures. Air and fuel flows to the engine were measured. A record of the engine operating conditions was kept enabling consistent conditions at the test points to be achieved to an accuracy of 5%. The results discussed here are the statistical mean of several tests. Throughout this research the tests were repeated taking samples from each test point on different days. These were found to be consistent and repeatable.

Table 1 Test Points

Speed(RPM)	BMEP(bar)
1500	1.0
1500	2.62
2000	2.0
2500	5.5
3500	Wide Open Throttle

Air fuel ratio 15:1
 Ignition timing adjusted to give peak pressure at 12 ATDC

The standard lubricating oil used is a CEC reference oil (RL 139/4) of viscosity 10W/30. The fuel is a reference unleaded petrol CEC RF-08-A-85, with knocking characteristic Octane numbers of RON 97.1, MON 87.4.

3 GAS CHROMATOGRAPHY, COMPARISON OF HYDROCARBON SPECIES FROM FUEL AND ENGINE EMISSIONS

The sample was carried to the gas chromatograph through a heated sample line without being diluted or filtered.

A Perkin Elmer 6000 gas chromatograph was used with a wall coated open tubular column, the stationary phase being, CP-Sil-5 CB, the column length 50m and the inside diameter 0.32 mm. This equipment gave good resolution of a wide range of hydrocarbons from C1 to C9. The method used is described in Table 2.

Table 2 Gas Chromatograph Method

Temperature Programme	
Temperature 1	= 30 °C
Iso time	= 2 minutes
Ramp 1	= 4 °C/minute
Temperature 2	= 200 °C
Injector Temperature	= 100 °C
Detector Temperature	= 250 °C
Carrier Gas	Helium
Flow Rate	1 ml/min at 20 °C
Injection	Automatic sampling valve, 0.1ml sample loop
Detection	Flame Ionisation Detector

From emission samples taken from the exhaust pipe. With the gas chromatograph method described above a selection of 13 species were chosen and identified with calibration gases. These species were a selection of products and fuel components representative of the main types of species alkanes, alkenes and aromatics. They accounted for approximately 75% of the area of the gas chromatograph trace. These are named and listed in Table 3.

Table 3 Major hydrocarbon species from emissions

Peak	Name
1	Methane
2	Ethene (ethylene)
3	Ethane
4	Propene (propylene)
5	Isobutene
6	Butane
7	pent-1-ene
8	Benzene
9	2,2,4, trimethyle pentane
10	2,4, dimethyle hexane
11	Toluene
12	P-Xylene and M-Xylene
13	O-Xylene

chromatograph plots from unleaded gasoline and emissions, that there is a significant reduction in the number of peaks detected in the emissions compared to the fuel. Unburned fuel species do not survive the combustion process in equal proportions. Some C1 to C3 hydrocarbons are not present in gasoline but, are products of incomplete combustion. Many components of fuel are not detected in the emissions. Dempster and Shore (4), identified a greater part of the hydrocarbon emissions as combustion products.

The flame ionisation detector connected to the gas chromatograph gives an output proportional to the carbon atoms present. Using calibration gas mixtures of known concentration allows the parts per million (ppm) concentration of carbon to be calculated. The amount of a particular compound is found by dividing the carbon atoms detected by the number of atoms in that compound.

4 RESULTS AND DISCUSSION

The cylinder to cylinder variations in air fuel ratio and therefore emissions due to the adapted TBI manifold creates problems when comparing these with the exhaust pipe emissions, because this becomes an average of all cylinders after the exhaust manifold, Figure 2 shows the air fuel ratios with the engine set at a ratio of 15:1 by using Spindt calculations from exhaust pipe emissions. The main difference being between the inside and outside cylinders, this holds for each test point used in these tests. To obtain a more representative sample from the exhaust ports an average sample was taken. To ensure an even flow of sample the sample circuit was double branched, Figure 3. before sampling commenced the air fuel ratios from the exhaust ports were compared against the exhaust pipe, close agreement was usually observed.

Measurements of hydrocarbon emissions before and after the manifold, Figure 4, indicate that decreases in emissions are greater as speeds and loads increase. This is better displayed in Figure 5 which shows the percentage change in the hydrocarbon emissions. The variations in

at low speed/load conditions there is no significant differences in the GC plots from before and after the exhaust manifold. However with higher speed and load a distinct change in the balance in the species occurs.

For more detailed discussion the species are divided into three groups, Alkanes, Alkenes and Aromatics. The Alkanes range from methane, a product of pyrolysis, to 2,4. dimethyle hexane a fuel component. A suitable way to demonstrate the changes in speciation is shown in Figure 6. Which compares the percentage changes for the Alkanes at each test point across the exhaust manifold. The negative bars indicate a decrease from the exhaust port, Figures 7 and 8 are plotted by the same method. The differences observed in Figure 6 are characterised by a large decreases in fuel species, especially 2,2,4. trimethyle pentane, and small increases in combustion products. The most dramatic change occurs at 2500 rpm 5.5 bar bmep.

The range of Alkenes is more restricted going from ethene (ethylene) to pent-1-ene a C5 hydrocarbon. Only Pent-1-ene is a fuel component. Figure 7 shows a similar trend to the Alkanes with the large decrease in pent-1-ene. The products are more erratic with increases at some speed load condition and decreases at others. Again the most significant change in fuel species occurs at 2500 rpm 5.5 bar bmep.

The Aromatics, Figure 8, are all fuel components and in general show reductions across the manifold which increase with speed and load upto 2500 rpm 5.5 bar bmep where as with other fuel species large reductions are observed. This is particularly the case for toluene and the xylenes. The lower reductions and slight increase at wide open throttle, of benzene is due to its also being a product of pyrolysis of heavier aromatics, Ninomiya and Biggers (5) observed that benzene in the exhaust also increases with increased toluene in the fuel. so as the break up of heavier aromatics increases the level of benzene increases. Toluene can also be formed by pyrolysis, hence the small increase at wide open throttle.

Table 4 Air Fuel Ratios and Temperatures

Test Point	Exhaust Port		Exhaust Pipe	
	AFR	T (°C)	AFR	T (°C)
1500rpm 1 bar	15	500	15	345
1500rpm 2.62 bar	14.9	550	15	415
2000rpm 2 bar	15.1	610	15	500
2500rpm 5.5 bar	15	700	15	545
3500rpm WOT	15.1	770	15	620

A familiar pattern for each group of species can be identified as the levels of fuel components decrease with increases in speed and load upto 2500 rpm 5.5 bar bmep, where a much larger reduction in fuel species occurs combined with an increase in pyrolysis products such as methane and ethane. At wide open throttle much smaller changes in the speciation are observed. However, as figure 5 indicates the largest reduction of total hydrocarbon emissions occurs at 3500 rpm wide open throttle.

The oxidation of hydrocarbons after combustion is dependent on temperature, residence time and oxygen content, which is stable at 1.4%. Table 4 shows average temperatures for each test point. The gas temperature at 2500 rpm 5.5 bar bmep is 700°C combined with the exhaust gas flow rate this gives the correct conditions for high levels of pyrolysis to take place, but insufficient time for full oxidation of the fuel species. This leaves a residue of pyrolysis products. The gas temperature at wide open throttle is high enough for higher levels of pyrolysis and for the oxidation of the products as they are formed. So the balance between fuel and products is closer to that detected at the exhaust port. An exception to this is an increase of 19% in benzene as a residual of larger aromatic compounds.

5 CONCLUSIONS

It has been shown that oxidation in the

exhaust manifold has a considerable impact on the hydrocarbon species emitted from the engine. Also that this speciation is affected by the speed and load of the engine as this alters the temperature and flow rate of the exhaust gas. The largest changes to speciation occurred at medium speeds and loads, characterised by the reduction of unburnt fuel and formation of methane and ethane from pyrolysis of the fuel.

Further work may realise the possibility that the exhaust manifold could be utilised further to assist the catalyst in reducing hydrocarbon emissions by changing the balance of species entering the catalyst.

ACKNOWLEDGMENT

The authors would like to thank AE Piston Products Ltd. and SERC for the supply of equipment and funds for this research.

REFERENCES

1. Sigworth, H.W. Myers, P.S. and Uyehara, O.A: The disappearance of ethylene, propylene, n-butane and 1-butane in spark ignition engine exhaust. SAE 700472
2. Bascunana, J.L. Skibinski, J. and Weaver, E.E: Rates of exhaust gas-air reactions. SAE 770639.

3. Kojima,K. Hirota,T. and Yakushiji,K. Effects of exhaust emission control devices and composition on speciated emissions of SI engines. Conference Proceedings Combustion in Engines, Technology, Applications and the Environment. IMechE. 1992 C448/015. pp 145-149.
4. Dempster,N.M. Shore,P.R: An investigation into the production of hydrocarbon emissions from a gasoline engine tested on chemically defined fuels. SAE 900354.
5. Ninomiya,J.S. and Biggers,B: Effects of toluene content in fuel on aromatic emissions in the exhaust. Journal of air pollution control. 1970. Vol. 20 No 9. pp 609-611.

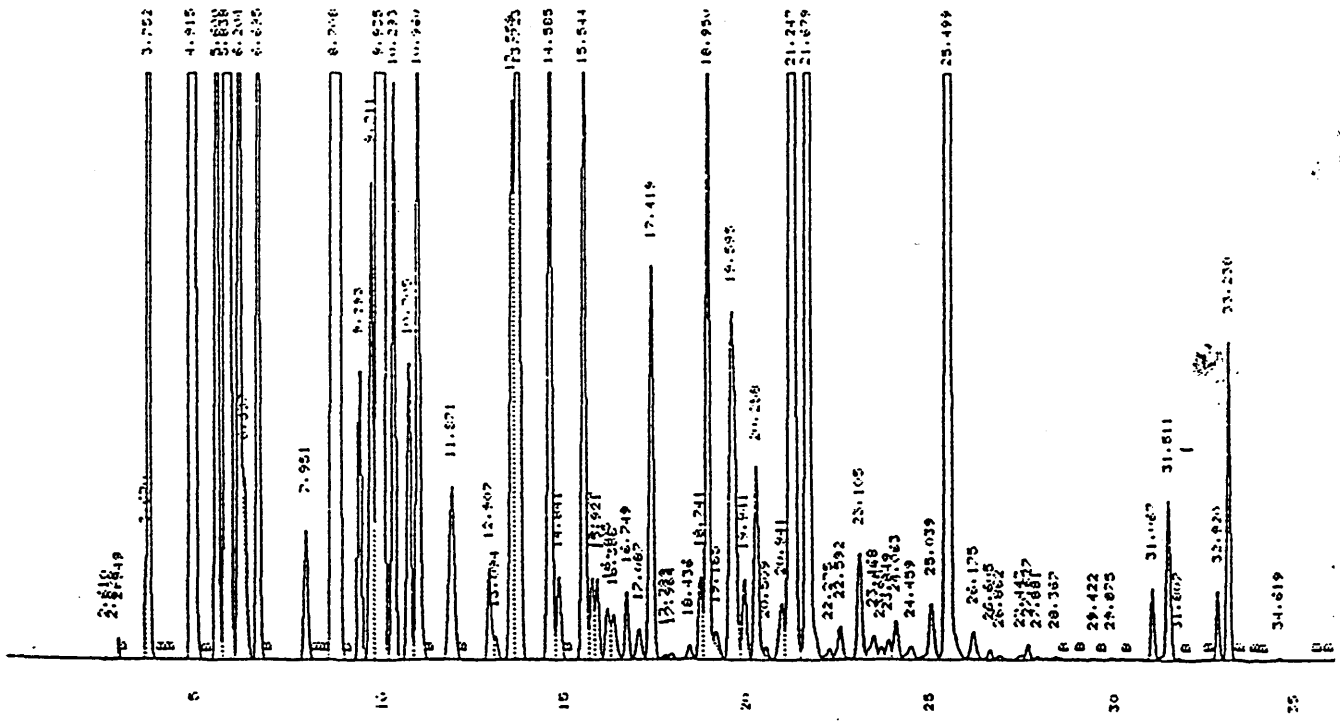


Figure 1, a, Gas chromatography plot of reference fuel

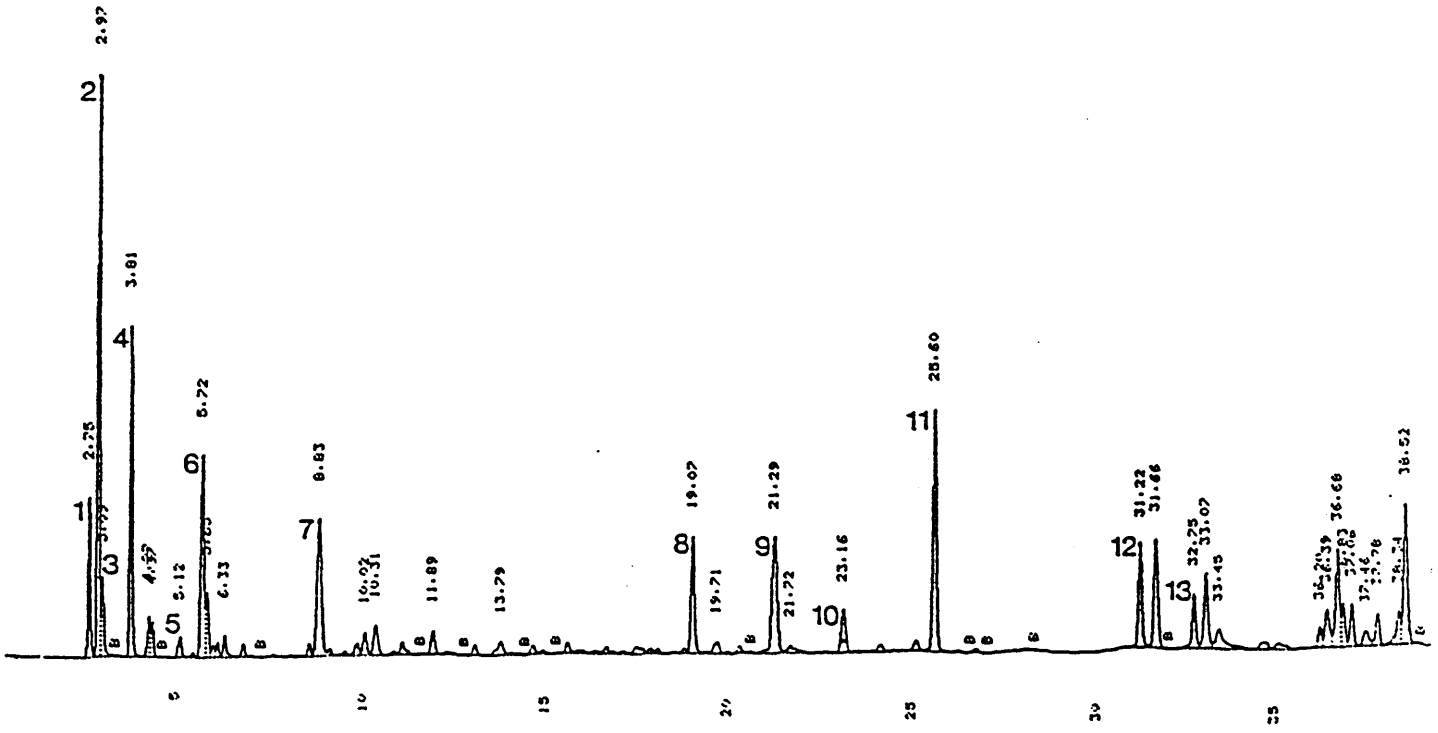


Figure 1, b, GC plot of emissions at 2500 rpm 5.5 bar bmep using standard pistons

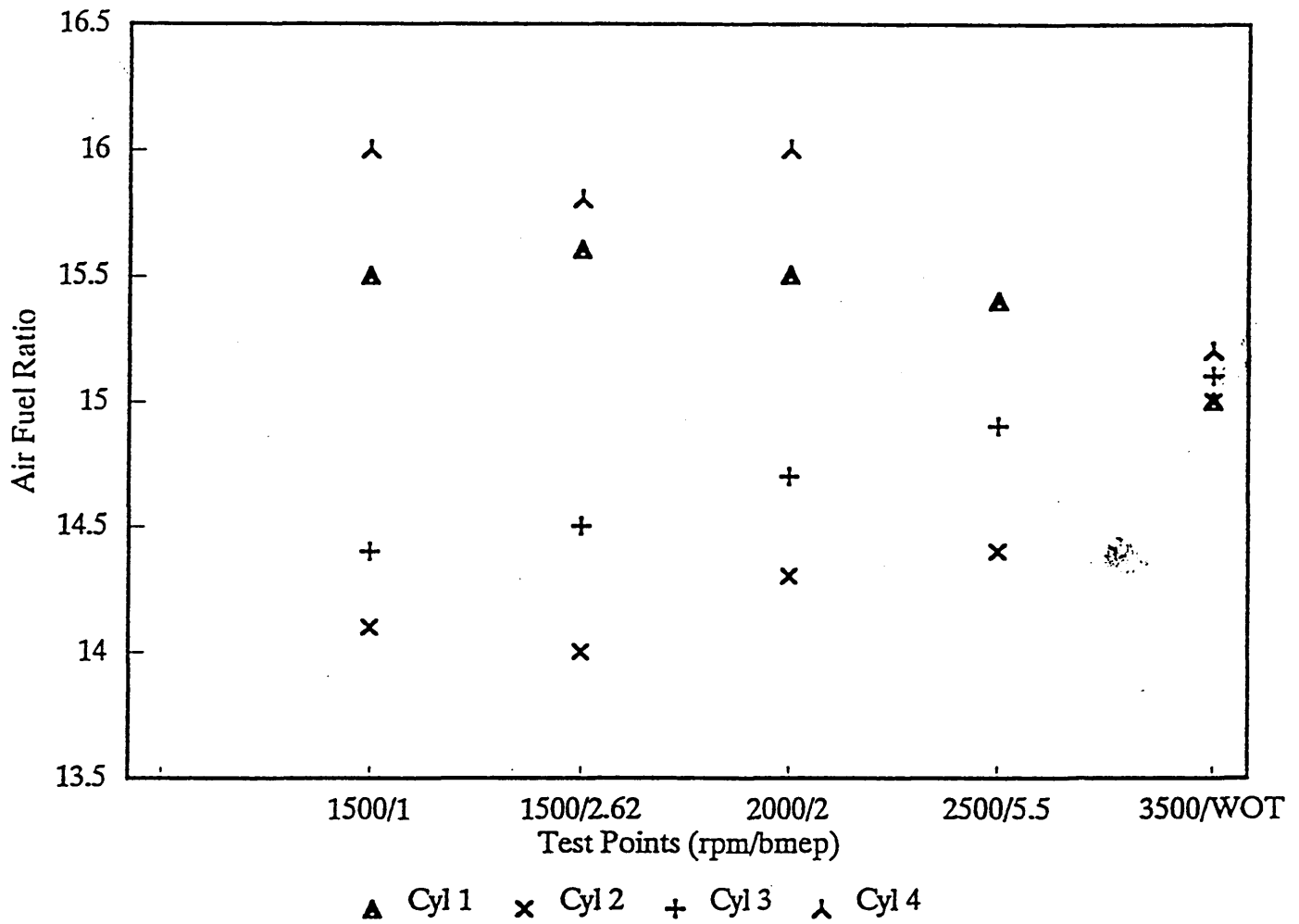


Figure 2 Variation in air fuel ratio between cylinders

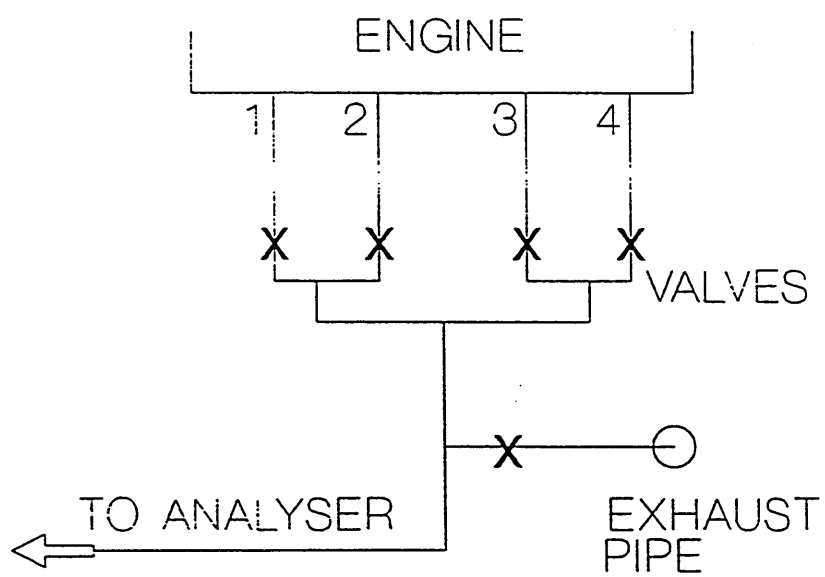


Figure 3 Modified sampling circuit

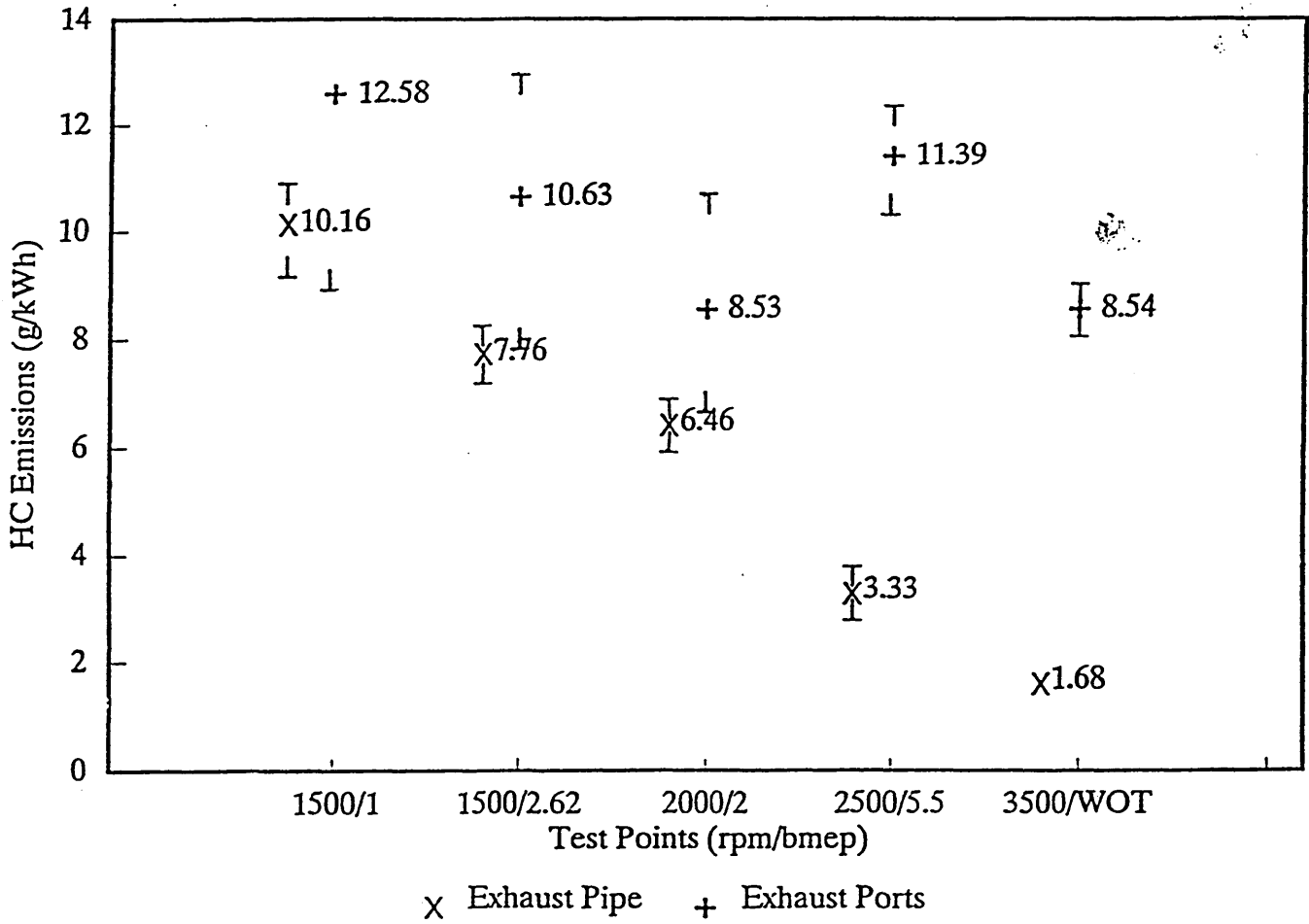


Figure 4 Comparison of hydrocarbon emissions from samples taken at the exhaust ports and pipe

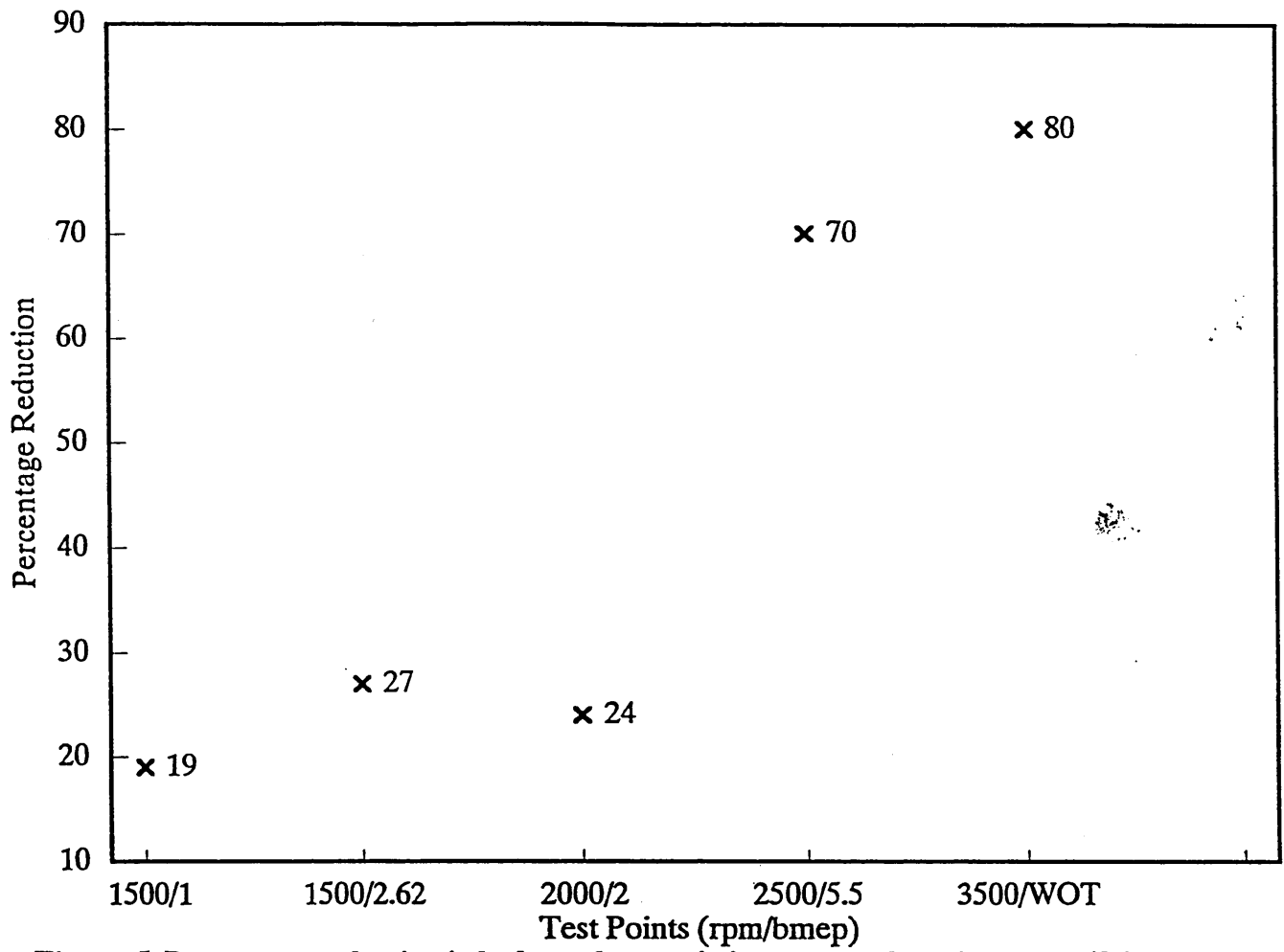


Figure 5 Percentage reduction in hydrocarbon emissions across the exhaust manifold

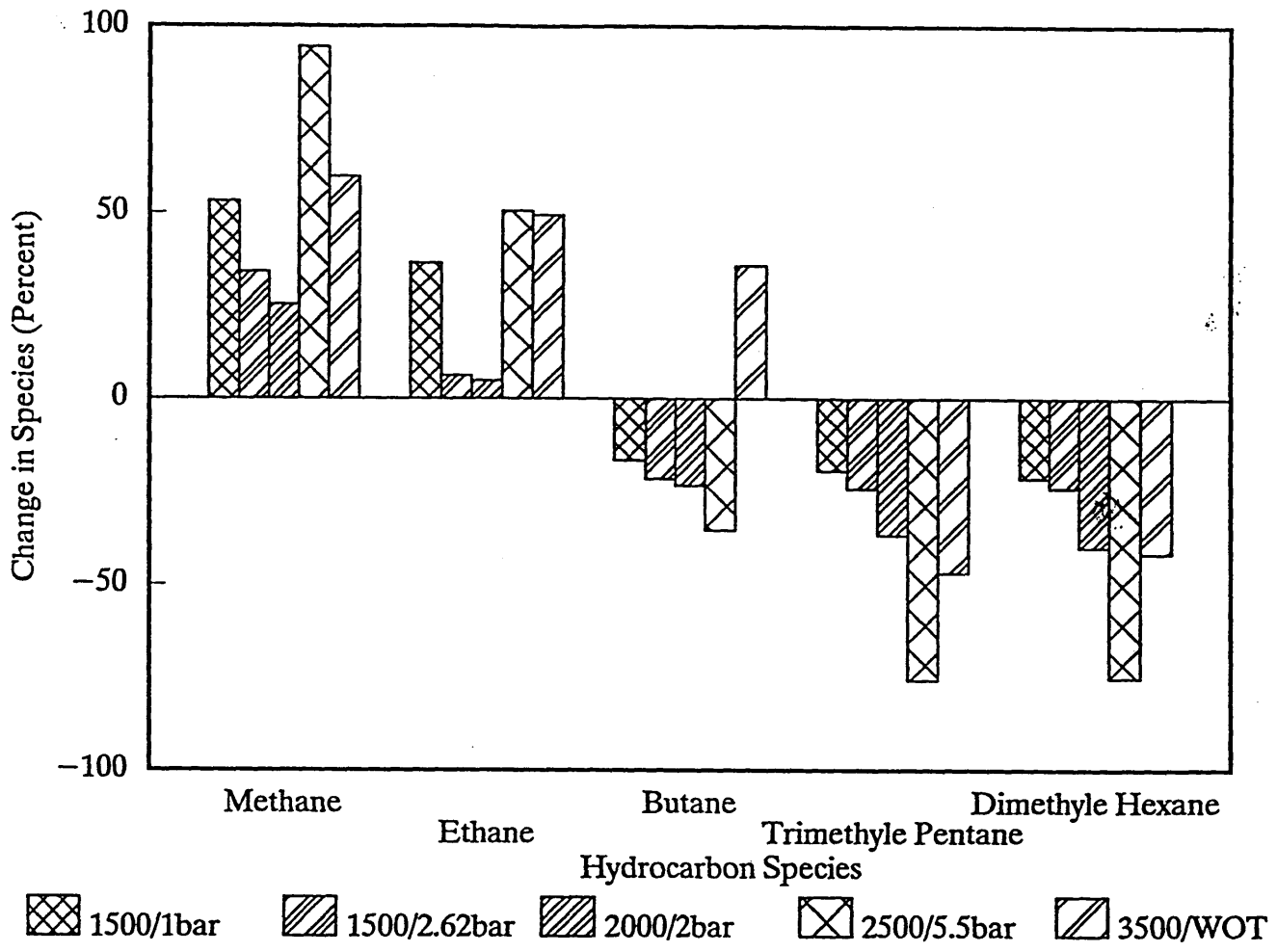


Figure 6 Percentage change in HC species (ALKANES) across the exhaust manifold

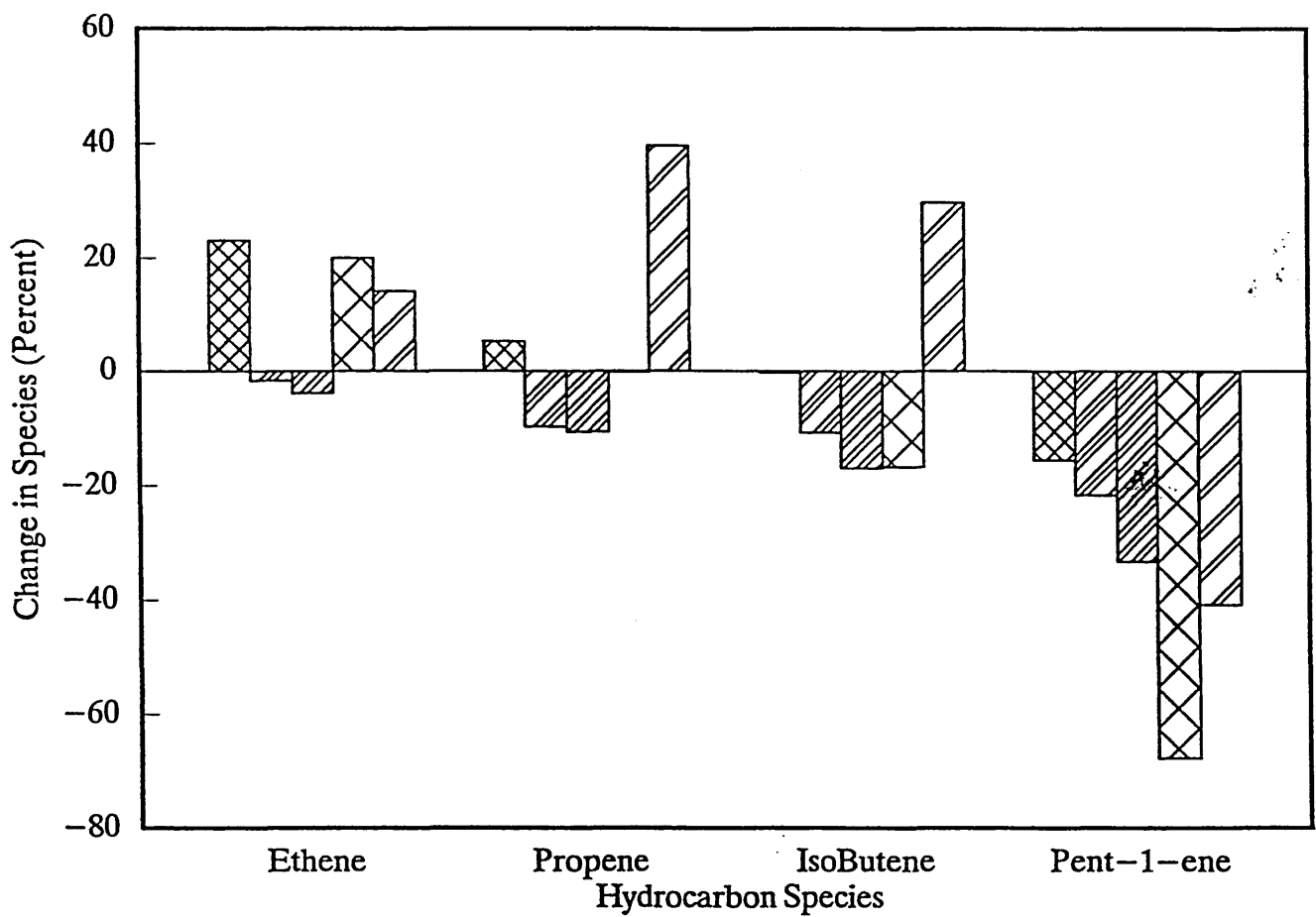


Figure 7 Percentage change in HC species (ALKENES) across the exhaust manifold

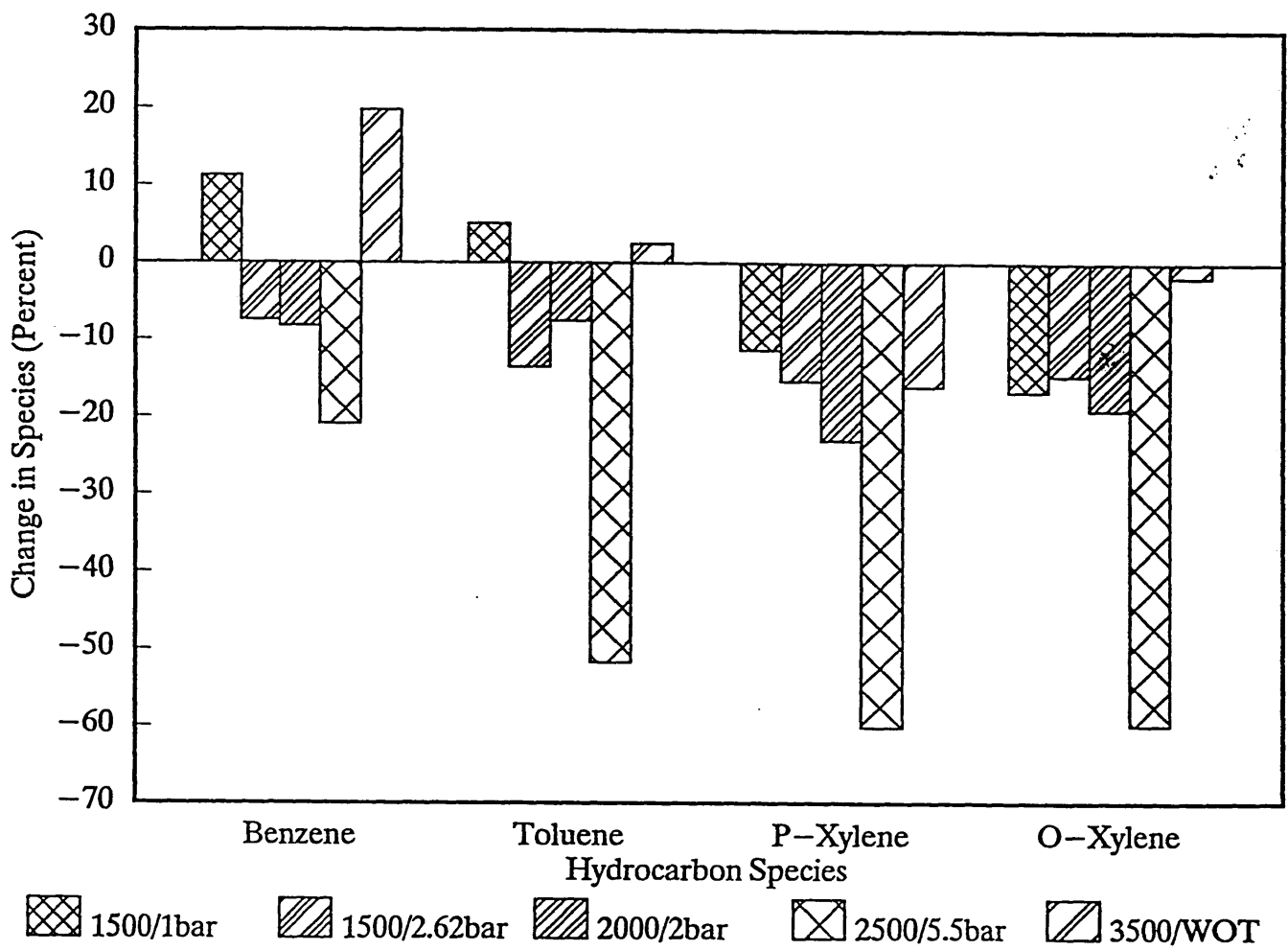


Figure 8 Percentage change in HC species (AROMATICS) across the exhaust manifold